



2809663247



REFERENCE ONLY

UNIVERSITY OF LONDON THESIS

Degree MD Year 2008 Name of Author ROBINSON, Grace
Victoria

COPYRIGHT

This is a thesis accepted for a Higher Degree of the University of London. It is an unpublished typescript and the copyright is held by the author. All persons consulting this thesis must read and abide by the Copyright Declaration below.

COPYRIGHT DECLARATION

I recognise that the copyright of the above-described thesis rests with the author and that no quotation from it or information derived from it may be published without the prior written consent of the author.

LOANS

Theses may not be lent to individuals, but the Senate House Library may lend a copy to approved libraries within the United Kingdom, for consultation solely on the premises of those libraries. Application should be made to: Inter-Library Loans, Senate House Library, Senate House, Malet Street, London WC1E 7HU.

REPRODUCTION

University of London theses may not be reproduced without explicit written permission from the Senate House Library. Enquiries should be addressed to the Theses Section of the Library. Regulations concerning reproduction vary according to the date of acceptance of the thesis and are listed below as guidelines.

- A. Before 1962. Permission granted only upon the prior written consent of the author. (The Senate House Library will provide addresses where possible).
- B. 1962-1974. In many cases the author has agreed to permit copying upon completion of a Copyright Declaration.
- C. 1975-1988. Most theses may be copied upon completion of a Copyright Declaration.
- D. 1989 onwards. Most theses may be copied.

This thesis comes within category D.

☒

This copy has been deposited in the Library of University College London

☐

This copy has been deposited in the Senate House Library,
Senate House, Malet Street, London WC1E 7HU.

The effects of sleep deprivation on brain fMRI activation during motion detection and tracking

Grace Robinson

Thesis submitted for MD degree, University of London

UMI Number: U593257

All rights reserved

INFORMATION TO ALL USERS

The quality of this reproduction is dependent upon the quality of the copy submitted.

In the unlikely event that the author did not send a complete manuscript and there are missing pages, these will be noted. Also, if material had to be removed, a note will indicate the deletion.



UMI U593257

Published by ProQuest LLC 2013. Copyright in the Dissertation held by the Author.
Microform Edition © ProQuest LLC.

All rights reserved. This work is protected against
unauthorized copying under Title 17, United States Code.



ProQuest LLC
789 East Eisenhower Parkway
P.O. Box 1346
Ann Arbor, MI 48106-1346

Abstract

Sleep deprivation is common and leads to inattention and impaired vigilance. Sleep deprived drivers have an increased road traffic accident rate. Police data suggest that sleep deprivation accounts for up to 23% of all accidents on UK roads. How sleep deprivation leads to impaired driving is uncertain.

The skills needed for error free driving are the detection of moving objects, and the ability to track. Work using Functional Magnetic Resonance Imaging (fMRI) has established which brain areas are active during tracking manoeuvres. This study used fMRI imaging to assess the effects of sleep deprivation on visual stimulation and visuo-motor tracking in normal subjects, hypothesising that sleep deprivation in normal subjects leads to impaired tracking and impaired motion detection, with reduced fMRI activation of the brain areas normally activated during performance of these skills. I hypothesised that similar effects would be seen in patients with the sleep fragmentation of OSA, and that any impairments would be reversed by successful CPAP treatment.

Ten normal subjects underwent visual stimulation and performed a tracking task during fMRI imaging, before and after total sleep deprivation. Tracking and steering simulator performance were impaired following sleep deprivation. fMRI analysis showed reduced activation of visual cortex area V5 (an area integral to visual motion detection) and increased frontal lobe activation following sleep deprivation. During tracking, there was preservation of precuneus activation following sleep deprivation. Coherent visual motion detection in 24 normal subjects showed impaired motion detection following sleep deprivation, in those subjects who were sleep deprivation vulnerable, correlating with the functional imaging abnormality demonstrated.

fMRI imaging during visual stimulation in 17 patients with obstructive sleep apnoea (OSA), before and after continuous positive airways pressure (CPAP) treatment showed increased activation of the frontal lobe pre treatment, and increased precuneus activation post treatment, but no differential visual cortex effect.

These results suggest potential mechanisms for the impaired driving seen in association with sleep deprivation and with the sleep fragmentation of untreated OSA. Impairment of attention, preservation of an 'idyling' or 'passive' state, and deficits in visual motion detection may contribute to the driving deficits seen.

Contents

	Page number
Abstract	1
Ethical Approval	5
Statement of Involvement	6
Aknowledgements	7
Introduction	8-10
 <i>Chapter 1 - Background</i>	
Effects of sleep deprivation	
Motor coordination and driving	11-17
Neurocognitive effects	18-20
Obstructive sleep apnoea	
Background	21-24
Driving effects of OSA	25-29
Functional Magnetic Resonance Imaging	
Background	30-35
fMRI analysis	36-43
Functional brain imaging and sleep	44-47
MRI studies and the resting or 'passive' state	48-50
Visuo-motor tracking	51-52
Coherent visual motion detection	53-56
Aims and Hypotheses	57-59
 <i>Chapter 2 - The effects of sleep deprivation on fMRI brain activation during visual stimulation and tracking</i>	
Introduction	60
Hypotheses	61
Developmental work	61-68
Methods	69-78
Results	79-84 & 101-106
Tables of results	85-87
Images of results	88-100 & 107-126
Discussion	127-138

Chapter 3 - The effect of total sleep deprivation on coherent visual motion and visual form detection in normal subjects

Introduction	139-140
Hypotheses	141
Methods	141-148
Results	149-153
Table of results	154
Graphs of results	155
Discussion	156-162

Chapter 4 - The effect of Obstructive Sleep Apnoea on visual stimulation and visuo-motor tracking, before and after continuous positive airways pressure treatment

Introduction	163
Hypotheses	163
Methods	164-169
Results	170-174
Tables of results	175-179
Images of results	180-188
Discussion	189-196

Chapter 5

General discussion	197-199
Future Work	200-201

Chapter 6

Publications	202
References	203-221

<i>Appendix</i>	222-273
------------------------	----------------

List of tables

	Page No
Table 1 - The subjects' baseline characteristics (study 1)	79
Table 2 - Normal subject data, after normal sleep and after sleep deprivation (study 1)	85
Table 3 - Non-fMRI results from study 1	87
Table 4 - Individual subject maximum pixel activation during visual stimulation, following mask thresholding, before and after sleep deprivation (study 1)	100
Table 6 - Individual subject maximum pixel activation during tracking, before and after sleep deprivation (study 1)	126
Table 7 - The subjects' baseline characteristics (study 2)	149
Table 8 - Data for subjects defined by their post sleep deprivation sleepiness status: 'sleepy' and 'non-sleepy', following normal sleep and following sleep deprivation (study 2)	154
Table 11 - The OSA patient baseline characteristics (study 3)	170
Table 12 - OSA patient data (study 3)	175
Table 13 OSA patient non-fMRI results (study 3)	179

Ethical Approval

Ethical approval for the work described in this thesis was obtained from the Central Oxford Research Ethics Committee (COREC reference 01.004). All work was carried out according to the committee's guidelines.

The work was undertaken at the Oxford Centre for Respiratory Medicine, Churchill Hospital, Oxford, at the Oxford Centre for Functional Magnetic Resonance Imaging of the Brain, John Radcliffe Hospital, Oxford and at the University Laboratory of Physiology, Oxford.

Funding for the work described was from a Research Training Fellowship awarded by the Oxford Health Services Research Committee.

Statement of Involvement

I carried out all the work described in this thesis other than the EEG analysis (used in study 2), which was performed by Dave Jones. The tracking paradigm and associated analysis programmes were designed by Professor Chris Miall.

Aknowledgements

I am grateful for the help and advice of the following people:

Rob Davies
John Stradling
Chris Miall
Paul Matthews
Stephen Spiro
Emma Jones
Debbie Nicoll
Debbie Smith
Beverley Langford
Joy Crosby
Colin Cox
Dave Jones
Jonathon Winter
Peter Hansen
Peter Hobden

Introduction

The rigors of modern life mean that sleep deprivation is very common. Sleep deprivation leads to sleepiness, which is the commonest cause of inattention and impaired vigilance. Sleep deprived drivers have an increased road traffic accident rate, and daytime sleepiness is a clear contributory factor to road traffic accidents [Horne JSR 1995, Horne BMJ 1995, Horne 1995, Lyznicki 1998]. Police data suggest that sleep deprivation accounts for up to 23% of all accidents on UK roads. The ability to drive safely is a vital skill; however road traffic accidents remain a major cause of morbidity and mortality. Worldwide, 1.2 million people die on roads per year [Webb 1995, WHO 2004]. The mechanism for the impaired driving of sleep deprivation is unknown.

Driving is a complex task, involving the integration of visual, tactile and auditory information, with translation into a coordinated motor output, involving speed control and alteration in lane position. Thus the skills needed for safe and error free driving are the detection of moving objects (motion detection), and the ability to track (the repeated adaptation of a motor response to a changing visual input). One or both of these skills or their component parts may be impaired by sleep deprivation. Both the detection of moving objects and the ability to track involve a number of complex neurological pathways; it is plausible that the sleep deprived brain is unable to use the appropriate brain areas to enable optimal performance of these skills.

Impaired attention and vigilance are more general, non-specific effects of sleep deprivation. A reduced state of vigilance is associated with sleep deprivation, and interference is thought to contribute, with an inability to ignore distracting targets in the sleep deprived state.

The studies in this thesis include an assessment of pure visual stimulation and visuo-motor tracking using brain functional magnetic resonance imaging (fMRI), and a functional test of coherent visual motion detection, in normal subjects before and after sleep deprivation. A deficit in the ability to detect moving objects might explain some of the tracking and steering impairments associated with sleep deprivation. In addition, a lack of sleep might impair the function of metabolically active brain areas. This is recognised in the frontal cortex following reduced sleep [Horne 1993, Harrison 1998, Harrison 1999].

Coordinated hand/eye tracking activates a number of brain regions, including areas in the motor cortex, cerebellum, extra striate visual cortex, the precuneus, ventral premotor areas and frontal cortex [Miall 2000, Miall 2001]. Hand tracking also activates area V5 / MT (the middle temporal area, in the extra-striate visual cortex), which is integral to the detection of coherent visual motion and involves a very metabolically active brain area [Oreja-Guevara 2004].

Work in this thesis has also assessed whether the motor skills used in steering and tracking are sensitive to the effects of sleep deprivation. These two studies were done in parallel because of the difficulties of carrying out sleep deprived functional fMRI work. A final study assessed the effects of sleep deprivation due to obstructive sleep apnoea (OSA) in a small number of patients, using the same paradigms. This aimed to establish whether any of the effects seen with sleep deprivation in normal subjects could also explain the deficits in driving and tracking associated with the sleep fragmentation of OSA, one of the commonest causes of sleep deprivation.

Thus the aims of this thesis were to establish some of the mechanisms for the impaired driving and tracking associated with sleep deprivation, to try to understand

the effects of sleep deprivation on brain fMRI activation and function during performance of some of the skills needed for safe and error free driving.

Effects of Sleep Deprivation

Motor coordination and driving

Road traffic accidents are a major cause of morbidity and mortality, ranking as the third leading cause of death in the United States [US Dept of Commerce 1990]. Worldwide, nearly 1.2 million people die on roads per year. This represents 2.6% of the global burden of disease and accounts for 23% of all deaths due to injury [Webb 1995]. The World Health Organisation (WHO) predicts that this number will rise by over 65% in the first decades of the 21st century, with most of this increase in the developing world [WHO 2004].

The commonest causative factors in road traffic accidents are sleepiness, inattention and alcohol. Sleepiness is a very common cause of inattention and impaired vigilance. Sleep deprivation is known to lead to an increased incidence of road traffic accidents, and accounts for between 16 and 23% of all accidents on UK roads (based on police data) [Horne 1999], and about 10%, based on drivers' self reports [Maycock 1997]. Worldwide estimates of road traffic accidents related to sleepiness vary widely, ranging from 1-3% in the United States [Lyznicki 1998], and up to 30% in Australia [Naughton 1991]. This type of accident is commonest in male drivers under the age of 30, and causes greater driver morbidity and mortality than other types of accidents. This is principally due to the absence of braking, and therefore a higher speed prior to impact. For this reason a higher cost is associated with each sleep related accident. A number of features are common to road traffic accidents associated with sleepiness: a single vehicle leaves the road, the driver makes no attempt to avoid the crash, the driver is alone in the vehicle, the crash is more

likely to be serious, and the accident is more likely to happen late at night, in the early hours, or in the mid afternoon.

Sleep deprivation leads to sleepiness, which has subjective, physiological and behavioural effects [Babkoff 1991, Pilcher 1996]. The associated reduction in vigilance levels has potentially serious implications for road users, as even short tasks can be affected by sleep deprivation. One hypothesis for the impaired performance seen with sleep deprivation is the 'lapse hypothesis' [Patrick 1896, Bills 1931]. This theory suggests that impaired performance is due to an increased frequency of lapses - either failure to respond or delayed responses. Drivers do not have to fall asleep at the wheel to have an accident; sleep deprivation leads to drowsiness, which makes drivers less attentive.

Clear time of day effects are seen with sleep related driving accidents, partly due to the circadian variation in sleepiness and alertness. Peaks in sleep related accidents are seen in the early morning (2am to 7am) and mid-afternoon [Horne JSR 1995, Langlois 1986, Pack 1995]. A significant association exists between drivers who identify themselves as sleepy and a subsequent sleepiness related road traffic accident [Connor 2002].

Sleepiness does not occur without warning, and there is evidence that the sensation of increased sleepiness correlates with increasing minor errors on simulated driving after a night of restricted sleep [Reyner, Psychophysiology 1998]. An effective measure to counter sleepiness is a 30 minute nap or the consumption of about 150mg of caffeine. The use of the car radio and cold air (winding down the window) whilst continuing to drive are only of benefit for short time period [Reyner 1998, Reyner 2002].

A number of studies have assessed the effects of sleep deprivation, alcohol intoxication and alerting agents such as caffeine, on driving simulator performance. Williamson et al assessed performance on a number of tasks, including tracking, reaction time, spatial memory and a test of vigilance [Williamson 2000]. The aim was to determine the number of hours of sleep deprivation required to produce a decrement in performance similar to that seen in subjects with a blood alcohol concentration (BAC) of 0.05%, the limit above which driving is considered hazardous [Howat 1991]. At the end of a 17 to 19 hour period of continuous wakefulness, performance on the tasks tested was comparable to that produced by alcohol intoxication to the legal limit. The earliest effects were seen on vigilance, with effects appearing later on a dual test of speed and hand / eye coordination. Longer periods of wakefulness were equivalent to higher alcohol doses. Dawson's 1997 study showed similar decrements after 17 hours of prolonged wakefulness, with impairments comparable to the effects of alcohol intoxication to the legal limit. This study also showed a progressive performance decrement on a monotonous motor coordination or tracking task from the baseline, of 1.16% with each 0.01% increase in blood alcohol concentration [Dawson 1997].

Additional work has shown that the combined effects of prolonged wakefulness and alcohol consumption produce greater decrements in driving performance than that produced by each condition alone, and that most drivers have a limited ability to appreciate the magnitude of their impairment following alcohol intoxication and sleep deprivation [Arnedt 2000, Philip 2003]. Low blood alcohol concentrations (at approximately half the UK legal limit, and not detected by police breathalysers) also impair simulated driving in sleep deprived subjects; this is not

associated with increased subjective sleepiness, but is associated with significant EEG changes [Horne 2003].

The effect of shift work on circadian rhythm results in impaired driving performance, with an increased road accident rate in shift workers. Shift work disrupts sleep patterns and increases sleep deprivation. Shift workers report a higher incidence of poor sleep and increased daytime sleepiness; they also consume more caffeine and alcohol than non-shift workers, and are more likely to use alcohol as a sleep aid [Richardson 1989]. Horne et al have also shown that the effect of the circadian propensity for sleepiness, in combination with the effect of a small amount of alcohol (BAC within the UK legal driving limit) leads to impairments in monotonous simulated motorway driving [Horne Ergonomics 1991].

The effect of alerting agents as a measure to counter the impaired driving performance associated with daytime sleepiness has been studied by a number of groups. Caffeine is known to increase levels of alertness, but it has been unclear whether this is associated with improved performance. Reyner has assessed the effect of 200mg caffeine compared to placebo on early morning simulated driving following a night of sleep restricted to 5 hours, or no sleep at all [Reyner 2000]. Following restricted sleep, caffeine significantly reduced adverse driving incidents and subjective sleepiness during a 2 hour drive. Following no sleep, the same caffeine dose reduced adverse incidents for the first 30 minutes of the drive, and improved subjective sleepiness for one hour.

Motor coordination and driving - potential mechanisms for impaired performance

A complex series of manoeuvres involving many different motor and neurocognitive processes lead to safe and error free driving. Matching the curvature of the road, and keeping a reasonable distance from the road edges are both achieved by steering. Steering depends on continuous visual feedback; different points of the road ahead supply important information to the driver. Visual feedback comes from monitoring of the angular deviation of the road from the vehicle's current position, and a 'preview' position on the road ahead, typically about 1 second in the future [Land 1995]. A view of both near (about 9m ahead) and far (about 16m ahead) road segments is needed to optimise position in lane, and follow road curvature, respectively. At higher speeds, the view of the far road is more important, with the near road mechanism for fine-tuning. A view of the near road alone is adequate for successful steering at lower speeds, like driving in fog.

A number of studies have explored the potential mechanisms for the impaired driving performance seen with sleep deprivation. Wu et al's 1991 positron emission tomography (PET) study describes reorganisation of cerebral metabolic activity following about 32 hours sleep deprivation in 8 normal subjects. No overall reduction in whole brain metabolism was identified, but relative decreases in metabolic activity were identified in the frontal, temporal and occipital lobes, the basal ganglia and thalamus. Reduction in brain activation in these areas was specifically associated with decrements in performance in a button pressing continuous performance task [Wu 1991].

Studies of the ability to process peripheral visual signals after sleep deprivation give another potential explanation for the driving impairment seen. With increasing monotonous driving, the driver's visual field alters, due to a 'tunnel vision'

type phenomenon. This leads to a reduced ability to process peripheral signals, and may partly explain the deterioration in driving performance, as adequate peripheral vision is important for driving. The 'useful visual field' (or useful field of view) corresponds to the area around the fixation point, from which information can be quickly extracted during a visual task [Mackworth 1965]. The 'useful visual field' also deteriorates with increasing fatigue, due to increasing interference and the inability to ignore distracting targets [Roge 2002, Roge 2003, Sekuler 2000]. It is also affected by arousal level [Roge 2001, Roge 2002].

Changes in saccadic eye movement velocity and pupil constriction latency may be additional contributing factors to the impaired visual processing seen post sleep deprivation, and have been assessed before and after sleep deprivation in a group of commercial drivers [Kendall 2006]. In this study, saccadic eye movement velocity was significantly impaired, with an increased pupil constriction latency, correlating significantly with sleep latency, following a week of restricted sleep.

In addition to the effects of sleep deprivation on motor function and driving, sleep is important for the consolidation of learned motor skills, as assessed by fMRI [Maquet 2003]. In this study, subjects were trained on a pursuit task, in which the target trajectory was visible on only the horizontal axis. Subjects were then randomised to a night of normal sleep or sleep deprivation, following the training period. Three days later, fMRI imaging showed task related increased brain activation in response to the learned task, compared to a new task trajectory. Performance was better in the group that slept following training, compared to the sleep deprived group, and correlated with increased activity in the superior temporal sulcus, cerebellum and frontal eye fields. This was interpreted as being due to sleep related changes in motor skill learning areas involved in eye smooth pursuit movements; showing that sleep

disrupts the slow processes that lead to memory consolidation. This study showed greater activation in the posterior superior temporal sulcus (STS) during performance of the learned trajectory following sleep deprivation than following normal sleep. The STS is anterior to area MT/V5 (middle temporal / visual cortex area V5, a motion sensitive area), and also responds to biological motion [Bonda 1996, Vaina 2001]. It is also close to the areas of the temporal lobe which are active during smooth pursuit eye movements [Schmid 2001]. Activation of this area is also reported during initiation of action [Iacoboni 2001], and is thought to be involved in goal-directed behaviour [Toni 1998]. It is suggested that, following training the subject builds up an internal model of the learned trajectory, which is consolidated during the post training night, and during a re-test of the learned trajectory. [Maquet 2003].

Effects of Sleep Deprivation

Neurocognitive effects

Sleep deprivation has a wide range of effects on neurocognitive function. Pilcher et al's 1996 meta-analysis of sleep deprivation studies involving 1,932 subjects showed that effects on mood were greater than effects on cognitive or motor performance [Pilcher 1996]. Overall, compared across all tasks, sleep deprived subjects performed at a level about 1.37 standard deviations below that of non-sleep deprived subjects. The study showed a large standard deviation (2.08) across effect sizes, demonstrating a range of performance amongst sleep deprived individuals. Overall, the effect size for partial sleep deprivation (2.04) was greater than that for both short-term (1.21) (defined as ≤ 45 hours) and longer-term (1.27) (defined as > 45 hours) sleep deprivation. The effect size was 3.16 for mood, 0.87 for motor performance, and 1.55 for deterioration in cognitive performance. In general, an effect size of 0.2 is considered small, 0.50 considered a medium effect, and an effect size of 0.80 or greater is considered large [Hedges 1985]. The reason for the greater impairment with partial sleep deprivation is thought to be a greater disruption of circadian rhythm, leading to deficits similar to those seen with sleep fragmentation due to obstructive sleep apnoea.

Chronic sleep restriction leads to significant cumulative and dose dependent effects on cognitive performance on a number of tasks. Regardless of the mode of sleep loss, the number of hours of wakefulness correlate with the number of lapses in function and alertness [Van Dongen 2003]. Similar performance decrements are seen following sleep restricted to 6 hours or less per night, showing that moderately small restrictions in sleep over a prolonged period are not benign. Subjective sleepiness

ratings during this study showed that subjects were largely unaware of their poor performance. Meta-analysis of the effects of short-term sleep deprivation on cognitive function showed greater effects on long and complex tasks, than the effects on shorter, easier tasks. For longer term sleep deprivation, there was a greater decrement on shorter tasks than longer ones.

Horne and Harrison have studied the effects of sleep deprivation on frontal cortex function, decision making and thinking ability [Harrison 1999, Harrison 2000]. In a number of total sleep deprivation experiments, Horne has shown that creative, or 'divergent' thinking ability is impaired following 32 hours sleep deprivation, with particular impairment of 'flexible thinking' - the ability to change strategy or generate original ideas. This is not thought to be due to motivational effects, as significant impairment is also seen in shorter, more stimulating tasks, which included an incentive to perform well [Horne 1988, Horne 1993].

Horne has shown that the prefrontal cortex is preferentially affected by sleep deprivation. This has led to the 'prefrontal cortex theory' of sleep deprivation. It is postulated that, because of the higher daytime metabolic rate of the prefrontal cortex, it is more susceptible to the effects of sleep deprivation, as it is unable to recover its normal function without adequate sleep [Horne 1993]. Patients with prefrontal cortex lesions typically have difficulty carrying out new, unfamiliar behaviours, and have concrete, unchanging perceptions. Alterations in speech are also seen, including reduced affect and intonation, with the generation of less complex and sophisticated sentences [Fuster 1989]. Short term memory is also impaired (which may be an attentional effect), and impairments of affect, leading to apathy and lack of initiative are also seen, as well as distractibility [Blagrove 1991]. Neuropsychological testing and brain imaging studies have shown similar effects on the prefrontal cortex in older

individuals, with impairment of prefrontal cortex function. This has led to the hypothesis of sleep deprivation in young healthy adults as a model for 'healthy aging'. [Harrison Sleep 2000].

Reductions in brain activity following sleep fragmentation have been measured with P300 brain wave mapping [Kingshott 2000]. This study used tone-induced sleep fragmentation [Martin 1996], making the sleep deprivation more akin to that seen in OSA. Event-related potentials were recorded during a visual information processing test. Overall, there was no reduction in cognitive performance or objective sleepiness with sleep fragmentation, though a reduction in P300 latency was seen at a number of sites, including in the frontal and temporal brain areas. This is postulated to represent a decrease in attention [Begleiter 1983]. Additional human studies have shown reduced amplitude and longer latency visual event related EEG potentials following 40 hours total sleep deprivation [Corsi-Cabrera 1999]. In this study, EEG amplitudes fell to around 20% of their post normal sleep size following sleep deprivation, and correlated with impaired performance in a reaction time task. This is postulated to be due to instability of the alertness mechanism following sleep deprivation, due to changes in thalamo-cortical gating systems [Steriade 1990].

In parallel with the above findings, motor cortical excitability has been found to be attenuated after sleep deprivation, as assessed using transcranial magnetic stimulation over the motor cortex, with the measurement of motor evoked potential amplitude and latency over the thenar eminence [Manganotti 2001]. A reduction in motor cortex excitability with increases in motor threshold was seen following sleep deprivation. This is thought to relate to changes in cortical excitability, via the involvement of inhibitory GABA neurones.

Obstructive Sleep Apnoea

Obstructive sleep apnoea (OSA) is one of the commonest causes of sleep deprivation. Study 3 in this thesis examined patients with OSA in a small pilot study. The mechanism for the sleep deprivation of OSA is different to that of the total sleep deprivation used in studies 1 and 2. However, the effects of untreated OSA on steering and tracking performance, and the road traffic accident rate are similar to those of sleep deprived normal subjects.

Prevalence

The sleep apnoea syndrome affects about 0.5 to 1% of the UK adult male population [Gislason 1988, Stradling 1991]; the exact prevalence of the condition varies with the methods and criteria used for diagnosis. The syndrome consists of obstructive apnoeas in association with daytime sleepiness [McNamara 1993], and warrants treatment with continuous positive airways pressure treatment (CPAP). OSA is therefore a very common cause of sleep deprivation and has been extensively investigated. It is covered here in some detail for this reason, and to demonstrate the wide ranging consequences of sleep deprivation, in particular on driving performance.

Pathophysiology

OSA is due to recurrent collapse of the muscular pharynx with sleep onset. Upper airway muscle tone falls with sleep [Remmers 1978], leading to reduced pharyngeal patency, and precipitating upper airway collapse in subjects with an anatomically narrowed airway. Complete airway collapse leads to apnoea, and partial collapse (hypopnoea) usually leads to snoring. The airway occlusion results in

asphyxia, which leads to hypoxaemia and mild hypercapnia, in association with sympathetic activation. Following airway compromise, frustrated respiratory efforts against a collapsed upper airway can lead to pleural pressures as low as -80cm water. Arousal from sleep occurs after a variable time period, probably triggered by the detection of the increased respiratory effort by pleural and / or pharyngeal receptors [Gleeson 1990], and is associated with return of the normal tone of the pharyngeal muscles. This re-opens the airway, with return to a normal blood oxygen level.

Apnoeas can last from a few seconds to over a minute. As sleep resumes, recurrent airway collapse leading to further apnoeas can occur, and the process may be repeated hundreds of times per night in patients with severe disease. The cycle of repeated airway collapse, and brain arousal leading to airway re-opening leads to severely fragmented sleep, causing the dominant symptom of the sleep apnoea syndrome - excessive daytime sleepiness [McNamara 1993]. It is the collapsibility of the pharynx that leads to upper airway collapse, and the commonest cause of this is an anatomically smaller airway, most commonly due to obesity, with the deposition of excess adipose tissue around the neck [Rodenstein 1990].

Factors reducing pharyngeal muscle tone such as alcohol [Taasan 1981], sedatives [Guilleminault 1990] or muscle weakness [Briskin 1978, McBrien 1996] will contribute to OSA. The overwhelming factor in OSA is obesity, with a predominant upper body distribution.

Diagnosis

The obstructive sleep apnoea syndrome is diagnosed by the presence of recurrent upper airway collapse in association with daytime hypersomnolence. The disease is usually defined by an arbitrary number of apnoeas per hour of sleep. A wide

range of apnoeas per hour will lead to differing degrees of sleepiness in different subjects. There are several reasons for this - individuals have different drives to sleepiness and wakefulness, and differing arousal thresholds. Differing sleep and wake work patterns mean that the degree of sleep disruption in one subject causing significant daytime sleepiness may not necessarily cause significant problems in another. This means that overall, the number of apnoeas per hour of sleep correlates very poorly with daytime symptoms, the main reason for treating OSA [Cheshire 1992, Poceta 1992]. In general an arbitrary cut off of around 10-15 apnoeas per hour of sleep is likely to represent moderately severe disease.

A raised Epworth Sleepiness Score (ESS) [Johns 1991, Johns 1994, Johns 1992, Johns 1993] in conjunction with evidence of sleep disruption due to sleep related upper airway obstruction is required for the diagnosis of sleep apnoea. The ESS indicates subjective sleepiness, and is also a useful marker of treatment response.

A sleep study is needed to confirm sleep disruption due to upper airway collapse, and quantifies the amount and pattern of snoring, along with the degree of respiratory obstruction, and the severity of the consequent sleep disruption. Full polysomnography (PSG) includes sleep electroencephalogram (EEG) and electromyogram recordings (EMG), which allows confirmation of sleep stage and sleep fragmentation. This is not always considered necessary, and the PSG itself can cause significant sleep disruption. The demonstration of oxygen desaturation in association with upper airway collapse (which can be measured by surrogate markers, such as the pulse transit time [Pitson 1995, Pitson 1998]), and the apnoea-hypopnoea index is cheaper, quicker, easier to set up and analyse, and the clinical outcomes are the same - the so called 'respiratory polysomnogram' [Bennett 1998].

Treatment

OSA management depends on the severity of the condition and the patient's treatment preferences. Mandibular advancement devices (MADs) [Schmidt 1991, Ferguson 1996] may be useful for patients with mild to moderate disease. Continuous positive airways pressure treatment (CPAP) is the most effective treatment for severe obstructive sleep apnoea [Sullivan 1981]. It corrects the upper airway obstruction, abolishing sleep disruption, by acting as a pneumatic splint to the upper airway during sleep. Randomised controlled trials have shown improvement of daytime sleepiness with nCPAP [Engelman 1994, Engelman 1998, Jenkinson 1999], which is usually improved after the first night of treatment, and certainly after two weeks [Lamphere 1989].

Surgical treatments for OSA are recommended in only a very small selected group of patients, if at all. Nasal surgery to an obstructed nasal airway may be considered if nasal obstruction is thought to be the major site of upper airway obstruction, but only improves snoring, and not frank upper airway collapse [Heimer 1983]. Palatal procedures, such as uvulopalatopharyngoplasty (UPPP) are rarely recommended, as the likelihood of long term OSA resolution and absence of significant morbidity following the procedure is very small [Harmon 1989, Caldarelli 1986]. Gastroplasty is occasionally performed for very obese patients, and it is possible that this operation will become increasingly commonly performed [Summers 1990] with the increasing population prevalence of obesity.

Effects of OSA - Driving

Daytime sleepiness is a clear contributory factor to road traffic accidents [Horne 1995, Horne 1999], and OSA is the commonest cause of excessive daytime sleepiness [National Commission on Sleep Disorders Research Report 1993, Wu 1996, Cassel 1996]. OSA has been reported in up to 5% of commercial drivers [Young 1997, Strohl 1994]. Patients with sleep deprivation due to OSA have an increased road traffic accident rate, and this has been shown by simulated steering data (laboratory conditions) and real road accident data. A number of mechanisms are likely to contribute to the increased risk, but the exact aetiology of the driving impairment in OSA is unclear.

Driving is a complex task, involving the integration of visual, tactile and auditory information, with translation into a coordinated motor output involving speed control and alteration in lane position. It is therefore not surprising that the sleep deprivation and / or neurocognitive impairment of OSA (and other forms of sleep deprivation) leads to impaired driving. During driving, attention is divided between control of the vehicle (which involves tracking, the primary task), and a secondary visual search task, to look for obstacles and pedestrians and so on. This is the basis for most of the steering simulators from which laboratory data in OSA (and sleep deprivation from other causes) has been accumulated [Land 1995, George 1996, George 1997, Hack 2000, Hack 2001].

A number of studies have shown that steering simulator performance is impaired in untreated OSA compared to matched controls, and that simulated steering performance improves with nCPAP treatment, though not quite to that of matched controls after one month's treatment [George 1997, George 2001, Findley 2000,

Juniper 2000, Hack 2001]. This improvement is reflected in a reduction in the real road accident rate following CPAP treatment in several studies [Cassel 1996, Kreiger 1997].

George et al's 1996 study using a divided attention steering simulator showed that patients with OSA and narcolepsy were relatively more impaired on the task of tracking, than the visual search task, compared to matched controls. This suggests that the patients chose to concentrate on the easier, secondary visual search task, rather than on the more difficult tracking task, and indicates a potential impairment of the ability to integrate the two search tasks needed for driving simultaneously, in the sleep deprived states of OSA and narcolepsy [George Sleep 1996].

An anonymous questionnaire study by Hortsman et al established a correlation between the severity of OSA and the likelihood of an accident, showing a motor vehicle accident rate of 13 per million kilometres driven in patients with severe OSA (apnoea-hypopnoea index (AHI) >34), compared to a risk of 1.1 per million kilometres driven, in patients with milder disease (AHI 10-34). The accident rate was 0.78 in an age and sex matched control group. The vehicle accident rate fell from 10.6 to 2.7 per million kilometres driven in a group of 85 OSA patients following treatment with nCPAP [Horstmann 2000].

Hack et al's randomised controlled study used a placebo control arm (sub-therapeutic CPAP), and demonstrated a significant improvement in simulated steering in a group of patients with moderate to severe OSA treated with therapeutic CPAP for one month, compared to those treated with sub-therapeutic CPAP [Hack 2000].

Steering performance (as assessed by deviation from the centre steering position on the Oxford Steering Simulator, a divided attention steering simulator) deteriorated following sub-therapeutic treatment, but improved in those treated with therapeutic

CPAP. Hack's 2001 study assessed OSA patient performance on a simulated steering task, in parallel with patients intoxicated to the legal limit for alcohol (mean blood alcohol level 71.6 mg/dl), or normal subjects deprived of sleep for one night. Control data for the OSA patients was provided following CPAP treatment, and after no alcohol, or after a night of normal sleep for the alcohol intoxicated and sleep deprived groups respectively. All three groups were significantly impaired compared to their control state, with the impairment in the OSA patients being more similar to that due to sleep deprivation, than that due to alcohol intoxication [Hack 2001].

Logistic regression analysis has been used to determine whether steering simulator performance can accurately predict driving performance on the real road, to help determine the usefulness of simulated steering tests in determining whether or not patients with OSA are fit to drive. Older age, female sex and self-reported alcohol consumption were found to most strongly negatively predict performance. Using this type of analysis, the number of off-road events was found to be independently associated with a previous road traffic accident; the Epworth Sleepiness Score was independently associated with episodes of falling asleep at the wheel and near miss accidents. This regression model was able to predict 100% of patients who did not have an accident, but could only identify 10% of those who did, suggesting an independent relationship between OSA patient real road driving ability and steering simulator performance. This suggests that computer steering simulators alone are not accurate enough to predict whether or not a patient with OSA is safe to drive on the real road [Turkington 2000, Turkington 2001]. However, real road accident data supports simulated steering data, confirming the higher accident rate in OSA patients. Improvement with CPAP has been confirmed by objective analysis of driver data in

Canada (Ontario Ministry of Transportation Motor Vehicle Collision data), where this information is available to the general public [George 2001].

The reduced road traffic accident rate with successful treatment of OSA is borne out by Findley et al's 2000 study, showing a reduction in objective reports of road traffic accidents in 36 subjects treated with CPAP over 2 years. This study showed a decrease of 0.07 crashes per driver per year, with no fall in accident rate in 14 patients who did not accept CPAP treatment [Findley 2000]. George et al's 2001 study showed that successful CPAP treatment prevented 75 serious road accidents in 210 patients during 3 years of treatment [George 2001].

Calculations have been made to determine the number of vehicle accidents that would be prevented by successfully treating severe sleep apnoea in the United States [Findley 2001]. It is estimated that treating 500 patients for 3 years would prevent 180 serious accidents, and this would result in the prevention of around 36 serious injuries; since 20% of reported crashes result in serious personal injury. It is estimated that the prevention of this number of serious accidents and injuries would save around US\$ 1 million per year.

Further studies have identified additional factors making patients with sleep deprivation due to OSA more prone to impaired driving. Juniper et al studied OSA patients and matched controls during a series of simulated drives, during which the whole of the oncoming road was visible, or only the near, or only the far portion was visible [Juniper 2000]. Patients with OSA were significantly impaired compared to matched control subjects on all types of drive, but were particularly impaired on the drives in which only a small part of the road ahead was visible to guide steering. This suggests that patients with OSA may be more impaired than normal subjects when a limited part of the road ahead is visible, such as driving in fog. This may reflect an

impairment of visual processing in sleep deprivation as a contributing factor to the steering impairment seen.

Driving Regulations

In the UK, the Driver and Vehicle Licensing Agency (DVLA) states that drivers must cease driving if the driver is excessively sleepy, whatever the cause of the sleepiness. Patients with OSA must inform the DVLA of their diagnosis and cease driving until treated. Driving can recommence once the disease is adequately treated. These regulations apply to Group 1 licence holders (ordinary licence). Group 2 drivers (public service and heavy goods vehicles) should cease driving until it is confirmed by a specialist that their condition is adequately treated (<http://www.dvla.gov.uk/medical.aspx>).

Functional Magnetic Resonance Imaging

Background

Functional brain imaging is the technique used to define the dynamic changes associated with brain activation, which may be motor, sensory or cognitive. There has been great interest in the advance and development of this brain imaging technique, and of its potential applications, over the last 10 to 15 years. The discovery of a change in local magnetic resonance (MR) signal around rat cerebral cortex veins, depending on the concentration of inspired oxygen, by Owaga and co-workers in 1990, laid the foundations for fMRI imaging. Owaga proposed that the MR signal reduction seen at lower inspired oxygen concentrations was due to the magnetic susceptibility of the blood [Owaga 1992], and ischaemia models produced similar findings. Subsequent human studies showed that brain activation lead to magnetic resonance signal increase, indicating an increase in local magnetic field inhomogeneity ($T2^*$). This could be modulated by the presence of intravoxel deoxyhaemoglobin levels, and suggested that blood oxygenation increased with activation, and that this could be used for brain mapping [Bandettini 1997].

Blood oxygen level dependent (BOLD) signal is generated because the magnetic field gradients produced by deoxyhaemoglobin reduce magnetic resonance signal. Brain activation is associated with a drop in the local oxygen extraction fraction (OEF), because of a relative increase in local cerebral blood flow. This leads to a fall in deoxyhaemoglobin concentration, which in turn leads to an increase in MR signal. The BOLD effect is not a direct measure of neuronal activity, and the mechanisms leading to increased local cerebral blood flow in association with synaptic activity are not fully understood. Neurotransmitter release and action

potential firing occur in the absence of additional energy; it is the removal of neurotransmitters and the restoration of ion gradients, which require energy. In addition, cerebral blood flow is not directly correlated with neuronal firing.

Magnetic resonance is the property of nuclei to have a magnetic 'moment', in the presence of a magnetic field. A nucleus excited in a magnetic field emits energy, at a frequency proportional to the strength of the applied magnetic field. Brain MR depends on the imaging of resonating brain nuclei, i.e. protons in brain water, which resonate in the presence of small magnetic field gradients, which are superimposed on the larger magnetic field of the imaging magnet, typically 1 to 1.5 Tesla (the unit of magnetic field strength). Spatial resolution is possible with the detection of the relative frequencies of the individual molecules by differences in their resonant frequencies.

Atomic nuclei have nuclear 'spin', and can behave as magnetic dipoles and assume either a high (behaving as if orientated against the applied magnetic field) or low energy state (behaving as if aligned with the magnetic field) in a magnetic field. Nuclear spins are excited from a low to a high energy state by the application of a magnetic field. MRI can detect their 'relaxation' back to a low energy state, by the detection of radiofrequency energy. The relaxation time is a constant, exponential process, the so called 'spin-lattice relaxation time', or T1 (the lattice is the environment within which the nuclei spin). Excited nuclei revert back to the 'relaxed' or lower energy state by regaining equilibrium with the applied magnetic field, over three T1 time periods.

Contrast is generated from tissues by the application of differing radio-frequency pulses. If excitation pulses are applied quickly (within the relaxation time of the nuclei), then the proportion of nuclear spins that can be excited is reduced, with

a subsequent reduction in resonance signal. The repetition time (TR) in the pulse sequence determines the frequency of pulse delivery. A shorter TR (i.e. faster rate of delivery of radiofrequency pulses) will lead to increased signal in those parts of the brain with a shorter relaxation time (T1) e.g. brain tissue, relative to those parts of the brain with a longer T1, e.g. cerebrospinal fluid.

Contrast can be generated by the alteration of three parameters in the pulse sequence. The energy per pulse of the radiofrequency excitation or 'flip angle' can be altered. The flip angle is the notional number of degrees of extent to which the net magnetisation spins the nucleus. The larger the flip angle, the longer the relaxation time. The rate at which radiofrequency pulses are applied also affects the contrasts seen. The shorter the TR, the less time for nuclear relaxation. The time delay to excitation (TE) will also alter the contrast.

Haemodynamic Response

Increased energy expenditure at neuronal synapses leads to increased regional cerebral blood flow, which probably results from increased uptake of glutamate, the main excitatory neurotransmitter [Magistretti 1996]. The BOLD response is fundamental to fMRI. It results from increased cerebral blood flow and therefore a relative excess of oxygenated blood, associated with neuronal excitation. The BOLD response is seen in the grey matter only, where synapses are found; the recorded signal represents synaptic activity, with a linear relationship between neuronal activity and the size of the BOLD response [Rees 2000].

Global and regional blood flow is under many controls, including sympathetic and hormonal mechanisms. Local regulators, such as hydrogen ions and carbon

dioxide act via nitric oxide, a potent cerebral vasodilator. Circulating factors such as serotonin, locally produced prostaglandins and drugs, such as theophyllines, can also modulate cerebral blood flow. Age related changes are also seen, with attenuation of blood flow with neuronal activation in older adults [Hock 1995].

BOLD signal is generated from the effect of the application of a magnetic field on haemoglobin. Oxyhaemoglobin is diamagnetic, whilst deoxyhaemoglobin is paramagnetic [Pauling 1936]. Paramagnetic materials have increased magnetic flux (i.e. the magnetic field is attracted to them), which results in changes in the applied magnetic field. As a result, deoxygenated blood increases the magnetic susceptibility of blood vessels relative to the surrounding brain tissue. This leads to the formation of local magnetic field gradients, which in turn cause a locally decreased tissue relaxation time in the tissue water surrounding the blood vessels. Brain activation leads to an increase in the local cerebral blood volume, with an associated increase in oxyhaemoglobin concentration, and a corresponding decrease in deoxyhaemoglobin concentration in the areas of increased neuronal activity [Ogawa 1992]. This is the basis of the BOLD response.

The haemodynamic response to neuronal activation is biphasic, with an initial dip (a hypo-oxic phase, lasting 0.5-1 seconds), followed by a longer hyper-oxic phase. The BOLD signal response is generated from the longer hyper-oxic phase. This phase reaches a plateau about 5-8 seconds after the onset of the applied stimulus, with an increase in blood flow of 50-70% [Liu 2000], providing physiological habituation does not occur. This increase is much greater than the increase in local oxygen utilisation, which increases by only 5-20%; hence the ratio of oxy to deoxyhaemoglobin increases, leading to increased signal intensity. Following

cessation of the stimulus there is a return of the BOLD response to baseline, which may be associated with an undershoot, during which the response remains negative for several seconds, and from which it slowly recovers over the course of a few seconds. Therefore overall, following the application of a short stimulus, the BOLD response takes place over 12-16 seconds [Bandettini 1997].

The application of any stimulus e.g. a potent visual stimulus, such as a flashing chequerboard can cause increases in regional brain perfusion of 50-70%. This leads to an increase in capillary oxygenation, increased blood oxygen delivery, and lowered deoxyhaemoglobin levels. Deoxyhaemoglobin reduces magnetic resonance signal, leading to positive signal changes, which are typically 2 to 3% of baseline signal. The magnitude of the BOLD response depends on the size and nature of the biological response as well as the magnetic field properties.

fMRI Experimental Design

Specific hypotheses, with an expected neuro-anatomical activation must be generated prior to the experimental study. Scan analysis involves the use of a General Linear Model (GLM), where predicted and expected responses are mapped. A 'block design' is a standard experimental technique, during which a stimulus is presented during a relatively long alternating period (e.g. 30 seconds), within which the same cognitive state is presumed to be maintained [Friston 1999]. This may be as simple as a 'rest' and 'active' state, with rest defined as relative to the active state. In this situation the shape of the haemodynamic response function can be assumed to be linearly related to the active periods.

Paradigm Design - block design

In a block task paradigm, one set of stimuli is presented in a discrete time, followed by another stimulus. The data is acquired during the 'block', and the activation during different time blocks is compared. Differing activity in differing regions can be compared between conditions, with the use of parametric and multifactorial designs. GLM analysis in this context depends on the assumption that the BOLD fMRI signal acquired is a direct measure of the haemodynamic response at that time. The model is generated from the factors which are expected to contribute to the signal acquired and many effects can be modelled for. For each voxel, the stimulus response is calculated by representing each time point by a linear equation. Thus for each time point in the data set, the BOLD response is the sum of the haemodynamic signal at that time, plus any variance generated by signal noise.

Strengths and weaknesses of fMRI

fMRI has many potential applications (as described above) and has been used in many imaging studies over a short period of time since its inception. One of the many potential weaknesses of fMRI as a research tool are the assumptions made about brain blood flow and neuronal firing, which form the basis of the BOLD signal response. fMRI brain activation is only an indirect measure of brain activation, and these assumptions include the fact that neural activation correlates very closely with changes in local cerebral blood flow and thus blood oxygenation levels, and that deoxy- and oxyhaemoglobin behave differently in a magnetic field. In addition there are limitations of the linear transformation methods used in the analysis of the fMRI response, as signal is averaged over a brain area of several voxels and a time period of several seconds. It is also assumed that one paradigm e.g. testing tracking will lead to

the same activation as another similar tracking paradigm. In addition the imaging techniques and experimental paradigms and data produced are based on group averaged data, with the assumption that all subjects respond in the same way to a stimulus. However huge advances have been made with the advent of fMRI, with it's ability to provide high resolution images with good spatial and temporal definition, with the ability to make repeated studies, because of it's relative safety. fMRI study results must be interpreted in the light of some of the potential limitations discussed above.

fMRI Analysis

General

Data is analysed voxel by voxel, following a number of steps of pre-processing, using standardised computer software programmes. The GLM is a multiple regression model, which runs a correlational analysis - correlating each voxel's time course with the time course of the model. Voxels (a three dimensional pixel volume) showing signal change varying with the stimulus are identified across the acquired data set. The data must be prepared prior to analysis, to minimise artefacts and to increase the signal to noise ratio. Potential analysis problems include small measured signal changes, so only relative signal changes can be assessed, and because a very large number of voxels are assessed simultaneously, there is a potential problem of multiple comparisons. For this reason, the significance threshold is much more stringent than in standard statistical tests, in proportion to the number of multiple comparisons. Data 'filtering' increases the signal to noise ratio, and post processing motion correction methods remove subject head movement artefact. High-resolution structural anatomical MRI data is also collected, on which to 'map' the functional data.

fMRI Analysis - Specifics

The aim of fMRI analysis is to detect those parts of the brain which show increased activity corresponding with stimulus application. A single brain volume (or image) is composed of voxels, each of which has an associated series of time points.

The data must be pre-processed and prepared for statistical analysis. A number of steps are employed:

1. The raw data is converted to volumes (images or scans) as the data is obtained as a digitised signal from the MRI receiver coil. This requires a Fourier transformation.
2. Slice timing correction - each slice in each volume is acquired at a slightly different time point. Adjustment must be made so that all the data in one volume appear to have been collected at the same time point.
3. Motion correction - each volume is transformed using rotation and translation so that all data volumes are aligned with each other.
4. Each volume is spatially filtered (blurred) to reduce noise. This increases the signal to noise ratio.
5. Intensity normalisation is applied - this adjusts each volume's intensity so that all voxels have the same mean intensity. This reduces the effects of global signal intensity changes over time.
6. Temporal filtering is applied, removing the unwanted components of a voxel's time series, without reducing the signal of interest. Components can be removed which vary more quickly or slowly than the signal of interest, helping to reduce noise. Low pass temporal filtering removes high frequency noise.
7. Head motion correction - rotation and translation in x, y and z planes is corrected.

Statistical Analysis

Statistical analysis determines which voxels are defined as being activated by the applied stimulation. The output is a statistical map showing which brain areas are activated in response to the stimulus. Each voxel's time series is analysed independently of the others (univariate analysis), but a multivariate analysis (using spatial information from neighbouring voxels, during cluster based thresholding) is used in the final stages of GLM analysis.

A model of the expected response to the applied stimulus is generated, and compared with the data obtained. The 'fit' of the model to the acquired data is assessed. A good fit with the data indicates that the brain activation was probably caused by the applied stimulus. A statistical map is then derived from the GLM, this undergoes thresholding, to decide at what level of significance the parts of the brain were activated. A significance level (p) threshold is selected, and applied to each and every voxel in the statistical map. Multiple comparisons, due to the large number of voxels in the brain, mean that a Bonferroni correction is needed - the significance at each voxel is divided by the number of voxels, which corrects for the problem of the large number of comparisons being made. More complicated models include variable numbers of explanatory variables (EVs), which explain the different processes within the data. The GLM is represented as a design matrix.

All of the GLM parameters are grouped together into a vector (β), with all the modelled data time courses grouped together in a matrix. The model is then fitted voxel by voxel to the data, and an estimate of 'goodness of fit' is generated for each voxel and column in the GLM. A good fit will generate a high parameter estimate (PE), images which are the best fit of the model to the data. The PE is converted to a T value, by comparison with the uncertainty in its estimation. $T = PE / \text{standard error}$,

and is a measure of how different the PE value is from zero. If the PE is low relative to its estimated uncertainty, then the model fit is not significant, and vice versa. The standard error image is directly related to the variance (signal noise) in the data. The T image is converted to a probability statistic (p) or Z score (a measure of p standard deviations) by standard statistical transformation. In practice, a threshold of $p < 0.01$ or 0.05 is chosen, which corresponds to a threshold t value, and all values whose t result passes the threshold are then selected. The output image is therefore essentially an image of Z statistics, showing how closely each voxel is related to each explanatory variable. Voxels of differing significance are shown in colour (ranging from red for lower significance, to yellow for highest significance). 'Contrasts' can be set up to examine whether or not one EV is more or less relevant to the data. All EVs must be independent of each other.

Thresholding the Z or T statistic map allows the brain activation at different levels of significance to be determined. There are several ways in which to do this, including setting a chosen p value, and applying it to each voxel in turn. Combining images and statistical data from a number of subjects is used to identify common activations in a group of subjects and also to increase the statistical power of low-level activations. For this to take place, the brain images from all subjects must be aligned into a common space. Statistical methods can then be applied across the subjects, using fixed-effects and random-effects analyses. A fixed-effect analysis assumes that all the subjects in the group show equal brain activation to the stimulus, and only takes into account within-session errors. Random-effect analysis includes between session errors, and is therefore valid for the whole population from which the group of subjects was drawn. Random effects results tend to be more conservative.

Registration is used to align the acquired functional data to standard high-resolution structural images. This enables activations to be interpreted anatomically, and functional assessments to be made. Registration involves transformation, translation and rotation to ensure good registration between images. Before registration can take place, processing of the structural brain image must occur. 'Brain extraction' involves the removal of non-brain structures, as it is these structures that can vary significantly between individuals. Data is then transformed into 'standard space'. This is usually the system of coordinates proposed by Talairach and Tournoux, enabling activations to be compared between subjects, and compared with anatomical landmarks from a standardised database. The Talairach and Tournoux brain atlas is a simple brain map, constructed from a detailed post-mortem study of one subject. Anatomical areas are defined by standard brain landmarks, enabling common brain structures to be identified by standardised coordinates, related to eight specific landmarks. The MNI (Montreal Neurological Institute) brain is a similar 'standard' brain. Both maps are used in the same way to define areas of activation to standardised coordinates or anatomical landmarks. MEDX software (<http://medx.sensor.com/products/medx/index.html>) can then be used to assess clusters of activation.

Brodmann Areas

Korbinian Brodmann (1868-1918) was an anatomist who divided the cerebral cortex into subdivisions of numbered regions, to aid anatomical mapping of specific areas. These divisions are based on cell types, arrangements and staining properties, and are used today to allow mapping of specific brain areas.

Imaging Constraints

Signal noise comes from many sources, and is a major constraint of fMRI imaging. Head and therefore brain movement, from both respiration and the cardiac cycle, and the subject's own movement (even if minimised with tape and head padding), contribute to signal noise. Respiration causes shifts in the static magnetic field, and even when stabilised, pulsatility of the CSF and brain parenchyma associated with the cardiac cycle causes interference. A high signal field strength (i.e. 1.5 Tesla) helps to reduce signal noise.

The fMRI experiment is carried out with the subject supine, in a small, enclosed space, in the presence of significant noise. This can present a number of problems. The noise of a 3-4 Tesla magnet can reach 120 dB. Subjects therefore need protection with earplugs and external headphones. During the experiment, there must be simultaneous presentation of the stimulus, which must be optimal and visible to the subject, with the collection of the MRI signal generated. The subject's available visual field may be limited to 15-20°, which, in addition to the small space within the magnet, may lead to claustrophobia in some subjects. The stimulus image is projected to the subject, and viewed with prism glasses. The subject is monitored by video, and continuous pulse and oxygen saturations are recorded. Subject boredom and sleepiness with repetitive stimuli is a potential problem. Scanning time can be relatively long because of the need to allow time between stimulus application and the scanning time of the whole brain, with recovery of the haemodynamic response.

The potential dangers of MRI imaging relate to pacemakers (which use an externally applied magnetic field to switch to operating mode), and other implanted magnetic objects, which could move within the magnetic field. The presence of metal

objects such as teeth braces, and metal hair clips can disrupt the magnetic field and the subsequently recorded signal.

Functional Brain Imaging and Sleep

Human functional brain imaging studies using positron emission tomography (PET) have shown changes in global and regional cerebral blood flow with sleep. Regional changes in cerebral glucose metabolism have also been demonstrated, with a reduction in cerebral blood flow with slow wave sleep, particularly in the prefrontal cortex. This correlates with Horne's hypothesis of prefrontal cortex susceptibility to sleep deprivation [Horne 1993].

The effects of sleep deprivation can be attributed to reductions in slow wave sleep [Horne 1993]. The precuneus (situated on the medial aspect of the parietal lobe) is one of the main areas deactivated during slow wave sleep [Andersson 1998]. This area of the association cortex has particularly high activity during wakefulness.

The impaired neurocognitive performance and driving impairment seen with sleep deprivation suggests a generalised decrease in brain function, which may be accompanied by reduced brain activation. The thalamus is particularly involved in attention and levels of alertness. PET studies using 18 fluorine-2-deoxyglucose (18-FDG), have shown a reduced global cerebral metabolic rate of glucose during the performance of serial addition and subtraction tasks, following 85 hours sleep deprivation [Thomas 2000]. In this study, subjects were scanned at 24 hour intervals during the period of sleep deprivation, with polysomnographic monitoring to ensure wakefulness during the scan period. Following 24 hours sleep deprivation, reduced brain activation was seen in the thalamus, prefrontal cortex and posterior parietal cortices. There were parallel reductions in alertness and cognitive performance.

fMRI studies have examined the relationship between sleep deprivation and brain activation, with varying task complexity and familiarity. Brain activation is

known to increase with task complexity, and decrease with task familiarity. In a series of brain fMRI studies, Drummond et al have shown that task dependent reductions and increases in brain activation occur in differing brain regions with sleep deprivation [Drummond 1999, Drummond 2000, Drummond 2001, Drummond 2004, Drummond 2005]. Serial subtraction tasks following 35 hours sleep deprivation, showed reduced activation in the posterior parietal cortices, bilateral prefrontal cortex and premotor areas, compared to following normal sleep. There were also parallel reductions in performance.

Arithmetic tasks are known to activate the prefrontal cortex and parietal lobes (brain regions particularly involved in working memory), and are also particularly susceptible to the effects of sleep deprivation [Thomas 2000]. However, brain fMRI verbal learning tasks performed post sleep deprivation show different brain responses, with increased frontal lobe activation compared to following normal sleep. The authors conclude that the brain's response to sleep deprivation may be cognitive task, rather than brain region specific [Drummond 2000, Drummond 2001]. A divided attention task, combining a verbal learning task and an arithmetic test has also been used [Drummond JSR 2001]. Increasing the difficulty of the arithmetic task reduces the performance of the verbal memory task. This is postulated to be because the processes compete for resources, as attention is divided between the two tasks. Total sleep deprivation in this context reduces performance further, as subjects become impaired in switching between the two tasks, with unequal performance deficits on the two tasks. Increased activation of brain areas involved in attention (the anterior cingulate and right prefrontal cortex) was seen following sleep deprivation. Activation of these areas may represent the recruitment of additional cognitive resources, aiming to preserve performance following sleep deprivation.

Additional studies by Drummond et al have assessed the extent of the cerebral compensatory response to task difficulty following up to 35 hours sleep deprivation. Performance on a logical reasoning task was unimpaired following sleep deprivation, and was associated with linear increases in cerebral activation, which correlated with increasing task difficulty after normal sleep. Following sleep deprivation, stronger linear responses were seen, in the bilateral parietal cortices, bilateral temporal cortex and dorsolateral prefrontal cortex. The authors conclude that task difficulty facilitates the cerebral response to the task [Drummond 2004]. This finding is confirmed by Chee et al who have studied the effects of sleep deprivation on working memory using fMRI. Following sleep deprivation, performance was preserved on the more complex task, but reaction times were slower. Reduced activation of the posterior cingulate and frontal cortex was seen post sleep deprivation [Chee 2004].

The anterior cingulate is thought to be involved with the ‘online’ monitoring of performance errors, particularly in situations where errors are more likely, such as following sleep deprivation [Carter 1998]. This may explain the increased anterior cingulate activation seen following sleep deprivation. The right prefrontal cortex is activated during attention requiring tasks [Cabeza 2000], and increased task attention (to perform at the same level), is needed in the reduced alertness state of sleep deprivation.

The mechanisms for the alteration in the cerebral and behavioural responses to sleep deprivation are unexplained, but the regional variation in brain activation seen is thought to relate to regional specialisation to specific cognitive demands [Drummond 2000, Drummond 2005]. However, it is clear that the brain is able to respond to the effects of sleep deprivation by the recruitment of additional brain regions, related both to the specific task being employed, and the generalised need for increased attention.

This highlights the plasticity of the brain, and its ability to adapt, even after the effects of long periods of sleep deprivation.

Further fMRI Studies

The resting or 'passive' state

A number of fMRI studies have shown task dependent increases and decreases in brain activity, in association with a 'passive state' such as passive viewing, or resting with the eyes closed. This raises the possibility that a baseline, or 'resting' brain state may exist, from which the brain is activated during transition to the 'active' state. Reductions or 'deactivations' in brain activity are thought to be related to additional physiological mechanisms, which remain incompletely understood, and seem to be task independent, varying little in their location across a range of activities [Shulman 1997, Mazoyer 2001]. This suggests that some brain regions perform very general, non-specific functions and are active across a number of tasks. It also suggests that there might be an organised brain system that is suspended during the performance of active tasks, but is present as a 'default' brain state.

In the resting state (i.e. lying quietly, with eyes closed in the MRI scanner), there is a close relationship between local cerebral blood flow and brain oxygen utilisation. There is spatial uniformity of the oxygen extraction fraction across the brain in the resting state, despite large variations in local oxygen consumption and blood flow within the grey and white matter regions of the brain. When a resting subject closes his eyes, areas of increased oxygen extraction fraction (OEF) (apparent reduced activation) are seen primarily in the extra-striate visual cortex, suggesting that for the visual cortex, the baseline state might be associated with having the eyes open. Eye opening increases blood flow in these areas [Raichle 2001].

The brain is about 2% of total body weight, but accounts for 20% of the body's oxygen consumption [Clark 1999]. One explanation for the high resting

cerebral blood flow is that up to 50% of the brain's baseline energy consumption is related to the maintenance of the resting state, and the synaptic transmission involved in this [Schwartz 1979, Mata 1980]. A number of studies have assessed brain activation in the resting state and suggest that a network of brain areas is active during a resting, passive state [Shulman 1997, Thompson 1990, Mazoyer 2001]. Activation in these areas is reduced during change to an active state, and the presence of sustained activation during an apparent resting state suggests a level of baseline neural activity / information processing. This suggests that an equilibrium exists between the metabolic requirements of neuronal activity of the active brain, and the level of blood flow in that particular area of the brain.

EEG, lesional and imaging studies have shown that the posterior cingulate cortex is involved in the assessment of the surrounding environment and with memory. It is also involved in monitoring eye movements [Olson 1993]. Additional studies have shown that this area is also involved in subject orientation and spatial awareness [Murray 1989] and is thought to be a 'tonically active' brain region. Along with the adjacent precuneus, the posterior cingulate cortex continuously gathers information about the surrounding environment [Raichle 2001]. There is an evolutionary hypothesis for this 'resting brain state'. This is that the detection of predators should be immediate, and not require the intentional diversion of additional attentional resources, but that these monitoring resources should be continuously available and allocated automatically. The medial prefrontal cortex also shows decreases in activity with focused attention, and this is thought to relate to an interplay between its role in cognitive processing and the emotional state of the subject [Simpson 2001].

PET studies have demonstrated that the anterior cingulate cortex is active in tasks with high cognitive and attention requirements, including tasks such as verbal fluency [Petersen 1988]. Neglect can occur with anterior cingulate lesions [Watson 1973]. Attention is closely related to motivation; there is a strong motivational component to any activity involving sustained attention. The anterior cingulate is thought to be closely involved with both motivation and attention [Vogt 1992]. The posterior parietal cortex is also involved in attention to visual stimuli to a specific location. fMRI studies show temporo-parietal junction (TPJ) activation in association with attention towards specific visual cues, both in voluntary orientation to maintain attention to a specific target location, and in re-orientating towards visual targets appearing at unattended locations [Corbetta 2000]. In addition, fMRI studies have shown activation of the right TPJ with the precuneus in target detection.

Functional imaging studies have defined a network of brain areas involved in visual attention. These areas comprise the posterior parietal cortex around the intra-parietal sulcus, and the frontal lobe (including the anterior cingulate and supplementary eye fields). These brain areas involved in the control of visual spatial attention, and are also those involved in the control of eye movements [Nobre 2001]. Visual spatial attention can be altered under voluntary or involuntary control. Brain imaging studies have shown that the mechanisms for these are likely to be the same [Friedrich 1998].

Visuo-Motor Tracking

Tracking, the ability to adapt a motor response to a changing visual input, is one of the fundamental skills used during driving. It is controlled by a number of complex, integrated mechanisms. Visual feedback is one of the key elements in the generation of smooth tracking manoeuvres, and is postulated to be under cerebellar control.

Successful driving involves the coordination of a number of motor and sensory skills. Many brain areas, with complex relationships are integral to this. The cerebellum has an important role in the control of coordinated movements [Bastian 1996, Muller 1994]. It is central to the control of limb joints and control between two limbs [Serrien 2000], and between the eye and hand in tracking tasks [Van Donkelaar 1994, Van Donkelaar 1997, Vercher 1994, Vercher 1996].

Functional imaging techniques have confirmed the role of the cerebellum in the control of visually guided movements [Jueptner 1996]. Miall et al have studied fMRI activation of the cerebellum with varying degrees of hand / eye coordination, showing increased cerebellar activation with independent tracking, compared to coordinated hand / eye tracking [Miall 2000, Miall 2001]. These studies have shown improved tracking performance with increasing coordination of eye and hand movements, and that the best tracking performance is achieved when the target for eye tracking anticipates the target for hand motion by 50-100 milliseconds, i.e. the ocular system slightly anticipates the manual system.

Miall et al's 2001 fMRI study showed that coordinated tracking also leads to activation of areas in the extrastriate visual cortex, the precuneus and areas in the ventral premotor region and frontal cortex [Miall 2001]. Precuneus activation during

tracking is thought to relate to the subjects' use of visual cues, as precuneus activation has been reported in association with visuo-spatial processing [Grafton 1992, Roland 1995, Fletcher 1996, Ghaem 1997]. Further studies have shown that hand tracking also activates area V5 / MT, which is integral to the detection of coherent visual motion. This is likely to relate to reciprocal connections between several motor areas related to movement performance (motor, premotor, striate and extra-striate) and the integration of visuospatial control mechanisms, probably through the visual control of forelimb movement [Oreja-Guevara 2004].

The neural correlates of driving have been described using fMRI. The brain areas activated reflect the integration of visuo-motor tracking skills and motion detection, all of which must be optimal for successful driving. A number of brain areas are activated, including areas in the occipital and parietal lobes bilaterally and the middle temporal area [Walter 2001].

Visual Motion Detection

The detection of coherent motion amidst incoherent motion, and the ability to judge the direction and speed in which objects are moving is of fundamental importance to driving [Raymond 1994, Gros 1998, Chen 1998].

fMRI and electroencephalogram (EEG) studies using random dot kinemetograms (RDKs) have established the role of the magnocellular pathway in the perception of coherent visual motion. Coherent motion is known to activate the middle temporal (MT) brain area, located at the parieto-temporo-occipital boundary. Primate single cell recording studies have demonstrated the presence of motion sensitive neurones in multiple visual areas of the dorsal pathways, projecting from the primary visual cortex (V1) through visual cortex area V5 and area MT, to higher visual areas within the parietal lobe. EEG and fMRI studies have shown activation of these areas during visual registration of coherent motion [Shalden 1996]. fMRI studies of biological motion also show activation in the anterior cerebellum [Grossman 2000]. The cerebellum is known to be involved in cognitive tasks, particularly those that involve judgements about whether or not motor activity is present [Fiez 1996]. Patients with cerebellar lesions perform poorly on tasks involving motion perception [Nawrot 1995].

fMRI studies have shown that processing of coherent visual motion is associated with activation of a number of extra-striate brain areas, in particular the occipital ventral surface, the intraparietal sulcus and the superior temporal sulcus, in addition to area V5 of the visual cortex [Braddick 2001]. Braddick et al have also found cuneus activation in association with coherent motion, but no activation of primary visual cortex areas V1 and V2. The visual cortex is organised into many

different specialised areas, spanning both cerebral cortices, numbered V1 to V8, all of which have been examined using fMRI [Serenio 1995, DeYoe 1996].

Functional imaging studies using fMRI show brain activation with motion to, as opposed to motion away from the observer. Activation is seen in the lateral inferior occipital cortex bilaterally, and in the right lateral superior occipital cortex, in areas that do not extend into area V5 [Wunderlich 2002]. The authors suggest that the early attentional and perceptual mechanisms needed for this type of visual processing are in the extra-striate visual cortex, in early visual processing areas.

Visual information is processed in parallel by two neural pathways from the retina to the visual cortex. These pathways remain segregated between the retina and input layers of the visual cortex, with two streams projecting to separate areas of the visual cortex. The ventral stream projects to the temporal cortex and is predominantly involved with providing information about the surface properties of objects, including colour and shape, enabling object recognition. The dorsal stream, which projects to the parietal cortex, provides information about the spatial properties of objects, including their motion, enabling object localisation.

In humans, visual information from the retina projects to the primary visual cortex (V1) by two linked, but independent pathways, the magnocellular and parvocellular pathways. The magnocellular pathway is more sensitive to low spatial frequency information than the parvocellular pathway, which is relatively more sensitive to high spatial frequency information, and stationary or slowly moving targets. Parvocells have low temporal resolution and process information used for form and wavelength discrimination. These cells project to areas of V1, to form the ventral stream, which terminates at the inferotemporal cortex. The magnocellular pathway contains cells which are sensitive to low spatial frequencies, flickering and

moving stimuli. They have high temporal resolution and process motion, depth and spatial information. Magnocells are large, with thickly myelinated axons, enabling high conduction velocities for the detection of rapid change. Coherent motion detection is the ability to detect motion, and depends on input from the magnocellular pathway. This pathway projects mainly to the dorsal stream of the visual cortex, terminating at the posterior parietal cortex. The pathways are segregated at the lateral geniculate nucleus (LGN), which is in the thalamus [Livingstone 1988, Maunsell 1983].

Random dot kinemetograms (RDKs) provide a measure of 'motion coherence threshold', the ability to detect coherent motion in an array of randomly moving dots, and are a validated method with which to measure magnocellular function [Talcott 1998, Talcott 2000, Cornelissen 1995, Cornelissen 1998]. RDKs consist of a visual stimulus composed of moving dots: a proportion of the dots move with a motion vector that is coherent over time, whilst the remaining dots randomly change their direction of movement over time, i.e. they move with Brownian motion. An individual's motion coherence threshold is the lowest proportion of dots that are needed to move coherently for the subject to correctly identify the direction of coherent motion from within the array of randomly moving dots. A high motion detection threshold indicates dysfunction of the magnocellular pathway and / or areas of the visual system receiving input from this pathway, as it is this pathway that is sensitive to flicker and motion [Talcott 1998].

The middle temporal (MT) cortical area is strongly served by cells from the magnocellular pathway, and single cell recording studies from this area have shown activity in response to random motion stimuli such as RDKs [Britten 1992, Talcott 2000]. Lesion studies in macaque monkeys have shown that defects in the

magnocellular pathway lead to motion blindness [Schiller 1990]. The sub-divisions of the human visual cortex have inter-subject variability in location, and this also applies to the middle temporal cortical area. Mapping studies using PET have identified the position of V5 / MT in 11 normal subjects, and the range of variability in position between subjects [Hasnain 1998, Watson 1973]. Across a number of mapping studies, variation of 4 to 8mm has been described for mapping a specific brain area, between subjects [Hunton 1996, Watson 1973, Ramsey 1996].

Attention is needed for successful visual processing, and there is evidence of a role for the thalamus in mediating interactions between attention and arousal mechanisms. Attention is modulated by arousal, and correlations between performance of attentional tasks and level of arousal are reported [Babkoff 1991]. However, the relationship is non-linear, with attention improving with moderate increases in arousal, but dropping off as high arousal levels are reached [Easterbrook 1959]. The neural correlates for arousal and attention are distinct, but are mediated by thalamic input.

Aims and Hypotheses

Hypotheses for study:

1. Sleep deprivation in normal subjects leads to impaired coherent visual motion detection with altered activation of the brain areas usually activated during this skill.
2. Sleep deprivation in normal subjects leads to impaired tracking and simulated steering, with altered activation of the brain areas usually activated during this skill.
3. Coherent visual motion detection as assessed by a random dot kinemetogram (RDK) is impaired following sleep deprivation, and is unimpaired following normal sleep.
4. The sleep fragmentation of untreated OSA is associated with impaired tracking, and leads to altered fMRI activation of visual cortex areas usually activated in association with this skill.
5. The altered brain activation of the visual cortex in untreated OSA improves with successful CPAP treatment, which also improves tracking and simulated steering.

Hypotheses 4 and 5 were established after preliminary examination of the data examining hypotheses 1 to 3.

Complete series of studies

Developmental Work - these studies and pilot studies were carried out as described below.

Study 1 - The effect of sleep deprivation on fMRI brain activation during pure visual stimulation and coordinated hand/eye tracking.

Preliminary work established:

- a) Whether the visual cortex is sensitive to the effects of sleep deprivation.
- b) Whether the brain areas involved in coordinated hand/eye motor tracking are sensitive to the effects of sleep deprivation.

These two studies were done in parallel because of the complexities of studying sleep deprived subjects with brain fMRI.

Study 2 - The effect of total sleep deprivation on coherent visual motion and visual form detection in normal subjects.

This study examined the ability to detect coherent visual motion and visual form, before and after a period of total sleep deprivation. The results from study 1 suggested that the visual cortex is sensitive to the effects of sleep deprivation; this study was a functional test of the brain areas affected by reduced sleep.

Study 3 - The effects of OSA on fMRI brain activation during visual stimulation.

This study assessed the effects of the sleep fragmentation of OSA on fMRI brain activation during pure visual stimulation. It aimed to establish whether the visual

cortex changes seen in sleep deprived normal subjects are also seen in patients with the sleep fragmentation of OSA.

Chapter 2

Study 1 - The effect of sleep deprivation on fMRI brain activation during pure visual stimulation and coordinated hand/eye tracking

Introduction

Study 1 assessed the effects of 28 to 32 hours total sleep deprivation on fMRI brain activation, during pure visual stimulation and during coordinated visuo-motor tracking. The effect of up to 32 hours total sleep deprivation on simulated steering was also assessed. Healthy subjects, with no pathological sleep condition were studied. All subjects had normal subjective and objective sleepiness at baseline.

Sleep deprivation leads to impaired driving, with an increased road traffic accident rate in sleepy drivers [Maycock 1997, Horne 1995, Naughton 1991]. Two of the fundamental skills needed for safe and error free driving are the detection of moving objects and the ability to track. One or both of these skills or their component parts may be impaired by sleep deprivation. Impairment of these functions may explain the deficits in driving ability seen with sleep deprivation. Both the detection of moving objects and the ability to track involve a number of complex neurological pathways, and it is plausible that the sleep deprived brain is unable to perform these skills optimally. Previous sleep deprivation fMRI studies have demonstrated task specific reductions in brain activation [Drummond 1999, Drummond 2000, Drummond 2004]. It is possible that up to 32 hours total sleep deprivation leads to reduced activation of specific brain areas integral to driving.

Hypotheses for study:

1. Sleep deprivation in normal subjects leads to impaired motion detection with reduced fMRI activation of the brain areas usually activated during performance of this skill.
2. Sleep deprivation in normal subjects leads to impaired tracking and simulated steering, with reduced fMRI activation of the brain areas usually activated during performance of this skill.

Developmental Work

Developmental work assessed the suitability of the assessment tools used in this study - the Oxford Steering Simulator (a divided attention steering simulator) and the Oxford Sleep Resistance (Osler) test. Both of these tests were developed at the Oxford Centre for Respiratory Medicine, and have been tested in Oxford and elsewhere. The tracking task used was developed by Professor Chris Miall in the Oxford University Laboratory of Physiology, and similar tracking paradigms have been used in both OSA and sleep deprivation studies. Two small pilot studies assessed the effects of total sleep deprivation on tracking performance, in normal subjects and in untreated OSA, prior to the start of study 1. This was to determine the training time and inter-individual variation in the performance of this task. Divided attention steering simulators have been used extensively in normal sleep deprived subjects and in patients with sleep deprivation due to OSA. There is limited previous experience using a joystick controlled tracking task in sleep deprivation, testing the tracking component of the steering simulator alone.

Developmental Work 1

Oxford Steering Simulator

Steering performance was assessed using the Oxford Steering Simulator, a test of steering / tracking which was developed in the Oxford Sleep Unit, based on the known visual physiology of steering [Land 1995, Hack 2000]. The test requires the subject to steer a computer 'car' down a pseudo-random winding road, necessitating 'tracking' or coordinated hand / eye manoeuvres to keep the car on the road. A regular search of the periphery is also needed, to monitor for target numbers in the four corners of the screen, corresponding with the distractions of real life driving, and measuring attention. The test / retest reliability of the steering simulator is good [Hack 2001]. The main outcome variables are tracking error (standard deviation from a theoretical ideal lane position), and response time to peripheral targets.

Developmental Work 2

Oxford Sleep Resistance Test

Objective daytime sleepiness was assessed by the Oxford Sleep Resistance (Osler) Test [Bennett 1997]. This is a behavioural maintenance of wakefulness test, based on the traditional EEG based maintenance of wakefulness test (MWT) [George AJRCCM 1996, George Sleep 1996]. The subject lies semi-recumbent in a dark and sound isolated room, and presses a button in response to a light emitting diode (LED), which is lit for one second every three seconds. The switch used is a touch sensitive proximity detector, with no alerting feedback 'click' provided to the subject as he presses the button. The maximum length of the test is 40 minutes. The test is terminated before this if the subject fails to respond to 7 consecutive light flashes (i.e.

21 seconds). The Osler test has been shown to be sensitive to treatment effects in patients with sleep disordered breathing (but not to placebo effects), and has been used successfully in a number of trials of CPAP in OSA [Juniper 2000, Hack 2000].

Developmental Work 3

Visuo-Motor Tracking Paradigm

The task consists of a joystick driven computer game, of coordinated hand / eye tracking manoeuvres. The subject is seated in front of a computer screen on which there is a stationary central cross hair. The subject controls the movement of a cursor by the use of a custom made joystick in their right hand. The cursor is actively displaced from the central cross hair following a random target waveform. The task is divided into 18-second blocks of varying target speed. Five blocks of different, random target speeds are followed by a rest period, during which the subject can rest.

The target waveform is composed of the summation of 6 sinusoids, with frequencies of 0.6, 2.0 and 2.6 hertz. Three frequencies are used for both the vertical and horizontal axes. All 6 sinusoids are given a random phase on each 18 second trial, which means that they are completely unpredictable from trial to trial, also varying in speed and extent; before summation into the final 2-dimensional trajectory. A new trajectory is generated every 18 second trial, by randomisation of the sinusoid frequencies. The trajectory is attenuated with a half-cosine function over the first and last 3 seconds of the trial, so that it starts and ends smoothly at the screen centre.

The subject's task is to compensate for the random cursor motion, by bringing the cursor back to the central cross hair at all times. An additional ocular target (a circle) ensures that the task is a test of coordinated hand / eye tracking. The ocular target moves in a reciprocal direction to that of the cursor. During co-ordinated

eye/hand tracking, the circle (ocular target) and square (hand target) move, requiring simultaneous ocular tracking and compensatory joystick control. Thus in coordinated tracking, the eye and hand movements are identical, inverted versions of each other; such that, the subject's eye and hand follow identical, simultaneous trajectories, enabling the subject to keep the cursor on the central cross hair.

The main outcome variables are tracking error (root mean squared (RMS) error) and lag time. Tracking error is the difference between the cursor position and the central cross hair, and is measured every 0.03 seconds, by cross correlation of the joystick and manual target trajectories. An ideal error score= 0 Arbitrary Units (AU) (i.e. no difference between the cursor position and the central cross hair). A very good error score is about 50 AU, a typical scores range between 80-100 AU. Poorly performing subjects achieve an error score of over 200 AU.

The lag time is the average time (milliseconds) between the ocular target and the joystick. This is calculated from a cross correlation between the target and joystick. Correlation ranges from +1 to -1. +1 means an identical waveform, -1 means identical, but inverted, and zero indicates that the target and joystick movements are completely uncorrelated. In each case, this can be independent of the lag (i.e. the joystick trajectory could be an identical shape to that of the target trajectory, but have a significant lag, which would lead to a high tracking error). The lag represents the visuo-motor control loop latency, a very similar measure to reaction time.

The initial analysis of the individual subject datasets used the in-house programme GRdualt (see appendix page 246). This programme analysed the data by speed (4 conditions, excluding rest). Data is produced for every 0.03 seconds of the 72, 18 second randomised tracking conditions. Secondary analysis involves a combined analysis across all subjects, during each condition, i.e. normal sleep and

sleep deprivation. This analysis used standard local programmes within the MATLAB software package (Mathworks Inc, US). The tracking data collected during fMRI scanning underwent additional pre-processing, using programmes GRdual_err_TR (see page 140) and GRdual_exSLP (see page 142). GRdual_err_TR removes any data collected during 6 scanner repetition times ('TRs') i.e. 18 seconds, from the beginning of the data. This time period corresponds with the scanner 'dummy' runs at the start of data collection, and is not meaningful data. GRdual_exSLP removes any microsleep (SLP) episodes from the data, and was also used for analysis of tracking data collected outside the scanner. Sleep episodes were defined as episodes where the joystick movement (i.e. the subjects hand movement) was less than $1/3^{\text{rd}}$ of the target velocity, for more than 2 seconds. These episodes were assumed to be due to microsleeps, or failure of attention by the subject. These episodes were removed from the data, and the remaining data spliced together.

Work by Miall et al has defined which brain areas are activated during visually guided manoeuvres using fMRI [Miall 2000, Miall 2001]. Parametrically varying the degree of coordination between the eye and hand has established that cerebellar BOLD signal increases as eye-hand coordination increases. In the original experiment [Miall 2001], subjects lay supine in the fMRI scanner, wearing prism glasses to view a rear projection screen placed 2.8m from their eyes. The $13^{\circ} \times 10^{\circ}$ display was generated by computer, at high resolution with an LCD projector. The movement of the joystick in two dimensions was encoded by the rotation of two polarised disks, detected by fibre optics, and converted to voltage signal, and sampled at 26 Hz. The green square cursor was $0.2^{\circ} \times 0.2^{\circ}$. The target for ocular tracking, a white circle was 0.2° in diameter. Joystick movement of approximately 6cm (75° of motion) was required to track the target. Manual joystick tracking was significantly better when the

target trajectories for eye and hand were identical and synchronous, than when they were unrelated. These experiments showed significant cerebellar activation during coordinated hand-eye tracking compared to isolated eye and hand movements. Only cerebellar activity varied in proportion to the degree of hand-eye coordination.

Developmental Work 4 - Pilot Studies

Pilot Study 1 - The effect of sleep deprivation on tracking performance

The effect of 28 hours total sleep deprivation on tracking performance was assessed in three subjects. Subjects were trained to stable performance on the tracking task. They were then assessed following a night of normal sleep at home, or after 28 hours total sleep deprivation (after a first night shift, having not slept the day before the shift). These assessments were done in random order. The subjects were one male and two females (mean age 35.3). Joystick movement was monitored and overall performance quantified from the average error in tracking, the average distance between the cross-hair and cursor position. Mean tracking error was 109.0 AU (SD 48.7) post normal sleep, and 185.8 (120.7) AU following sleep deprivation, ($p < 0.0001$, paired t-test).

Pilot Study 2 - The effect of OSA on tracking performance

The effect of the sleep fragmentation of untreated OSA on tracking performance was assessed in 9 patients (8 male). OSA was diagnosed from a one night respiratory polysomnographic study. The mean $>4\%$ oxygen saturation dip rate was 32.1 (SD 10.9) and the mean baseline Epworth Sleepiness Score (ESS) was 15.4 (SD 4.9). Subjects were right handed, current drivers (all driving $>10,000$ miles per year), who abstained from stimulants including caffeine. The subjects performed the

tracking task before and after one months' treatment with therapeutic CPAP. Thirteen control subjects (12 male) matched for age, sex, handedness and driving, also completed the tracking task. Joystick movement was monitored and overall performance quantified from the average tracking error. Untreated patients with OSA had a significantly higher mean tracking error than controls; pre-treatment OSA patient mean tracking error was 268.2 AU (SD 67.0), controls 114.3 AU (SD 26.2), $p < 0.0001$ (unpaired t-test). Both pre and post CPAP treatment of OSA, tracking error correlated with increasing target speed. A significant improvement in mean tracking error was seen following treatment; post-treatment OSA patient mean tracking error was 198.2 AU (SD 75.4), mean improvement 69.1 AU (SD 72.3), $p < 0.02$ (paired t-test).

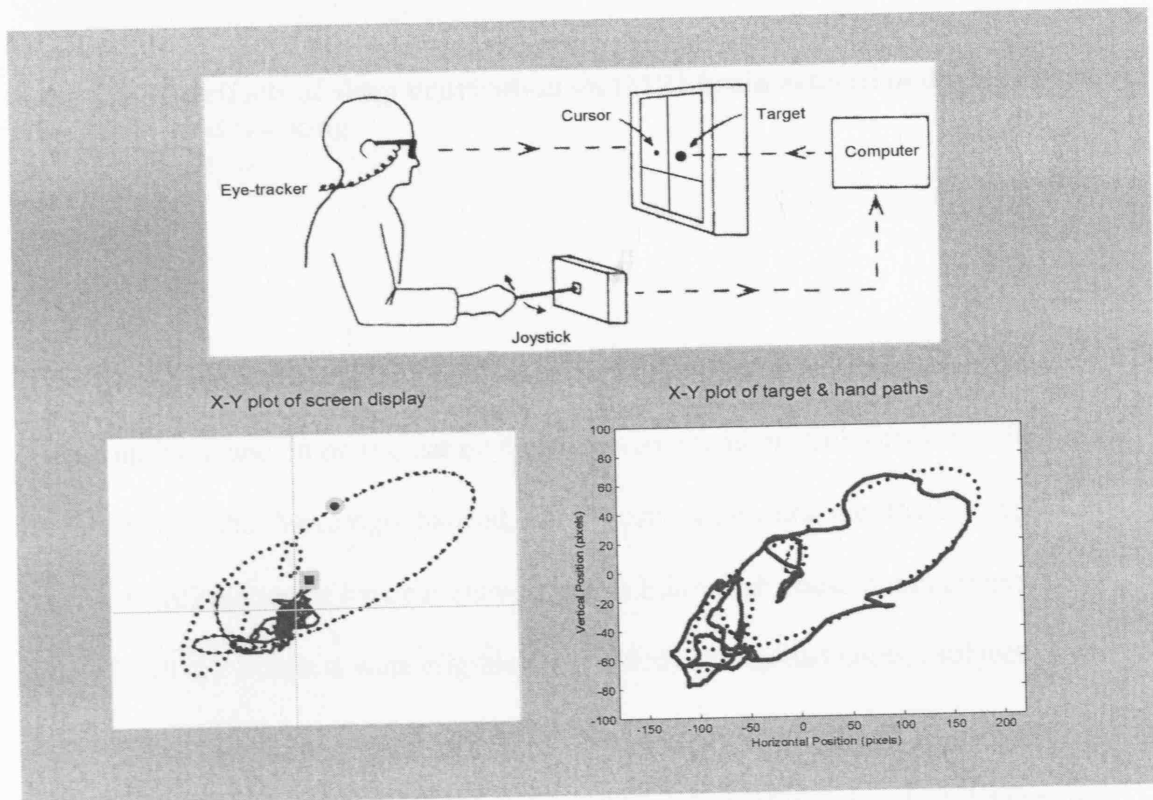


Figure 1 - Pictorial representation of the tracking task (from Professor Miall)

Top panel - a subject performing the tracking task. The subject uses the joystick to centre the target (large black dot) on the central cross hair. The target is continuously and randomly displaced from the cross hair. The target for ocular tracking is the smaller black dot ('cursor'), which moves in a reciprocal direction to that of the target. The subject is instructed to keep the target on the central cross hair at all times whilst using the ocular target to guide in which direction to move his hand, in order for the target to return to the central cross hair.

Bottom left panel - a plot of the screen display of a subject performing the task. The dotted line is the trajectory of the ocular target (circle); the complete line represents the subjects' cursor movement (square) to re-centre the target.

Bottom right panel - a plot of the target and hand paths. The dotted line is the trajectory of the ocular target; the complete line represents the subject's cursor movement (using the joystick) in following the ocular target, to re-centre the cursor on the central cross.

Study 1 - The effects of sleep deprivation on fMRI brain activation during visual stimulation and tracking

Methods

Subjects

10 normal subjects, with no history of neurological disease or pathological sleep condition, and on no regular medication were recruited. Subjects were eligible for the study if they were right handed, non-claustrophobic and met fMRIB safety criteria. Confirmation of handedness was by the Edinburgh Handedness Inventory [Oldfield 1971]. Subjects were eligible for the study if they had normal subjective and objective sleepiness at baseline. Subjective sleepiness was confirmed by the Epworth Sleepiness Score (ESS) [Johns 1991, Johns 1992, Johns 1993, Johns 1994]. Objective sleepiness was measured by the Osler test [Bennett 1997]. In addition, all subjects had to be regular drivers and hold a current UK driving licence. Subjects had the study protocol explained to them in detail, and were provided with written study details, before signing a consent form, at least 24 hours later.

Study Techniques (for protocol appendix page 222)

1. Baseline / eligibility assessment (Visit 1)

Subjects completed a questionnaire about their normal sleep and an ESS. To be eligible for the study the ESS had to be normal (≤ 9), with a normal objective sleepiness at baseline (i.e. a maintenance of wakefulness test (MWT) of 40 minutes). The Edinburgh Handedness Inventory was completed. A questionnaire about normal caffeine, alcohol and cigarette consumption was completed. Subjects confirmed that they were regular drivers, with no history of neurological or pathological sleep condition. Subjects completed the fMRI safety assessment questionnaire. An

information letter was supplied if it had not already been given, and the timing of the rest of the study, and the protocol for the sleep deprivation night was discussed.

2. Tracking and steering simulator training (Visit 2)

Subjects were trained to stable performance on the Oxford Steering Simulator and the tracking task. During the training visit, the rest of the study protocol was explained again in detail. Subjects had an opportunity to visit the fMRI scanner. The consent form was signed.

Tracking Paradigm Training

The tracking task was used as described on page 63. Subjects were trained to stable performance on the task. Before attempting the task, the paradigm was explained to the subject, who initially observed a short practice run. Training commenced with hand tracking only, at low speed. Once hand tracking alone had been mastered, hand / eye tracking started, initially at low speed. The speed increased to the maximum, and the subject practiced the task at this speed for about 10 minutes. Following training to stable performance in the sitting position, the subject was trained to use the task supine, using prism glasses to view the task on a computer screen, about 1.5 metres from their face. This was to replicate the set up in the MRI scanner, where the task is performed in a limited space, with the subject supine. The subject performed the same maximum speed task in the supine position. Total training time was around 40 minutes.

Oxford Steering Simulator Training

Subjects were trained to stable performance on the Oxford Steering Simulator. The training time to stable performance has been established [Juniper 2000, Hack 2000], and is about 16 minutes in a naïve subject. To ensure optimal performance was reached, the subjects practiced the task for two ten minute sessions. The speed was set to medium, with all of the road visible (standard defaults).

3. Assessment after normal sleep (Visit 3)

This assessment was done after a night of normal sleep at the subjects' home. Prior to this assessment, the subjects had received an actigraph watch to wear for a minimum of 20 hours prior to the start of the study period, to ensure normal daytime activity, and a normal nights sleep before the assessments. Subjects rose at 8am on the day before the assessment, and were instructed to complete a normal days activities. They were instructed to be in bed with the light out by 11pm, and were asked to rise by 8am on the day of visit 3. Following a normal mornings activities, the subjects attended the Oxford FMRIB Centre at the John Radcliffe Hospital at 2pm.

A. Visuo-motor tracking during fMRI scanning

Subjects performed the tracking task as practiced during the training visit. Following a standard safety check, the subject was positioned in the MRI scanner using a standard protocol. The subject's head was restrained with support. Ear-plugs and sound insulating headphones were worn to minimise sound interference. Having checked the panic button and attached an oxygen saturation probe (for continuous monitoring of pulse rate and oxygen saturation), the subject was moved into the MRI scanner. The joystick was placed by the right hand, positioned at the subject's side,

with the arm supported with padding. The tracking task was projected onto a screen at the subject's feet, about 3 metres from the face. This was seen through prism lenses, with vision corrected if necessary. Any episode of sleep during scanning was identified from the failure of joystick movement. Standard Echo-Planar Imaging (EPI) using a 3 Tesla Siemens-Varian scanner and a standard whole-head coil was used. Axial MRI images were acquired as 21 x 6mm slices of the cerebrum and cerebellum, using a 3 second repetition time (TR) for 60 volume acquisitions, with a nominal voxel size of 3 x 3mm in plane. This is a standard signal acquisition sequence, used routinely and successfully in many studies in the Oxford FMRIB centre (www.fmrib.ox.ac.uk). The structural image was acquired with a standard sequence to give slices of 256 x 256 voxels.

During the scanner set-up period, (including preliminary shimming and localising scans, lasting about 10 minutes) the subject had a further opportunity to practice the tracking task. Communication with the subject was via the subject's headphones, and continuous video monitoring of the subject was on view at all times from the control room. The joystick was calibrated before the start of the tracking task. Real time tracking data was collected simultaneously with the fMRI data, during performance of the task.

B. Visual stimulation during fMRI scanning

This test was performed immediately after completion of the tracking task. The visual stimulation paradigm was projected onto a screen at the subject's feet, again visualised with prism glasses. The subject was instructed to look at the centre of the screen at all times. The visual stimulation program consists of an 8 hertz yellow / blue chequerboard, alternating at 125 milliseconds per frame. The total test time was

3 minutes, with 3 cycles of 30 seconds on, followed by 30 seconds off. There are no data output files related to this paradigm. The scanner set up was the same as for the tracking task, with a 3 second repetition time (TR) for 60 volume acquisitions.

fMRI Analysis

Scan analysis was carried out using software in FEAT (FMRIB's Easy Analysis Tool), an extension of Medx (Sensor Systems, Virginia, USA). The scans from each session were realigned, to correct for motion artefact, using a rigid body transformation, with the first scan as a reference. The six parameters for the rigid body transformation were estimated using a least squares approach. All images from each subject were then transformed into a standard space (normalising spatial transformation). This process matched each scan to a template image using a 12 parameter affine (linear) and quadratic (non-linear) three-dimensional transformation.

Analysis of the fMRI tracking data pre and post sleep deprivation aimed to determine whether a brain activation deficit could explain the impairments in tracking and steering associated with sleep deprivation. Tracking and driving require complex neurological processes, controlled by a number of pathways, integrated by a number of brain areas. Analysis of the activation of specific brain areas aimed to establish whether reduced activation of these areas might be associated with the impaired steering and tracking associated with sleep deprivation. Specific brain areas of interest, integral to tracking and steering are the motor cortex, cerebellum and areas involved in the detection of motion. Additional areas of interest are the frontal lobe (involved in task attention), and the precuneus (involved in assessment of the surrounding environment).

The fMRI tracking data was analysed at variable threshold levels. Analysis of the tracking data involves a complex general linear model and a large number of variables. Eight COPE images are generated for each subject - four for each of the four tracking speeds, one for all speeds combined, one for increasing speed, one for decreasing speed, and one for tracking error. Programmes in Medx were used to generate local maxima and coordinates for the various parameter estimate (PE) images. These were then assessed by the computerised version of the Talairach and Tournoux 1958 brain atlas.

fMRI Statistical Analysis

The subject, condition and co-variate effects were estimated using a General Linear Model at each voxel. To test hypotheses about regionally specific conditions or co-variate effects, the estimates were compared using linear compounds or contrasts. For the visual stimulus, two explanatory variables were set - one with the chequerboard 'on' and the other with the chequerboard 'off'. For the tracking task, six explanatory variables were used: the four tracking speeds, tracking error and sleep episodes (derived from the MATLAB data analysis). Seven contrasts were used - 4 of which were the four different tracking speeds. The additional 3 contrasts were all tracking speeds combined (i.e. any tracking speed), increasing speed and decreasing speed. The resulting set of voxel values for each contrast tested constituted a statistical parametric map (SPM) of the *t* statistic (*t*). SPM maps were then combined across subjects using fixed effects and random effects models. For further fMRI analysis details see appendix, page 234.

The *t* statistics were transformed into the unit normal distribution (*Z*), at varying threshold levels. The resulting foci were then characterised in terms of spatial

extent (k) and peak height (u). The significance of each region was estimated using approximations from the theory of Gaussian Fields, by thresholding at $Z < 2.3$. From this theory, the probability that the observed number of voxels (or bigger), could have occurred by chance [$p(n_{\max} > k)$], or that the peak height observed (or higher) could have occurred by chance [$p(Z_{\max} > u)$] over the entire brain volume was analysed. Differing thresholds were set: using clusters or voxels, uncorrected threshold, or no threshold, each with a variable p value (0.01 and 0.05)

Significant clusters were then rendered as colour images onto a standard brain (e.g. MNI 305, the standard brain image of the Massachusetts Neurological Institute) or a group averaged brain. Locations of cluster maxima were reported, and these were identified by reference to the spatial coordinates of the standard statistical parametric mapping (SPM) brain templates [Talairach 1958].

C. Structural MRI scan

A 3mm T1-weighted structural MRI scan, using whole brain images in the axial plane was obtained for each subject, to allow anatomical localisation of the subsequent BOLD signal changes within the cerebellum and motor cortical areas. Functional MRI time-series were analysed using tools in FEAT (fMRIB's Easy Analysis Tool) (www.fmrib.ox.ac.uk/fsl). Briefly, images were motion corrected, low pass filtered, and smoothed with a 5mm FWHM kernel. Signal changes were then tested using a gaussianised T/F statistic. Functional images were then co-registered with the T1 anatomical image. Signal change was measured on individual subjects, with group contrasts performed using a random effects model and using a region of interest (ROI) based analysis, in anatomically defined regions of interest. For detailed MRI analysis see appendix page 234.

D. Steering simulator assessment

The steering simulator assessment and MWT were performed after fMRI imaging. Subjects performed a 30 minute simulated drive, the speed was set to 'medium', and the entire road visible. The main outcome measures were standard deviation from centre drive lane position and response time to peripheral target stimuli.

E. Maintenance of wakefulness test

The final test performed was the maintenance of wakefulness test. The Oxford Sleep Resistance (Osler) test was used.

4. Assessment after sleep deprivation (Visit 4) NB Visits 4 and 5 in random order

Sleep Deprivation Night Protocol

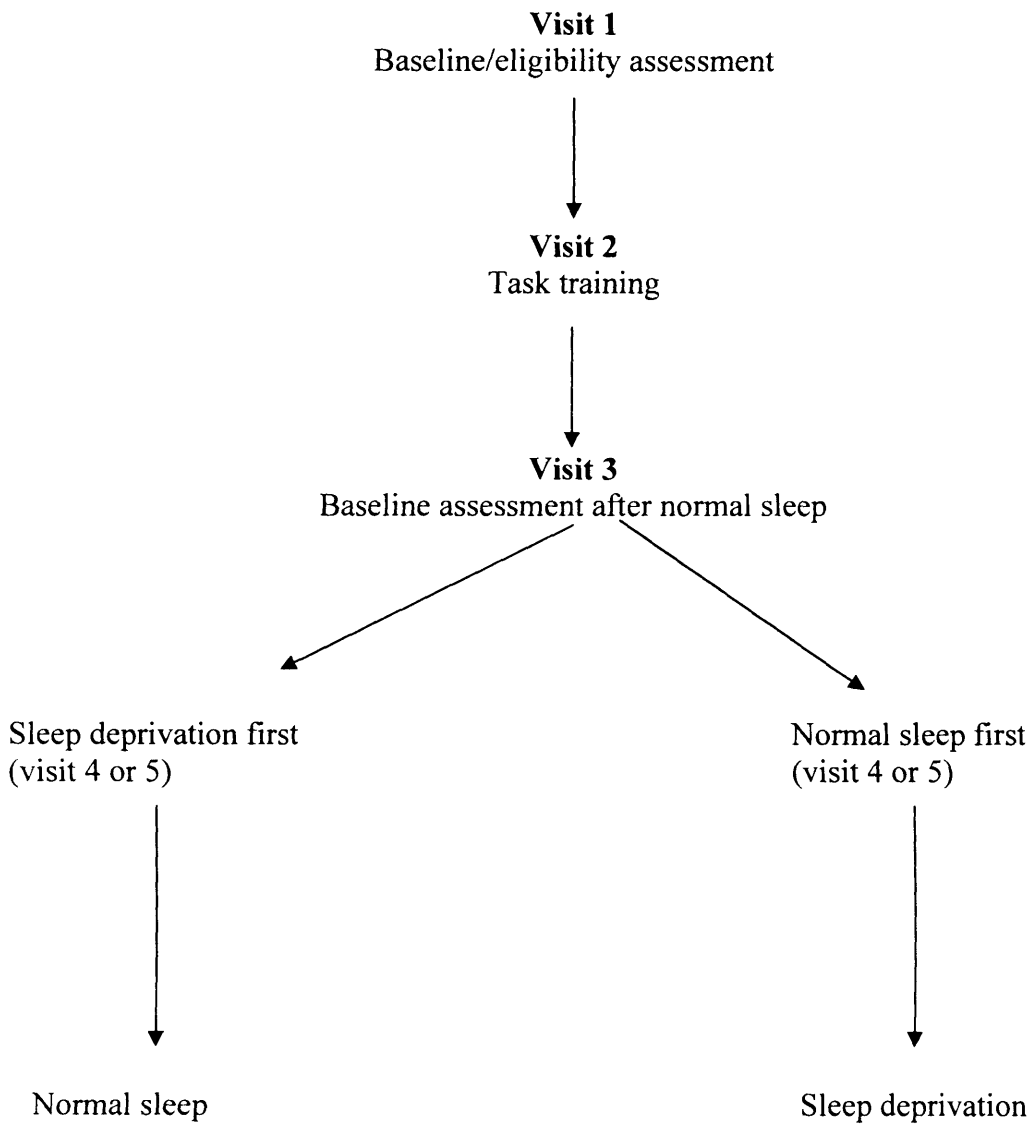
This assessment was done after a night of sleep deprivation, which was supervised at the Oxford Centre for Respiratory Medicine, Churchill Hospital, Oxford. Prior to the assessment, all subjects received an actigraph watch to wear for a minimum of 20 hours prior to the start of the study period. This was to ensure a day of normal activities, and to confirm that the subjects were awake throughout the duration of the sleep deprivation night. Subjects rose at 8am on the day before the assessment night, and were instructed to complete a normal day's activities. They were instructed to arrive at the Churchill Hospital by 10pm (or were collected by car, if they preferred). They were advised to bring work and games to occupy themselves overnight. Videos and board games were provided. A maximum of four subjects were supervised overnight. Food (sandwiches and fruit) was provided. No high glucose food, which could have had an alerting effect, caffeine containing food or drinks,

alcohol or cigarettes were permitted. Breakfast was provided from 8am. Following a normal mornings activities, the subjects attended the Oxford FMRIB Centre at the John Radcliffe Hospital at 2pm. The assessments were carried out exactly as for visit 3. Subjects went home in a taxi following the afternoon of assessments. They were advised to stay at home for the rest of the evening, and were advised not to drive, or sign important documents until the following day. Randomisation to visits 4 and 5 was by a series of pre-sealed, numbered opaque envelopes, and was performed by a research nurse who was not otherwise involved in the study.

5. Assessment after normal sleep (Visit 5) NB Visits 4 and 5 in random order

This was carried out in exactly the same way as for visit 4.

Study 1 The effect of total sleep deprivation on visual stimulation and visuo-motor tracking in normal subjects



Chapter 2 - Results from study 1

The effect of sleep deprivation on fMRI brain activation during pure visual stimulation and coordinated hand/eye tracking

Ten normal subjects completed the study. There was no difference between the data collected at baseline (visit 3, including a desensitisation scan) and the data collected after normal sleep (visit 4 or 5). The results presented here are a comparison of the data collected after sleep deprivation and after normal sleep (visits 4 and 5, in random order). All subjects had normal subjective and objective sleepiness at baseline; their baseline data are shown in table 1 (below). Table 2 (page 85) shows the full individual subject baseline data and table 3 (page 87) shows the non fMRI study data.

Age (years)	27.1 (6.4)
Baseline ESS	5.5 (2.8-7.0)
Baseline MWT (minutes)	40 (40-40)

Table 1 - The subjects' baseline characteristics

Results are mean and (standard deviation). Interquartile range (IQR), 25-75% is presented for the non-normally distributed data.

ESS= Epworth Sleepiness Score, MWT= maintenance of wakefulness (Osler) test.

Maintenance of Wakefulness Data

All 10 subjects had normal objective sleepiness at baseline, reaching the full 40 (40-40) minutes on the Osler test. This was in keeping with their normal subjective sleepiness at baseline, with a median ESS of 5.5 (2.8-7.0) The median post sleep

deprivation Osler was 9.4 (3.8-24.5, difference 24.2 minutes (95% CI 15.1 to 33.6, $p < 0.0001$)), paired t-test.

Steering Simulator Data

There was a significant deterioration in steering simulator performance following the sleep deprivation night. Mean steering error (standard deviation from the centre drive lane position, in arbitrary units (AU)) was 0.13 (0.09-0.15) AU following normal sleep, and 0.40 (0.14-3.2) AU following sleep deprivation, difference 1.20 AU (95% CI -2.42 to 0.03) $p < 0.05$, paired t-test. As for the tracking task, there was a greater range of performance following sleep deprivation, with some subjects' performance deteriorating by a factor of more than 20. Mean reaction time to register peripheral target stimuli was also impaired following sleep deprivation. Mean reaction time was 1.74 (1.5-2.3) seconds following normal sleep, and 2.26 (1.7-2.9) seconds post sleep deprivation, difference 0.30 seconds (95% CI -0.03 to -0.57) $p < 0.03$, paired t-test. The range of performance and deterioration in peripheral target reaction time was relatively less than the impairment on the steering task, suggesting that the subjects chose to concentrate on the less difficult, target registration task, than on the more difficult steering task. No subjects missed any peripheral targets following normal sleep, and two missed one each, following sleep deprivation.

Tracking Data

There was a significant deterioration in tracking performance following the sleep deprivation period: mean tracking error following normal sleep was 120.1 (94.5-129.4) AU, mean post sleep deprivation tracking error was 233.2 (154.0-276.0) AU, difference 101.4 AU (95% CI -148.1 to -54.6) $p < 0.001$, paired t-test. Mean tracking

lag time following normal sleep was 167.5 (134.1-199.2) ms, mean post sleep deprivation tracking lag time was 253.2 (175.5-337.0) ms, difference 82.1 ms (95% CI -127.8 to -36.5) $p < 0.003$, paired t-test.

Actigraphy Data

Actigraphy data was collected on all subjects for a minimum of 20 hours before each study period. Analysis of the actigraphy data confirmed that subjects had undisturbed sleep during their night of normal sleep at home. It also confirmed a night of activity during the sleep deprivation period, and that subjects remained active until their afternoon of assessments following the sleep deprivation night. The raw actigraphy data is not presented in this thesis.

Statistical Analysis

Further statistical analysis was carried out with SPSS software, version 14.0. Relationships between normal sleep and sleep deprivation data were explored with Pearson's correlation. The MWT following sleep deprivation correlated with drive reaction time following sleep deprivation, $r = -0.79$, $p < 0.006$, showing that reaction time to measure peripheral targets was worse in those subjects who were more sleepy following sleep deprivation. Tracking error following normal sleep correlated with driving error (SD from centre drive lane position) following normal sleep, $r = 0.63$, $p < 0.05$, showing that these two tests encompass some of the same parameters.

fMRI Results - Visual Stimulus

fMRI analysis was carried out as described, with each individual subject's scan analysed, following preprocessing. A group analysis, of all ten subjects scans generated a group averaged image showing significant clusters as coloured areas overlying the group averaged structural brain scan. Differential brain activation in the two states - following normal sleep and following sleep deprivation was then assessed by subtraction analysis, showing the relevant brain areas activated in each sleep state. Differing threshold levels were applied to these analyses and the corresponding anatomical areas were then determined. There was no difference between the visual fMRI data collected at visit 3 (baseline) or after normal sleep (visit 4 or 5), thus the data presented are a comparison of the data collected after normal sleep (visit 4 or 5) and after the period of total sleep deprivation (visit 4 or 5) in random order.

Figure 2 shows the fMRI group averaged data following normal sleep, and figure 3 shows the same group averaged data following sleep deprivation (both n= 10). Both of these analyses use a FLAME (FMRIB's local analysis of mixed effects) analysis, with $p= 0.01$, $Z= 2.3$. Figure 4 shows the design matrix for an individual subject's visual stimulation analysis. Figures 5 and 6 show the design matrices for the visual stimulation group analysis, and for the visual stimulation group subtraction analysis, respectively.

Figure 7 shows a higher level subtraction analysis - group averaged data following normal sleep minus group averaged data following sleep deprivation. Figure 8 also shows a higher level subtraction analysis - group averaged data following sleep deprivation minus group averaged data following normal sleep. The respective tables show the Medx coordinates and associated Talairach atlas anatomical sites. These images show the brain areas differentially activated in the two

different sleep states. Figure 7 shows the brain areas only activated following normal sleep, and not following sleep deprivation, and vice versa for figure 8. Statistical thresholding determines the level of significance of the areas activated. These data are active using a FLAME analysis, ordinary least squares, $p = 0.05$, $Z = 2.3$. The areas of highest activation are in yellow (4.2 AU), with areas of less significant activation in orange and red (1.6 AU).

For both of these group averaged subtraction analyses, the maximum pixel activation levels are modest, probably reflecting the relatively small subject number, however, clear differences in brain activation are seen following the two different sleep states. Following normal sleep, activation is seen in the occipital lobe, around Brodmann Area (BA) 19, with no frontal lobe activation. Following sleep deprivation, activation is seen predominantly in the frontal lobes, with lesser activation of areas in the left temporal lobe, and no occipital lobe activation.

Further Visual Cortex Analysis

Featquery (a software programme within FEAT, to interrogate data for maximal voxel activation, after thresholding using a predefined mask), was used to further define areas of activation within the visual cortex. Masks were generated using standard programmes in Medx, using known coordinates, and were tested at a number of threshold levels.

Mask 1 (defining visual cortex area V5 / MT) was constructed using data from Hasnain et al (see appendix page 245). Mask 2 defined the primary visual cortex (areas V1 and V2), without area V5. Both masks were applied to the differential visual stimulation data, at varying threshold levels.

Testing using the visual cortex masks showed activation following normal sleep, but not following sleep deprivation, at an uncorrected threshold of $p = 0.01$. There was no difference in the size or statistical significance of the visual cortex areas activated, with or without thresholding using the above masks. Maximal pixel values for the group subtraction data are shown in figures 9 and 10, and their corresponding tables of coordinates. The mask data confirms activation of the peripheral visual cortex following normal sleep, but not following sleep deprivation. This suggests an effect of sleep deprivation on this specific visual cortex area.

Table 4 (page 100) shows the individual subject maximum pixel activation during visual stimulation, following thresholding with visual cortex masks. Overall there was greater activation of area V5 following normal sleep than following sleep deprivation, and this was statistically significant.

Subject	Age	BMI	Handed	ESS	Trk Lag		Trk Err		Drive Err		Rx Time		2s		Osler	
					NSlp	SlpDep	NSlp	SlpDep	NSlp	SlpDep	NSlp	SlpDep	NSlp	SlpDep	NSlp	SlpDep
1	20	26.9	30	1	166.60	240.40	106.80	299.40	0.09	3.02	1.83	1.81	0	0	40	7.5
2	20	23.1	26	7	187.60	354.60	117.90	273.50	0.15	0.68	2.59	2.90	0	1	40	1.1
3	31	22.9	30	6	168.40	286.30	123.00	223.20	0.07	0.51	1.78	2.32	0	0	40	11.5
4	29	24.2	30	6	206.30	265.60	128.80	165.50	0.12	0.24	1.53	1.89	0	0	40	23.3
5	28	19.3	30	3	144.60	196.90	93.90	119.40	0.13	0.14	1.70	2.19	0	0	40	28.1
6	21	26.1	27	8	154.70	185.20	131.00	243.10	0.14	4.60	1.69	2.41	0	1	40	5.5
7	25	22.2	30	7	99.10	97.50	77.20	79.30	0.08	0.09	1.51	1.47	0	0	40	13.3
8	33	21.2	30	5	196.80	403.10	122.20	283.20	0.15	3.60	2.19	2.97	0	0	40	4.2
9	40	23.2	29	5	102.50	146.40	94.70	250.00	0.12	0.13	2.73	3.01	0	0	40	2.6
10	24	23.0	30	2	259.20	331.10	147.30	220.00	0.28	0.29	1.19	0.75	0	0	40	40

Table 2
Normal subject data, after normal sleep and after sleep deprivation

Subject = subject name (alphabetical order)

BMI = Body Mass Index (Kg / m^2)

Handed = score on Edinburgh Handedness Inventory (>25 = strongly right handed)

NSlp = data after normal sleep

SlpDep = data after sleep deprivation

TrkLag = tracking lag time (milliseconds)

TrkErr = tracking error (Arbitrary Units)

DriveErr = drive error (standard deviation from centre drive lane position)

RxTime = reaction time to register peripheral targets

2s = number of 2s missed

Osler = minutes reached on Osler test (behavioural maintenance of wakefulness test)

	Normal Sleep	Sleep Deprivation	Difference (95% CI)	p
MWT (minutes)	40 (40-40)	9.4 (3.8-24.5)	24.2 (15.1 to 33.6)	p< 0.0001
Drive Error (arbitrary units)	0.13 (0.09-0.15)	0.40 (0.14-3.2)	1.20 (-2.42 to 0.03)	p< 0.05
Drive RT (seconds)	1.74 (1.5-2.3)	2.26 (1.7-2.9)	0.30 (-0.03 to -0.57)	p< 0.03
Tracking Error (arbitrary units)	120.1 (94.5-129.4)	233.2 (154.0-276.0)	101.4 (-148.1 to -54.6)	p< 0.001
Tracking Lag (msecs)	167.5 (134.1-199.2)	253.2 (175.5-337.0)	82.1 (-127.8 to -36.5)	p< 0.003

Table 3 Non-fMRI results from study 1

Results are mean and (standard deviation). Interquartile range (IQR), 25-75% is presented for the non-normally distributed data.

MWT = maintenance of wakefulness test

Drive Error = standard deviation of centre drive lane position

Drive RT = drive reaction time to register peripheral targets

Tracking Error = tracking error

Tracking Lag = tracking lag time

CI = confidence interval

p = paired t-test

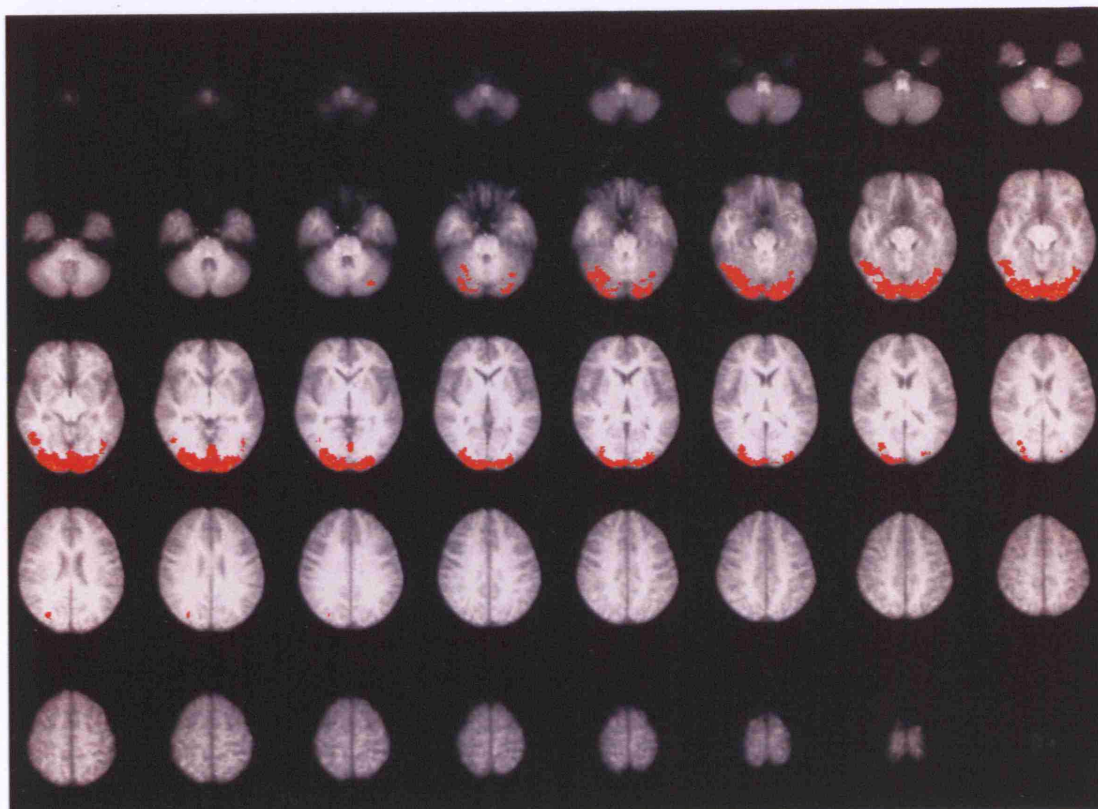


Figure 2

Visual stimulation: group averaged data (n= 10) after **normal sleep**.
FLAME analysis, $p= 0.01$, $Z= 2.3$.



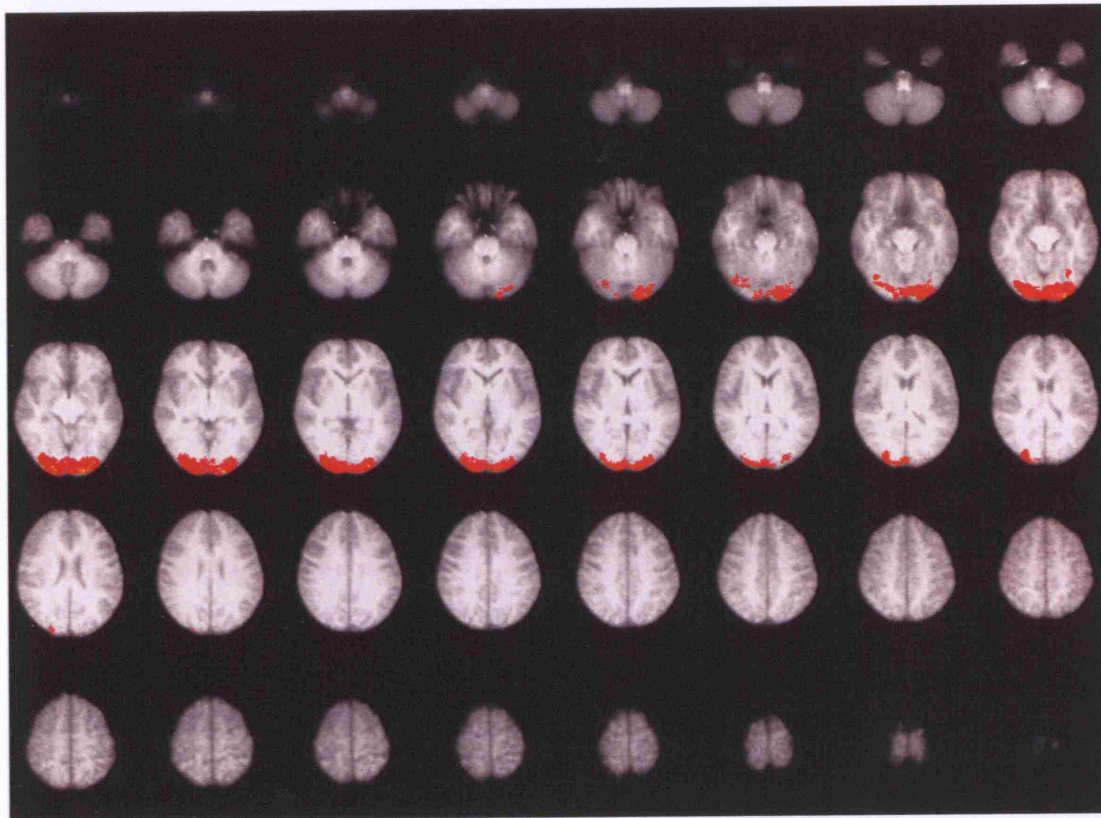


Figure 3

Visual stimulation: group averaged data (n= 10) after **sleep deprivation**.
FLAME analysis, $p= 0.01$, $Z= 2.3$.



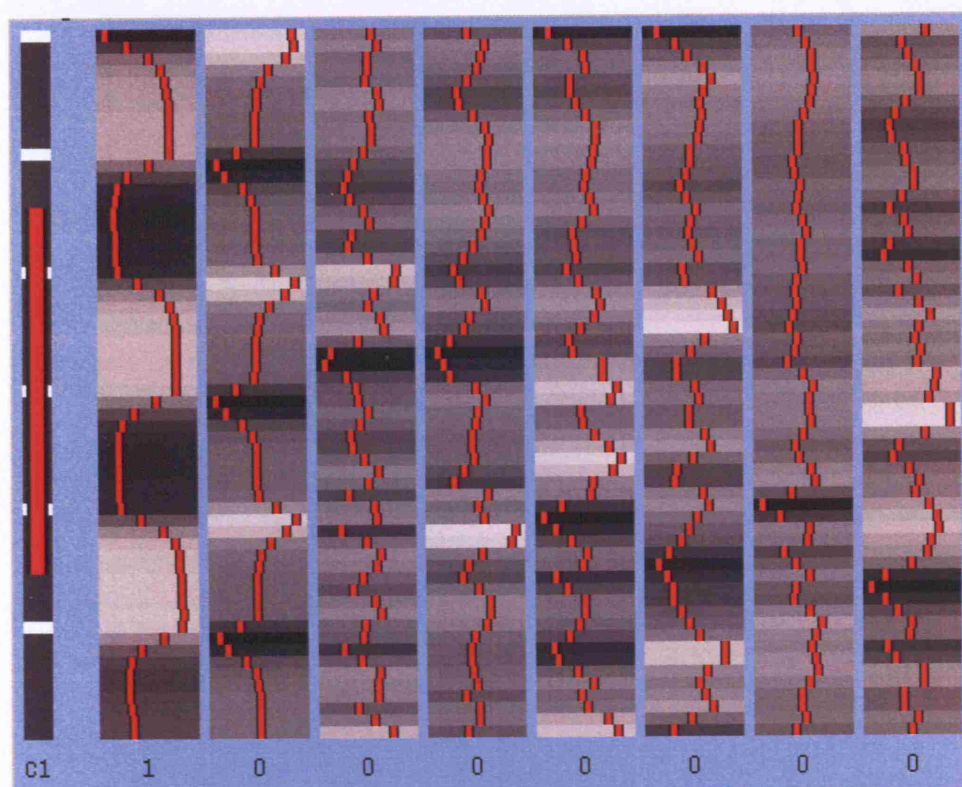


Figure 4

The design matrix and parameter contrasts for an individual subject's visual stimulation analysis (the columns are 1 to 8, from left to right). The bar on the left is a graphical representation of time - the white bars mark the position of every 10th volume. The red bar shows the length of the longest temporal cycle which is passed by the high pass filter. Time is represented by the vertical axis, each column (left to right) represents a different explanatory variable. EV (explanatory variable) 1 (columns 1 and 2 - column 2 is the first derivative of column 1) explains the chequerboard flashing on and off, and columns 3 to 8 explain head motion correction. Columns 3 and 4 explain movement in the X plane, columns 5 and 6 explain the movement in the Y plane, and columns 7 and 8 explain the movement in the Z plane. Columns 4, 6 and 8 are the first derivatives of columns 3, 5 and 7 respectively. The parameter contrasts are shown in the bottom panels. The red lines and black-white sections represent the same thing: the variation of the waveform with time. Each row is a different contrast vector, and each column refers to the weighting of the relevant EV.

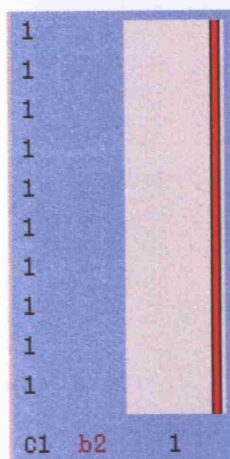


Figure 5
The design matrix for the visual stimulation group analysis.

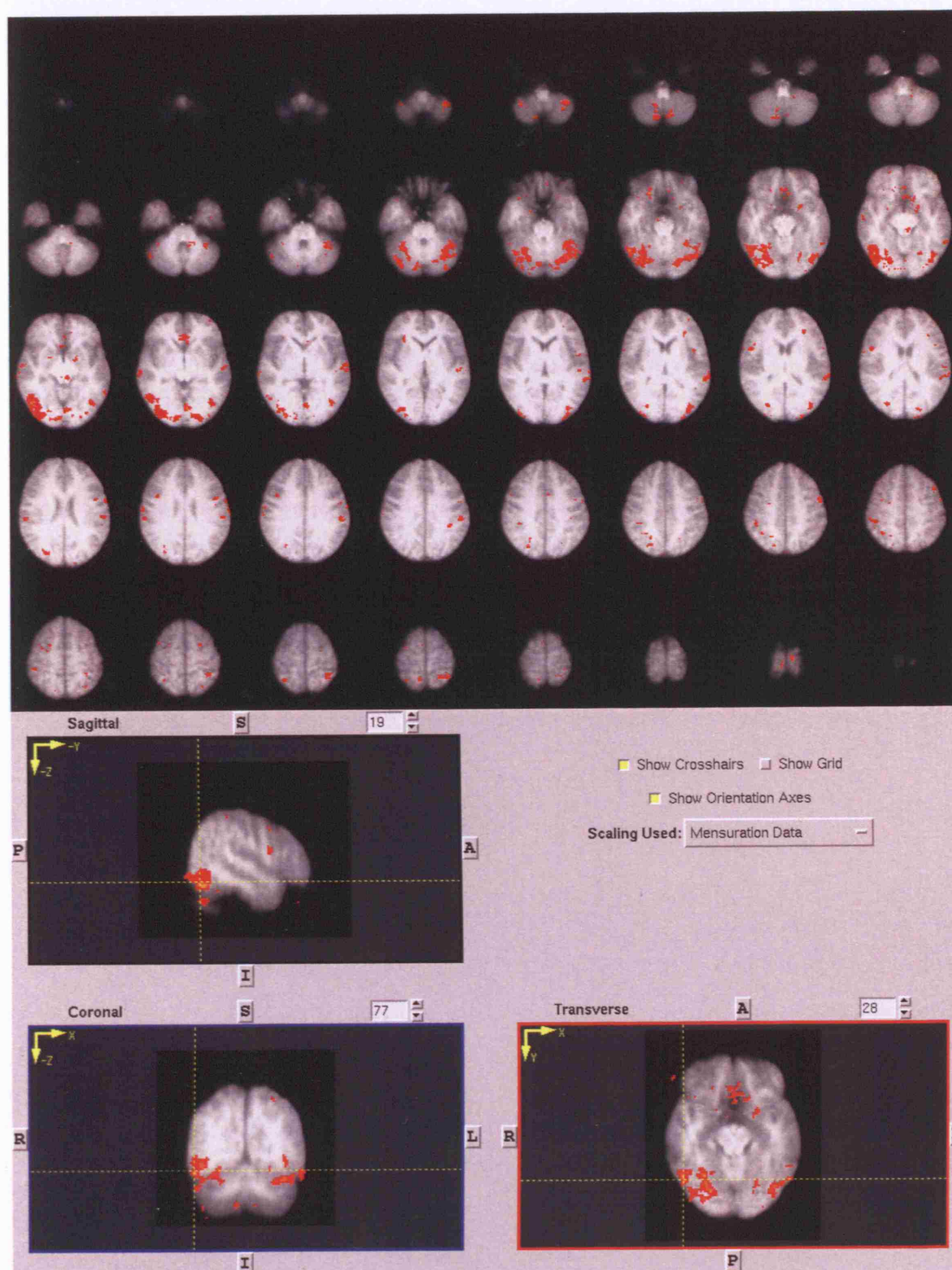


Figure 7
 Visual stimulation: group averaged subtraction data (n= 10) **normal** sleep minus sleep deprivation.
 FLAME analysis, uncorrected OLS, $p= 0.05$.



Medx coordinates	Maximum pixel value	Talairach Datapoint
-44, -68, -18	4.12	L occipital lobe, BA 19
30, -86, -2	3.61	L inf occipital gyrus
42, -72, -4	3.60	L inf occipital gyrus, BA 19
46, -64, -8	3.58	R occipital lobe
30, -58, -14	3.58	L occipital lobe, BA 19

Table 7

Maximum areas of pixel activation during visual stimulation: normal sleep minus sleep deprivation, with their Medx coordinates and Talairach atlas anatomical sites.

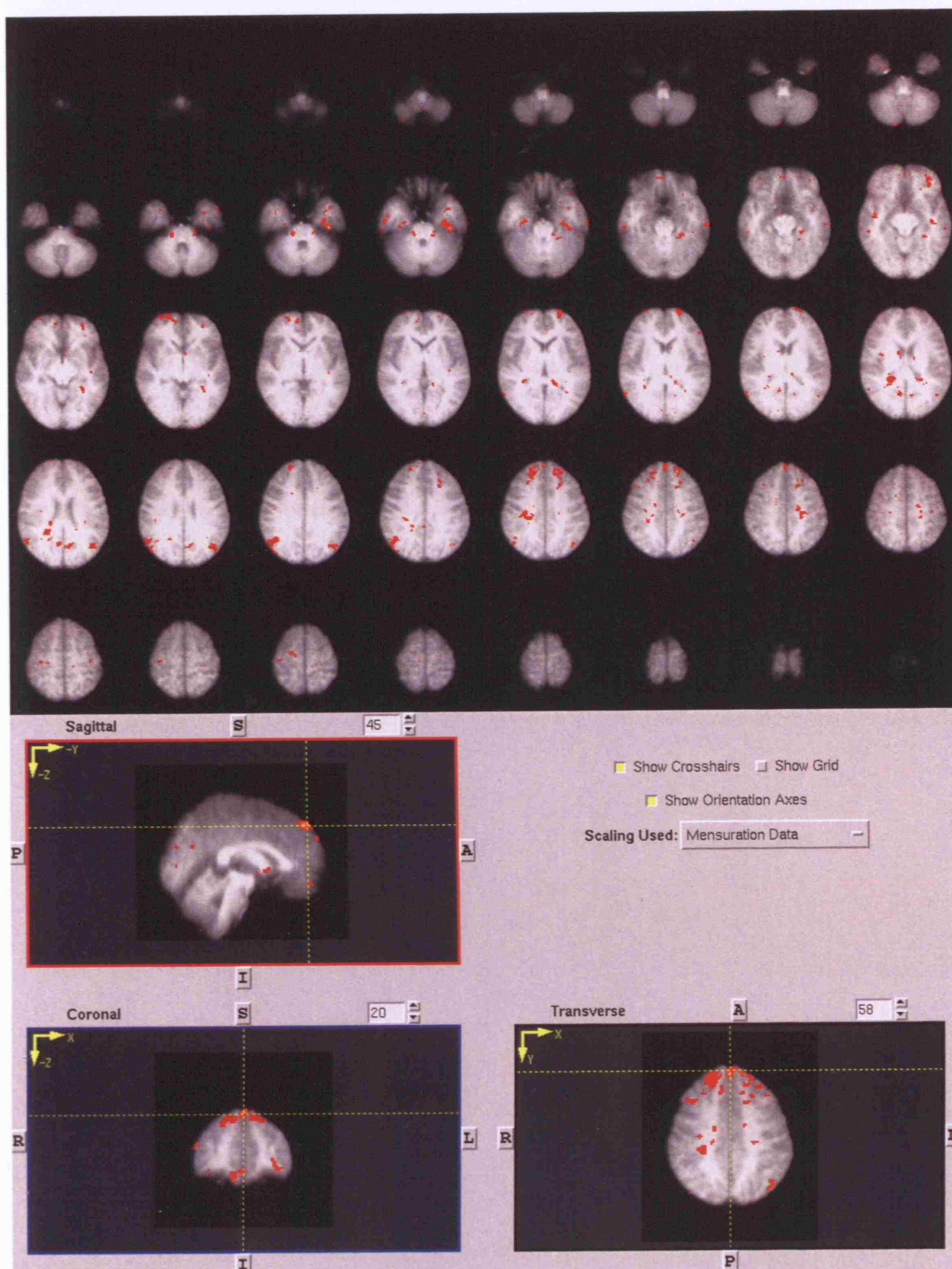


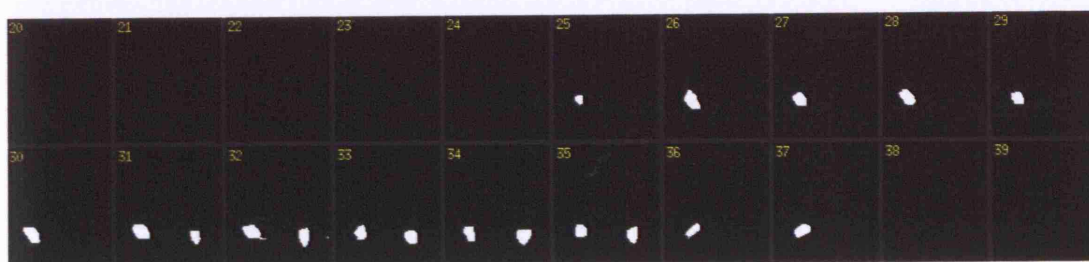
Figure 8
 Visual stimulation: group averaged subtraction data (n= 10) **sleep deprivation** minus normal sleep.
 FLAME analysis, uncorrected OLS, $p= 0.05$.



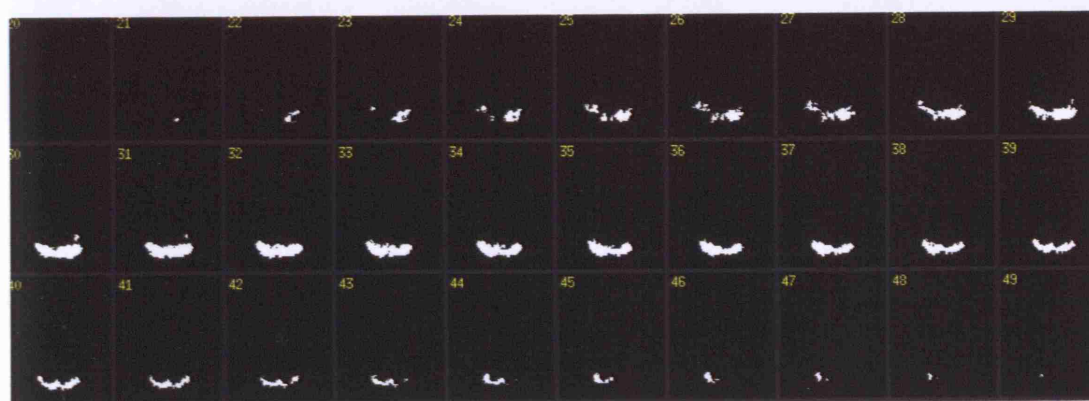
Medx coordinates	Maximum pixel value	Talairach Datapoint
2, 48, 46	4.05	R frontal lobe, BA 8
-30, 8, -36	3.51	L sup temporal gyrus, BA 38
-42, -22, -26	3.51	L inf temporal gyurs, BA 20
-68, -10, -30	3.45	L precentral gyrus, BA 6

Table 8

Maximum areas of pixel activation during visual stimulation: sleep deprivation minus normal sleep, with their Medx coordinates and Talairach atlas anatomical sites.



Visual Cortex Mask 1 - area V5/MT.



Visual Cortex Mask 2 - areas V1 and V2.

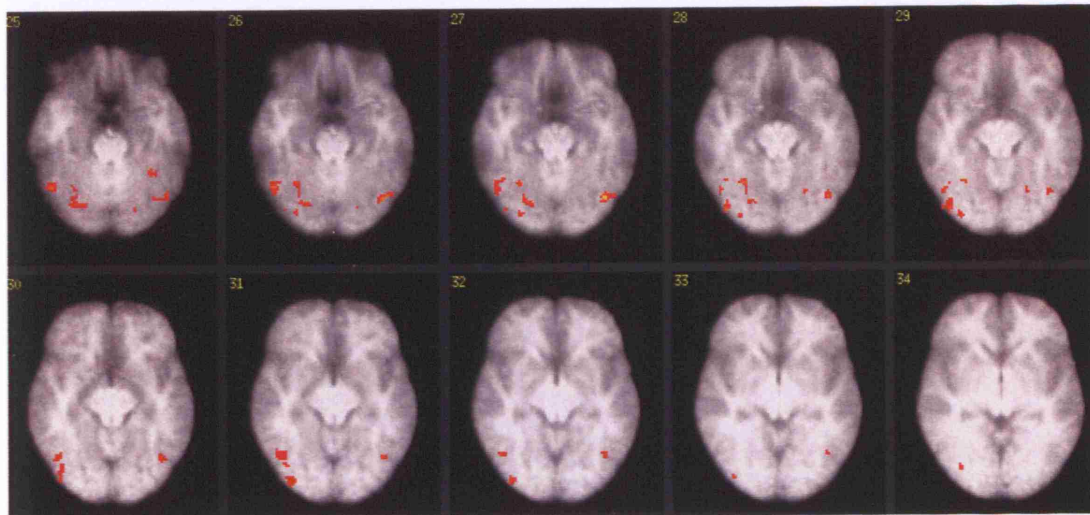


Figure 9 - Visual stimulation subtraction group analysis: activation with **mask 1** (area V5/MT); **normal sleep** minus sleep deprivation, uncorrected analysis, $p=0.01$.
Table of coordinates below.

Medx Coordinates	Maximum pixel value	Talairach Datapoint
-40, -68, -18	4.03	L Occipital lobe, BA 19
30, -56, -16	3.67	R Posterior Cerebellum
50, -58, -20	3.63	R Temporal Lobe, BA 37
34, -74, -24	3.63	R Posterior Cerebellum

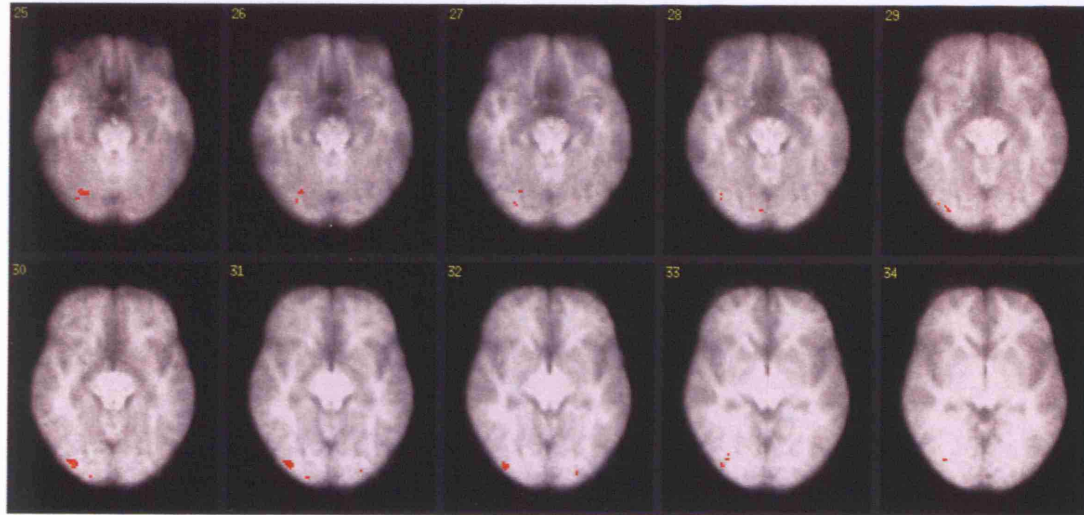


Figure 10 - Visual stimulation subtraction group analysis: activation with **mask 2 (primary visual cortex)**; **normal sleep** minus sleep deprivation, uncorrected analysis, $p=0.01$. Table of coordinates below.

Medx Coordinates	Maximum pixel value	Talairach Datapoint
34, -86, -12	3.58	R Inferior Occipital Gyrus, BA 18
42, -80, -14	3.29	R Inferior Occipital Gyrus, BA 18
26, -72, -22	3.28	R Posterior Cerebellum
38, -84, -6	3.01	R Inferior Occipital Gyrus, BA 18

Subject	Max N Slp V5 (mask 1)	Max Slp Dep V5 (mask 1)	Max N Slp V1V2 (mask 2)	Max Slp Dep V1V2 (mask 2)
6517	989.6	461.0	1327.0	862.5
6520	533.1	992.1	1035.2	1558.8
6518	415.6	375.9	1017.0	743.6
5492	1471.4	1081.8	1688.2	1488.8
5870	957.3	1027.2	1177.9	1125.7
5491	910.0	619.4	1050.7	659.7
5490	1392.3	1080.2	1588.3	1586.5
5493	1727.8	1180.3	1727.8	1204.7
5601	931.0	667.5	1321.1	667.5
5600	938.3	638.6	1266.1	1127.1
Mean SD	1026.6 (405.1)	812.4 (290.6)	1320.0 (267.2)	1105.5 (357.3)
p		p=0.05		p=0.72

Table 4

Individual subject maximum pixel activation during visual stimulation, following mask thresholding, before and after sleep deprivation.

V5 (mask 1) = V5 visual cortex mask

V1V2 (mask 2) = area V1 and V2 visual cortex mask

Max = maximal voxel activation (Arbitrary Units)

N Slp = after normal sleep

Slp Dep = after sleep deprivation

p = paired t-test

fMRI Results - Tracking

Analysis of the fMRI tracking data pre and post sleep deprivation aimed to determine whether a brain activation deficit could explain the impairments in tracking and steering associated with sleep deprivation. Tracking and driving require complex neurological processes, controlled by a number of pathways, integrated by a number of brain areas. Analysis of the activation of specific brain areas aimed to establish whether reduced activation of these areas might be associated with the impaired steering and tracking associated with sleep deprivation. Specific brain areas of interest, integral to tracking and steering are the motor cortex, cerebellum and areas involved in the detection of motion. Additional areas of interest are the frontal lobe (involved in task attention), and the precuneus (involved in assessment of the surrounding environment).

The fMRI tracking data was analysed as previously described, at variable threshold levels. Analysis of the tracking data involves a complex general linear model and a large number of variables. Eight COPE images are generated for each subject - four for each of the four tracking speeds, one for all speeds combined, one for increasing speed, one for decreasing speed, and one for tracking error. Programmes in Medx were used to generate local maxima and coordinates for the various parameter estimate (PE) images. These were then assessed by the computerised version of the Talairach and Tournoux 1958 brain atlas.

There was no difference between the fMRI data collected during tracking at visit 3 (baseline) or after normal sleep (visit 4 or 5). Thus the data presented are a comparison of the data collected after normal sleep (visit 4 or 5) and after the period of total sleep deprivation (visit 4 or 5) in random order.

Tracking - all speeds

Figure 11 shows the group averaged tracking data at 'all' speeds, following normal sleep, and figure 12 shows the same data following sleep deprivation (both $n=10$). Both of these analyses uses a FLAME (FMRIB's local analysis of mixed effects) analysis, with $p=0.01$, $Z=2.3$. Figure 12 shows an unexpected area of apparent white matter activation in the cortex, for which there are several potential explanations. This may represent an area of spatial blurring. The group analysis here requires the registration of different brain areas into a common 3 dimensional space, requiring spatial blurring, thus the average cluster location seen here may not be the exact position of the 'hot spot' of highest activation on the original individual scans. White matter activation is possible, as this brain type does have some local blood supply, and may therefore show some weak functional activation, compensating for local metabolic changes, though this activation would be expected to be fairly small however. The other potential explanation is that this activation represents the tail of a cluster in overlapping grey matter.

Figure 13 shows the design matrix for an individual subject's tracking analysis. Figures 14 and 15 show the design matrices for the group tracking analysis, and for the tracking group averaged subtraction analysis respectively.

Tracking - increasing speed

Figures 16 and 17 show group averaged representative brain slices following normal sleep, and following sleep deprivation respectively. These show how brain activation alters with increasing tracking speed, decreasing tracking speed, and with tracking error. Figure 16 shows frontal lobe activation at speed 25, with increasing motor cortex activation corresponding with increasing tracking speed, with cerebellar

activation appearing at the highest tracking speed (speed 250). Figure 17 shows the same representative brain slices following sleep deprivation. In contrast to normal sleep, this figure shows the absence of frontal cortex activation at low tracking speeds, and relatively less increased motor cortex activation with increasing speed. Figure 18 (and its respective table of coordinates) shows group averaged tracking data activation at increasing tracking speed, normal sleep minus sleep deprivation. There was no cerebellar activation at higher tracking speeds.

Tracking - speed 25 and 'all' speeds

Figures 19 to 21 show group averaged subtraction tracking analyses: group averaged data following normal sleep minus group averaged data following sleep deprivation, and vice versa. The brain areas differentially activated in the different sleep states are shown. Initial analysis assessed differential brain activation at low and high tracking speeds, as the primary tracking outcome is tracking error, which is closely related to tracking speed. Statistical thresholding of the activation areas seen determines the level of significance of the areas activated. These data are active using a FLAME uncorrected analysis, $p=0.05$ or $p=0.01$, $Z=2.3$. The areas of highest activation are in yellow, with areas of less significant activation in red.

Figure 19 shows group averaged tracking data at tracking speed 25, normal sleep minus sleep deprivation. Figure 20 shows group averaged tracking data at tracking speed 25, sleep deprivation minus normal sleep. Figure 21 show group averaged tracking data at 'all' tracking speeds, normal sleep minus sleep deprivation. The associated table show the activation maximum pixel values and their corresponding anatomical coordinates.

The maximum pixel levels are fairly modest, probably reflecting the small subject number, but clear differences in brain activation are seen. Activation of areas in the anterior cerebellum and right cingual gyrus are seen at low tracking speeds, following normal sleep, but not following sleep deprivation. Activation of the left temporal lobe occurred at 'all' tracking speeds following normal sleep, but not following sleep deprivation. Activation of the precuneus was seen following sleep deprivation, but not following normal sleep. The associated tables show the activation maximum pixel values, with their corresponding anatomical coordinates. Activation of the right frontal lobe, right cingulate gyrus and left posterior cerebellum, are seen

in association with increasing speed following normal sleep, but not following sleep deprivation.

Further tracking Analysis

Further assessment of other brain regions, the cerebellum and the precuneus (involved in attention and awareness of the surrounding environment) was carried out using anatomically defined masks using varying threshold levels. For tracking masks see page 123.

Precuneus: figure 22 shows precuneus activation following sleep deprivation, at speed 25 ($p= 0.01$, $Z= 2.3$). The corresponding table shows the anatomical coordinates. No other analysis showed precuneus activation. This suggests that the precuneus is active following sleep deprivation only, and at low tracking speeds. There was no precuneus activation following normal sleep.

Cerebellum: figure 23 shows a small area of activation in the posterior cerebellum following normal sleep, at speed 250. This area was not active following sleep deprivation, and may explain why tracking is impaired in this state, as it is under partial cerebellar control.

Table 6 (page 115) shows individual subject maximum pixel activation during tracking, following mask thresholding. There is a significant difference in maximum pixel activation following thresholding with the precuneus mask. Significantly greater activation of this area was seen following sleep deprivation, than following normal sleep. The precuneus is part of a network of brain areas which is 'tonically active' in

the 'resting' or 'passive' state, and is thought to be involved in subject orientation and spatial awareness.

The relative increase in precuneus activation following sleep deprivation suggests that the brain is in a 'resting' state, and not functioning as it would, if fully 'active'. The impaired tracking seen with sleep deprivation may therefore be partially explained by the persistence of precuneus activation. Movement to an 'active' state, where tracking is optimal may be impaired by the persistence of precuneus activation.

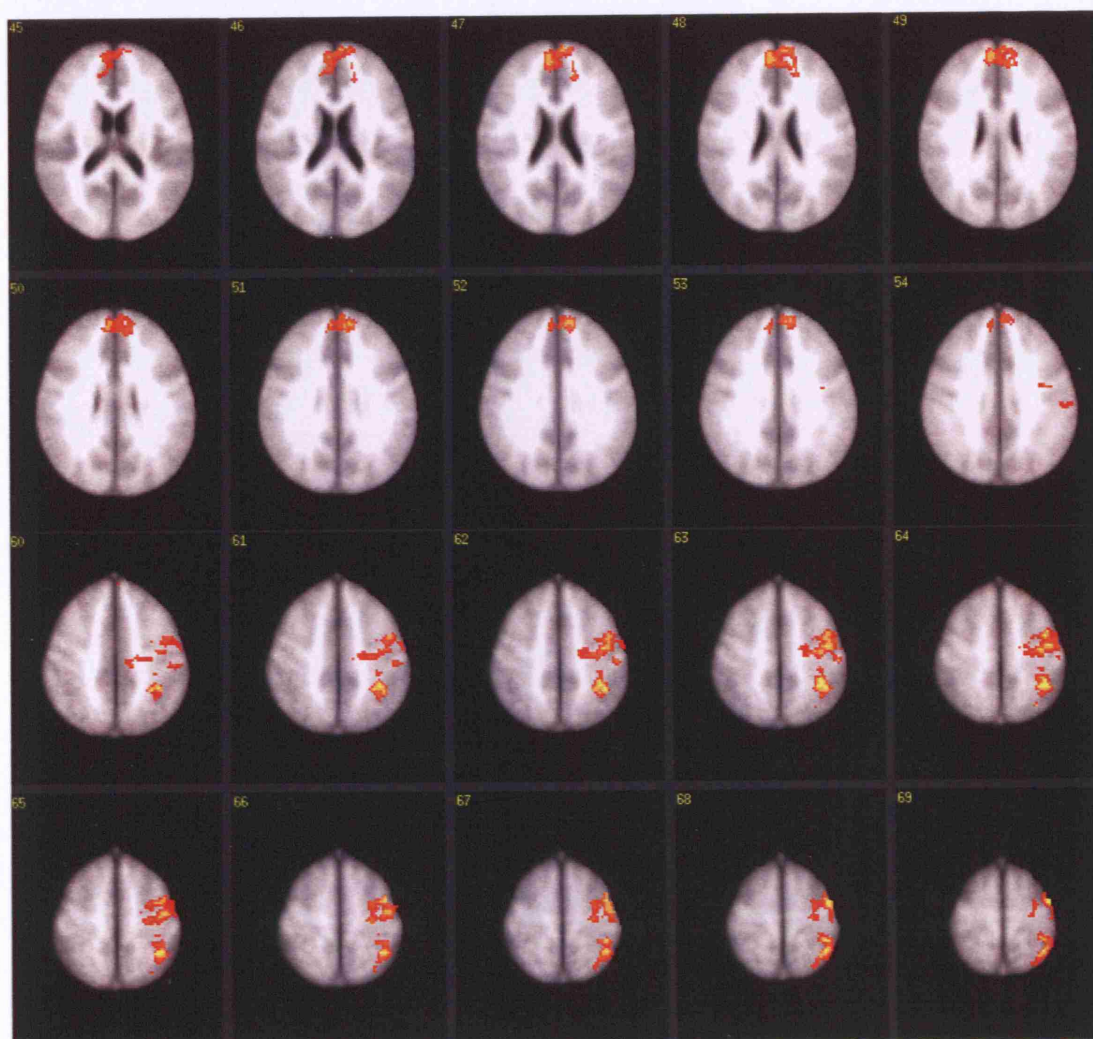


Figure 11
Tracking speed 'all': group averaged data (n= 10) after **normal sleep**.
 FLAME cluster analysis, $p= 0.01$, $Z= 2.3$.



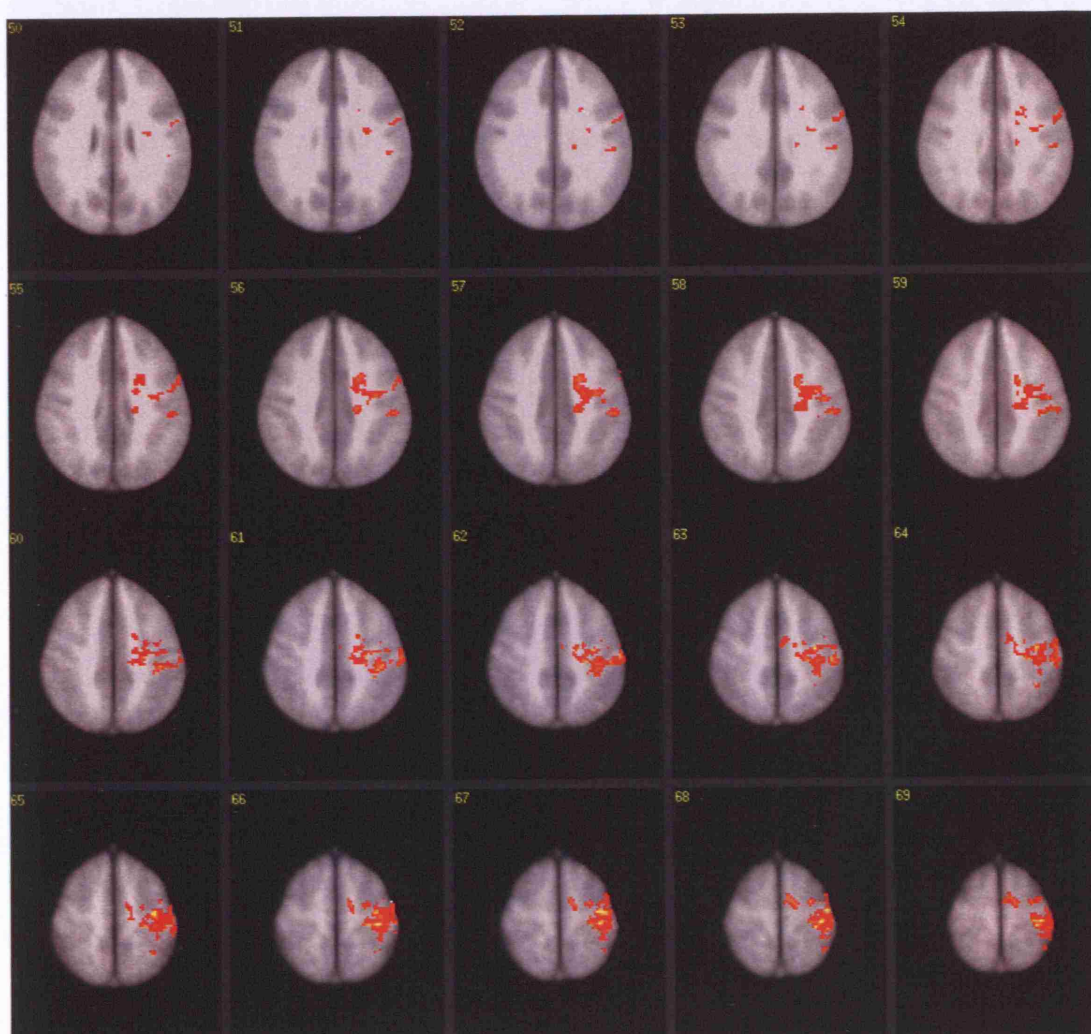


Figure 12
Tracking speed 'all': group averaged data (n= 10) after **sleep deprivation**.
 FLAME cluster analysis, $p= 0.01$, $Z= 2.3$.



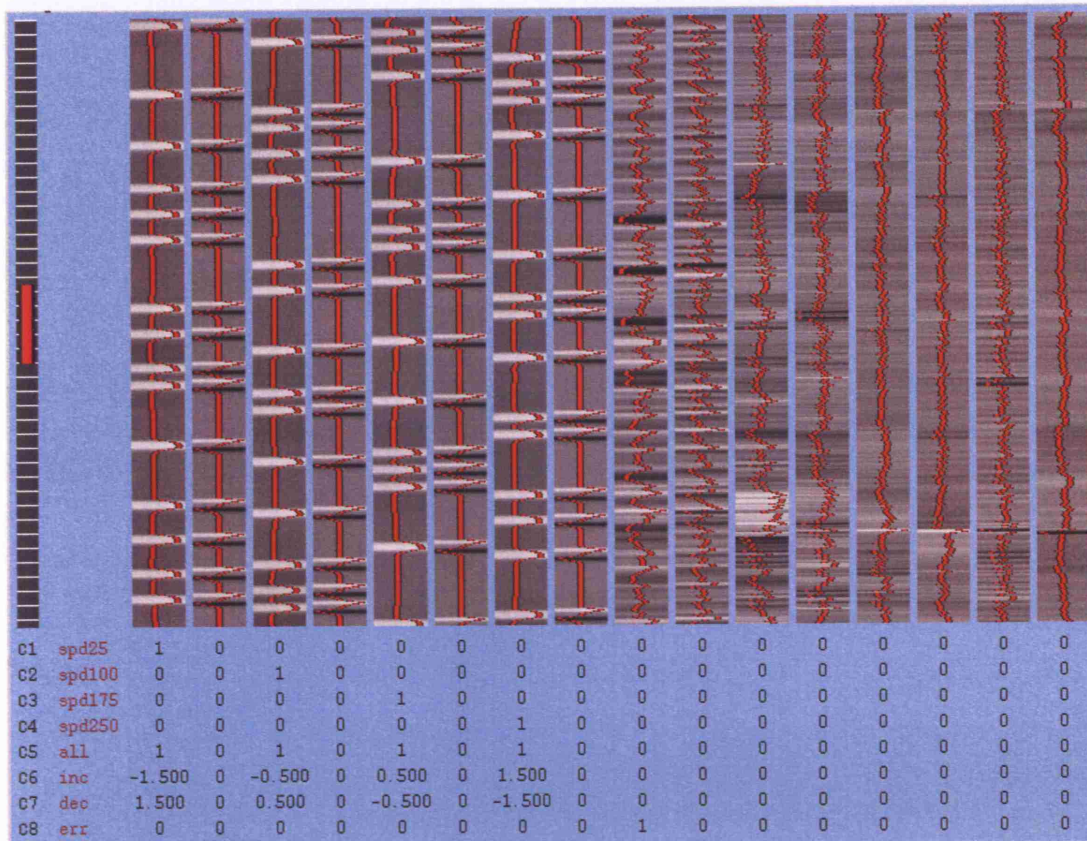


Figure 13

The design matrix for an individual subject's tracking analysis (the columns are 1 to 16, from left to right). EV1 (explanatory variable 1) in columns 1 and 2 (column 2 is the first derivative of column 1) explains the lowest speed (C1: spd25). Columns 3 to 8 explain increasing speeds (speed 100 to speed 250: spd100 to spd250). EV5 explains all speeds (all), EV6 explains increasing speed (inc), EV7 explains decreasing speed (dec) and EV8 explains tracking raw error (err).

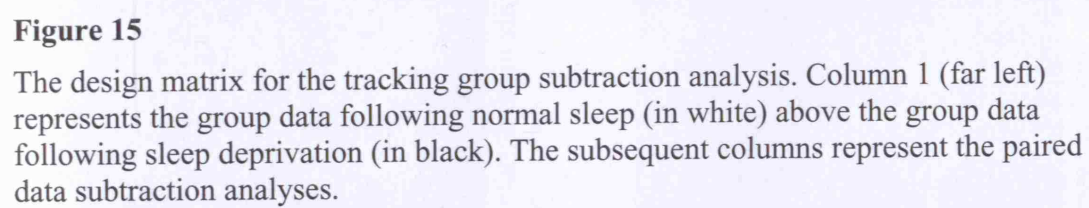
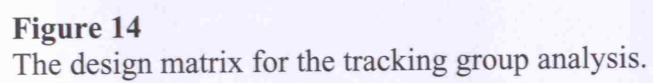
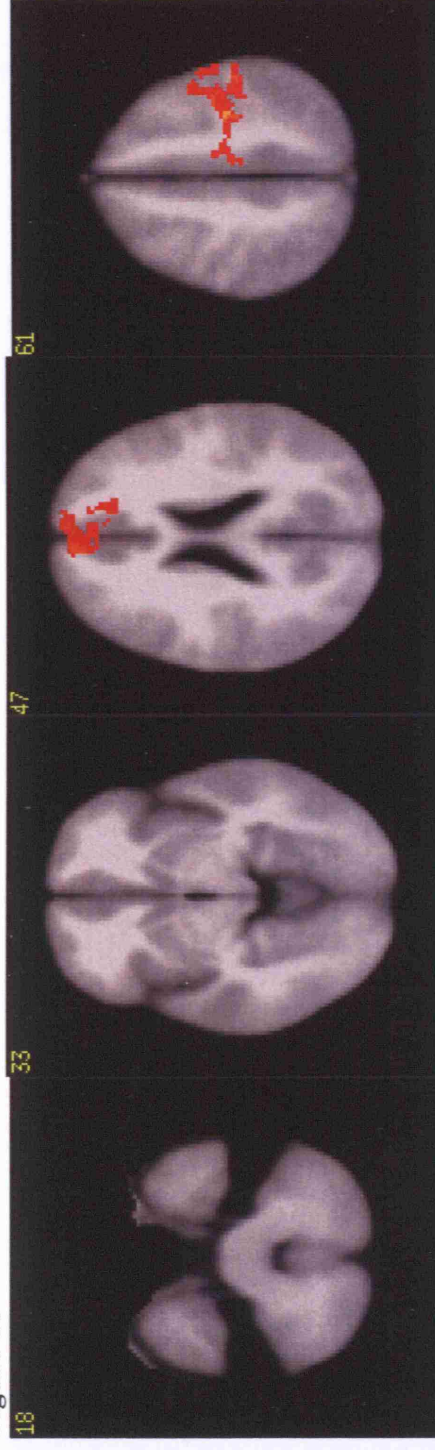
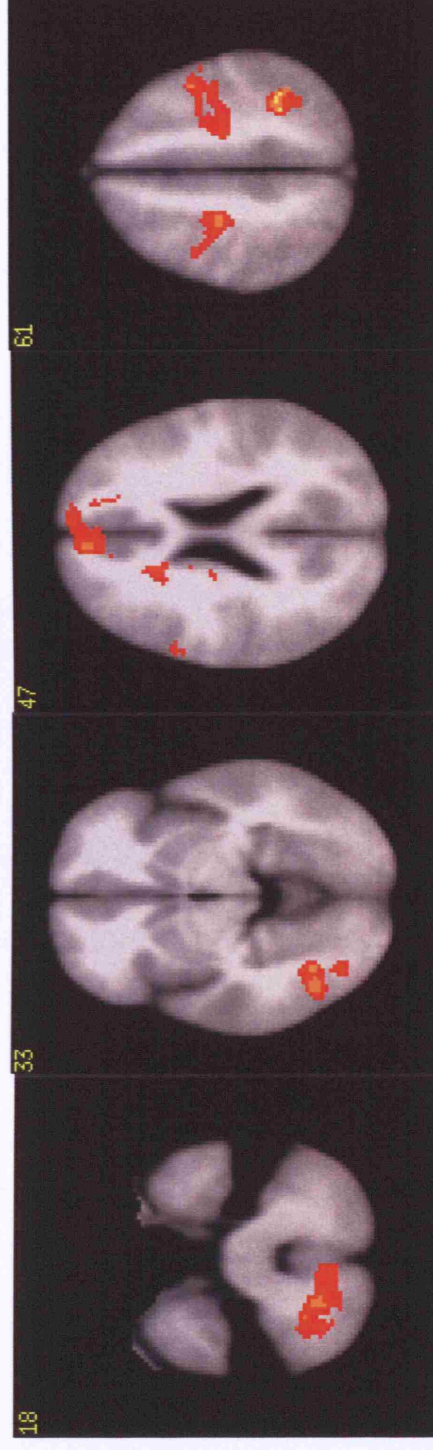


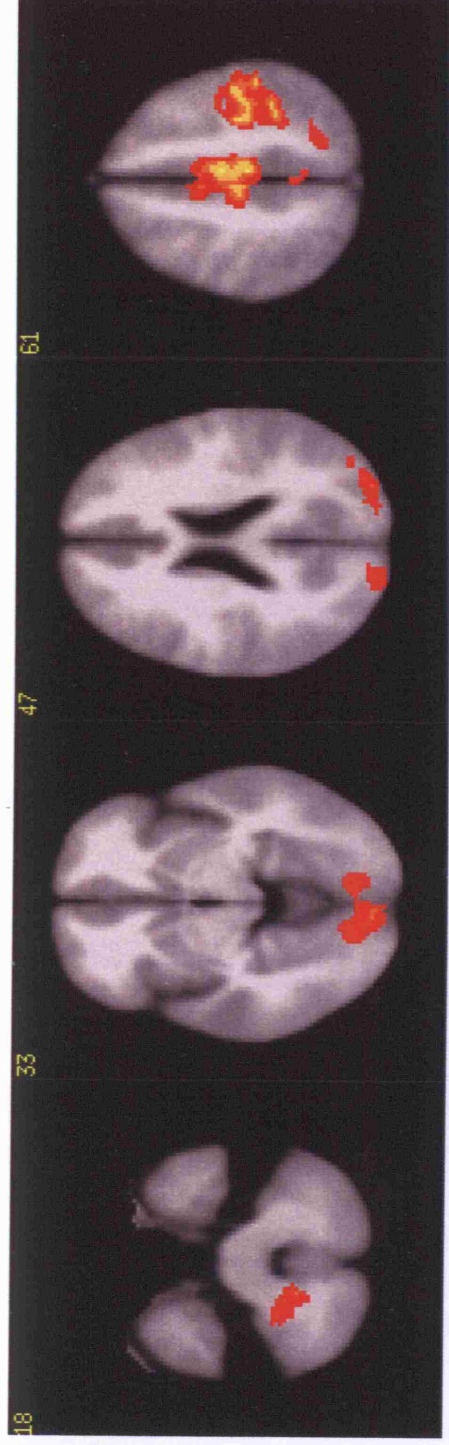
Figure 16



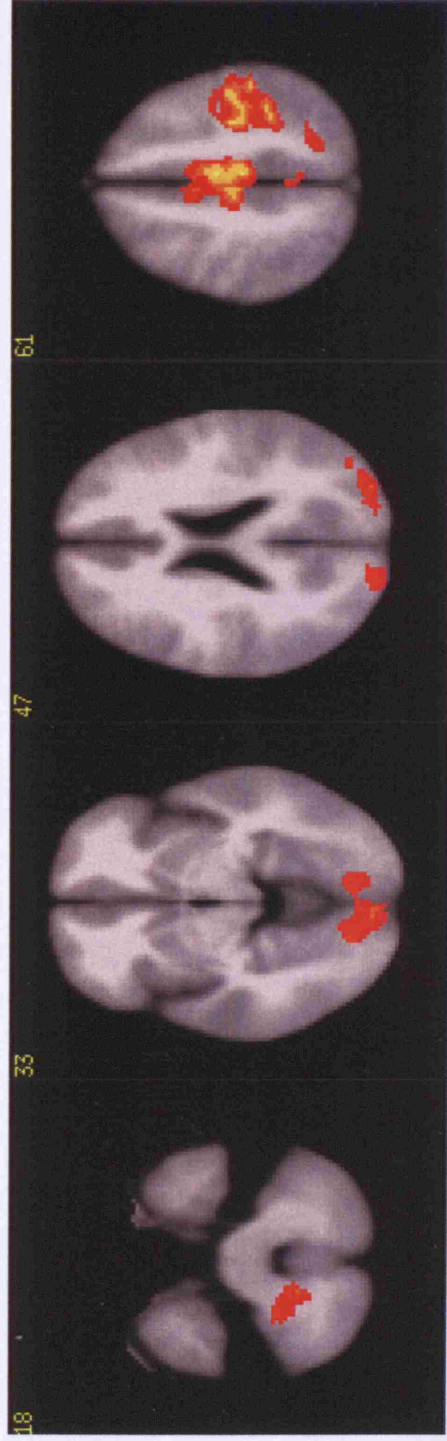
Representative brain slices - tracking after normal sleep: speed 25.



Representative brain slices - tracking after normal sleep: speed 250.

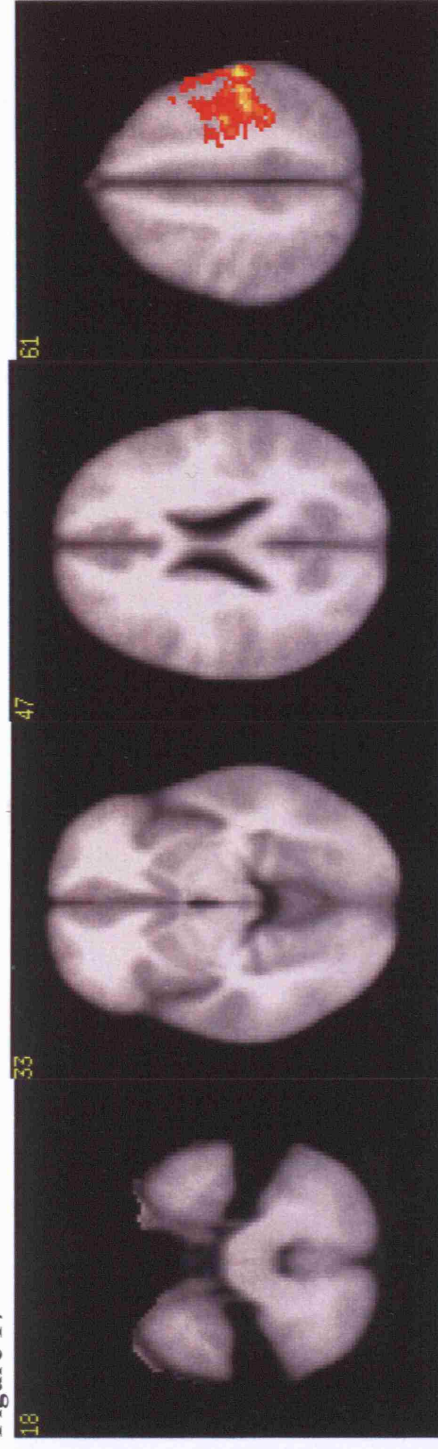


Representative brain slices - tracking after normal sleep: tracking error.

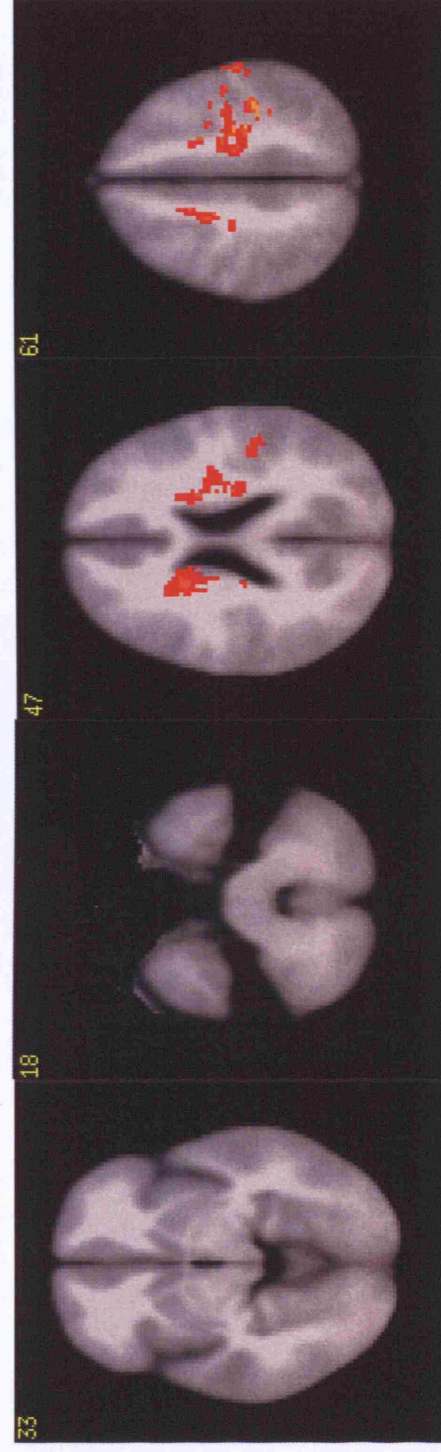


Representative brain slices - tracking after normal sleep: tracking error.

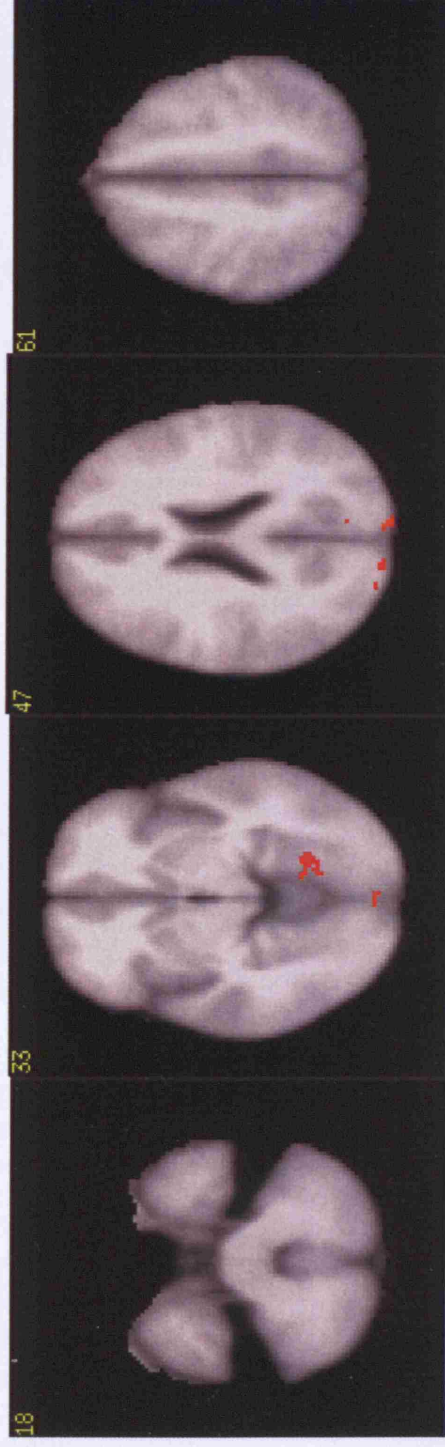
Figure 17



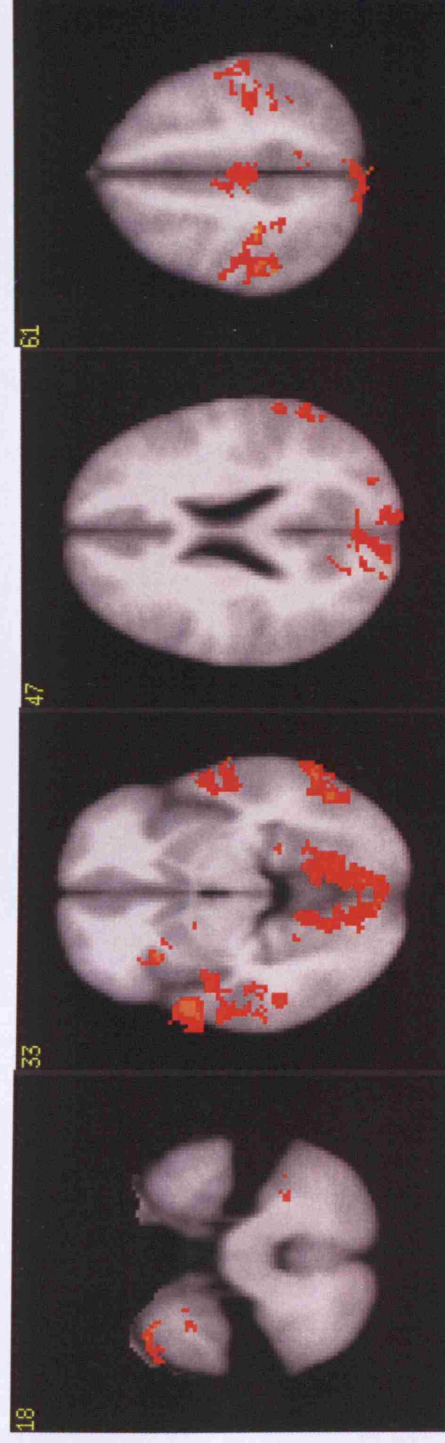
Representative brain slices - tracking after sleep deprivation: speed 25.



Representative brain slices- tracking after sleep deprivation: speed 250.



Representative brain slices - tracking after sleep deprivation: decreasing speed.



Representative brain slices - tracking after sleep deprivation: tracking error.

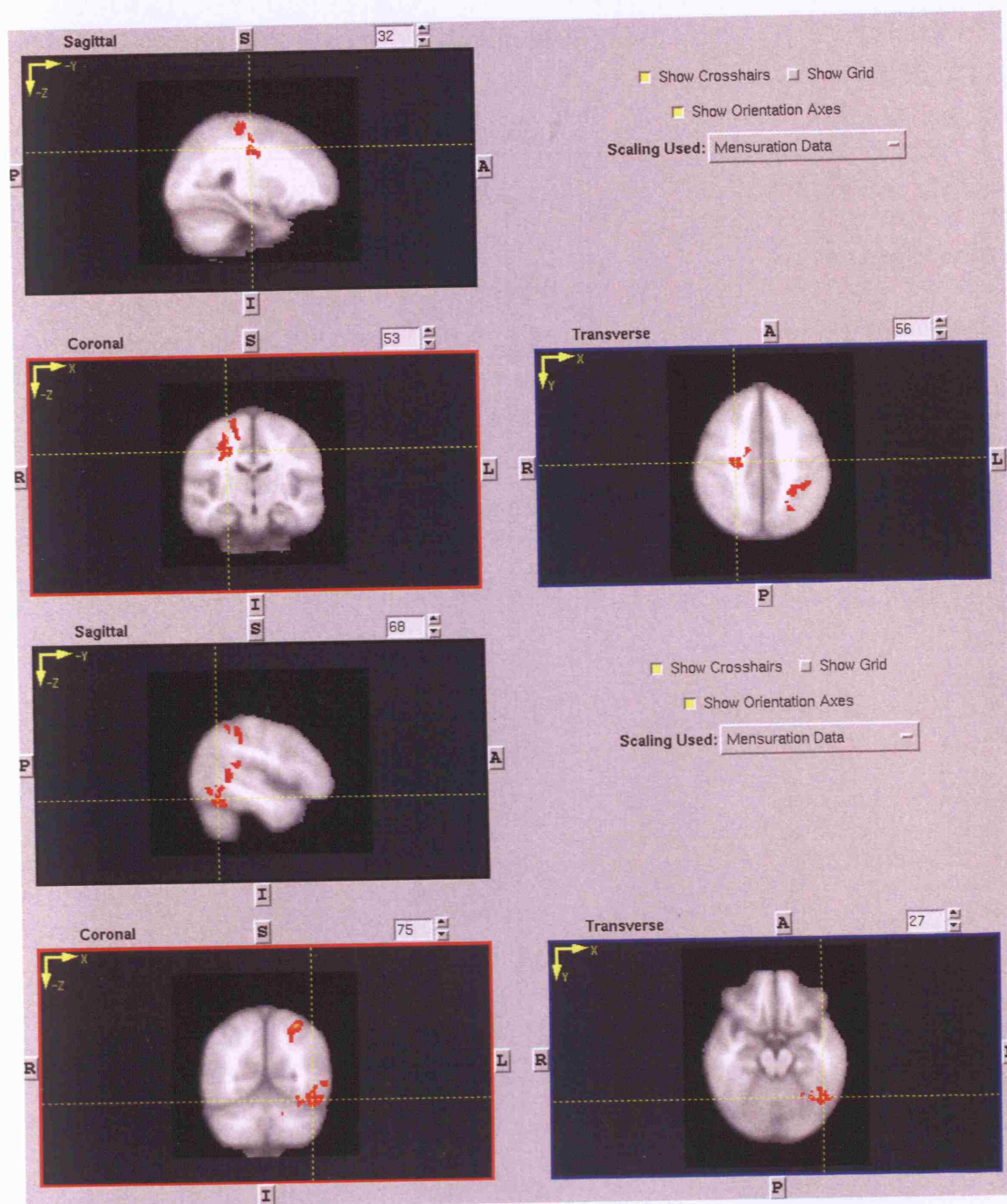


Figure 18

Figure 18
Increasing speed: normal subject group averaged subtraction data (n= 10) **normal**
sleep minus sleep deprivation. OLS cluster analysis, $p= 0.05$, $Z= 2.3$.

Medx coordinates	Maximum pixel value	Talairach Datapoint
-30, -58, 56	4.00	L sup parietal lobule, BA 7
16, -4, 46	3.66	R cingulate gyrus, BA 24
18, -16, 58	3.27	R frontal lobe, BA 6
-44, -46, 8	3.25	L middle temporal gyrus
-16, -56, -32	3.25	L posterior cerebellum

Table 18

Maximum areas of pixel activation during tracking at increasing speed (inc), normal sleep minus sleep deprivation, with their Medx coordinates and Talairach atlas anatomical sites.

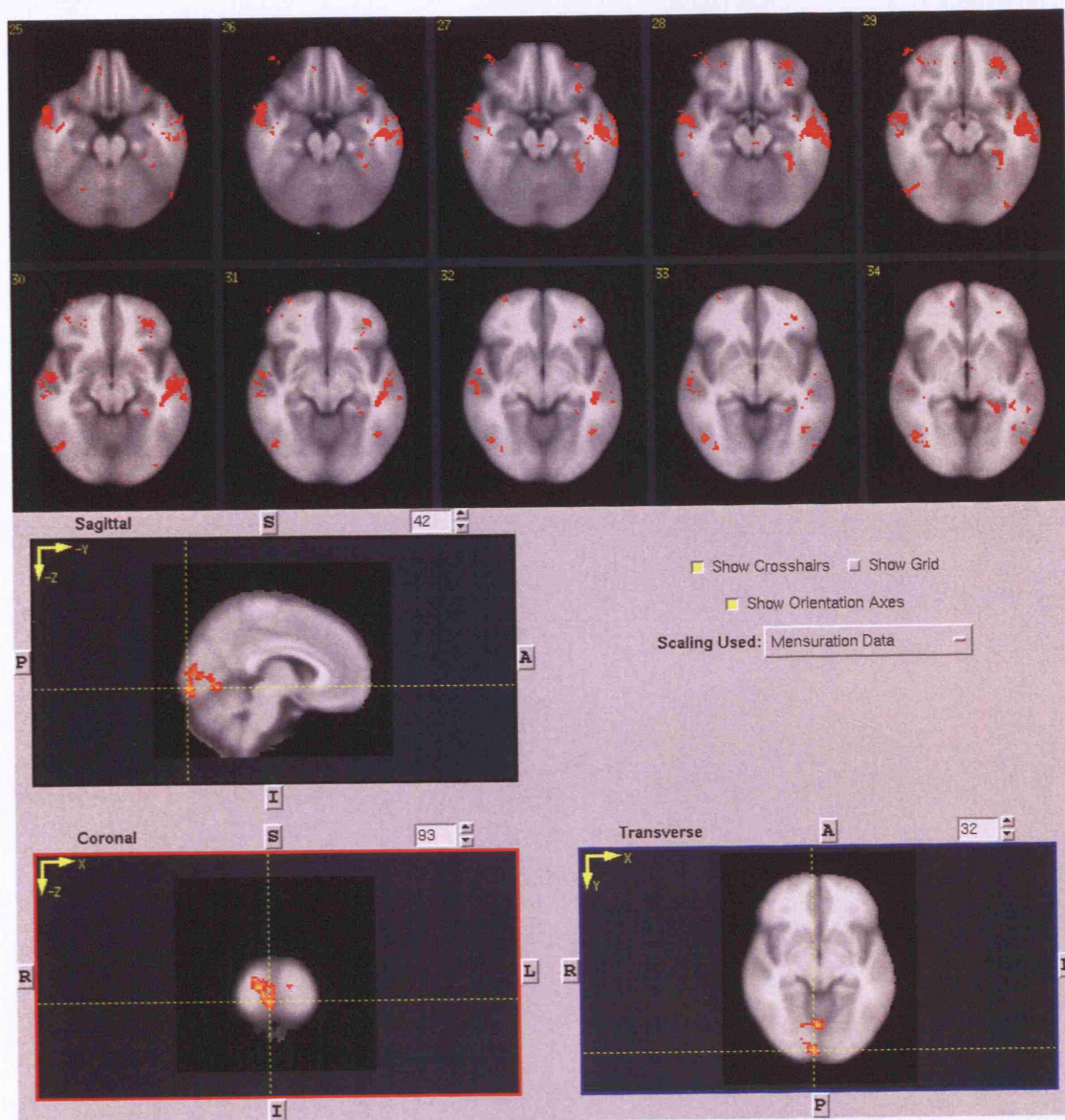


Figure 19
Tracking speed 25: normal subject group averaged subtraction data (n= 10) **normal**
sleep minus sleep deprivation.
 FLAME cluster analysis, $p= 0.01$, $Z= 2.3$.

Medx coordinates	Maximum pixel value	Talairach Datapoint
20, -92, 10	3.72	Right middle occipital gyrus, BA 18
14, -86, -10	3.71	Right Lingual gyrus, BA 18
8, -92, 6	3.70	Right cerebellum, BA17
6, -68, -6	3.67	Right anterior lobe cerebellum

Table 19
Maximum areas of pixel activation during tracking at speed 25, normal sleep minus sleep deprivation, with their Medx coordinates and Talairach atlas anatomical sites.

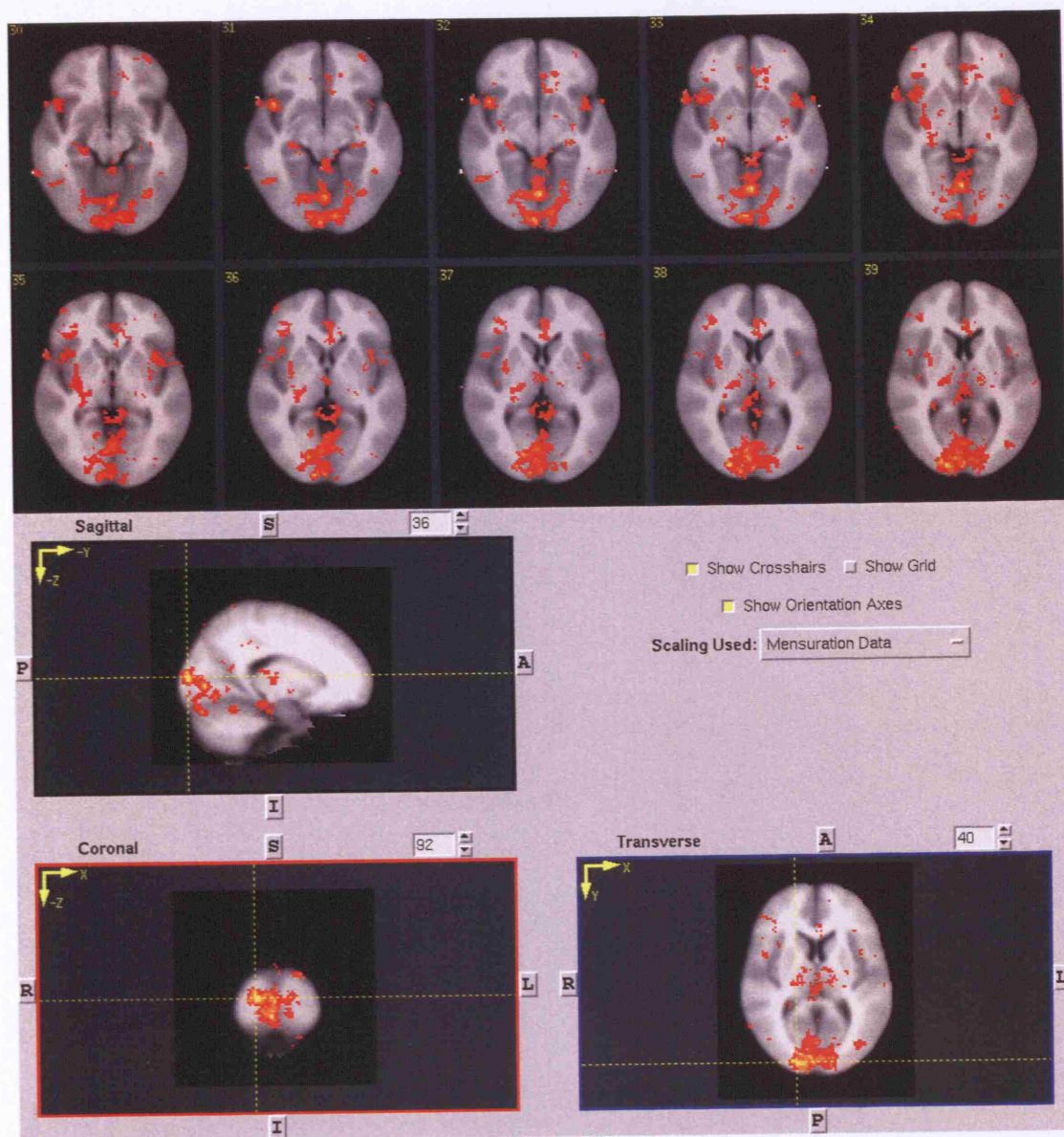


Figure 20
Tracking speed 25: normal subject group averaged subtraction data (n= 10) **sleep deprivation** minus normal sleep.
 FLAME uncorrected analysis, $p= 0.05$, $Z= 2.3$.

Medx coordinates	Maximum pixel value	Talairach Datapoint
16, -92, 4	5.8	R occipital lobe, cunues, BA 17
2, -90, 2	5.7	R occipital lobe, cunues, BA 17
2, -66, -10	5.7	R anterior cerebellum
0, -74, -12	4.80	L posterior cerebellum

Table 20
Maximum areas of pixel activation during tracking at speed 25, sleep deprivation minus normal sleep, with their Medx coordinates and Talairach atlas anatomical sites.

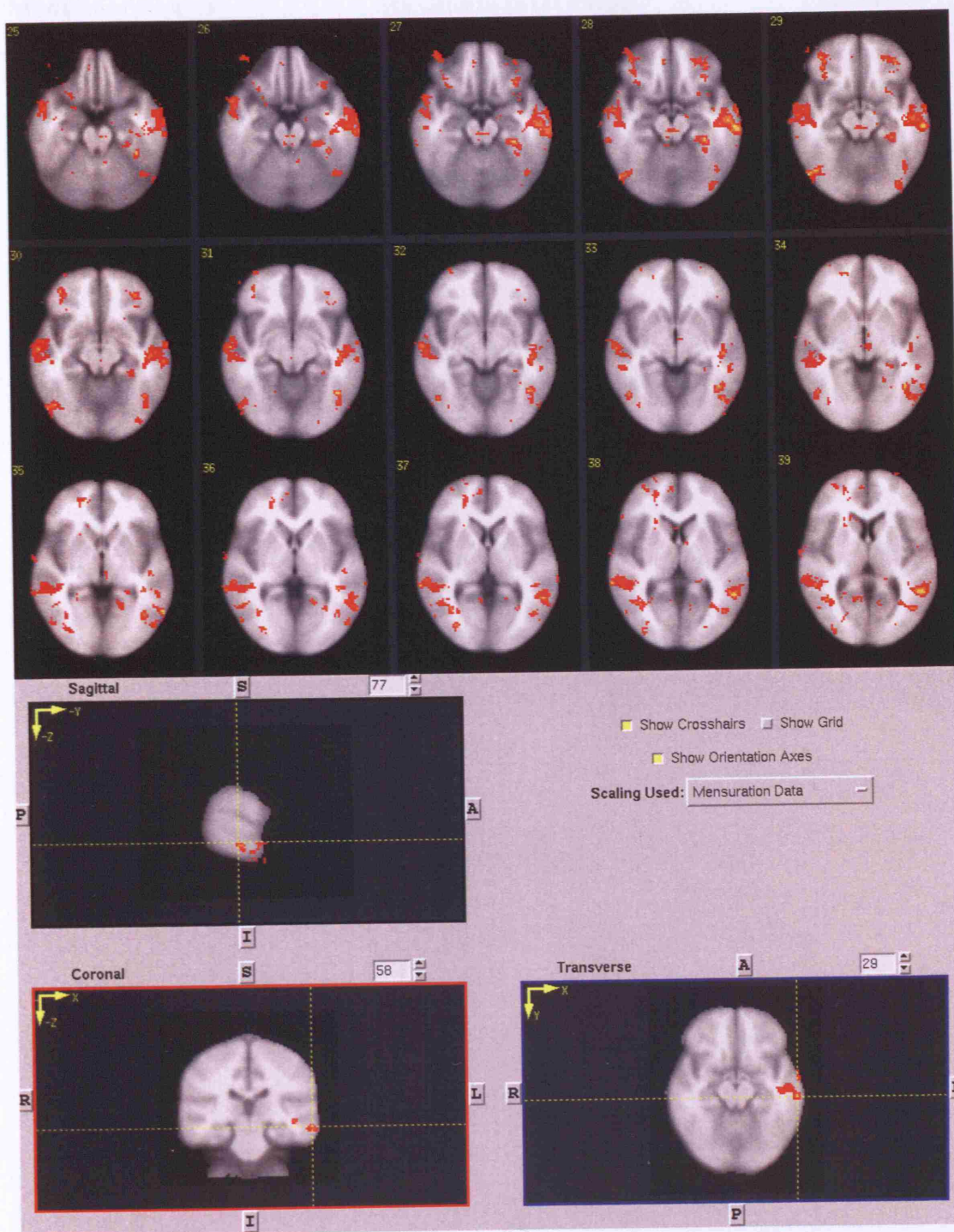


Figure 21
Tracking speed ‘all’: normal subject group averaged subtraction data (n= 10)
normal sleep minus sleep deprivation. OLS cluster analysis, $p= 0.05$, $Z= 2.3$.

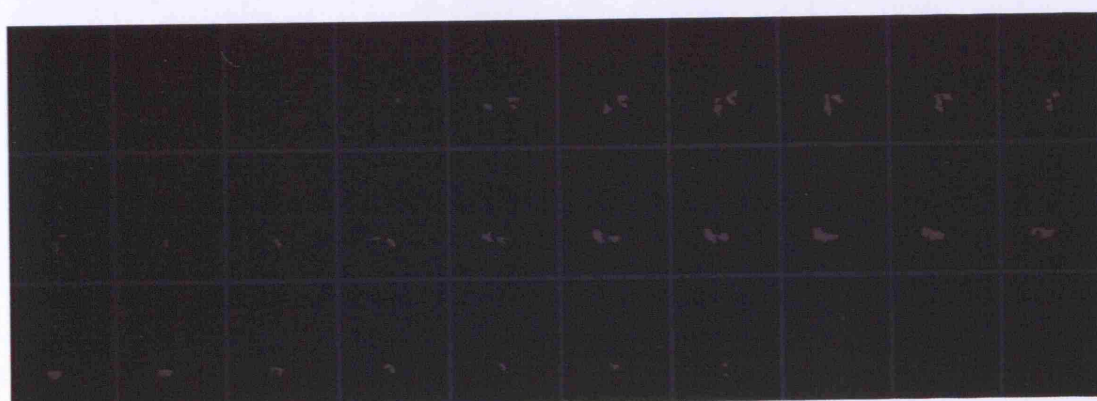
Medx coordinates	Maximum pixel value	Talairach Datapoint
-56, 16, -26	3.30	Left sup temporal gyrus, BA 38
-46, -18, -12	3.17	Left temporal lobe, BA 21
-60, -10, -30	3.14	Left inf temporal gyrus, BA 20

Table 21

Maximum areas of pixel activation during tracking speed (all), normal sleep minus sleep deprivation, with their Medx coordinates and Talairach atlas anatomical sites.



Tracking mask 1 - precuneus



Tracking mask 2 - cerebellum

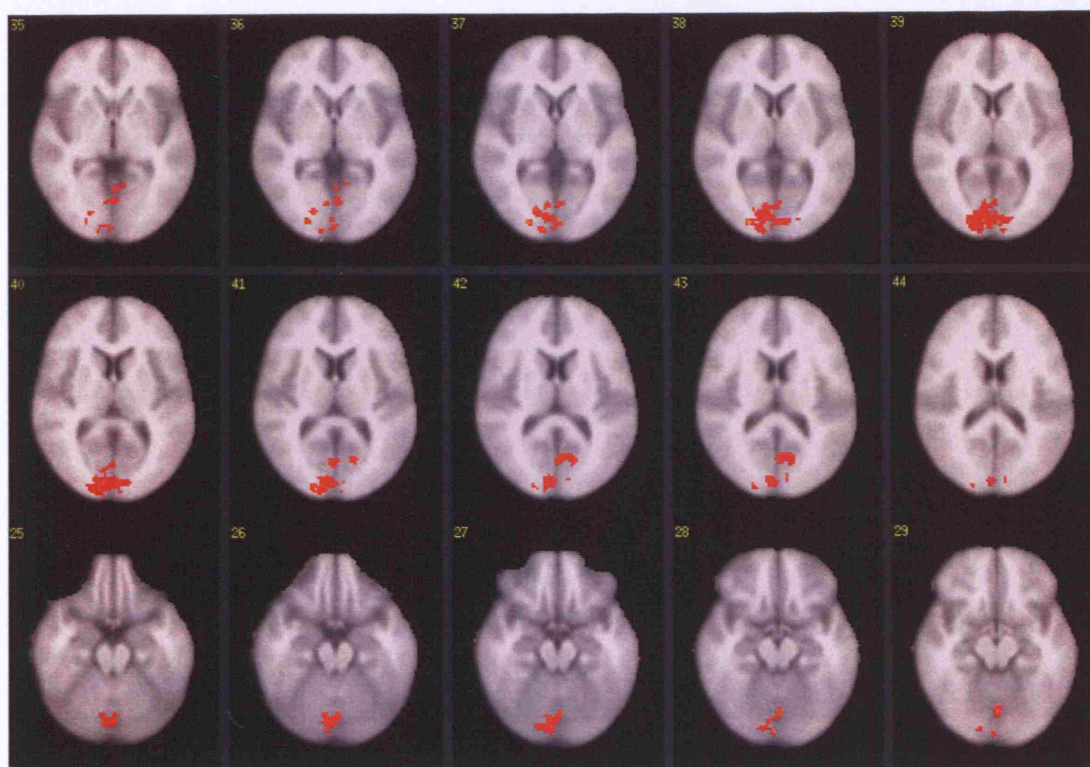


Figure 22

Tracking subtraction group analysis: activation with **precuneus mask; sleep deprivation** minus normal sleep, at speed 25. OLS cluster analysis, $p=0.01$, $Z=2.3$. Table of coordinates below.

Medx Coordinates	Maximum pixel value	Talairach Datapoint
18, -94, 10	4.04	Right occipital lobe, cuneus, BA 18
10, -88, 8	3.64	Right occipital lobe, cuneus, BA 17
12, -94, 2	3.63	Right occipital lobe, cuneus, BA 17
-4, -90, 6	3.63	Left occipital lobe, cuneus, BA 18
0, -66, -8	3.58	Left anterior lobe cerebellum

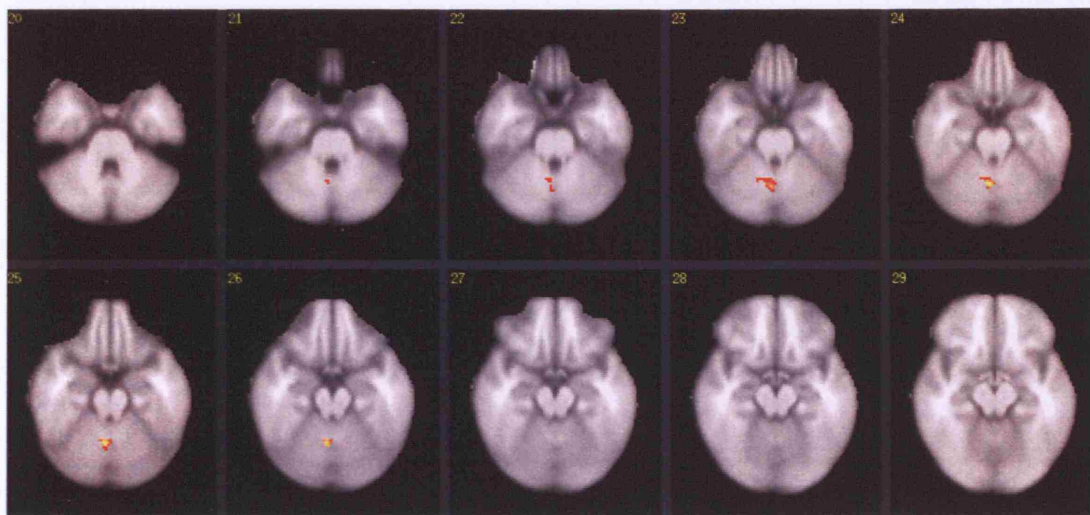


Figure 23 Mask analysis - tracking subtraction group analysis: activation with **cerebellar mask; normal sleep** minus sleep deprivation, at **speed 250 'spd250'**. OLS uncorrected analysis, $p=0.05$, $Z=2.3$. Table of coordinates below.

Medx Coordinates	Maximum pixel value	Talairach Datapoint
34, -66, -36	2.98	R posterior cerebellum
6, -72, -58	2.90	-
14, -66, -32	2.67	R posterior cerebellum

Subject Number	Max Precuneus NSlp	Max Precuneus SDep	Max Cerebellum NSlp	Max Cerebellum SDep
6517	85.8	173.4	78.3	76
6520	99.7	193.5	137.6	59
6518	13.2	169.3	55.6	62
5492	166.7	258.2	218.3	128.7
5431	115.3	361.6	107.5	173.3
5491	47.7	78.8	99.7	63.6
5490	115.8	174.1	158.3	107.5
5493	103.9	404.2	78.6	480.5
5601	59	132	64.4	87.9
5600	46.3	111.4	50.7	79.5
Mean	85.3	205.7	104.9	131.8
SD	44.5	105.6	52.9	127.6
p		0.02		0.56

Table 6

Individual subject maximum pixel activation during tracking (AU), before and after sleep deprivation.

NSlp = normal sleep, SDep = sleep deprivation.

Summary and discussion of results from study 1

The effect of sleep deprivation on fMRI brain activation during pure visual stimulation and coordinated hand/eye tracking

This initial study aimed to define the impairment in tracking and steering simulator performance, along with the brain activation changes, during visuo-motor tracking and visual stimulation, following up to 32 hours total sleep deprivation, in normal subjects. It enabled the complex study protocol to be fully tested in a group of healthy normal subjects, and established the baseline of impairment in subjects with no pathological sleep condition. All subjects had normal subjective and objective sleepiness at baseline (a study entry criteria). Subjects were assessed after 28 to 32 hours supervised total sleep deprivation.

Maintenance of wakefulness data

There was a range of objectively measured sleepiness following the sleep deprivation period, with a significant reduction in the number of minutes awake on the post sleep deprivation MWT. There was also a large range of sleepiness across the subjects, but no baseline predictors of post sleep deprivation MWT.

These results demonstrate the wide range of the effect of sleep deprivation in normal individuals, after a single extended period without sleep. There are several potential explanations for this. Banks et al have demonstrated the range of Osler test defined objective sleepiness in randomly selected normal subjects, with the lower limit of normal extending from about 26 minutes on a standard 40 minute Osler test [Banks 2004]. Kim et al have studied normal subjects, aiming to determine factors related to subjective daytime sleepiness in a normal population cohort [Kim 2007]. The study found a number of factors related to subjective sleepiness propensity

including lower education status and body mass index, as well as female gender and higher sleep debt for some areas, and male gender and older age for other areas. Thus subjective daytime sleepiness has a large number of determinants, making separating out predictors of subjective or objective sleepiness within this small study difficult. In addition, there are a number of drives to sleepiness, and similarly a number of drives to wakefulness, with much inter-individual variation. The number of hours sleep required by individuals varies considerably, with a reduced number of hours sleep leading to subjective impairment, but not necessarily an objective performance deficit, and vice versa. The subjects studied may have had a variable number of hours sleep per night in the week before the study, even though a one-off baseline MWT, and single ESS were within normal limits at the start of the study.

Divided Attention Steering Simulator

Subjects had their simulated steering performance assessed after normal sleep and after the period of total sleep deprivation. The two main outcome variables are the standard deviation from the centre drive lane position, and the time to register regularly appearing peripheral target stimuli (and the number of targets not registered at all). The measure of standard deviation from the ideal centre drive lane position is essentially a measure of tracking performance, and involves a constant alteration of steering position to track the curvature of the road. The registration of peripheral targets measures vigilance and attention, and the ability to concentrate on the two parallel tasks, dividing attention equally between the primary steering task, and the peripheral visual target registration task.

On average, the subjects performed less well following the sleep deprivation period. There was a greater range of steering performance following sleep

deprivation, with some subjects' performance deteriorating by a factor of more than 20. The mean reaction time to register peripheral target stimuli was also impaired following sleep deprivation.

This deterioration in steering performance is comparable to that seen by Hack et al [Hack 2001], who studied steering simulator performance following sleep deprivation, following alcohol intoxication and in untreated OSA. George et al have also assessed simulated steering following varying degrees of sleep deprivation [George 1996, George 1997]. These studies and others have confirmed the deterioration in steering and tracking performance seen with increasing sleep deprivation. The mechanism for the impaired performance is not clear, but it is likely to relate to a combination of impaired attention, low vigilance levels, and possibly deficits in motor coordination, that lead to an impaired ability to track accurately and effectively. The lapse hypothesis [Patrick 1896, Bills 1931] has been postulated as one contributing mechanism - whereby the lowered arousal level of sleep deprivation leads to increasing 'lapses' of concentration, either leading to delayed responses or a failure to respond altogether. The deterioration in steering performance is significant; Williamson et al have shown that a period of continuous sleep deprivation of 17 to 19 hours causes steering simulator performance decrements comparable to those seen with alcohol intoxication to the legal limit, with longer periods of wakefulness comparable to higher alcohol concentrations [Williamson 2000]. The effects of circadian rhythm may also contribute [Horne 1991, Horne 1996, Pack 1994, Langlois 1986].

The range of performance and deterioration in peripheral target reaction times in the subjects studied here was relatively less than the impairment on the steering task, suggesting that the subjects chose to concentrate on the less difficult, target

registration task, than on the more difficult steering task. This may also reflect deficits in attention, and the inability to coordinate two tasks simultaneously. No subjects missed any peripheral targets following normal sleep, and two subjects missed one target each, following sleep deprivation. This suggests that in the sleep deprived state, subjects are unable to divide attention equally between the two tasks, and that their limited vigilance and attention levels mean that only one task can be performed at a time, and with increased errors. This differential effect on performance of the two different tasks following sleep deprivation has also been shown by George et al, where patients sleep deprived due to narcolepsy, or due to untreated OSA were studied [George 1996].

Tracking data

Tracking data was collected during fMRI scanning after normal sleep, and following the sleep deprivation period. The main outcome variables are root mean squared (RMS) tracking error (Arbitrary Units) and lag time (milliseconds). There was a significant deterioration in tracking performance following the sleep deprivation period. As for the simulated steering, there was a range of deterioration between individual subjects, with some subjects' tracking error deteriorating by very little, and some by a factor of nearly three. Tracking raw error and lag time were both similarly impaired following sleep deprivation, in comparison to the differential deterioration seen in the two components of the steering simulator task. This is probably because the lag time is an integral measure of the tracking task, and not a separate component which can be 'ignored' in the same way that the registration of peripheral targets seems to have been, during simulated steering. As in the simulated steering task there was a greater range of performance following sleep deprivation,

showing that some subjects are relatively less impaired than others following the period of sleep deprivation.

The same mechanisms causing impaired tracking following sleep deprivation are likely to lead to impaired simulated steering, as tracking is the skill integral to steering; simulated steering is really another, more sophisticated way of measuring tracking. There are likely to be a combination of mechanisms causing the impairment, including deficits in motor coordination, reduced attention and vigilance levels, and the inability to concentrate on the task, and ignore peripheral distracting targets. Additional potential explanations include motor processing deficits and impaired visual processing; including possible reductions in the useful field of view.

One additional factor contributing to the poor performance post sleep deprivation might be the possible relationship between memory consolidation and sleep deprivation. Sleep is needed for the laying down of new memory, with impaired recollection of learned tasks in subjects sleep deprived on the post learning night [Maquet 1999]. REM sleep is particularly important for the laying down of new memory, and there is likely to be a reduction in REM sleep post sleep deprivation [Saxvig 2007, Marshall 2007]. This may be an additional factor contributing to the poor performance seen. Poor memory consolidation of all the learned tasks is one possible contributing factor to the poor performance seen, however the subjects task training was several nights before the sleep deprivation nights, and always included at least 5 nights of normal sleep prior to any study nights.

fMRI data - Visual stimulation

Subjects underwent passive viewing of a potent visual stimulus before and after the period of total sleep deprivation. The yellow/blue flashing chequerboard

caused maximal activation in the occipital cortex bilaterally, as expected. However differences in activation of the extra striate visual cortex and other brain areas were seen in the two different sleep states. Subtraction group scan analysis following normal sleep showed activation in the occipital lobe, around BA 19, with no frontal lobe activation. Subtraction group scan analysis following sleep deprivation showed activation predominantly in the frontal lobes, with lesser activation of areas in the left temporal lobe, and no occipital lobe activation. This suggests that sleep deprivation somehow leads to reduced activation of occipital lobe visual cortex areas, and that these areas may be more susceptible to the effects of sleep deprivation, needing sleep to restore normal activation and function.

The visual cortex area differentially activated following normal sleep falls within the boundaries of area V5/MT [Hasnain 1998]. Hasnain et al's coordinates are 73% sensitive for the detection of area V5 in the left cerebral hemisphere, and 82% sensitive for the right cerebral hemisphere. It is expected that a stimulus containing movement, such as a flashing chequerboard will activate this motion sensitive area of the visual cortex. Individual subject maximum pixel activation during visual stimulation confirmed greater activation of area V5 following normal sleep, than following sleep deprivation.

Area V5 of the visual cortex is integral to the detection of subtle visual motion [Maunsell 1983, Livingston 1988], and this has been confirmed in fMRI and primate lesional studies [Talcott 2000, Eden 1996]. This current data shows that sleep deprivation leads to impaired activation of area V5, but gives no information about the function of this visual cortex area in the sleep deprived state. There are several potential explanations for these findings. It is possible that sleep deprivation leads to a global, non-specific 'deactivation' of various brain areas, and that this effect is seen on

this specific visual cortex area. PET studies using 18-fluorine-2-deoxyglucose (18-FDG), have shown a reduced global cerebral metabolic rate of glucose during the performance of specific tasks following 85 hours of total sleep deprivation [Thomas 2000]. Drummond et al have shown in a series of fMRI studies, that task dependent reductions and increases in brain activation occur in different brain regions with sleep deprivation. The mechanism for the alteration in the cerebral and behavioural responses to sleep deprivation are unexplained, but the regional variation in brain activation seen is thought to relate to regional specialisation to specific cognitive demands [Drummond 1999-2004]. It is clear that the brain is able to respond to the effects of sleep deprivation by the recruitment of additional brain regions, related both to the specific task being employed, and the generalised need for increased attention. Motor cortical excitability has also been found to be attenuated after sleep deprivation, as assessed using transcranial magnetic stimulation over the motor cortex, so a global change in brain activation is a potential explanation [Civardi 2001].

However, if this is the explanation, then a similar, non-specific 'deactivation' effect on the primary visual cortex, and the rest of the brain might have been expected, but no similar effect was seen. An alternative explanation is that the highly metabolically active magnocells supplying the magnocellular pathway (and strongly serving visual cortex area V5/MT), are more susceptible to the effects of sleep deprivation. It is likely that these cells need sleep in order to restore normal function, hence the specific area of reduced activation seen. This might also apply to the frontal cortex, where highly active neurones are more susceptible to the effects of sleep deprivation. Though in this current study bilateral frontal lobe activation was seen following sleep deprivation, not reduced activation, as might have been expected.

Frontal lobe activation is usually seen in association with task attention [Peers 2005].

The increased frontal cortex activation suggests that the subjects may have had to attend to the task to a greater degree when sleep deprived than following normal sleep, and are having to work harder to perform even at a reduced level.

Horne has shown that prefrontal cortex function is preferentially affected by sleep deprivation, and this has led to the 'prefrontal cortex theory' of sleep deprivation. This current study has shown increased activation of the frontal lobe following sleep deprivation, during performance of another, unrelated task. No measures of frontal lobe function were made in this study, but the increased activation is more likely to fit with greater frontal lobe function, rather than decreased function following sleep deprivation, which is contrary to Horne's theory. Global, non-specific and task specific responses to sleep deprivation are recognised, the recruitment of additional brain regions, including those related to the need for increased attention is recognised [Drummond, Thomas 2000]. The increased post sleep deprivation frontal lobe activation seen in this study may be a reflection of this.

The above results raised questions as to whether impaired function of visual cortex area V5 is associated with its reduced fMRI activation following sleep deprivation, and whether this might provide a potential explanation for some of the driving and tracking deficits seen with sleep deprivation.

fMRI data - Visuo-Motor Tracking

Tracking error and lag time were significantly impaired following sleep deprivation. Specific brain areas of interest, integral to tracking and steering are the motor cortex, cerebellum, frontal lobe (involved in task attention), and areas involved in the detection of motion.

During tracking, activation of the motor cortex and areas in the cerebellum was seen, as expected [Miall 2000, Miall 2001, Culham 1998]. Differential brain activation was seen pre and post sleep deprivation. The cuneus was the only area active after sleep deprivation, which was not active after normal sleep. This brain area is one of a number of areas active during passive 'resting', and is considered to be 'tonically active', continuously gathering information about the world around us [Shulman 1997, Mazoyer 2001, Laureys 1999]. The adjacent precuneus is active in tasks involving navigation, visual-spatial processing and visual imagery, as well as tracking [Roland 1995, Ghaem 1997]. The cuneus has been described as a 'central controller', or 'polymodal integration centre', and is more active in the resting condition than during performance of a task [Raichle 2001]. This suggests that in the state of sleep deprivation, the subjects were unable to move from a passive 'resting' state, to an active state, required for accurate tracking. Activation of the precuneus during tracking is likely to relate to the integration of visuo-spatial cues into the planning of coordinated movements [Miall 2001], and its increased activation, in association with cuneus activation after sleep deprivation suggests that greater visuo-spatial processing may have occurred after sleep deprivation, for subjects to try and maintain adequate tracking performance. Raichle et al have also shown that other areas of 'deactivation' in the resting state are seen in the extra-striate visual cortex, principally in the parietal and occipital lobes, suggesting that activation in these areas may be attenuated when focused attention is required, reflecting a diversion of resources to the task. The evolutionary theory behind this is that the detection of, for example predators, should not require the intentional allocation of attentional resources, but should be automatic and continuously available [Raichle 2001]. These brain areas also have a high baseline resting metabolic rate, and this may also explain

their susceptibility. This current study did not identify activation of these specific areas.

Increasing speed following normal sleep lead to activation of the cerebellum, and right cingulate gyrus. These areas were not active following sleep deprivation. Previous studies have shown activation of the frontal lobes and cerebellar nuclei with new motor learning [Jueptner 1997]. The subjects were trained to stable performance on the task, but it is possible that they continued to learn with further task performance. The frontal lobe was active following normal sleep and sleep deprivation suggesting that subjects paid attention to the task [Nobre 2001]. Previous fMRI studies have suggested the activation of a 'default mode network' of brain areas in association with poorer performance on reaction time tasks following sleep deprivation. This network includes the frontal and posterior midline regions. The right frontal cortex activation and poor tracking performance in this current study may reflect the move to a 'default' mode of brain function [Drummond 2005]. Additional sleep deprivation studies suggest that increased compensatory brain activation is task dependent, and that the activation of non-specific brain areas can be both beneficial to the task, and interfere with task performance, depending on the brain regions involved [Drummond 2005, Drummond 2006].

The cerebellum is involved in control of movement [Miall 2000], as well as attention, error detection and correction, and motor learning [Jenkins 1997, Clower 2001, Clower 2005, Flament 1986]. Increased cerebellar activity has been seen with higher tracking errors with independent, as opposed to coordinated hand eye tracking [Miall 2001]. Tracking speed and velocity errors are known to activate the cerebellum, but these were not associated with increased cerebellar activation following sleep deprivation in this study. In motor learning tasks, where errors are

initially high, greater cerebellar activity is seen early on, with reducing cerebellar activity as the task is learnt [Jenkins 1997, Imamizu 2000]. Increased anterior and posterior cerebellar activation was seen in this study with normal sleep, where tracking errors were lower than following sleep deprivation. This increased activation might be related to greater attention to the task, with greater error detection and correction (explaining better tracking performance) than following sleep deprivation.

The neural correlates of both active and passive driving (during which the subject holds the steering wheel, while the researcher steers the car) have been assessed during fMRI scanning. Similar brain activation is seen in both steering conditions. As expected, the areas activated correlate with the activation seen during performance of the tracking paradigm, in particular activation in the occipital and parietal regions bilaterally, the sensorimotor cortex and cerebellum [Walter 2001]. A similar fMRI study has assessed the neural correlates of driving at a safe distance - a task in which the subject uses a joystick to control his driving speed, in order to remain at a constant distance from the car ahead, which travels at a variable speed. Again similar areas of activation are seen, with activation of the cerebellum, basal ganglia, premotor cortex and thalamus [Uchiyama 2003]. These are similar to the areas of activation seen in this study.

There was no differential motor cortex activity after normal sleep and after sleep deprivation. This suggests similar motor cortex activation in the two sleep states, despite the increase in tracking error following sleep deprivation (which might be expected to be associated with greater joystick movement and therefore greater motor cortex activation).

Summary

This study has shown significantly impaired driving and tracking performance in association with objective sleepiness following up to 32 hours total sleep deprivation. Sleep deprivation is associated with reduced activation of visual cortex area V5, an area integral to the detection of motion. Persistence of precuneus/cuneus activation during tracking following sleep deprivation suggests that subjects may be unable to move from a passive 'resting' state, to an active state, required for accurate task performance.

Chapter 3

Study 2 - The effect of total sleep deprivation on coherent visual motion and visual form detection in normal subjects

Introduction

Analysis of the fMRI visual stimulation data from study 1 raised a number of further questions. This study showed reduced activation of visual cortex area V5 following sleep deprivation, with no reduction in activation following normal sleep. This area of the visual cortex is integral to the detection of subtle visual motion [Maunsell 1983, Livingston 1988]. Reduced activation of this brain area in the sleep deprived state may help to explain the tracking and driving impairment associated with sleep deprivation, if it is associated with a functional impairment of coherent visual motion detection. Further exploration of this impairment, with an investigation as to whether there is an associated behavioural impairment in visual motion detection was carried out.

Two neural pathways are involved in the detection of coherent visual motion, carrying information from the retina to the visual cortex. The magnocellular and parvocellular pathways are linked, but independent. The magnocellular pathway is more sensitive to low spatial frequency information, moving or flickering stimuli. Magnocells have high temporal resolution and process motion, depth and spatial information. The magnocellular pathway projects to the dorsal stream of visual processing, terminating at the posterior parietal cortex. The parvocellular pathway is sensitive to high spatial frequency information, stationary or slow moving targets. This pathway projects to the ventral stream of visual processing, terminating at the

inferotemporal cortex. The pathways are segregated at the lateral geniculate nucleus (LGN), a six-layered structure in the thalamus.

Study 2 explored the detection of subtle coherent visual motion in normal subjects, before and after up to 32 hours total sleep deprivation. An impairment of visual motion detection might explain some of the deficits associated with sleep deprivation. The perception of visual motion is of central importance to driving and tracking; the detection of weak coherent motion amidst incoherent motion, and the ability to judge the speed at which objects are moving are vital driving skills.

The test of motion detection used was a random dot kinemetogram (RDK), which provides a sensitive measure of magnocellular pathway processing [Talcott 1998, Talcott 2000, Cornelissen 1995, Cornelissen 1998]. The magnocellular pathway contains cells that are sensitive to low frequency spatial information, such as moving or flickering stimuli. An RDK requires the subject to detect a coherently moving signal embedded in signal 'noise' (incoherent motion). It provides a measure of the 'motion coherence threshold'.

fMRI and primate lesional studies using RDKs have established area V5 of the peripheral visual cortex as central to the perception of visual motion [Talcott 2000, Eden 1996]. Single cell recording studies, recording activity in cortical area MT (middle temporal) in response to random motion, have shown that RDKs provide a sensitive measure of magnocellular pathway function [Britten 1992, Schiller 1990]. Area MT is strongly served by the magnocellular pathway.

The detection of 'form' or shape is processed by a separate area of the visual cortex and a different neural pathway - the parvocellular pathway. Parvocells are less metabolically active than the magnocells which detect visual motion, and might therefore be less susceptible to the effects of sleep deprivation.

Hypotheses for study:

1. Coherent visual motion detection as assessed by an RDK is impaired following sleep deprivation, and is unimpaired following normal sleep.
2. The detection of visual form or shape is unimpaired following sleep deprivation.

Methods

Subjects

Twenty-four normal subjects, with no history of neurological disease or sleep condition, and on no regular medication were studied. The subjects were 14 female and 10 male, with a mean age of 23.9 (SD 5.4) years. Subjects were eligible for the study if they had normal subjective and objective sleepiness at baseline. Subjective sleepiness was confirmed by the Epworth Sleepiness Score (ESS) [Johns 1991, Johns 1992, Johns 1993, Johns 1994], and objective sleepiness was measured by the Osler test [Bennett 1997]. Subjects confirmed that they were regular drivers, holding a current UK driving licence. Subjects had the study protocol explained to them in detail, and were provided with written study details, before signing a consent form at least 24 hours later.

Study Techniques (for protocol see appendix page 259)

1. Baseline / eligibility assessment (visit 1)

All subjects had their height (metres) and weight (Kg) measured, and their body mass index (BMI, Kg / m²) was calculated. Subjects completed a questionnaire about their normal sleep and sleeping patterns, and completed an ESS. To be eligible for the study the ESS had to be normal (≤ 9). The subjects had to have normal objective sleepiness at baseline, with a normal MWT of 40 minutes. A questionnaire

about usual caffeine, alcohol and cigarette consumption was completed. Subjects confirmed that they were regular drivers, with no history of neurological or pathological sleep condition. An information letter was supplied if it had not already been given, and the timing of the rest of the study, and the protocol for the sleep deprivation night was discussed.

2. Tracking, driving and motion detection training (visit 2)

Subjects were trained to stable performance on the Oxford Steering Simulator and the tracking task. Training on the form and motion detection paradigms also took place. During the training visit, the rest of the study protocol was explained again in detail. Movement monitoring by actigraphy was also explained. The consent form was signed.

Tracking training - this was done exactly as for study 1.

Oxford Steering Simulator training - this was done exactly as for study 1.

Motion and Form Detection training

The random dot kinemetogram (RDK) comprises a patch of high luminance white dots (each one pixel), presented on a black background, in two panels [Talcott 1998, Cornelissen 1995, Cornelissen 1998, Hansen 2001]. The paradigm is viewed on a standard computer screen, in low light conditions, with the computer screen about 1 metre from the subjects face. One panel contains a variable proportion of dots moving with horizontal coherent motion, either left or right across the screen. The remaining dots move with the same speed, but without coherent motion. In the second panel all

the dots move with Brownian motion i.e. entirely randomly. Which of the two panels contains the coherent motion is randomly selected each trial. Coherent motion is defined as the percentage of dots moving together in a single direction across the horizontal axis of the screen, i.e. the ratio of target stimulus elements to the remaining noise elements. The task therefore requires the subject to detect a signal embedded in signal 'noise'. Each dot stays on the screen for only two animation frames before it disappears and is regenerated at a random position within the stimulus area (70 Hz). This means that the subject cannot follow the trajectory of a single dot to determine the direction of coherent motion, thus the visual system has to integrate the local motion vectors of a number of dots before the perception of global motion emerges.

The percentage of coherent horizontally moving dots within a given frame is determined by the subjects' detection threshold, varying by a step up, step down, forced-choice ladder. Coherence starts at 75%, which is easily detected by all subjects, and increases by a factor of 1.4 for every incorrect response; decreasing by a factor of 1.1 for every correct response. Auditory feedback is provided, whereby a high tone is given for each correct response and a low tone for each incorrect response. This enables the subject to monitor his performance in real time, as the task is completed. Every 5th trial is a 'catch trial', at 75% coherence, to assess attention to the task. It is expected that no errors are made on the catch trials. Subjects are asked to fixate on a central white cross hair, in the centre of the animation frame, which remains on the screen for the duration of the task. The subject indicates the direction of coherent motion by pressing one of two predetermined keyboard buttons. Subjects are instructed to guess if they are unsure of the correct response. Each trial is repeated three times, with the geometric mean of the three trials determining the subjects' motion detection threshold in percentage (%). Thresholds are measured by the

geometric average of the last 8 of 10 reversal points within the series of trials. The motion detection threshold time is also measured, in milliseconds. The total stimulus time is determined by the speed at which the subject reaches his limit of motion detection threshold, and varies for each subject. Figure 24 is a pictorial representation of the motion detection paradigm.

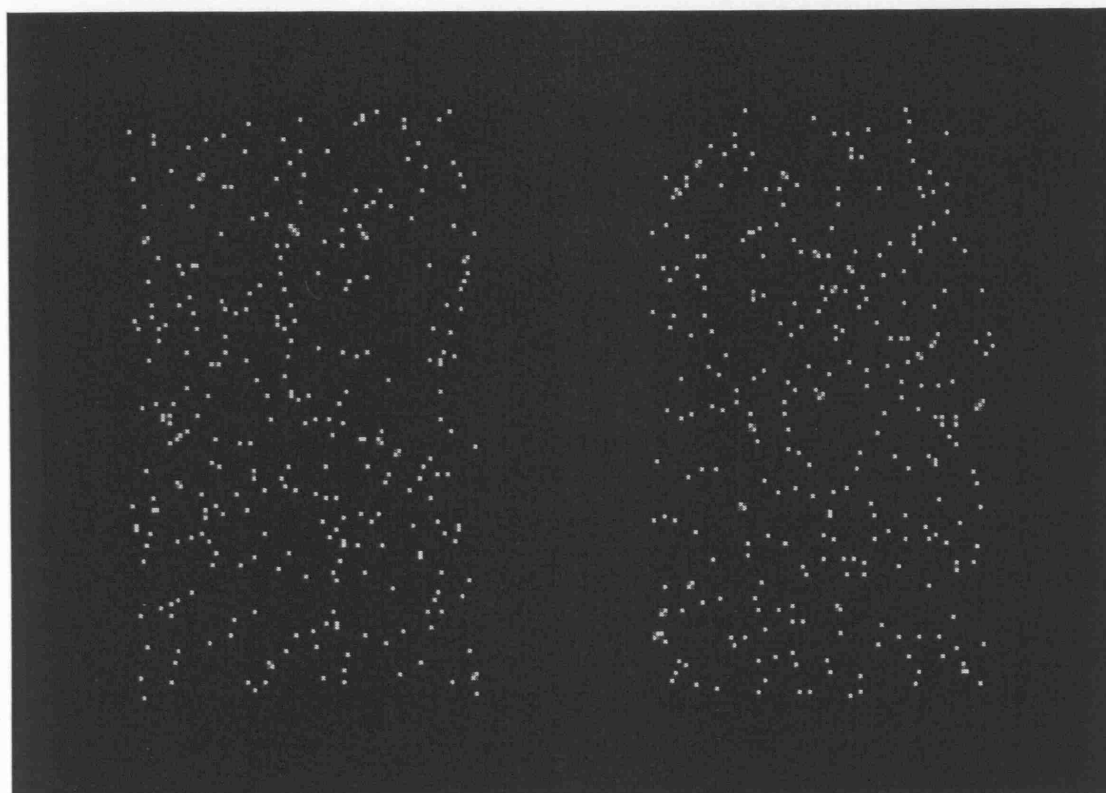


Figure 24 - a random dot kinematogram showing the two panels of dots.

Visual form detection uses a similar two panel task to that of motion detection [Sigmundsson 2003]. The coherent form / shape (dashes configured in a circle) is embedded in a panel of 'noise' in which identical white dashes are configured randomly. In the control panel, the dashes are configured entirely randomly, so the panel consists of noise elements only. An identical step up, step down forced-choice staircase is used, with the task starting at 75% coherence. The detection threshold is defined as the proportion of coherently orientated line segments necessary to detect the circle shape. Figure 25 is a pictorial representation of the form detection paradigm.

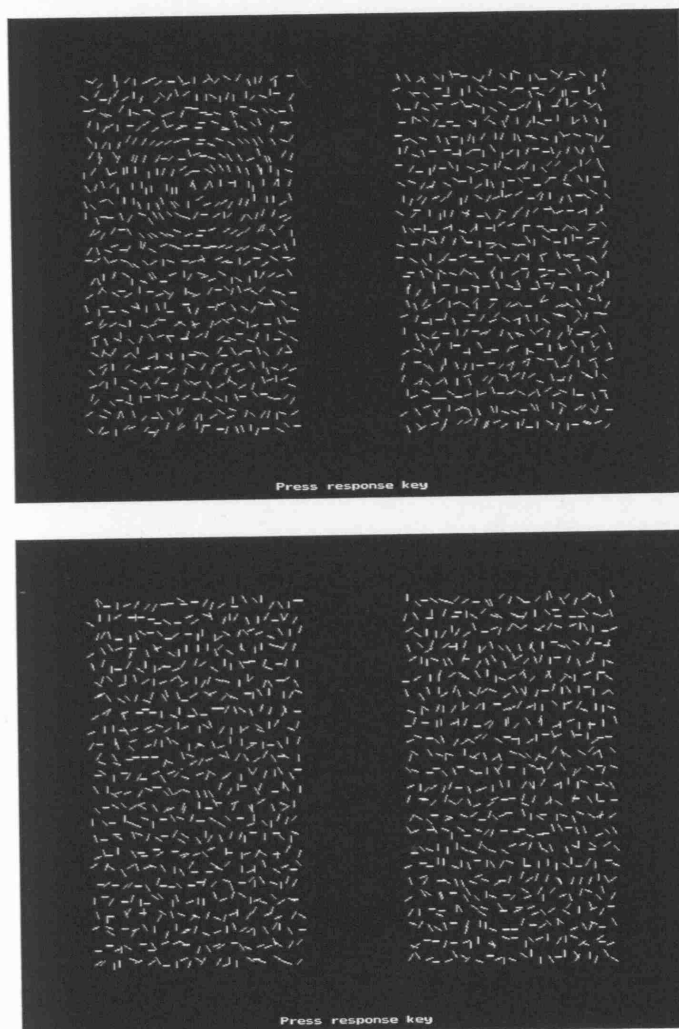


Figure 25 - the form detection paradigm. The top diagram shows an easy paradigm, with the 'form' in the top left panel, and the control panel on the right. The bottom diagram is more difficult, with the 'form' in the bottom right panel.

Continuous eye movement video recording is used to confirm eye opening and visual fixation during the motion and form detection tasks. Continuous EEG recording (Embletta, Medcare, Iceland) during the performance of these tasks was used to confirm wakefulness, and the absence of sleep episodes.

Training on each paradigm takes about 20 minutes and ceased when stable performance is reached. This is determined by on-line monitoring of performance showing detection thresholds generally ceasing to improve after about 15 minutes.

3. Assessment after normal sleep (visit 3)

Visits 3 and 4 carried out in random order

This assessment was done after a night of normal sleep at the subjects' home, exactly the same as for study 1. Following a normal mornings activities, the subjects attended the Oxford Centre for Respiratory Medicine, at the Churchill Hospital, at 2pm, where all the assessments were made. Randomisation to visits 3 and 4 was by a series of pre-sealed, numbered, opaque envelopes, and was performed by a research nurse who was not otherwise involved in the study.

A. Coherent visual motion and visual form detection

These two tests were performed exactly as described in section 2. Continuous EEG and eye movement video recording confirmed eye fixation and attention to the task.

B. Tracking assessment

Subjects performed the tracking task, sitting in front of a computer screen, as practiced during the training visit. The program used was identical to that used in

study 1 in the fMRI scanner (for normal sleep deprived subjects), lasting a total of 21.6 minutes.

C. Steering simulator assessment

Subjects performed a 30 minute simulated drive, exactly as in study 1. As for the practice runs, the speed was set to 'medium', with the entire road visible. Data was collected for subsequent analysis. The two main outcomes are standard deviation from centre drive lane position and response time to peripheral target stimuli.

D. Maintenance of wakefulness test

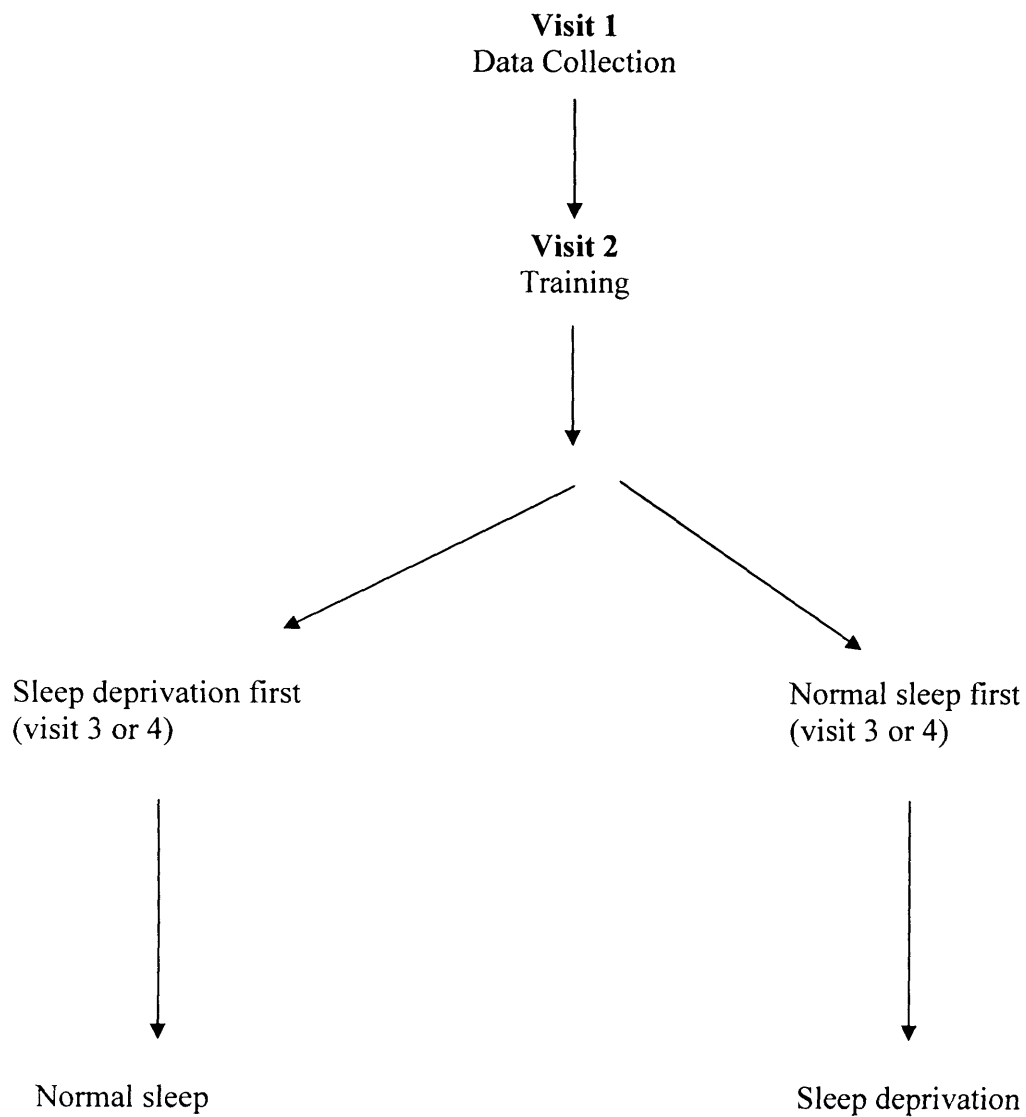
The final test performed was the maintenance of wakefulness test. The Osler test was used.

4. Assessment after sleep deprivation (visit 4)

Visits 3 and 4 carried out in random order

This assessment was done after a night of supervised sleep deprivation at the Oxford Centre for Respiratory Medicine, Churchill Hospital, Oxford. This was carried out exactly as for study 1 (see page 76). Assessments were carried out exactly as for visit 3, from 2pm.

Study 2 The effect of total sleep deprivation on visual motion and form detection in normal subjects



Chapter 3 - Results

Study 2 - The effect of total sleep deprivation on coherent visual motion and visual form detection in normal subjects

Twenty-four normal subjects completed the study. The results presented here are a comparison of the data collected after normal sleep and after sleep deprivation (visits 3 and 4, carried out in random order). All subjects had normal subjective and objective sleepiness at baseline; their baseline data are shown in table 7.

Age (years)	23.9 (5.4)
Male / Female	10 / 14
Baseline ESS	5.0 (4.0-7.8)
Baseline MWT (minutes)	40 (40-40)

Table 7 The subjects' baseline characteristics. Results are presented as mean and (standard deviation), or median and (interquartile range, (25-75%)) for non-normally distributed data. ESS= Epworth Sleepiness Score, MWT= maintenance of wakefulness test.

Maintenance of Wakefulness Data

All 24 subjects had normal objective sleepiness at baseline, reaching the full 40 (40-40) minutes on the Osler test. This was in keeping with their normal subjective sleepiness at baseline, with a median ESS of 5.0 (4.0-7.8). Following the sleep deprivation period, there was a wide range of objective sleepiness across the 24 subjects. Eleven of the 24 subjects had a normal MWT post sleep deprivation, and 13 of the 24 subjects had a reduced post sleep deprivation MWT. A pre hoc decision was

made to analyse the subjects based on their post sleep deprivation MWT, because of the wide range of inter-individual variation in response to sleep deprivation. The 11 subjects with normal post sleep deprivation objective sleepiness (median MWT 40) were defined as 'sleep deprivation resistant' (SDR). The 13 subjects with a significantly reduced MWT (median MWT 19.2), were defined as 'sleep deprivation vulnerable' (SDV). The difference between the two groups following sleep deprivation was 23.3 minutes, 95% confidence interval (CI) 19.4 to 27.3, $p < 0.0001$, unpaired t-test. Age and baseline subjective sleepiness (ESS) did not predict post sleep deprivation objective sleepiness status.

Coherent Visual Motion Detection

There was a statistically significant deterioration in motion detection threshold following the sleep deprivation period, in the sleep deprivation vulnerable subjects – defined from their post sleep deprivation MWT (see above). For sleep deprivation resistant subjects, the mean post normal sleep motion detection threshold was 6.7 (5.3-9.3) % vs 6.9 (5.2-10.5) % post sleep deprivation, mean difference 1.03, 95% CI -3.8 to 1.8, $p > 0.4$, paired t-test. For the SDV subjects, the post normal sleep mean motion detection threshold was 8.6 (5.4-11.0) % vs 10.8 (7.7-14.6) % post sleep deprivation, mean difference 2.2, 95% CI -4.0 to -0.32, $p < 0.03$, paired t-test. The two groups of subjects did not have significantly different motion detection thresholds at baseline, to account for the post sleep deprivation difference, mean difference 0.70, 95% CI -3.4 to 4.8, $p > 0.4$, unpaired t-test. Pre and post sleep deprivation motion detection threshold reaction times (msecs) were not significantly different when analysed according to the subjects' post sleep deprivation objective sleepiness status: mean difference 0.31 msecs, 95% CI -0.80 to -0.18, $p > 0.2$, paired t-test for the SDR

subjects, and mean difference 0.03msecs, 95% CI -0.60 to -0.54, $p > 0.9$, paired t-test for the SDV subjects. Performance on the catch trials (75% coherence) was good, with 4 subjects each missing one motion catch trial following normal sleep, and 2 subjects each missing one motion catch trial following sleep deprivation.

Visual Form Detection

There was no impairment in visual form detection following sleep deprivation in the subjects defined as SDV or SDR. Mean visual form detection threshold for the SDR subjects was 22.4 (15.6-25.7) % following normal sleep and 22.2 (16.0-26.3) % following sleep deprivation, difference 0.12 (95% CI -3.33 to 3.55, $p > 0.9$, paired t-test). Mean visual form detection threshold for the SDV subjects was 19.3 (13.7-23.4) % following normal sleep and 20.2 (18.5-22.3) % following sleep deprivation, difference 1.7 (95% CI -4.3 to 0.9, $p > 0.2$, paired t-test).

Oxford Steering Simulator

There was a deterioration in driving ability following sleep deprivation, with a greater, but non statistically significant deterioration in driving error for the SDV subjects. For the SDR subjects, mean driving error was 0.13 (0.08-0.20) AU following normal sleep, and 0.14 (0.10-0.18) AU following sleep deprivation, difference 0.53, 95% CI 0.61 to 1.67, $p > 0.33$, paired t-test. For the SDV subjects, mean driving error was 0.09 (0.80-0.10) AU following normal sleep, and 0.20 (0.43-0.93) AU following sleep deprivation, difference 0.41, 95% CI 0.17 to 0.98, $p > 0.15$, paired t-test.

Tracking

The tracking data was analysed exactly as for study 1. There was a significant deterioration in tracking performance following the sleep deprivation period in the SDV subjects. For the SDV subjects: mean post normal sleep tracking error was 110.5 (84.4-132.1) AU vs 125.4 (97.5-185.0) AU after sleep deprivation, difference 31.2 (95% CI 12.8 to 49.7), $p < 0.003$, paired t-test. Mean tracking lag time for the SDV subjects was 122.7 (101.1-144.5) msec after normal sleep, 138.2 (113.2-210.7) msec after sleep deprivation, difference 30.2 (95% CI 13.3 to 47.1), $p < 0.02$, paired t-test. In the SDR subjects, only mean lag time was statistically significantly worse following sleep deprivation: 147.0 (94.1-202.1) msec after normal sleep vs 166.5 (130.2-191.4) msec after sleep deprivation, difference 30.8 (95% CI 7.51 to 54.0), $p < 0.01$, paired t-test. The difference in tracking error between the two sleep states in the SDR subjects was 26.4 (95% CI -60.1 to 7.20) $p = 0.1$. Overall results are in table 8 (page 154).

Actigraphy Data

Actigraphy data was collected on all subjects for a minimum of 20 hours before each study period. The actigraph watch was worn for the night of normal sleep at the subjects' home, and for the period of supervised sleep deprivation, with the watch only removed at the end of each study period. Analysis of the actigraphy data confirmed that subjects had undisturbed sleep during their night of normal sleep at home. It also confirmed a night of activity during the sleep deprivation period, and that subjects remained active until their afternoon of assessments following the sleep deprivation night.

Summary of results

The results from study 2 correlate with the functional imaging data from study 1, showing a functional impairment of coherent visual motion detection following sleep deprivation. This effect was seen in those subjects vulnerable to the effects of restricted sleep, with measured objective sleepiness following sleep deprivation. This suggests that the reduced brain activation of visual cortex area V5 following sleep deprivation is associated with a functional impairment of this brain region, leading to deficits in motion detection ability. This may be one mechanism by which sleep deprivation leads to impaired tracking and driving.

No impairment of visual form detection was identified in those subjects resistant or vulnerable to the effects of sleep deprivation. This suggests that the brain area responsible for this function is less susceptible to the effects of sleep deprivation. This may be due to the lower metabolic rate of parvocells, serving this neural pathway. Impairments in simulated steering performance and tracking were also seen, independent of objective sleepiness status, as expected from previous studies.

Table 8. Data for subjects defined by their post sleep deprivation sleepiness status: 'sleepy', or sleep deprivation vulnerable (SDV, n=13) and 'non-sleepy', or sleep deprivation resistant (SDR, n=11), following normal sleep and following sleep deprivation

	Condition	After normal sleep	After sleep deprivation	Difference (95% CI)	p
n= 13 'Sleepy'	MWT	40 (40-40)	19.2 (9.2-20.7)	23.3 19.4 to 27.3	<0.0001
n=11 'Non-sleepy'	MWT	40 (40-40)	40 (40-40)	-	-
'Sleepy'	Motion Threshold	8.6 (5.4-11.0)	10.8 (7.7-14.6)	2.2 -4.0 to -0.32	<0.03
'Non-sleepy'	Motion Threshold	6.7 (5.3-9.3)	6.9 (5.2-10.5)	1.03 -3.8 to 1.8	>0.4
'Sleepy'	Form Threshold	19.3 (13.7-23.4)	20.2 (18.5-22.3)	1.7 -4.3 to 0.9	>0.2
'Non-sleepy'	Form Threshold	22.4 (15.6-25.7)	22.2 (16.0-26.3)	0.12 -3.33 to 3.55	>0.9
'Sleepy'	Tracking Error	110.5 (84.4-132.1)	125.4 (97.5-185.0)	31.2 12.8 to 49.7	<0.003
'Non-sleepy'	Tracking Error	112.3 (84.6-143.3)	119.7 (94.9-139.3)	26.4 7.2 to 60.1	>0.11
'Sleepy'	Tracking Lag Time	122.7 (101.1-144.5)	138.2 (113.2-210.7)	30.2 13.3 to 47.1	<0.002
'Non-sleepy'	Tracking Lag Time	147.0 (94.1-202.1)	166.5 (130.2-191.4)	30.8 7.51 to 54.0	<0.01

All results are median with (25%-75% IQR).

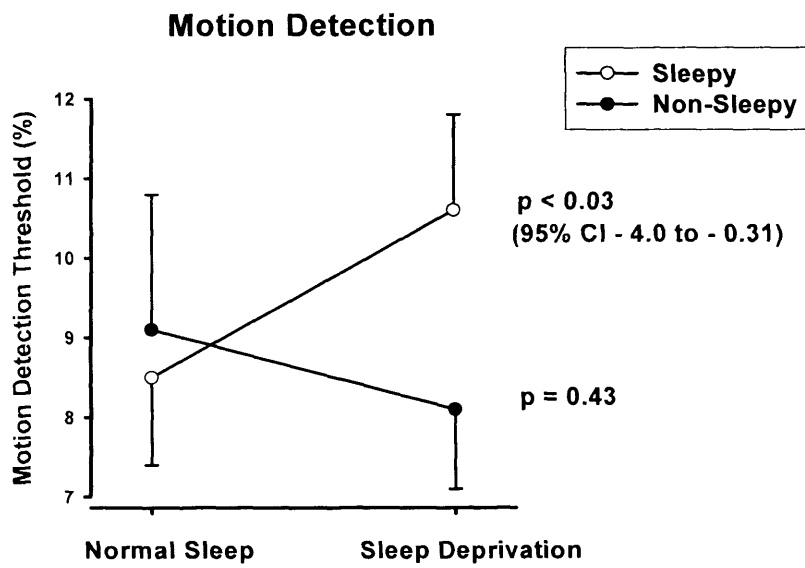
MWT = maintenance of wakefulness test (Oxford Sleep Resistance Test)

Motion Threshold = motion detection threshold (%)

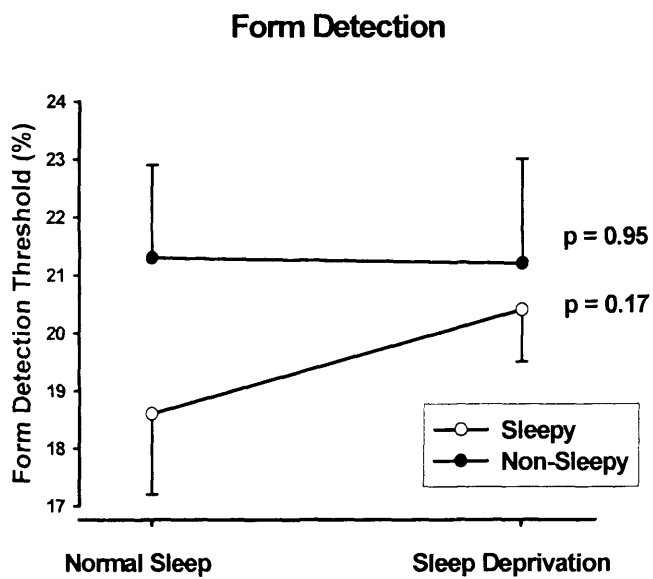
Form Threshold = form detection threshold (%)

Tracking Error = raw tracking error (arbitrary units)

Tracking Lag Time (msecs)



Graph 1 – Motion detection threshold, as defined by post sleep deprivation objective sleepiness, before and after sleep deprivation.



Graph 2 – Form detection threshold, as defined by post sleep deprivation objective sleepiness, before and after sleep deprivation.

Summary and discussion of results from study 2

The effect of total sleep deprivation on visual motion and form detection in normal subjects

Analysis of the fMRI visual stimulation data from study 1 raised a number of further questions. Reduced activation of visual cortex area V5 in the sleep deprived state may be a potential mechanism to explain the tracking and driving impairment associated with sleep deprivation, if it is associated with a functional impairment of the ability to detect motion. Further exploration of this impairment, with an investigation as to whether there is an associated behavioural impairment in visual motion detection was carried out.

Maintenance of wakefulness data

All subjects had normal objective and subjective sleepiness at baseline (a study entry criteria). Following sleep deprivation there was a wide range of objective sleepiness. Subjects were defined as SDR or SDV depending on their post sleep deprivation MWT. This division of the subjects was made pre hoc, because of the wide phenotypic differences in response to sleep deprivation.

Previous imaging studies suggest that sleep deprivation vulnerable (SDV) and sleep deprivation resistant (SDR) subjects are different in terms of the fMRI brain activation seen pre and post sleep deprivation, so there are likely to be real reasons why the two groups in this study might behave differently. Sleep deprivation resistant subjects have greater fMRI brain activation during a working memory task than sleep deprivation vulnerable subjects, and this is associated with performance differences [Mu].

There were no predictors of post sleep deprivation objective sleepiness status. This study used a single MWT to determine objective sleepiness. This has been shown to discriminate sleepiness due to OSA from normal subjects, as effectively as an EEG based MWT [Bennett 1997]. The completion of a sleep diary might have helped to guide in which subjects sleep deprivation might have lead to greater impairments, for example in those subjects with a degree of chronic sleep deprivation, in whom a one-off MWT might have been too insensitive to detect subtle baseline impairments

Coherent Visual Motion Detection data

The studies outlined in chapter 3 were designed to assess whether the differentially reduced activation of visual cortex area V5 (seen in study 1), was associated with a functional impairment in coherent visual motion detection. The motion detection paradigm (a random dot kinemetogram) was designed with a step up, step down, forced-choice ladder, where subjects reach their individual threshold of motion detection ability. This means that the threshold reached for each subject is the maximum for that individual, effectively reducing variation in inter-subject performance.

I hypothesised that the detection of visual form would be unimpaired following sleep deprivation. ‘Form’ is detected by a separate area of the visual cortex and different neural pathway, the parvocellular pathway. Parvocells are less metabolically active than magnocells (which detect coherent visual motion), so may be less susceptible to the effects of sleep deprivation. Only reduced activation of motion sensitive visual cortex areas was seen following sleep deprivation in study 1, thus the form paradigm was a control task.

The motion and form detection data was analysed dependent on the subjects post sleep deprivation objective sleepiness. This was an *a priori* decision, because of the wide range of post sleep deprivation objective sleepiness seen; with subjects clearly at two ends of the spectrum of susceptibility to the effects of sleep deprivation. The subjects with normal post sleep deprivation objective sleepiness provided a control group for those subjects with reduced post sleep deprivation objective sleepiness.

Only those subjects with increased objective sleepiness following sleep deprivation were impaired on the coherent visual motion detection task. Those subjects with normal objective sleepiness following sleep deprivation were unimpaired on the task. This data confirms the functional imaging data from study 1, showing that the reduced activation of visual cortex area V5 post sleep deprivation is associated with a functional impairment, and a reduced ability to detect coherent visual motion.

The most plausible explanation for this finding is that the high metabolic activity of the magnocellular pathway means that normal function of the pathway (and therefore motion detection) is impaired when a lack of sleep prevents restoration of normal daytime cellular function. This hypothesis fits with Horne's prefrontal lobe theory.

Impaired attention to the task is another potential explanation; poor attention occurs with the low arousal level associated with sleep deprivation. However, this did not seem to be the case: performance on the regularly spaced 'catch trials' (75% coherence) was not impaired in either the SDV or SDR groups. This suggests that, despite their objective sleepiness, the SDV subjects were able to pay attention to the

task, and detect the easiest trials, but that the skills needed for the harder trials were inadequate.

There was a wide range of objective sleepiness following the period of total sleep deprivation. In those subjects who were susceptible to the effects of sleep deprivation, there was reduced fMRI activation and reduced functional performance of the visual cortex area integral to visual motion detection. The ability to detect motion is a skill integral to driving; drivers must be able to anticipate the speed of approaching vehicles, and judge the speed of their own vehicle to avoid obstacles, and steer safely in the centre of the road. An impaired ability to detect motion and inability to 'see' an oncoming vehicle is a potential contributing mechanism for the impaired driving associated with sleep deprivation.

Visual Form Detection data

This paradigm provided the control test for the coherent visual motion detection task. There was no impairment of the ability to detect visual form following sleep deprivation, whether or not subjects were sleepy by objective measures. This data is in keeping with the functional imaging data collected in study 1. The detection of form is by parvocells, which connect with the parvocellular pathway. This pathway is sensitive to high spatial frequency information, stationary or slow moving targets, and projects to the ventral stream of visual processing, terminating at the inferotemporal cortex. Parvocells have a lower metabolic rate than the magnocells which are integral to motion detection, and may therefore be less susceptible to the effects of sleep deprivation. Whether or not the subjects were impaired in terms of their post sleep deprivation MWT, there was no impairment in the ability to detect

form. This may also be a skill that is less important during driving, and does not seem to be affected by sleep deprivation.

Tracking data

The deterioration in tracking performance following sleep deprivation was comparable to that seen in study 1, with an increase in tracking error and tracking lag time following sleep deprivation. A greater deterioration was seen in the SDV subjects. The tracking test is complex, and contains components testing a number of skills. The detection of motion is integral to the performance of the task. The deterioration in performance suggests that the combined skills tested are sensitive to sleep deprivation.

Tracking lag time probably reflects the visuo-motor control loop latency, and is therefore very similar to drive reaction time [Miall 2000]. This could easily change with level of alertness, as there is no specific brain area controlling it. A change in alertness is a potential explanation for the changes seen; the functional imaging data from study 1 showed changes in frontal cortex activation with sleep deprivation, an area which is integral to attention and vigilance maintenance [Nobre 2001]. There were also changes in activation of the cuneus and cerebellum with sleep deprivation, which may help to explain the tracking performance deficits seen. The cerebellum is known to be integral to the control of movements under visual guidance [Miall 2000, Miall 2001], as well as being involved in attention [Coull 2004], sensory processing [Gao 1996], error detection [Flament 1986], and motor learning [Clower 2001, Clower 2005]. Reduced cerebellar activation was seen post sleep deprivation. Another explanation is that the tracking impairment is due to the reduction in motion detection

ability, which may contribute to impaired tracking, as the motion of the cursor is detected inaccurately.

Divided Attention Steering Simulator data

As expected, there was a deterioration in driving performance following the sleep deprivation period. This deterioration in steering and much greater range of performance following sleep deprivation was comparable to that seen in study 1. There was a similar deterioration in the detection of peripheral visual targets.

Steering simulator performance was more impaired in the SDV than SDR subjects. Similar to the tracking task, the steering simulator assesses a number of the skills needed for safe and successful driving, and subtle differences in performance of, for example motion detection and tracking may be too small for the test to detect.

There is evidence that performance post sleep deprivation varies with the task selected, with length and pace of the task also being important. Similarly, the effects on motor performance depend on the type and duration of the task [Martin 1996]. Variations in performance might have been due to the subjects perceptions of the task, with some subjects finding the task more monotonous than others, leading to the differences in performance seen. Caffeine is known to increase levels of alertness, and has been shown to lead to improved performance following sleep deprivation. De Valck's 2003 study showed that 300mg of slow release caffeine improved lane drifting on a 45 minute simulated drive after a night of up to 7.5 hours sleep [De Valk 2003]. In a similar study, a 'functional energy drink' containing 80mg caffeine with glucose and sucrose lead to significantly reduced driving incidents and subjective sleepiness compared to placebo, following a night of restricted sleep [Reyner 2002]. The subjects in this current study were assessed after no stimulants of any kind

(including high glucose foods), and no record of their usual caffeine intake was made. Thus it is difficult to know whether or not the absence of caffeine consumption during the sleep deprivation night was a confounding factor, and if caffeine levels on the post sleep deprivation night would have been very different from normal in these subjects.

Summary

This study confirmed the fMRI visual stimulation data from study 1, showing a functional impairment in coherent visual motion detection ability following sleep deprivation, in those subjects susceptible to the effects of sleep deprivation. Impairments in steering simulator and tracking performance were also seen. The impaired ability to detect subtle visual motion may be an explanation for the driving impairments associated with sleep deprivation.

Chapter 4

Study 3 - The effects of obstructive sleep apnoea on fMRI brain activation during visual stimulation, before and after CPAP treatment

Introduction

Study 3 examined a small number of patients with OSA and aimed to establish whether the visual cortex changes seen in sleep deprived normal subjects are also seen in patients with OSA, a very common cause of sleep deprivation and daytime sleepiness. A functional assessment of visual motion detection was not made. Tracking and simulated steering were also assessed, and objective measures of daytime sleepiness were made before and after continuous positive airways pressure (CPAP) treatment. A power calculation was not carried out for this preliminary study, which also aimed to assess whether the complex trial protocol was manageable in a cohort of obese individuals with OSA.

The sleep deprivation of OSA is different to the relatively short period of total sleep deprivation used to sleep deprive the subjects in studies 1 and 2. However untreated OSA is associated with a high road traffic accident rate, and treatment of OSA with CPAP leads to a rapid improvement in both the daytime symptoms of hypersomnolence and an improvement in road traffic accident rate, with a measurable improvement in simulated steering and tracking.

Hypotheses for study:

1. The sleep fragmentation of untreated OSA is associated with impaired tracking and driving, which improve with the resolution of OSA with CPAP treatment.
2. The sleep fragmentation of untreated OSA is associated with reduced fMRI activation of visual cortex area V5.

3. CPAP treatment of OSA alters fMRI brain activation of specific visual cortex areas.

Subjects were eligible for the study if they had moderately severe OSA, with ≥ 10 , $>4\%$ oxygen saturation dips per hour due to upper airway collapse, on respiratory polysomnography. They also had to have sufficient daytime hypersomnolence to warrant treatment with nasal continuous positive airways pressure (nCPAP). Assessments were made before and after a minimum of 5 weeks CPAP treatment.

Methods

Subjects

Patients attending the Sleep and Respiratory Trials Unit, at the Oxford Centre for Respiratory Medicine, Oxford, UK were recruited. Patients were eligible for the study if they were aged over 18 years, and had proven obstructive sleep apnoea with more than 10 dips of $>4\%$ oxygen saturation per hour on overnight sleep study, and had daytime hypersomnolence, with an Epworth Sleepiness Score (ESS) ≥ 10 .

Obstructive sleep apnoea was diagnosed from a one-night in-patient respiratory polysomnographic study. Patients' body movements, heart rate and transient pulse transit time (PTT) falls were recorded as measures of arousal from sleep. The PTT signal and body movements were recorded on video. They are robust markers of arousal, and along with arterial oxygen saturation, snoring and increases in the respiratory swing in PTT, are accurate in diagnosing and quantifying OSA severity [Pitson 1998] (Win-Visi monitoring system, Stowood Scientific Instruments, Oxford, UK). The results of the sleep study were scored automatically, with manual

review to ensure data accuracy. OSA was diagnosed from review of all data, including the video recording.

The severity of sleep apnoea was then quantified numerically as the number of dips in oxygen saturation of greater than 4% for every hour of the study. This index is one of the best predictors of response to nCPAP [Bennett 1998], correlates well with conventional apnoea-hypopnoea index (AHI) measurements [Pitson 1998], and is the most consistent index between repeat studies of patients with OSA [Vazquez 2000].

Right handed, non-claustrophobic, regular drivers meeting fMRIB safety and the above inclusion criteria were invited to participate in the study. Because of the relatively small space within the MRI scanner, subjects with a chest diameter ≥ 54 cm, and those weighing over 110 Kg were excluded. Subjects had the study protocol explained to them in detail, and were provided with written study details, before signing a consent form, at least 24 hours later.

Study Techniques (for protocol see appendix page 262)

1. Baseline / eligibility assessment (Visit 1)

All subjects had their height (metres) and weight (Kg) measured, and their body mass index (BMI, Kg / m²) was calculated. Neck circumference was measured at the level of the cricothyroid membrane [Davies 1992].

To be eligible for the study the ESS had to be ≥ 10 . A questionnaire about normal caffeine, alcohol and cigarette consumption was completed. Subjects confirmed that they had no history of neurological disease, were regular drivers, driving over 10,000 miles per year, and in possession of a current UK driving licence. Subjects completed the fMRI safety assessment questionnaire. An information letter

was supplied if it had not already been given, and the timing and detailed protocol of the rest of the study, including the CPAP setup was discussed.

2. Tracking and driving training (Visit 2)

Subjects were trained to stable performance on the Oxford Steering Simulator, and the tracking task. Subjects had an opportunity to visit the fMRI scanner. If this visit was declined, the fMRI scanner setup was discussed in some detail. The consent form was signed.

Tracking Paradigm Training

The tracking training programme length and speed were identical to those used in study 1, and the training protocol was performed in an identical manner. The tracking task used for OSA patient testing was shorter (12.9 minutes, compared with 21.6 minutes for the normal subjects), and did not reach such high maximal speeds as that for the normal, sleep deprived subjects. This was because pilot study 2 had shown that at low target speeds, the subjects with untreated OSA were able to manage the test well, but at higher target speeds, they were unable to cope with the test, producing error scores four or five fold those seen in the normal subjects at comparable speeds. The target speed range was therefore reduced, to the maximum target speed of four fifths that used in normal subjects.

Oxford Steering Simulator Training

Training on the Oxford Steering Simulator was exactly as for study 1.

3. Assessment pre CPAP treatment (Visit 3)

Following a normal mornings activities, the subjects attended the Oxford FMRIB Centre at the John Radcliffe Hospital at 2pm.

A. Visual stimulation during fMRI scanning

B. Structural MRI scan

C. Visuo-motor tracking

D. Steering simulator assessment

E. Maintenance of wakefulness test

All of the above assessments were performed exactly as described for the sleep deprived normal subjects in visit 3.

4. CPAP set-up (Visit 4)

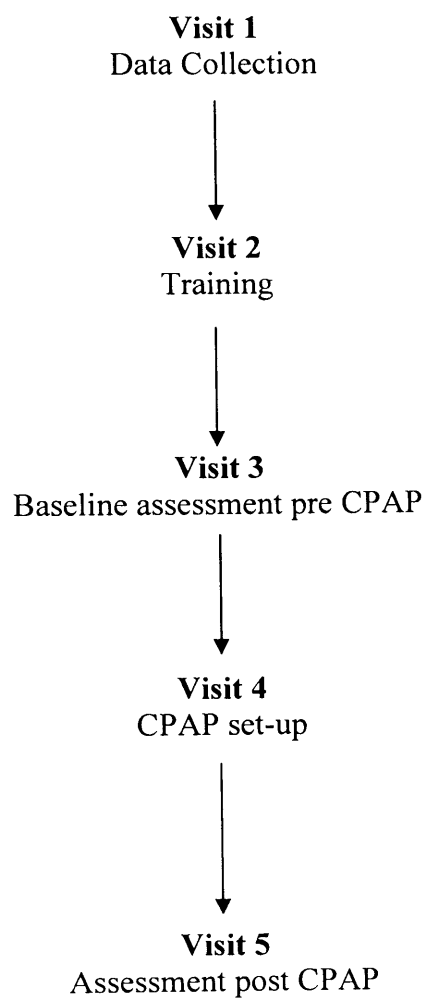
Patients underwent the standard Oxford out-patient CPAP induction programme. Having watched a video and learnt about CPAP, the subjects had a one to one specialist nurse led session, during which mask fit was optimised. Therapeutic CPAP was generated using an automatic CPAP machine (Autoset, Resmed, Abingdon, UK). Following CPAP set-up, a specialist nurse team assisted patients with telephone advice for any CPAP difficulties during the treatment period, and masks were adjusted as necessary.

5. Assessment after CPAP treatment (Visit 5)

This was carried out exactly as for visit 3, and took place a minimum of 5 weeks after the start of CPAP treatment. After completion of the assessments, CPAP compliance, median pressure and mask leak data was downloaded from the subject's

CPAP machine. Subjects were given a fixed pressure machine, with the pressure derived from the 95th percentile pressure from the autoadjusting CPAP machine. Travel expenses were paid, and the subject was booked into a routine CPAP follow-up clinic.

Study 3 The effects of OSA on fMRI brain activation during visual stimulation before and after CPAP treatment



Results - Chapter 4

Study 3 - The effects of obstructive sleep apnoea on fMRI brain activation during visual stimulation, before and after CPAP treatment

Seventeen patients with OSA were recruited to study 3. All subjects were regular drivers, driving at least 10,000 miles per year. No patients had any history of neurological disease. One subject had treated hypertension and type II diabetes. No subjects had any other relevant past medical history. Mean CPAP treatment time was 7.4 (2.8) weeks, and depended on access to the fMRI scanner. Mean CPAP compliance was comparable with that of the other Oxford trials of CPAP in OSA, with a mean of 5.4 (2.3) hours per night.

The results presented are a comparison of the data collected before and after CPAP treatment (visits 3 and 5). The subjects baseline data is shown in table 11. Table 12 shows the individual subject data.

Age (years)	47.4 (10.7)
BMI (Kg / m²)	29.3 (25.9-30.6)
4% oxygen desaturation (dips / hour)	31.0 (16.0-41.7)
Baseline ESS	15.0 (14.8-18.0)
Baseline MWT (minutes)	17.4 (5.8-40)
CPAP treatment time (weeks)	7.4 (5.5-9.0)
CPAP compliance (hrs / night)	6.3 (3.6-7.3)

Table 11 The OSA patient baseline characteristics. Results are presented as mean and (standard deviation), and interquartile range, (25-75%) for the non-normally distributed data. BMI= body mass index, ESS= Epworth Sleepiness Score, MWT= maintenance of wakefulness test, CPAP= continuous positive airway pressure.

Maintenance of Wakefulness Data

The median pre-treatment MWT was 17.4 (5.8-40) minutes, in keeping with the subjects daytime hypersomnolence, with a median baseline ESS of 15.0 (14.0-18.0). Following CPAP treatment, the median MWT was 40 (19.9-40) minutes, difference 10.6 minutes (95% CI -19.2 to 1.4) $p > 0.02$, paired t-test. The median post treatment ESS was 5.0 (3.0-8.0), difference 9.8 (95% CI 7.1 to 12.6) $p < 0.0001$, paired t-test. Despite their subjective daytime hypersomnolence at baseline, 5 subjects had a normal MWT.

Steering Simulator Data

There was a minor overall improvement in steering simulator performance following CPAP treatment. Mean steering error (standard deviation from the centre drive lane position, in arbitrary units) was 1.02 (2.27) AU pre-treatment, and 0.15 (0.72) AU following CPAP treatment, difference 0.87 (95% CI -0.33 to 2.07) $p > 0.14$. As for the tracking task, there was a wide range of performance pre-treatment.

The mean reaction time to register peripheral targets was improved to a greater degree following CPAP; mean reaction time was 2.55 (0.92) seconds pre treatment, and 1.95 (0.71) seconds post treatment, difference 0.60 (95% CI 0.33 to 0.86) $p < 0.0001$, paired t-test. The mean number of peripheral targets missed pre treatment was 0.68 (1.7), with 0.25 (0.7) missed post treatment, difference 0.44 (95% CI -0.23 to 1.11) $p > 0.19$, paired t-test.

Tracking Data

The tracking data collected before and after CPAP treatment was analysed exactly as for study 1, using in-house MATLAB analysis programmes. There was no

measurable improvement in tracking performance following CPAP treatment. Pre CPAP treatment mean tracking error was 143.0 (44.4) AU, post treatment mean tracking error was 130.1 (35.2) difference 12.5 (95% CI -6.6 to 31.5) $p > 0.18$, paired t-test. The baseline (pre-treatment) OSA patient tracking performance was comparable to that of the normal subjects, studied in study 1, following normal sleep (mean tracking error 120.1 (94.5-129.4) post normal sleep). However the tracking task used for the OSA patients was easier than that used for the normal subjects, and this may explain the similar results obtained. There was a small change in tracking lag time following CPAP treatment, improving from 221.9 (69.4) msec pre treatment, to 197.3 (64.1) msec post treatment, difference 24.6 (95% CI -2.5 to 51.6) $p > 0.72$, paired t-test. Table 13 shows the OSA patient non-fMRI study data.

fMRI Results - Visual Stimulation

The OSA patient fMRI individual scan analysis, group analysis, and group comparison / subtraction analyses were carried out exactly as for study 1, following preprocessing, using software in FEAT. Statistical analysis was carried out using a GLM, and the same design matrices as for study 1. Estimates were compared using the same linear compounds or contrasts. Differential brain activation in the two states, pre and post CPAP treatment was assessed by subtraction analysis.

Figure 26 shows the fMRI group averaged OSA patient data pre CPAP treatment, and figure 27 shows the same data following CPAP treatment (both $n = 17$). Both of these analyses use a FLAME cluster analysis, with $p = 0.01$, $Z = 2.3$. The design matrices for an individual OSA patient's visual stimulation analysis, the visual stimulation group analysis and the visual stimulation group subtraction analysis GLM were identical to those used in study 2 (see figures 28, 29 and 30 respectively).

There was no differential activation of the visual cortex pre and post CPAP treatment, contrary to my hypotheses about visual cortex motion sensitive areas pre and post CPAP treatment. However differences were seen in other brain areas, in particular the cerebellum, parietal and frontal lobes. Figures 31 and 32 show subtraction group analyses - group averaged data pre CPAP minus group averaged data post CPAP, and group averaged data post CPAP minus group averaged data pre CPAP, respectively. These images show the brain areas differentially activated in the two different states, with their maximal pixel activation and Talairach coordinates. Differential activation of the right frontal lobe and left post central gyrus are seen pre CPAP treatment, with predominant activation of areas in the left parietal lobe, cerebellum and cuneus following CPAP treatment.

Further analysis of specific anatomical areas of the visual cortex (as in study 1) failed to demonstrate any significant difference in visual cortex activation pre and post CPAP treatment.

Statistical Analysis

Further statistical analysis was carried out with SPSS software, version 14.0. Relationships between pre and post treatment data were assessed with Pearson's correlation. There was a significant correlation between pre treatment tracking error and baseline OSA severity (dip rate), $r = 0.67$, $p < 0.05$. There were no baseline predictors of driving or tracking performance, or improvement in performance.

Summary of Results

The post visual stimulation differential brain activation pre and post CPAP treatment in the OSA patients differed to that seen before and after sleep deprivation, in study 1. Areas of differential brain activation were not confined to the visual cortex motion sensitive areas. Pre CPAP treatment (i.e. in the sleep deprived state) maximum activation was in the right frontal lobe. Following CPAP treatment, predominant activation was in the left parietal lobe and cuneus. There was no differential activation of the visual cortex.

Despite reasonable CPAP compliance, not all subjects had good resolution of their daytime symptoms post CPAP treatment. There was a trend towards improved simulated steering and tracking performance, but this was not statistically significant.

Subject	Age	Dip	ESS Pre	ESS Post	BMI	CPAP Comp	Trk Lag PreCPAP	Trk Lag PostCPAP	Trk Err PreCPAP	Trk Err PostCPAP
1	42	31.5	14	3	30.1	6.38	213.7	131.9	139.2	104.4
2	58	31.4	17	2	26.4	7.24	128.3	138.4	107.0	95.4
3	61 (F)	39.8	15	15	35.7	4.07	228	-	134.6	-
4	57	19	18	5	26.3	2.5	292.8	259.5	189.1	138.4
5	31	80.3	21	2	34.5	8.05	330.1	348.6	262.0	201.7
6	43	13.5	15	6	23.9	6.36	146.8	188.3	86.2	102.7
7	44	14	19	8	25.5	0.48	221.2	202.7	124.9	131.5
8	38	11.5	17	4	30.3	7.2	162.6	233.8	107.6	189.4
9	58	36	18	4	26.3	7.54	189.4	164.1	170.8	135.6
10	43	15	15	7	31.1	4.34	208	149.4	121.5	96.1
11	25	30.4	15	8	30.4	3.04	187.3	132.6	110.8	86.7
12	37	67.3	12	3	32.8	4.52	290.1	246.5	164.8	146.6
13	50 (F)	17	19	7	29.3	6.52	362.8	249.9	174.0	150.5
14	53	31	16	5	23.5	7.32	177.5	108.8	112.3	88.4
15	54	24	10	11	28.0	2.59	167.6	180.6	121.5	140.0
16	49 (F)	43.6	14	0	24.5	6.3	250.7	224.3	153.1	151.0
17	62	46	12	10	30.3	8.11	-	185.1	-	108.1

Subject	Drive Err PreCPAP	Drive Err PostCPAP	Rn Time PreCPAP	Rn Time PostCPAP	2s PreCPAP	2s PostCPAP	Osler PreCPAP	Osler PostCPAP
1	0.12	0.09	2.1	1.6	0	0	8.2	40
2	0.19	0.11	3.0	2.3	0	1	11.4	40
3	9.07	0.24	3.8	2.4	4	0	40	40
4	0.11	0.16	1.9	1.4	0	0	40	26.8
5	2.4	0.11	3.2	2.2	0	0	31.7	40
6	0.09	0.08	1.9	1.3	0	0	3.4	40
7	0.13	0.14	2.6	1.6	0	0	40	40
8	0.38	0.13	4.5	3.9	6	3	17.4	40
9	0.13	0.12	2.5	2.8	0	0	40	40
10	0.17	0.12	2.9	1.5	0	0	15.3	40
11	0.09	0.08	1.7	1.7	0	0	29.6	40
12	0.17	0.12	1.7	1.4	0	0	12.6	12.7
13	2.33	0.19	2.9	2.7	0	0	1.3	3.1
14	0.16	0.16	1.1	1.0	0	0	25.2	40
15	0.15	0.15	4.0	2.3	1	0	40	13.2
16	0.58	0.37	1.9	1.5	0	0	2.9	40
17	-	-	-	-	-	-	1	3.7

Table 12 - OSA Patient Data. All results are mean and (standard deviation)

Age (years)
Dip = >4% oxygen saturation dips per hour
ESS pre = pre treatment Epworth Sleepiness Scale
ESS post = post treatment Epworth Sleepiness Scale
BMI = Body Mass Index (Kg / m ²)
CPAP Comp = CPAP compliance (mean hrs / night)
Trk Lag pre CPAP = Tracking lag time (milliseconds) pre CPAP treatment
Trk Lag post CPAP = Tracking lag time (milliseconds) post CPAP treatment
Trk Err pre CPAP = Tracking error (Arbitrary Units) pre CPAP treatment
Trk Err post CPAP = Tracking error (Arbitrary Units) post CPAP treatment
Drive Err pre CPAP = Drive Error (standard deviation from centre drive lane position) pre CPAP
Drive Err post CPAP = Drive Error (standard deviation from centre drive lane position) post CPAP
Rn Drive pre CPAP = Drive reaction time (Rn) to register peripheral targets pre CPAP (seconds)
Rn Drive post CPAP = Drive reaction time (Rn) to register peripheral targets post CPAP (seconds)

2s pre CPAP = number of 2s missed pre CPAP (drive peripheral targets)

2s post CPAP = number of 2s missed post CPAP (drive peripheral targets)

Osler pre CPAP = minutes reached on Osler test (MWT) pre CPAP

Osler post CPAP = minutes reached on Osler test (MWT) post CPAP

n =17	Pre CPAP	Post CPAP	Difference (95% CI)	p
ESS	15.0 (14.0-18.0)	5.0 (3.0-8.0)	9.8 (7.1 to 12.6)	0.0001
MWT (minutes)	17.4 (5.8-40)	40 (19.9-40)	10.6 (-19.2 to 1.4)	0.026
Drive Error (arbitrary units)	1.02 (2.27)	0.15 (0.72)	0.87 (-0.33 to 2.07)	0.144
Drive RT (seconds)	2.55 (0.92)	1.95 (0.71)	0.60 (0.33 to 0.86)	0.0001
Tracking Error (arbitrary units)	143.0 (44.4)	130.1 (35.2)	12.5 (-6.6 to 31.5)	0.18
Tracking Lag (msecs)	221.9 (69.4)	197.3 (64.1)	24.6 (-2.5 to 51.6)	0.07

Table 13 OSA patient non-fMRI results

Results are mean and (SD) or median and (IQR) if not normally distributed.

ESS = Epworth Sleepiness Score

MWT = maintenance of wakefulness test (Oxford Sleep Resistance Test)

Drive Error = standard deviation of centre drive lane position

Drive RT = drive reaction time to register peripheral targets

Tracking Error = raw tracking error

Tracking Lag = tracking lag time

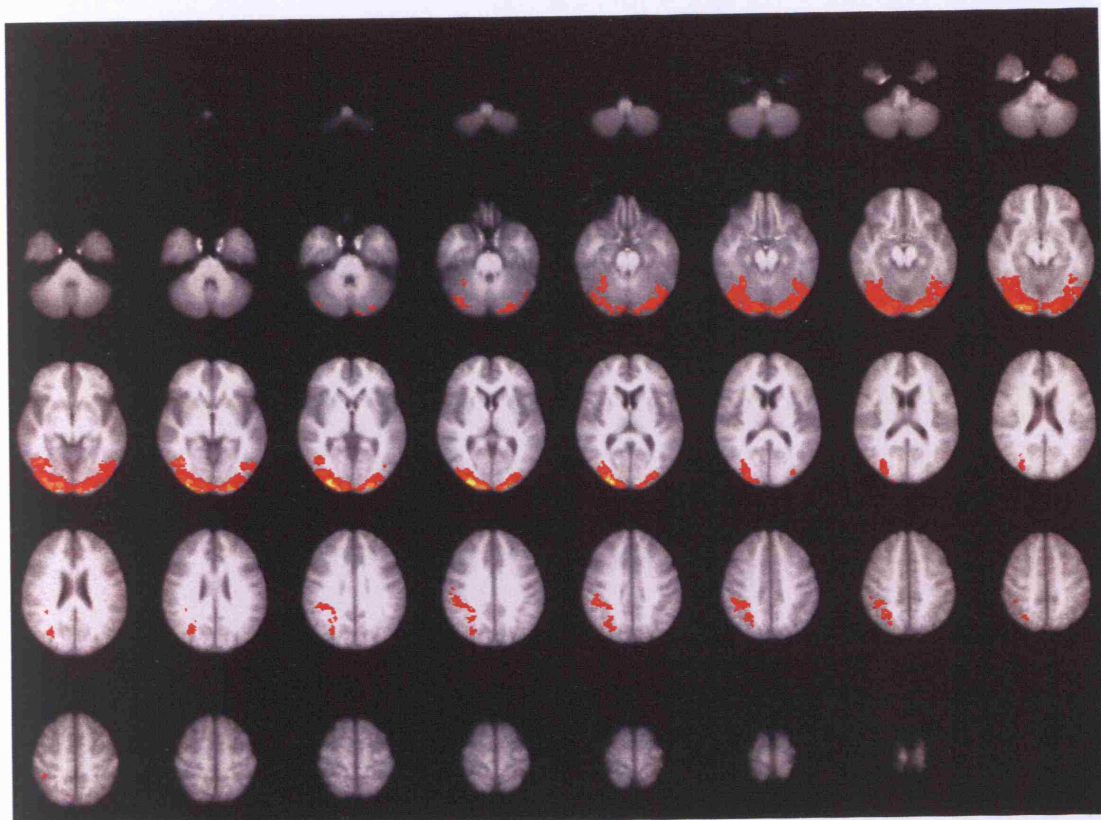


Figure 26

Visual stimulation: group averaged OSA patient data, **pre CPAP** treatment (n= 17).
FLAME cluster analysis, $p= 0.01$, $Z= 2.3$.



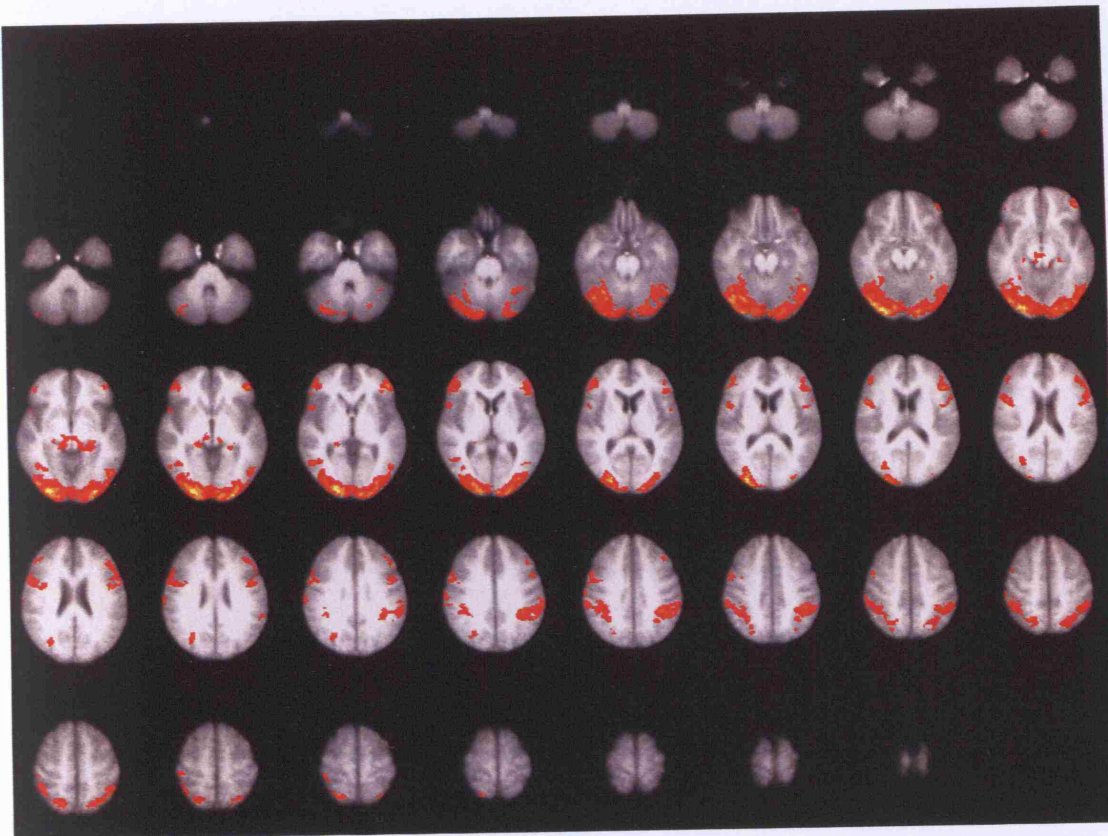


Figure 27
 Visual stimulation: group averaged OSA patient data, **post CPAP** treatment (n= 17).
 FLAME cluster analysis, $p= 0.01$, $Z= 2.3$.



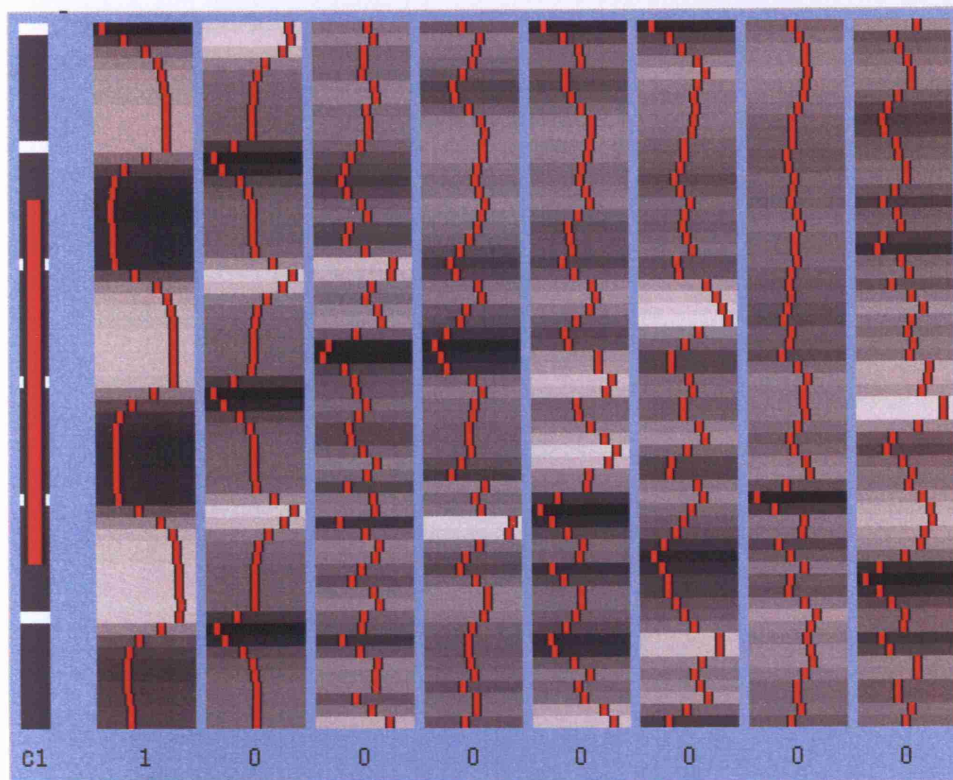


Figure 28

The design matrix for an individual OSA patient's visual stimulation analysis (the columns are 1 to 8, from left to right).

EV (explanatory variable) 1 (columns 1 and 2 - column 2 is the first derivative of column 1) explains the chequerboard flashing on and off, and columns 3 to 8 explain head motion correction. Columns 3 and 4 explain movement in the X plane, columns 5 and 6 explain the movement in the Y plane, and 7 and 8 explain the movement in the Z plane. Columns 4, 6 and 8 are the first derivatives of columns 3, 5 and 7 respectively.

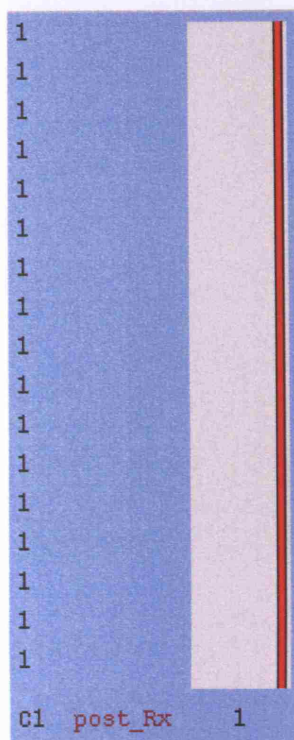


Figure 29
The design matrix for the visual stimulation OSA patient group analysis (n=17).

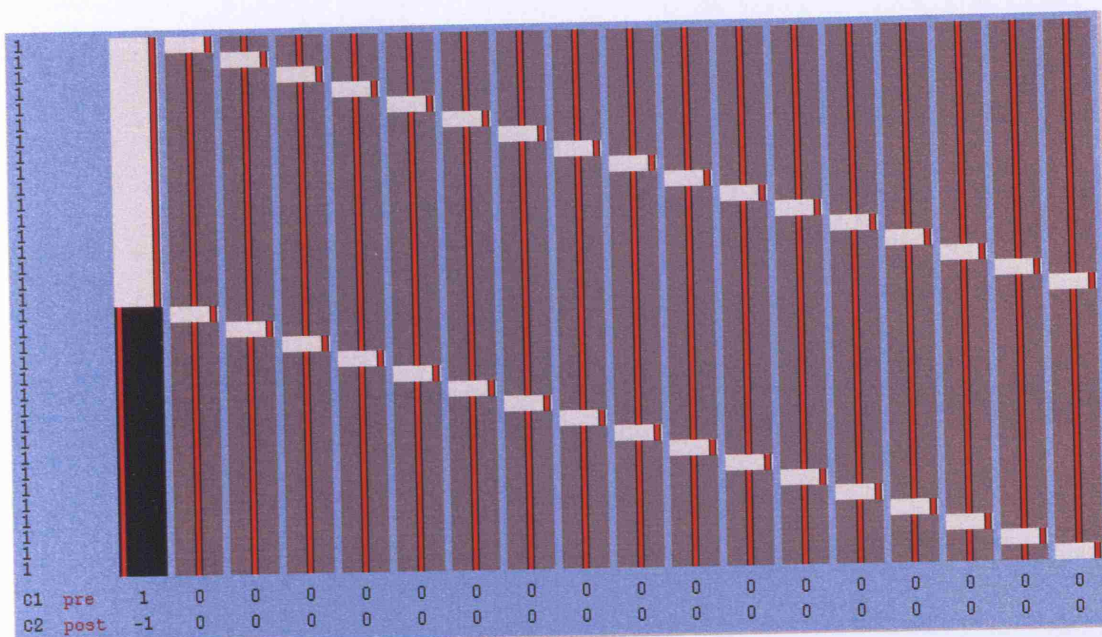


Figure 30

The design matrix for the OSA patient visual stimulation subtraction group analysis. Column 1 (far left) represents the group data pre CPAP treatment (in white) above the group data following CPAP treatment (in black). The subsequent columns represent the paired data subtraction analyses.

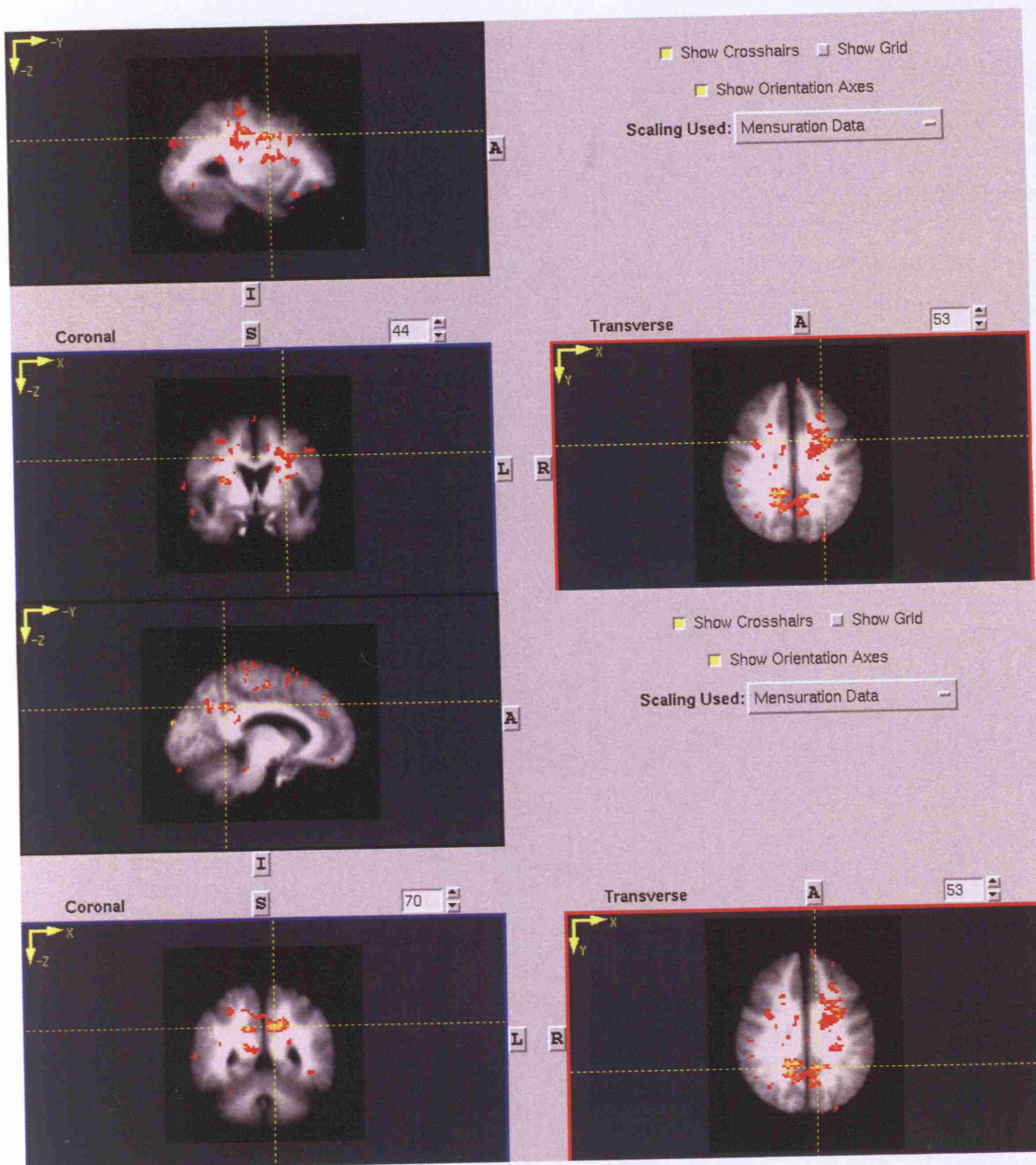


Figure 31
Visual stimulation: OSA patient group averaged subtraction data (n= 17) pre CPAP minus post CPAP.
Threshold uncorrected analysis, $p = 0.05$.



Medx coordinates	Maximum pixel value	Talairach Datapoint
10, 12, 62	3.83	R sup frontal gyrus, BA 6
-34, -18, 28	3.40	L post central gyrus
- 20, -22, 42	3.40	R frontal lobe, BA 31

Table 31

Maximum areas of pixel activation during visual stimulation, pre CPAP minus post CPAP, with their Medx coordinates and Talairach atlas anatomical sites.

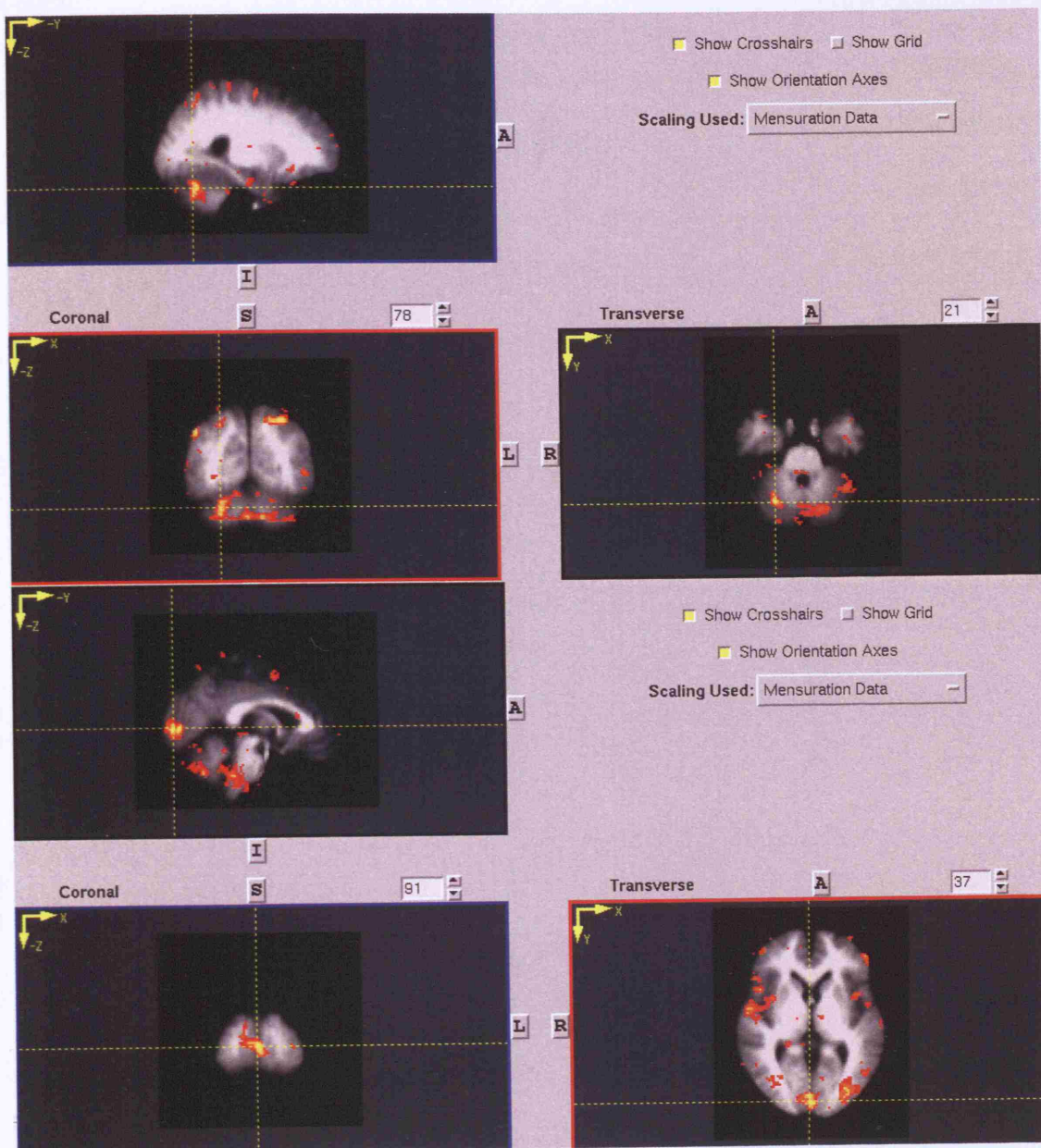


Figure 32

Visual stimulation: OSA patient group averaged subtraction data (n= 17) **post CPAP** minus pre CPAP. This is in comparison to pre CPAP minus post CPAP (see figure 31).

Threshold uncorrected analysis, $p= 0.05$.



Medx coordinates	Maximum pixel value	Talairach Datapoint
-34, -42, 44	3.85	L parietal lobe, BA 40
-26, -64, 50	3.84	L parietal lobe, BA 7
0, -90, 2	3.83	L cerebrum, cuneus, BA 7
-46, -38, 42	3.83	L inf parietal lobe, BA 40

Table 32
Maximum areas of pixel activation during visual stimulation, post CPAP minus pre CPAP, with their Medx coordinates and Talairach atlas anatomical sites.

Summary and discussion of results from study 3

The effect of OSA on visual stimulation before and after CPAP treatment

The fMRI visual cortex changes from study 1 were assessed in a group of subjects with OSA before and after CPAP treatment. This was to assess whether the changes seen in normal, sleep deprived subjects were present in patients with the sleep fragmentation of OSA, and whether the same impairment of visual motion detection could also explain the raised road traffic accident rate of untreated OSA.

The subjects studied were representative of a typical patient population with OSA, with the majority being male (80%), with a mean age of 47.4 (10.7) and a median BMI of 29.3 (25.9-30.6). The patients had significant daytime hypersomnolence at baseline, in keeping with moderately severe OSA. Mean CPAP compliance was comparable with that of the other Oxford trials of CPAP in OSA, with a median of 6.3 (3.6-7.3) hours per night.

Maintenance of Wakefulness data

There was a small improvement in daytime symptoms post CPAP treatment, though not as great as that seen in previous Oxford trials of CPAP in OSA [Pepperell 2002, Jenkinson 1999]. The median pre-treatment MWT was 17.4 (5.8-40) minutes, which improved to 40 (19.9-40) minutes post CPAP treatment, difference 10.6, 95% CI -19.2 to 1.4 $p > 0.02$, paired t-test. The ESS fell to within the normal range post CPAP treatment, and a greater improvement in median post treatment objective sleepiness might have been expected with this. Despite significant daytime symptoms at baseline, five subjects had a normal MWT, however only three of these subjects had a normal MWT post treatment.

Despite a mean CPAP compliance of over 6 hours per night, this patient group's post treatment performance was not as good as might have been expected. CPAP mask discomfort and air leaks were no greater than expected. The reasons for the limited improvement are uncertain; some of the ESS fall may have been regression to the mean. It is possible that this population's OSA was not severe enough at baseline, to enable a significant difference to be detected. However the mean baseline >4% dip rate was comparable with that of other Oxford trials of CPAP in OSA (mean 32.4 (SD 19.1). The subjects studied may have been a different subject sub-population, chosen because of their not too severe obesity, so they could fit into the MRI scanner. This may partially explain the small fMRI changes identified.

The subjects scored themselves as less subjectively sleepy post CPAP treatment, and this therapy is known to have a significant placebo effect [Profant]. It is also possible that, because of their participation in a research study, the subjects under scored their post treatment daytime symptoms. A randomised trial of therapeutic versus sub-therapeutic CPAP in this setting would help to resolve some of these issues.

Divided Attention Steering Simulator data

There was a non-statistically significant improvement in steering simulator performance following CPAP treatment. The mean time to register peripheral targets was significantly improved after treatment ($p < 0.0001$). The relatively greater improvement in target registration time suggests that these subjects (like the sleep deprived normal subjects) chose to concentrate on the easier, target recognition task, than on the more challenging steering task, and that dividing attention between the two tasks simultaneously may have been too difficult pre treatment. This corresponds

with previous data [George 1996]. The improvement in steering performance occurred despite some overall persisting post treatment residual objective sleepiness. Previous studies have demonstrated a poor correlation between post sleep deprivation objective sleepiness and objective performance measures, with wide variations in performance between individuals dependent on the period of sleep deprivation [Cutler 1979]. Pilcher et al's meta-analysis showed that overall, compared across a range of tasks, sleep deprived subjects perform at a level about 1.37 standard deviations below non-sleep deprived subjects [Pilcher 1996].

This data is comparable with published data assessing steering simulator improvement with CPAP treatment in OSA patients. A number of studies have shown that steering simulator performance is impaired in untreated OSA patients compared to matched controls, and that simulated steering performance improves with CPAP treatment, though not quite to that of matched controls after one month's treatment [George 1997, George 1996, George 2001, Findley 2000, Juniper 2000, Hack 2001]. This improvement in simulated steering is reflected in a reduction in the real road accident rate post CPAP treatment in several studies [Cassel 1996, Kreiger 1997]. Questionnaire data suggests that patients with more severe OSA have a greater number of accidents [Hortsmann 2000]; this current data shows a significant correlation between pre treatment tracking error and baseline OSA severity (dip rate), $r = 0.67$, $p < 0.05$.

Tracking data

There was a non-statistically significant improvement in tracking error following CPAP treatment, with a similar small improvement in tracking lag time. These improvements were much smaller than those seen with steering simulator

performance post CPAP. It is possible that the incomplete resolution of the daytime symptoms of OSA led to persistent visual motion detection deficits, impaired motor coordination, impaired attention or vigilance maintenance, hence the limited improvement seen.

However, the OSA patients pre treatment tracking performance (i.e. in the 'sleep deprived' state) was comparable to that of the normal subjects performance post sleep deprivation; similarly, the OSA patients post treatment tracking performance (i.e. in the 'normal sleep' state) was less impaired than that of the normal subjects following normal sleep. Pre OSA treatment and sleep deprived normal subject data was comparable for tracking lag time. These comparisons may reflect the differences in type of sleep deprivation occurring in the two subject groups. It is possible that a one-off period of prolonged total sleep deprivation has very different neurological and therefore functional effects than the chronic (often for more than 10 years), low level recurrent brain arousal (leading to sleep fragmentation) of OSA. However the ultimate effects on driving performance and road traffic accident rate seem to be similar.

These differences may also be partly explained by the easier tracking task completed by the OSA patients. The maximum target speed for the OSA patients was four fifths that used for the normal subjects, with a total task time of 12.9 minutes, compared to 21.6 minutes for the normal subjects, which may have lead to improved attention to the task. Kim et al's 2007 study examined the relationship between sleep disordered breathing and performance on a number of psychomotor vigilance tasks, in subjects studied as part of the Wisconsin Sleep Cohort. Multiple linear regression analysis showed a significant negative association between measures of sleep disordered breathing and task lapses / false responses, independent of sex or BMI, in subjects aged over 65 years, concluding that sleep disordered breathing in a community based

population is associated with impaired psychomotor vigilance. The population studied here is younger, but the performance effects seen are certainly similar [Kim 2005, Kim 2007].

fMRI data - Visual stimulation

The OSA patient visual stimulation data was different to that of the sleep deprived normal subjects. There was no differential activation of the visual cortex pre and post CPAP treatment. However differences were seen in other brain areas, in particular the cerebellum, parietal and frontal lobes.

Differential activation of the right frontal lobe and left post central gyrus were seen pre (and not post) CPAP treatment, with predominant activation of areas in the left parietal lobe, cerebellum and cuneus post (and not pre) CPAP treatment. These are all small changes and must be interpreted with caution in this small pilot study, but raise some important areas for further investigation, and may help to explain some of the performance abnormalities seen in untreated OSA.

The small changes in brain activation may relate to a global brain effect due to OSA, or may relate to persistent residual post CPAP treatment OSA effects. As discussed above, this subject group appears to be somewhat atypical, with limited performance improvements post CPAP. There may also be inter-individual variations in fMRI activation. The OSA patients moved more within the scanner (despite head restraint), and this may have lead to degradation of fMRI signal (despite the use of motion correction software). It is also possible that OSA patients in general generate less fMRI signal than normal subjects, because of cerebrovascular and micro-vascular changes, too small to be detected on standard structural MRI scans. OSA is an

independent risk factor for hypertension, and it is well known that these patients have a high incidence of cerebrovascular and cardiovascular disease [Peker 2006].

Activation of areas in the frontal lobe pre CPAP treatment suggests increased attention to the task in the sleep deprived state. Posterior parietal and frontal areas are also integral to visuo-spatial attention [Corbetta 2000]. There was no frontal lobe activation following CPAP treatment, suggesting that the subjects may have needed to divert fewer attentional resources to the task, when no longer sleep deprived.

The left parietal lobe was more active after CPAP treatment. This brain area has been shown to be active in spatial and temporal attention [Coull 2004], with particular activation of a left hemisphere dominant fronto-parietal system for the orientation of attention in time. The brain areas involved in the control of spatial attention (vital if a subject is able to perform a task) are the same as those involved in the control of eye movements. It is thought that eye movements represent the most basic orientating response, as they can be shifted accurately and rapidly depending on the task [Nobre 2001].

The left cuneus was active after CPAP treatment. A number of studies have demonstrated activation of specific brain areas during passive 'resting', including the posterior and anterior cingulate (very close to the cuneus / precuneus), left frontal areas, and cerebellar foci. These areas are thought to be 'tonically active' and continuously gathering information about the world around us [Shulman 1997, Mazoyer 2001, Laureys 1999]. These areas are more active in the resting condition than during performance of a task. The anterior precuneus has been shown to be deactivated during various cognitive tasks, as opposed to passive conditions; the posterior precuneus has been reported to be active during 'conscious effortful recollection of episodes' [Buckner 1996]. Why the left precuneus was active after the

restoration of normal sleep in this study is uncertain, and is at odds with the precuneus activation demonstrated post sleep deprivation in normal subjects, during tracking. It may be an area whose activation is task dependent, though a previous study in sleep deprived normal subjects demonstrated deactivation of the right precuneus following 48 hours total sleep deprivation in a non-verbal recognition memory task [Bell-McGinty 2004].

A small area in the right posterior cerebellum was active after CPAP treatment. The cerebellum is integral to the control of visual feedback and is involved in attention (most commonly the left superior cerebellum) [Allen 2005].

Previous fMRI studies of untreated OSA (during a verbal learning task) have demonstrated increased activation of several brain areas, including the bilateral frontal gyri, cingulate gyrus, thalamus and cerebellum, compared to normal subjects. The authors postulate that this is due to a cerebral adaptive compensatory response, with the recruitment of additional brain areas similar to that seen in healthy, sleep deprived normal subjects [Drummond 1999-2004]. This study only showed increased frontal lobe activation pre treatment, and this may be because the visual stimulation task used is a 'passive' viewing task, that does not lead to the recruitment of additional brain areas which an 'active' verbal task might.

Time limitation meant that a functional assessment of visual motion detection using an RDK could not be made in this small pilot study, and this is an important area for future research, including a larger number of subjects, and specifically assessing visual cortex activation and function. This may lead to a greater understanding of the limitations and effects of brain recovery due to plasticity in other neurological diseases.

Summary

The post visual stimulation differential brain activation pre and post CPAP treatment in the OSA patients differed to that seen before and after sleep deprivation, in study 1. Areas of differential brain activation were not confined to the visual cortex motion sensitive areas. Pre CPAP treatment (i.e. in the sleep deprived state) maximum activation was in the right frontal lobe. Following CPAP treatment, predominant activation was in the left parietal lobe and cuneus. There was no differential activation of the visual cortex.

Despite reasonable CPAP compliance, not all subjects had good resolution of their daytime symptoms post CPAP treatment. There was a trend towards improved simulated steering and tracking performance, but this was not statistically significant.

General Discussion

The three studies in this thesis aimed to investigate a possible mechanism for the impaired driving and increased road traffic accident rate associated with sleep deprivation. The effect of total sleep deprivation on brain activation during visual stimulation and visuo-motor tracking was assessed in a group of normal subjects. fMRI data from this study suggested a differential brain activation effect on the visual cortex, and this was investigated further in study 2 using a functional test of visual motion detection. This showed an impaired ability to detect coherent visual motion in the sleep deprived state, a potential explanation for some of the sleep deprivation associated deficits in driving and tracking. The fMRI visual cortex changes were assessed in a small patient study, in a group of subjects with OSA before and after CPAP treatment. This study showed no differential visual cortex activation, but activation of other brain areas before and after treatment of OSA.

Study 1 showed significantly impaired driving and tracking performance in association with objective sleepiness following up to 32 hours total sleep deprivation in a group of healthy, normal subjects. It showed that sleep deprivation is associated with reduced activation of visual cortex area V5, an area integral to the detection of motion, suggesting that this brain area may be more susceptible to the effects of sleep deprivation than the rest of the visual cortex, and reduced activation of this area may explain some of the impairments in tracking seen.

Brain activation differences were also seen during the tracking paradigm. Greater cerebellar activation occurred with increasing tracking speed following normal sleep, and no anterior or posterior cerebellar activation was seen in the sleep

deprived state. This raises the possibility that cerebellar activation and potentially therefore cerebellar function is impaired in the absence of normal, restorative sleep.

Activation of the precuneus at low tracking speeds was seen following sleep deprivation, but not following normal sleep. Persistence of precuneus/cuneus activation during tracking following sleep deprivation suggests that subjects may be unable to move from a passive 'resting' state, to an active state, required for accurate task performance, and this may be one potential mechanism for the impaired tracking and driving seen.

The results from study 2 correlate with the functional imaging data from study 1, showing a functional impairment of coherent visual motion detection following sleep deprivation. This effect was seen in those subjects vulnerable to the effects of restricted sleep, with measured objective sleepiness following sleep deprivation. This suggests that the reduced brain activation of visual cortex area V5 following sleep deprivation is associated with a functional impairment of this brain region, leading to deficits in motion detection ability. This may be one mechanism by which sleep deprivation leads to impaired tracking and driving. No impairment of visual form detection was identified in those subjects resistant or vulnerable to the effects of sleep deprivation. This suggests that the brain area responsible for this function is less susceptible to the effects of sleep deprivation. This may be due to the lower metabolic rate of parvocells, serving this neural pathway. Impairments in simulated steering performance and tracking were also seen, independent of objective sleepiness status, as expected from previous studies.

The initial study in OSA patients pre and post CPAP treatment showed non-specific brain activation changes, mostly related to task attention and visuo-spatial awareness. No differential visual cortex changes were seen. Small improvements in

steering and tracking performance were seen with CPAP treatment, but there was residual overall objective sleepiness post treatment, which may confound interpretation of the fMRI findings.

Thus the effects of sleep deprivation are widespread and complex, a number of specific and non-specific brain activation changes are seen with sleep deprivation in normal subjects, and with the sleep deprivation of OSA.

Future Work

The results of these studies raise a number of further questions, which could be assessed in future studies. An assessment of the effects of sleep deprivation on coherent visual motion detection in a much larger number of subjects, with a range of objective and subjective sleepiness at baseline, using a specific V5 sensitive paradigm (such as an RDK) in the fMRI scanner would ensure specific effects on the visual cortex. The ability to measure subject attention during data collection would also improve the study. This would mean the use of an eye tracker device, or EEG in the scanner, and not just the surrogate marker of joystick movement, which was used in the tracking task.

Future work to ascertain the mechanism for the impairment in visual motion detection would determine the importance of the persistence of precuneus activation post sleep deprivation. One unanswered question is whether the reduced activation of visual cortex area V5 in the sleep deprived state is impaired because it 'can't' be activated, because of a metabolic impairment of the magnocellular pathway, or because it 'won't' be activated, because it is unable to move from a resting / idling state, because of the persistence of precuneus activation. The studies presented in this thesis have shown evidence for both these effects of sleep deprivation as a potential mechanism, the data presented here supports the 'can't be activated' theory, and that the metabolic effects on the sensors in the magnocellular pathway are affected by sleep deprivation.

Further investigation would help to determine more specific effects of sleep deprivation, and how the brain recovers function of these areas with normal sleep. It might aid understanding of the recovery of brain function and plasticity in other

neurological conditions. The study of an alerting agent such as modafinil or caffeine in this context might help to ascertain a mechanism.

The next study to take the assessment of brain activation in OSA patients forward would be a randomised controlled trial of subjects treated with therapeutic or sub-therapeutic CPAP. This would remove any placebo effect of therapeutic CPAP, and would enable an assessment of the true effects of the treatment, and resolution of OSA on performance and brain fMRI activation. A study including patients with a wide range of OSA, and a range of subjective and objective sleepiness at baseline would add to the usefulness of the data collected.

Publications

The publications arising from this thesis are listed below.

Abstracts:

Robinson GV, Hansen PC, Miall RC, Stradling JR, Davies RJO. Visual motion detection is impaired in normal subjects following total sleep deprivation. *Am J Resp Crit Care Med* 2004, 169; 7: A869.
Oral presentation at the American Thoracic Society Annual Meeting, 2004.

Robinson GV, Miall RC, Matthews PM, Stradling JR, Davies RJO. Brain functional MRI during visuo-motor tracking in OSA - changes with CPAP treatment. *Am J Resp Crit Care Med* 2004, 169; 7: A869.
Oral presentation at the American Thoracic Society Annual Meeting, 2004.

Robinson GV, Hansen PC, Miall RC, Stradling JR, Davies RJO. Visual motion detection is impaired following total sleep deprivation in normal subjects. *Thorax* 2003, 58; S3: T6.
Oral presentation at the British Thoracic Society Winter Meeting, 2003.

Robinson GV, Miall RC, Matthews PM, Jones EM, Winter JL, Stein JF, Stradling JR, Davies RJO. Brain fMRI activation and evoked potentials during visual stimulation and visuo-motor tracking in normal subjects before and after sleep deprivation. *Am J Resp Crit Care Med* 2003, 167; 7: A16.
Oral presentation at the American Thoracic Society Annual Meeting, 2003.

Robinson GV, Miall RC, Matthews PM, Jones EM, Winter JL, Stein JF, Stradling JR, Davies RJO. fMRI activation and evoked potentials during visual stimulation and visuo-motor tracking in normal subjects before and after sleep deprivation. *Thorax* 2002, 57; S3: S17.
Oral presentation at the British Thoracic Society Winter Meeting, 2002.

Robinson GV, Miall RC, Matthews PM, Davies RJO.
Differential changes in occipital cortex activation to a visual stimulus following total sleep deprivation - an fMRI study.
Poster presentation at the American Society for Neurosciences Annual Meeting, 2002.

Robinson GV, Doyle J, Pepperrell JCT, Maskell NA, Miall RC, Stradling JR, Davies RJO. Visuo-motor tracking function in patients with Obstructive Sleep Apnoea before and after nasal CPAP treatment. *Thorax* 2001, 56; S3: 28.
Oral presentation at the British Thoracic Society Winter Meeting, 2001.

References

- Allen G, McColl R, Barnard H, Ringe WK, Fleckerstein J, Culham CM. Magnetic resonance imaging of cerebellar prefrontal and cerebellar parietal functional connectivity. *Neuroimage* 2005; 28: 39-45.
- Andersson JL, Onoe H, Hetta J, Lidstrom K, Valind S, Bromer JE, Watanbe Y, Langstrom B. Brain networks affected by synchronised sleep visualised by positron emission tomography. *J Cereb Blood Flow Metab* 1998; 18: 701-715.
- Arnedt JT, Wilde GJ, Munt PW, Maclean AW. Simulated driving performance following prolonged wakefulness and alcohol consumption: separate and combined contributions to impairment. *J Sleep Res* 2000; 9: 233-241.
- ASDA Standards of Committee Practice. Practice parameters for the treatment of snoring and obstructive sleep apnea with oral appliances. *Sleep* 1995; 18: 511-513.
- Babkoff H, Capsy T, Mikulincer M. Subjective sleepiness ratings: the effects of sleep deprivation, circadian rhythmicity and cognitive performance. *Sleep* 1991; 14: 534-539.
- Banderet LE, Strokes JW, Francesoni R. Artillery teams in simulated sustained combat: performance and other measures. In: *Biological rhythms, Sleep and shift work* (Ed LC Johnson); 1981: 459-477. New York: Spectrum.
- Bandettini PA, Kwong KK, Davis TL, Totell RB, Wong EC, Fox PT, Belliveau JW, Weisshoff RM, Rosen BR. Characterisation of cerebral blood oxygenation and flow changes during prolonged brain activation. *Human Brain Mapping* 1997; 5: 93-109.
- Banks S, Barnes M, Tarquinio N, Pierce RJ, Lack HC, McEvoy RD. The maintenance of wakefulness test in normal healthy subjects. *Sleep* 2004; 27: 799-802.
- Bastain AJ, Martin TA, Keating JG, Thach WT. Cerebellar ataxia: abnormal control of interaction torques across multiple joints. *J Neurophysiology* 1996; 76: 492-509.
- Beaumont M, Batejat D, Pierard C, Coste O, Doireau P, Van Beers P, Denis JB, Laqarde D. Slow release caffeine and prolonged (64-hr) continuous wakefulness: effects on vigilance and cognitive performance. *J Sleep Res* 2001; 10: 265-276.
- Bechara A, Tranel D, Damasio H, Adolphs R, Rockland C, Damsaio AR. Double dissociation of conditioning and declarative knowledge relative to the amygdale and hippocampus in humans. *Science* 1995; 269: 1115-1118.
- Begleiter H, Porjesz B, Chou CL, Aunon JL. P3 and stimulus incentive value. *Psychophysiology* 1983; 20:

Bell-McGinty S, Habeck C, Hilton HJ, Rakitn B, Scarmeau N, Zarahn E, Flynn J, Delapaz R, Basner R, Stern Y. Identification and differential vulnerability of a neural network in sleep deprivation. *Cereb Cortex* 2004; 14: 496-502.

Bennett LS, Barbour C, Langford B, Stradling JR, Davies RJ. Health status in obstructive sleep apnoea: relationship with sleep fragmentation and daytime sleepiness, and effects of continuous positive airway pressure treatment. *Am J Respir Crit Care Med* 1999; 159: 1884-90.

Bennett LS, Stradling JR, Davies RJO. A behavioural test to assess daytime sleepiness in obstructive sleep apnoea. *J Sleep Res* 1997; 6: 142-5.

Bennett LS, Langford BA, Stradling JR, Davies RJ. Sleep fragmentation indices as predictors of daytime sleepiness and nCPAP response in OSA. *Am J Respir Crit Care Med* 1998; 158: 778-786.

Beppu H, Nagaoka M, Tanaka R. Analysis of cerebellar motor disorders by visually guided elbow tracking movement II. Contribution of the visual cues on slow pursuit. *Brain* 1987; 110: 1-18.

Bills AG. Blocking: a new principle of mental fatigue. *Am J Psychol* 1931; 43: 230-245.

Blagrove M, Alexander C, Horne J. The effects of sleep deprivation on a test of field-independence. *Sleep Res* 1991; 20A: 458.

Bonda E, Petrides M, Ostry D, Evans A. Specific involvement of human parietal systems and the amygdala in the perception of biological motion. *J Neurosci* 1996; 16: 3737-3744.

Braddick OJ, O'Brien JM, Wattam-Bell J, Atkinson J, Hartley T, Turner R. Brain areas sensitive to coherent visual motion. *Perception* 2001; 30: 61-72.

Briskin JG, Lehrman KL. Shy-Drager syndrome and sleep apnea. In: Guilleminault C, Dement WC, Eds. *Principles and Practices of Sleep Medicine*. Philadelphia: Saunders, 1978; 317-322.

Britten KH, Shalden MN, Newsome WT, Movshon JA. The analysis of visual motion: A comparison of neuronal and psychophysical performance. *J Neuroscience* 1992; 12: 4745-4765.

Brown SH, Kessler KR, Hefter H, Cooke JD, Freund HJ. Role of the cerebellum in visuomotor coordination I. Delayed eye and arm initiation in patients with mild cerebellar ataxia. *Exp Brain Res* 1993; 94: 478-488.

Buckner RL, Raichle ME, Miezin FM, Petersen SE. Functional anatomic studies of memory retrieval for auditory and visual pictures. *J Neurosci* 1996; 16: 6219-6235.

Cabeza R, Nyberg L. Imaging cognition II. An empirical view of 275 PET and fMRI studies. *J Cog Neurosci* 2000; 12: 1-47.

Caldarelli DD, Cartwright R, Lillie JK. Severity of sleep apnea as a predictor of successful treatment by palatopharyngoplasty. *Laryngoscope* 1986; 96: 945-947.

Carter CS, Braver TS, Barch DM, Botvinick MM, Noll D, Cohen JD. Anterior cingulate cortex, error detection, and the online monitoring of performance. *Science* 1998; 280: 747-749.

Cassel W, Ploch T, Becker C, Dugnus D, Peter JH, Von Willert P. Risk of traffic accidents in patients with sleep-disordered breathing: reduction with nasal CPAP. *Eur Respir J* 1996; 9: 2606-2611.

Chee MW, Choo WC. Functional imaging of working memory after 24 hours of total sleep deprivation. *J Neurosci* 2004; 24: 4560-4567.

Chen Y, Bedell H, Frishman LJ. The precision of velocity discrimination across spatial frequency. *Perception and psychophysics* 1998; 60: 1329-1336.

Cheshire K, Engelmann H, Deary I, Shapiro C, Douglas NJ. Factors impairing daytime performance in patients with the sleep apnoea / hypopnoea syndrome. *Arch Intern Med* 1992; 152: 538-541.

Civardi C, Boccagni C, Vicentini R, Bolamperti L, Tarletti R, Varrasi C, Monaco F, Cantello R. Cortical excitability and sleep deprivation: a transcranial magnetic stimulation study. *J Neurol Neurosurg Psychiatry* 2001; 71: 809-12.

Clark DD, Sokoloff L. in basic neurochemistry. Molecular, cellular and medical aspects (Eds Siegel GJ, Agranoff BW et al). Lippincott-Raven 1999.

Clower DM, West RA, Lynch JC, Strick PL. The inferior parietal lobule is the target of output from the superior colliculus, hippocampus, and cerebellum. *J Neurosci* 2001; 21: 6283-91.

Clower DM, Dum RP, Strick PL. Basal ganglia and cerebellar inputs to 'AIP'. *Cereb Cortex* 2005; 15: 913-20.

Connor J, Norton R, Ameratunga S, Robinson E, Civil I, Dunn R, Bailey J, Jackson R. Driver sleepiness and risk of serious injury to car occupants: population based control study. *BMJ* 2002; 324: 1125.

Corbetta M, Kincade JM, Ollinger JM, McAvoy MP, Shukman GL. Voluntary orienting is dissociated from target detection in human posterior parietal cortex. *Nature Neuroscience* 2000; 3: 292-297.

Cornelissen PL, Hansen PC, Gilchrist I, Cormack T, Essex J, Frankish C. Coherent motion detection and letter position encoding. *Vision Res* 1998; 38: 2181-2191.

Cornelissen P, Hansen PC, Hutton JL, Evangeliou V, Stein JF. Magnocellular visual function and children's single word reading *Vision Research* 1998; 38: 471-482.

Cornelissen P, Richardson A, Mason A, Fowler S, Stein JF. Contrast sensitivity and coherent motion detection measured at photopic luminance levels in dyslexics and controls. *Vision Research* 1995; 35: 1483-1494.

Corsi-Cabrera M, Arce C, Del Rio-Portilla IY, Perez-Garci E, Guevara MM. Amplitude reduction in visual event related potentials as a function of sleep deprivation. *Sleep* 1999; 22: 181-189.

Coull JT. fMRI studies of temporal attention: allocating attention within, or towards, time. *Brain Res Cogn Brain Res* 2004; 21: 216-26.

Coull T, Jones ME, Egan TD, Frith CD, Maze M. Attentional effects of noradrenaline vary with arousal level: selective activation of thalamic pulvinar in humans. *Neuroimage* 2004; 22: 315-22.

Coull JT, Vidal F, Nazarian B, Macer F. Functional anatomy of the attentional modulation of time estimation. *Science* 2004; 303: 1506-8.

Culham JC, Brandt SA, Cavanagh P. Cortical fMRI activation produced by attentive tracking of moving targets. *J Neurophysiol* 1998; 80: 2657-2670.

Cutler NR, Cohen HB. The effect of one night's sleep loss on mood and memory in normal subjects. *Compr Psychiatry* 1979; 20: 61-6.

Davies RJO, Ali NJ, Stradling JR. Neck circumference and other clinical features in the diagnosis of the obstructive sleep apnoea syndrome. *Thorax* 1992; 47: 101-105.

Dawson D, Reid K. Fatigue, alcohol and performance impairment. *Nature* 1997; 338: 235.

De Valk E, De Groot E, Cluydts R. Effects of slow-release caffeine and a nap on driving simulator performance after partial sleep deprivation. *Percept Motor Skills* 2003; 96: 67-78.

DeYoe EA, Carman GJ, Bandettini P, Glickman S, Wieser J, Cox R, Miller D, Nietz J. Mapping striate and extrastriate visual areas in human visual cortex. *Proc Nat Acad Science USA* 1996; 93: 2382-2386.

Drummond SP, Brown GG, Stricker JL, Buxton RB, Wong EC, Gillin JC. Sleep deprivation induced reduction in cortical functional response to serial subtraction. *Neuroreport* 1999; 10: 3745-3748.

Drummond SP, Brown CG. The effects of total sleep deprivation on cerebral performances to cognitive performance. *Neuropsychopharm* 2001; 25: S68-73.

Drummond SP, Brown GG, Gillin JC, Stricker JL, Wong EC, Buxton RB. Altered brain responses to verbal learning following sleep deprivation. *Nature* 2000; 403: 655-657.

Drummond SP, Bischoff-Grethe A, Dinges DF, Aaylon L, Mednick SC, Meloy MT. The neural basis of the psychomotor vigilance task. *Sleep* 2005; 28: 1059-1068.

Drummond SP, Meloy MJ, Yanagi MA, Orff HJ, Brown GG. Compensatory recruitment after sleep deprivation and the relationship with performance. *Psychiatry Research* 2005; 140: 211-223.

Drummond SP, Gillin JC, Brown GG. Increased cerebral response during a divided attention task following sleep deprivation. *J Sleep Res* 2001; 10: 85-92.

Drummond SP, Brown GG, Salamat JS, Gillin JC. Increasing task difficulty facilitates the cerebral compensatory response to total sleep deprivation. *Sleep* 2004; 27: 445-451.

Easterbrook JA. The effect of emotion on cue utilisation and the organisation of behaviour. *Psychol Review* 1959; 66: 183-201.

Eden G, Vanmeter J, Rumsey J, Zeffino TA. Abnormal processing of visual motion in dyslexia revealed by functional brain imaging. *Nature* 1996; 382: 222-233.

Engelmann HM, Martin SE, Deary IJ, Douglas NJ. Effect of continuous positive airway pressure treatment on daytime function in sleep apnoea / hypopnoea syndrome. *Lancet* 1994; 343: 572-575.

Engelman HM, Hirst WS, Douglas NJ. Under reporting of sleepiness and driving impairment in patients with sleep apnoea/hypopnoea syndrome. *J Sleep Research* 1997; 6: 272-275.

Engelmann HM, Martin SE, Kingshott RN, Mackay TW, Deary IJ, Douglas NJ. Randomised placebo controlled trial of daytime function after continuous positive airway pressure (CPAP) therapy for sleep apnoea / hypopnoea syndrome. *Thorax* 1998; 53: 341-345.

Ferguson KA, Ono T, Lowe AA, Keenan SP, Fleetham JA. A randomised crossover study of an oral appliance vs nasal continuous positive airway pressure in the treatment of mild-moderate obstructive sleep apnea. *Chest* 1996; 109: 1269-1275.

Fiez JA. Cerebellar contributions to cognition. *Neuron* 1996; 16: 13-15.

Findley LJ, Weiss W, Jabour R. Drivers with untreated sleep apnea. *Arch Int Med* 1991; 151: 1451-1452.

Findley LJ, Suratt PM. Serious motor vehicle crashes - the cost of untreated sleep apnoea. *Thorax* 2001; 56: 505.

- Findley LJ, Unverzagt ME, Surratt PM. Automobile accidents in patients with obstructive sleep apnoea. *Am Rev Respir Disease* 1988; 138: 337-340.
- Findley LJ, Surratt PM. Serious motor vehicle crashes: the cost of untreated sleep apnoea. *Thorax* 2001; 56: 505.
- Findley L, Smith C, Hooper J, Dineen M, Surratt PM. Treatment with nasal CPAP decreases automobile accidents in patients with sleep apnea. *Am J Respir Crit Care Med* 2000; 161: 857-859.
- Fiset P, Paus T, Daloze T, Bachman SB, Evans AC. Brain mechanisms of propofol induced loss of consciousness in humans: a positron emission tomography study. *J Neurosci* 1999; 19: 5506-5513.
- Flament D, Hore J. Movement and electromyographic disorders associated with cerebellar dysmetria. *J Neurophysiol* 1986; 55: 1221-33.
- Fletcher PC, Shallice T, Frith CD, Frackowiak RS, Dolan RJ. Brain activity during memory retrieval. The influence of imagery and semantic cueing. *Brain* 1996; 119: 1587-1596.
- Friedrich FJ, Egly R, Rafal RD, Beck D. Spatial attention deficits in humans: A comparison of superior parietal and temporal-parietal junction lesions. *Neuropsychol* 1998; 12: 193-207.
- Friston KJ, Zarahn E, Josephs O, Henson RN, Dale AM. Stochastic designs in event-related fMRI. *Neuroimage* 1999; 10: 607-619.
- Fuster JM. *The prefrontal cortex*. 1989; New York: Raven Press.
- Gao JH, Parsons LM, Bower JM. Cerebellum implicated in sensory acquisition and discrimination rather than motor control. *Science* 1996; 272: 545-7.
- George C. Reduction in motor vehicle collisions following treatment of sleep apnoea with nasal CPAP. *Thorax* 2001; 56: 508-512.
- George CF, Boudreau AC, Smiley A. Comparison of simulated driving performance in narcolepsy and sleep apnea patients. *Sleep* 1996; 19: 711-717.
- George CF, Boudreau AC, Smiley A. Effects of nasal CPAP on simulated driving performance in patients with obstructive sleep apnoea. *Thorax* 1997; 52: 648-653.
- George CF, Boudreau AC, Smiley A. Simulated driving performance in patients with obstructive sleep apnea. *Am J Respir Crit Care Med* 1996; 154: 175-81.
- George CF, Nickerson PW, Hanly PJ, Millar TW, Kryger ML. Sleep apnoea patients have more automobile accidents. *Lancet* 1987; 2: 447.

Ghaem O, Mellet E, Crivello F, Tzourio N, Mazoyer B, Berthoz A, Denis M. Mental navigation along memorised routes activates the hippocampus, precuneus and insula. *Neuroreport* 1997; 8: 739-744.

Gislason T, Almqvist M, Eriksson G, Taube A, Boman G. Prevalence of sleep apnea syndrome among Swedish men – an epidemiological study. *J Clin Epidemiol* 1988; 41: 571-576.

Gleeson K, Zwillich CW, White DP. The influence of increasing ventilatory effort on arousal from sleep. *Am Rev Respir Dis* 1990; 142: 295-300.

Grafton ST, Mazziotta JC, Woods RP, Phelps ME. Human functional anatomy of visually guided finger movements. *Brain* 1992; 115: 565-587.

Gros B, Blake R, Hiris E. Anisotropies in visual motion perception: a fresh look. *J Op Soc America* 1998; 15: 2003-2011.

Grossman E, Donnelly M, Price R, Pickering D, Morgan V, Neighbor G, Blake R. Brain areas involved in perception of biological motion. *J Cog Neuroscience* 2000; 12: 711-720.

Guilleminault C, Stoohs R, Duncan S. Snoring (I). Daytime sleepiness in regular heavy snorers. *Chest* 1991; 99: 40-48.

Guilleminault C. Benzodiazepines, breathing and sleep. *Am J Med* 1990; 88: 25S-28S.

Hack MA, Davies RJO, Mullins R, Choi S, Ramdassingh-Dow S, Jenkinson S, Stradling JR. Randomised prospective parallel study of therapeutic versus sub-therapeutic nasal continuous positive airway pressure on simulated steering performance in patients with obstructive sleep apnoea. *Thorax* 2000; 55: 224-231.

Hack MA, Choi SJ, Vijayapalan P, Davies RJ, Stradling JR. Comparison of the effects of sleep deprivation, alcohol and obstructive sleep apnoea (OSA) on simulated steering performance. *Respir Med* 2001; 95: 594-601.

Hansen PC, Stein JF, Orde SR, Winter JL, Talcott JB. Are Dyslexics' Visual Deficits Limited to Measures of Dorsal Stream Function? *NeuroReport* 2001; 12: 1527-1530.

Harmon JD, Morgan W, Chaudhary B. Sleep apnea: morbidity and mortality of surgical treatment. *South Med J* 1989; 82: 161-164.

Harrison Y, Horne YA, Rothwell A. Prefrontal neuropsychological effects of sleep deprivation in young adults-a model for healthy aging? *Sleep* 2000; 23: 1067-1073.

Harrison Y, Horne JA. One night of sleep loss impairs innovative thinking and flexible decision making. *Organ Behav Hum Decis Process* 1999; 78: 128-145.

Harrison Y, Horne JA. Sleep loss and temporal memory. *Q J Exp Psychol* 2000; 53: 271-279.

- Harrison Y, Horne JA. Sleep impairs short and novel language tasks having a prefrontal focus. *J Sleep Res* 1998; 7: 95-100.
- Hasnain MK, Fox PT, Woldorff MG. Intersubject variability of functional areas in the human visual cortex. *Human Brain Mapping* 1998; 6: 301-315.
- Hedges LV, Olkin I. Statistical methods for meta-analysis. Orlando Fl.: Academic Press, 1985.
- Heimer D, Scharf SM, Lieberman A, Lavie P. Sleep apnea syndrome treated by repair of deviated nasal septum. *Chest* 1983; 84: 184-185.
- Hock C, Muller-Spahn SF, Schuh-Hofer HS, Hofmann DM, Dirnagl U, Villringer A. Age dependency changes in cerebral haemoglobin oxygenation during brain activation: a near infra-red spectroscopy study. *J Cereb Blood Flow and Metabolism* 1995; 15: 1103-1108.
- Horne JA, Reyner LA. Sleep related vehicle accidents. *BMJ* 1995; 310: 565-567.
- Horne JA, Reyner LA. Driver sleepiness. *J Sleep Res* 1995; 4: S2: 23-29.
- Horne J, Reyner L. Vehicle accidents related to sleep: a review. *Occup and Environ Med* 1999; 56: 289-294.
- Horne JA, Reyner LA, Barrett PR. Driving impairment due to sleepiness is exacerbated by low alcohol intake. *Occup and Environ Med* 2003; 60: 689-692.
- Horne JA, Baumber CJ. Time of day effects of alcohol intake on simulated driving performance in women. *Ergonomics* 1991; 34: 1377-1383.
- Horne J. Sleep loss and 'divergent thinking' ability. *Sleep* 1988; 11: 528-536.
- Horne JA. Human sleep, sleep loss and behaviour. Implications for the prefrontal cortex and psychiatric disorder. *Brit J Psychiatry* 1993; 162: 413-419.
- Horstmann S, Hess CW, Bassetti C, Mathis J. Sleepiness related accidents in sleep apnea patients. *Sleep* 2000; 23: 383-389.
- Howat P, Sleet D, Smith I. Alcohol and driving: is the 0.05% blood alcohol concentration justified? *Drug and alcohol review* 1991; 10: 151-166.
- Hunton DL, Miezin FM, Buckner RL. An assessment of functional-anatomical variability in neuroimaging studies. *Hum Brain Mapp* 1996; 4: 122-139.
- Iacoboni M, Koski LM, Brass M, Bekkering M, Woods RP, Dbeau MC, Mazziotta JC, Rizzalatti G. Reafferent copies of imitated actions in the right superior temporal cortex. *Proc Nat Acad Sci USA* 2001; 98: 13995-13999.

Imamizu H, Miyauchi S, Tamada T, Susaki Y, Takino R, Putz B, Yoshioka T, Kawato M. Human cerebellar activity reflecting an acquired internal model of a new tool. *Nature* 2000; 403: 192-5.

Jenkins IH, Passingham RE, Brooks DJ. The effect of movement frequency on cerebral activation: a positron emission tomography study. *J Neurol Sci* 1997;151: 195-205.

Jenkinson CW, Davies RJO, Mullins R, Stradling JR. Comparison of therapeutic and subtherapeutic nasal continuous positive airway pressure for obstructive sleep apnoea: a randomised prospective parallel trial. *Lancet* 1999; 353: 2100-2105.

Johns MW. Sleepiness in different situations measured by the Epworth Sleepiness Scale. *Sleep* 1994; 17: 703-710.

Johns MW. A new method for measuring daytime sleepiness: the Epworth Sleepiness Scale. *Sleep* 1991; 14: 540-545.

Johns MW. Reliability and factor analysis of the Epworth Sleepiness Scale. *Sleep* 1992; 15:376-81.

Johns MW. C Daytime sleepiness, snoring, and obstructive sleep apnea. The Epworth Sleepiness Scale. *Chest*.1993;103:30-6.

Jueptner M, Jenkins IH, Brooks DJ, Frackowiak RS, Passingham RE. The sensory guidance of movement: a comparison of the cerebellum and basal ganglia. *Exp Brain Res* 1996; 112: 462-474.

Jueptner M, Stephan UM, Frith CD, Brooks DJ, Frackowiak RS, Passingham RE. Anatomy of motor learning: I frontal cortex and attention to action. *J Neurophysiol* 1997; 77: 1313-1324.

Juniper M, Hack MA, George CF, Davies RJ, Stradling JR. Steering simulation performance in patients with obstructive sleep apnea and matched control subjects. *Eur Respir J* 2000; 15: 590-595.

Kendall AP, Kautz MA, Russo MB. Effects of sleep deprivation on lateral visual attention. *Int J Neurosci* 2006; 116: 1125-1138.

Kim H, Young T. Subjective daytime sleepiness: dimensions and correlates in the general population. *Sleep* 2005; 28: 625-34.

Kim H, Dinges DF, Young T. Sleep-disordered breathing and psychomotor vigilance in a community-based sample. *Sleep* 2007; 30:1309-16.

Kingshott RN, Cosway RJ, Deary IJ, Douglas NJ. The effect of sleep fragmentation on cognitive processing using computerised topographic brain mapping. *J Sleep Res* 2000; 9: 353-357.

- Krieger J, Meslier N, Lebrun T, Levy P, Phillip-Joet E, Saily JC, Racineaux JL. Accidents in obstructive sleep apnea patients treated with nasal continuous positive airway pressure: a prospective study. *Chest* 1997; 112: 1561-1566.
- La Berge D, Brown V. Theory of attentional operations in shape identification. *Psychol Rev* 1989; 96: 101-124.
- Lamphere J, Roehrs T, Wittig R, Zorich F, Conway WN, Roth T. Recovery of alertness after CPAP in apnea. *Chest* 1989; 96: 1364-1367.
- Land M, Horwood J. Which parts of the road guide steering? *Nature* 1995; 377: 339-40.
- Langlois PH, Smolensky MH, His BP, Wein FW. Temporal patterns of reported single-vehicle car and truck accidents in Texas USA during 1980-1983. *Chronobiol Int* 1986; 2: 131-146.
- Laureys S, Goldman S, Phillips C, Franck G, Maquet P. Impaired effective cortical connectivity in vegetative state, preliminary study using PET. *Neuroimage* 1999; 9: 377-382.
- Lauerys S, Lemaire C, Maquet P, Phillips C, Franck G. Cerebral metabolism during vegetative state and after recovery to consciousness. *J Neurol Neurosurg Psychiatry* 1999; 67: 121-122.
- Liu HL, Pu Y, Nicherson LD, Liu Y, Fox PT, Guo JH. Comparison of the temporal response in perfusion and BOLD-based event-related functional MRI. *Mag Resonance in Medicine* 2000; 43: 768-772.
- Livingstone MS, Hubel DH. Segregation of form, colour, movement and depth: Anatomy, physiology and perception. *Science* 1988; 240: 740-749.
- Lyznicki JM, Doege TC, Davies RM, Williams MA. Sleepiness, driving and motor vehicle crashes. *JAMA* 1998; 279: 1908-1913.
- Mackworth NH. Visual noise causes tunnel vision. *Psychonom Sci* 1965; 3: 67-68.
- Magistretti PJ, Pellerin L. The contribution of astrocytes to the 18-2-deoxyglucose signal in PET activation studies. *Molecular Psychiatry* 1996; 1: 445-452.
- Manganotti P, Palermo A, Patuzzo S, Zanatte G, Fiuschi A. Decrease in motor cortical excitability in human subjects after sleep deprivation. *Neurosci Letters* 2001; 304: 153-156.
- Maquet P, Faymonville ME, Degueldre C, Delfibre G, Franck G, Luxen A, Laurey M. Functional neuroanatomy of hypnotic state. *Biol Psychiatr* 1999; 45: 327-333.
- Maquet P, Schwartz S, Passingham R, Frith CD. Sleep-related consolidation of a visuomotor skill: brain mechanisms as assessed by functional magnetic resonance imaging. *J Neuroscience* 2003; 23: 1432-1440.

Marshall L, Born J. The contribution of sleep to hippocampus-dependent memory consolidation. *Trends Cogn Sci*. 2007;11442-50.

Martin BJ, Roll JP, DirRenzo N The interaction of hand vibration with oculomotor manual coordination in pursuit tracking. *Aviat Space Environ Med* 1991; 62: 145-152.

Martin SE, Engelman HM, Deary IJ, Douglas NJ. The effect of sleep fragmentation on daytime function. *Am J Respir Crit Care Med* 1996; 153: 1328-1332.

Mata M, Fink DJ, Schwartz WJ, Sokoloff L. Activity-dependent energy metabolism in rat posterior pituitary primarily reflects sodium pump activity. *J Neurochem* 1980; 34: 213-215.

Maunsell JH, Van Essen DC. The connections of the middle temporal visual area (MT) and their relationship to a cortical hierarchy in the macaque monkey. *J Neurosci* 1983; 3: 2563-2586.

Maycock G. Sleepiness and driving: the experience of UK car drivers. *Accid Anal Prev* 1997; 29: 453-462.

Mazoyer B, Zago L, Mellet E, Civecllo F, Jolot M, Petit L, Tzourio-Mazoyer N. Cortical networks for memory and executive functions sustain the resting state in man. *Brain Res Bull* 2001; 54: 287-298.

McBrien F, Spraggs PD, Harcourt JP, Croft CB. Abductor vocal cord palsy in the Shy-Drager syndrome presenting with snoring and sleep apnoea. *J Laryngol Otol* 1996; 110: 681-682.

McNamara SG, Grunstein RR, Sullivan CE. Obstructive sleep apnoea. *Thorax* 1993; 48: 754-764.

Menon RS, Kim S-G. Spatial and temporal limits in cognitive neuroimaging with fMRI. *Trends in Cognitive Neuroscience* 1996; 272: 551-554.

Miall RC, Imamizu H, Miyauchi S. Activation of the cerebellum in co-ordinated eye and hand tracking movements - an fMRI study. *Exp Brain Research* 2000; 135: 22-23.

Miall RC, Reckess GZ, Imanizu H. The cerebellum coordinates eye and hand tracking movements. *Nat Neurosci* 2001; 4: 638-644.

Mitler MM, Gujavarty S, Brownman CP. Maintenance of wakefulness test: a polysomnographic technique for evaluating treatment efficacy in patients with excessive somnolence. *Electroencephalog Clin Neurophysiol* 1982; 53: 658-661.

Mu Q, Mishory A, Johnson KA, Bohring DE, George MS. Decreased brain activation during a working memory task at rested baseline is associated with vulnerability to sleep deprivation. *Sleep* 2005; 28: 386-388.

Muller F, Dichgans J. Discoordination of pinch and lift forces during grasp in patients with cerebellar lesions. *Exp Brain Res* 1994; 101: 485-492.

Murray EA, Davidson M, Gaffan D, Ollon DS, Suoni S. Effects of fornix resection and cingulate cortex ablation on spatial memory in rhesus monkeys. *Exp Brain Res* 1989; 74: 173-186.

Naughton M, Pierce R. Sleep apnoea's contribution to the road toll. *Aust NZ J Med* 1991; 21: 833-883.

National Commission on Sleep Disorders Research report Vol 1. Summary and Executive report. Bethesda MD: National Institutes of Health 1993.

Nawrot M, Rizzo M. Motion perception deficits from midline cerebellar lesions in humans. *Vis Research* 1995; 35: 723-731.

Nobre AC. The attentive homunculus: Now you see it. Now you don't. *Neuroscience Biobehav Rev* 2001; 25: 477-96.

Oldfield RC. The assessment and analysis of handedness: the Edinburgh inventory. *Neuropsychologia* 1971; 9: 97-113.

Olson CR, Msil SY, Goldberg ME. Posterior cingulate cortex and visuo-spatial cognition: properties of single neurons in the behaving monkey. In: *Neurobiology of the cingulate cortex and limbic thalamus*. Boston 1993.

Oreja-Guevara C, Kleiser R, Paulus R, Kruse W, Seitz RT, Hoffman KP. The role of V5 (hMT+) in visually guided hand movements: an fMRI study. *Eur J Neurosci* 2004; 19: 3113-3120.

Owaga S, Tank DW, Menon R, Ellermann JM, Merkle H, Kim SG, Ugurbil K. Intrinsic signal changes accompanying sensory stimulation: functional brain mapping with magnetic resonance imaging. *Proc Nat Acad Sciences USA* 1992; 89: 5951-5955.

Pack AI, Pack AM, Rodgman E, Cucchiara A, Dinges DF, Schwab CW. Characteristics of crashes attributed to the driver having fallen asleep. *Accid Anal Prev*. 1995; 27: 769-75.

Pack I, Maishin G, Rogers WC, George CF, Dinges DF Impaired performance in commercial drivers-role of sleep apnea and short duration sleep. *Am J Respir Crit Care Med* 2006; 174: 446-454.

Patrick GTW, Gilbert JA. On the effects of loss of sleep. *Psychol Rev* 1896; 3: 469-483.

Pauling L, Coryell C. The magnetic properties and structure of hemoglobin, oxyhemoglobin, and carbon monoxymoglobin. *Proc Nat Acad Sciences USA* 1936; 22: 210-216.

Peers PV, Ludwig CJ, Rorden C, Cusack R, Bundesen C, Driver J, Antoun N. Attentional functions of the parietal and frontal cortex. *Cereb Cortex* 2005; 15: 1469-1484.

Peker Y, Carlson J, Hedner J. Increased incidence of coronary artery disease in sleep apnoea: a long-term follow-up. *Eur Resp J* 2006; 28: 596-602.

Pepperell JCT, Ramdassingh-Dow S, Crosthwaite N, Mullins R, Jenkinson C, Stradling J, Davies RJ. Ambulatory blood pressure after therapeutic and sub-therapeutic continuous positive airway pressure for obstructive sleep apnoea: a randomised controlled trial. *Lancet* 2002; 359: 204-209.

Petersen SE, Fox PT, Posner MI. Positron emission tomographic studies of the cortical anatomy of single-word processing. *Nature* 1988; 331: 585-589.

Philip P, Sagaspe P, Taillard J, Moore N, Charles A, Bioulac B. Fatigue, sleep restriction and performance in automobile drivers: a controlled study in a natural environment. *Sleep* 2003; 26: 277-280.

Pilcher JJ, Huffcutt AI. Effects of sleep deprivation on performance: a meta-analysis. *Sleep* 1996; 19: 318-326.

Pitson DJ, Stradling JR. Autonomic markers of arousal during sleep in patients undergoing investigation for obstructive sleep apnoea, their relationship to EEG arousals, respiratory events and subjective sleepiness. *J Sleep Research* 1998; 7: 53-59.

Pitson DJ, Stradling JR. Value of beat-to-beat blood pressure changes, detected by pulse transit time, in the management of the obstructive sleep apnoea/hypopnoea syndrome. *Eur Resp J* 1998; 12: 685-692.

Pitson DJ, Sandell A, Van Den Hout R, Stradling JR. Use of the pulse transit time as a measure of inspiratory effort in patients with obstructive sleep apnoea. *Eur Respir J* 1995; 8: 1669-1674.

Poceta JS, Timms RM, Jeong DU, Ho SL, Erman MK, Mitler MM. Maintenance of wakefulness test in obstructive sleep apnea syndrome. *Chest* 1992; 101: 893-897.

Portas CM, Rees G, Howesman O, Josephs O, Turner R, Frith CD. A specific role for the thalamus in mediating the interaction of attention and arousal in humans. *J Neuroscience* 1998; 18: 8979-8989.

Profant J, Ancoli-Israel S, Dimsdale JE.. A randomised controlled trial of 1 week of continuous positive airway pressure treatment on quality of life. *Heart Lung* 2003; 32: 52-58.

Raichle ME, Macleod AM, Sayder AZ, Powers WS, Gunsard DA, Shulman GL. A default mode of brain functioning. *Proc Nat Acad Sciences USA* 2001; 98: 676-682.

Ramsey NF, Kirby BS, Van Gelderen PV, Esposito G, Mooren CT, Weinberger DR. Functional mapping of human sensorimotor cortex with BOLD fMRI correlates highly with H₂¹⁵O PET rCBF. *J Cereb Blood Flow Metab* 1996; 16: 755-764.

Raymond JE. Directional anisotropy of motion sensitivity across the visual field. *Vision Research* 1994; 24: 1029-1038.

Rees G, Friston K, Koch C. A direct quantitative relationship between the functional properties of human and macaque V5. *Nat Neuroscience* 2000; 3: 716-723.

Remmers JE, deGroot WJ, Sauerland EK, Anch AM. Pathogenesis of upper airway occlusion during sleep. *J Appl Physiol* 1978; 44: 931-938.

Reyner LA, Horne JA. Falling asleep whilst driving: are drivers aware of prior sleepiness? *Int J Legal Med* 1998; 111: 120-123.

Reyner LA, Horne JA. Early morning driver sleepiness: effectiveness of 200mg caffeine. *Psychophysiology* 2000; 37: 251-256.

Reyner LA, Horne JA. Evaluation 'in-car' countermeasures to sleepiness: cold air and radio. *Sleep* 1998; 21: 46-50.

Reyner LA, Horne JA. Efficacy of a 'functional energy drink' in counteracting driver sleepiness. *Physiol Behav* 2002; 75: 331-335.

Richardson GS, Miner JD, Czeisler CA. Impaired driving performance in shiftworkers: the role of the circadian system in a multifactorial model. *Alcohol Drugs Driving* 1989; 5: 265-273.

Rodenstein DO, Doms G, Thomas Y, Liistro G, Stanescu DC, Culee C, Aubert-Tullers G. Pharyngeal shape and dimensions in healthy subjects, snorers, and patients with obstructive sleep apnoea. *Thorax* 1990; 45: 722-727.

Roge J, Keilbasa L, Muzet A. Deformation of the useful visual field with state of vigilance, task priority, and central task complexity. *Percept and Motor Skills* 2002; 95: 118-130.

Roge J, Muzet A. Variations of the level of vigilance and of behavioural activities during simulated automobile driving. *Accident Analysis and Prevention* 2001; 33: 181-186.

Roge J, Pebayle T, El Hannachi S, Muzet A. Effect of sleep deprivation and driving duration on the useful visual field in younger and older subjects during simulator driving. *Vision Research* 2003; 43: 1465-1472.

Roland PE, Gulyas B. Visual memory, visual imagery and visual recognition of larger field patterns by the human brain: functional anatomy by positron emission tomography. *Cereb Cortex* 1995; 5: 79-93.

Russo M, Thomas M, Thorne D, Hall S, Krichman J, Balkin T. Occulomotor impairment during chronic partial sleep deprivation. *Clin Neurophysiol* 2003; 114: 723-736.

Sadeh A, Acebo C. The role of actigraphy in sleep medicine. *Sleep Med Rev* 2002; 6: 113-124.

Sangal RB, Thomas L, Mitler MM. Maintenance of wakefulness test and multiple sleep latency test: measurement of different abilities in patients with sleep disorders. *Chest* 1992; 101: 898-902.

Saxvig IW, Lundervold AJ, Grønli J, Ursin R, Bjorvatn B, Portas CM. The effect of a REM sleep deprivation procedure on different aspects of memory function in humans. *Psychophysiology* 2007; XX

Schmid A, Rees G, Frith C, Barnes G. An fMRI study of anticipation and learning of smooth pursuit eye movements in humans. *Neuroreport* 2001; 12: 1409-1414.

Schmidt Nowara WW, Meade TE, Hays MB. Treatment of snoring and obstructive sleep apnea with a dental orthosis. *Chest* 1991; 99: 1378-1385.

Schwartz WJ, Smith CB, Davidsen L, Mata M, Fink DJ, Gainer H. Metabolic mapping of functional activity in the hypothalamo-neurohypophysial system of the rat. *Science* 1979; 205: 723-725.

Schiller PH, Logoethetis NK, Charles ER. Role of colour-opponent and broad band channels in vision. *Visual Neuroscience* 1990; 5: 321-346.

Sekuler AB, Bennett PJ, Mamelak M. Effects of aging on the useful field of view. *Exp Aging Res* 2000; 26: 103-120.

Sereno MI, Dale AM, Reppas JB, Kwong KK, Belliveau JW, Brady TJ, Rosen BR, Tootell RB. Borders of multiple visual areas in humans revealed by functional magnetic resonance imaging. *Science* 1995; 268: 889-893.

Serrien DJ, Wiesendanger M. Temporal control of a bimanual task in patients with cerebellar dysfunction. *Neuropsychologia* 2000; 38: 558-565.

Shalden MN, Britten KH, Newsome WT, Moyshon JA. A computational analysis of the relationship between neuronal and behavioural responses to visual motion. *J Neuroscience* 1996; 16: 1486-1510.

Shulman G. Common blood flow changes across visual tasks: I. Increases in subcortical structures and cerebellum, but not in non-visual cortex. *J Cog Neuroscience* 1997; 9: 623-6247.

Shulman G. Common blood flow changes across visual tasks: II. Decreases in cerebral cortex. *J Cog Neuroscience* 1997; 9: 648-663.

- Sigmundsson H, Hansen PC, Talcott JB. Do 'clumsy' children have visual deficits. *Behav Brain Res*. 2003; 139: 123-9.
- Simpson JR, Snyder AZ, Gusnard DA, Raichle ME. Emotion-induced changes in human medial prefrontal cortex: I. During cognitive task performance. *Proc Acad Sci USA* 2001; 98: 683-687.
- Simpson JR, Drevets WC, Snyder AZ, Gusnard DA, Raichle ME. Emotion-induced changes in human medial prefrontal cortex: II. During anticipatory anxiety. *Proc Acad Sci USA* 2001; 98: 688-693.
- Smith C. Sleep states and memory processes. *Brain Behav Res* 1995; 69: 137-145.
- Smith SM, Zhang Y, Jenkinson M. Accurate, robust, and automated longitudinal and cross-sectional brain change analysis. *Neuroimage* 2002; 17: 479-489.
- Steriade M, Llinas RR, Lopes da Silva FH. Basic mechanisms of cerebral rhythmic activities. *Electroenceph Clin* 1990; 76: 481-508.
- Stradling JR, Crosby JH. Predictors and prevalence of obstructive sleep apnoea and snoring in 1001 middle aged men. *Thorax* 1991; 46: 85-90.
- Strickgold R, James L, Hobson JA. Visual discrimination learning requires sleep after training. *Nat Neurosci* 2000; 3: 1237-1238.
- Strohl K, Bonnie R, Findley L. Sleep apnea, sleepiness and driving risk. *Am J Respir Crit Care Med* 1994; 150: 1463-1473.
- Sikes RW, Vogt BA, Swadlow HA. Neuronal responses in rabbit cingulate cortex linked to quick-phase eye movements during nystagmus. *J Neurophysiol* 1988; 59: 922-936.
- Sullivan CE, Issa FG, Berthon-Jones M, Eves L. Reversal of obstructive sleep apnea by continuous positive airway pressure applied through the nares. *Lancet* 1981; 1: 862-865.
- Summers CL, Stradling JR, Baddeley RM. Treatment of sleep apnoea by vertical gastropasty. *Br J Surg* 1990; 77: 1271-1272.
- Taasan VC, Block AJ, Boysen PG, Wynne JW. Alcohol increases sleep apnea and oxygen desaturation in asymptomatic men. *Am J Med* 1981; 71: 240-245.
- Talairach J & Tournoux J. Stereotaxic localisation of central gray matter. *Neurochirurgia (Stuttg)* 1958; 1: 88-93.
- Talcott JB, Hansen PC, Willis-Owen C. Visual magnocellular impairments in adult developmental dyslexics. *Neuro-Ophthalmology* 1998; 20: 187-201.

Talcott JB, Hansen PC, Assoku EL, Stein JF. Visual motion sensitivity in dyslexia: Evidence for temporal and energy integration deficits. *Neuropsychologia* 2000; 38: 935-943.

Thach WT, Goodkin HP, Keating JG. The cerebellum and the adaptive coordination of movement. *Annu Rev Neurosci* 1992; 15: 403-442.

Thomas M, Sing H, Belenky G, Welsh A, Balwinski S, Redmond D. Neural basis of alertness and cognitive performance impairments during sleep deprivation. I: effects of sleep deprivation on waking human regional brain activity. *J Sleep Res* 2000; 4: 335-352.

Thompson R. Neural mechanisms of classical conditioning in mammals. *Phil Trans Royal Soc London* 1990; 329: 161-170.

Thulborn KR, Carpenter PA, Just MA. Plasticity of language-related brain function during recovery from stroke. *Stroke* 1999; 30: 749-754.

Toni I, Krams M, Turner R, Passingham RE. The time course changes during motor sequence learning: a whole brain fMRI study. *Neuroimage* 1998; 8: 50-61.

Torrance EP. Torrance tests of creative thinking - norms and and technical manual. Lexington, Massachusetts: Ginn, 1974.

Turkington PM, Sircar M, Allgar V, Elliott MW. Relationship between obstructive sleep apnoea, driving simulator performance, and risk of road traffic accidents. *Thorax* 2001; 56: 800-805.

Turkington PM, Sircar M, Elliot MW. The relationship between OSA, driving simulator performance and risk of road traffic accidents. *Thorax* 2000; 55 (Suppl 3): 54.

Turkington PM, Sircar M, Saralaya D, Elliott MW. Time course of changes in driving simulator performance with and without treatment in patients with sleep apnoea hypopnoea syndrome. *Thorax* 2004; 59: 56-59.

Uchiyama Y, Ebe K, Kozato A, Okada T, Sadoto N. The neural substrate of driving at a safe distance: an fmri study. *Neurosci Lett* 2003; 352: 199-202.

US Dept of Commerce. US Bureau of the Census Statistical Abstract of the United States: 1990, 7th Edn. Washington DC: US Department of Commerce, 1990.

Vaina LM, Solomon J, Chowdhury C, Sinha P, Belliveau JW. Functional neuroanatomy of biological motion perception in humans. *Proc Nat Acad Sci USA*. 2001; 98: 11656-11661.

Van Dongen HP, Maislin G, Mullington JM. The cumulative cost of additional wakefulness: dose-response effects on neurobehavioral functions and sleep physiology from chronic sleep restriction and total sleep deprivation. *Sleep* 2003; 26: 117-126.

- Van Donkelaar P, Lee RG. Interactions between the eye and hand motor systems: disruptions due to cerebellar dysfunction. *J Neurophysiol* 1994; 72: 1674-1685.
- Van Donkelaar P. Eye-hand interactions during goal-directed pointing movements. *Neuroreport* 1997; 8: 2139-2142.
- Vazquez JC, Tsai WH, Flemons WW, Masuda A, Brant R, Hajduk E, Whitelaw WA, Remmers JE. Automated analysis of digital oximetry in the diagnosis of obstructive sleep apnoea. *Thorax* 2000; 55: 302-307
- Vercher JL, Magenes G, Prablanc C, Gauthier GM. Eye-head-hand coordination in pointing at visual targets: spatial and temporal analysis. *Exp Brain Res* 1994; 99: 507-523.
- Vercher JL, Gauthier GM, Guedon O, Blouin J, Cole J, Lamare Y. Self moved target eye tracking in control and deafferented subjects: roles of arm motor coordination. *J Neurophysiol* 1996; 76: 1133-1144.
- Vogt BA, Finch DM, Olson CR. Functional heterogeneity in the cingulate cortex: the anterior executive and posterior evaluative regions. *Cereb Cortex* 1992; 2: 435-443.
- Walter H, Vetter SC, Grothe J. The neural correlates of driving. *Neuroreport* 2001; 12: 1763-1767.
- Watson RT, Heilman KM, Cauthen JC, King FA. Neglect after cingulectomy. *Neurology* 1973; 23: 1003-1007.
- Watson JDG, Myers R, Frackowiak RSJ, Hajnal JV, Woods RP, Mazziotta JC, Shipp S. Area V5 of the human brain. *Cereb Cortex* 1993; 3: 79-94.
- Webb WB. The cost of sleep related accidents: a re-analysis. *Sleep* 1995; 18: 276-280.
- WHO: A 5-year WHO strategy for Road Accident Prevention, www.who.int/world-health-day/2004.
- Williamson AM, Feyer AM. Moderate sleep deprivation produces impairments in cognitive function and motor performance equivalent to legally prescribed levels of alcohol intoxication. *Occup Environ Med* 2000; 57: 649-655.
- Worsley KJ, Evans AC, Marrett S, Neelin P. A three-dimensional statistical analysis for CBF activation studies in human brain. *J Cerebral Blood Flow and Metabolism* 1992; 12: 900-918.
- Wu JC, Gillin JC, Buchsbaum MS, Hershey T, Hazlett E, Sicotte N, Bunney MC. The effect of sleep deprivation on cerebral glucose metabolic rate in humans assessed with positron emission tomography. *Sleep* 1991; 14: 155-162.

Wu H, Yan GF. Self reported automobile accidents involving patients with obstructive sleep apnoea. *Neurology* 1996; 46: 1254-1257.

Wunderlich G, Marshall JC, Amunts K, Weiss PL, Mohlberg H, Zafiris O, Zilles K, Fink GR. The importance of seeing it coming: a functional magnetic resonance study of motion-in-depth towards the human observer. *Neuroscience* 2002; 112 : 535-540.

Young T, Blunstein J, Finn L, Palta M. Sleep-disordered breathing and motor vehicle accidents in a population based sample of employed adults. *Sleep* 1997; 20: 608-613.

.

.

.

Study 1 - Protocol

The effect of total sleep deprivation on visual stimulation and visuo-motor tracking in normal subjects.

Visit 1 - Data Collection / study eligibility

Name and contact details

Age

Height (Metres)

Weight (Kg)

BMI (Kg / m²)

Epworth Sleepiness Score (must be ≤ 9)

Osler test (must reach 40 minutes)

Edinburgh Handedness Inventory

Medication Yes / No

Past medical history

UK driving licence Yes / No

Miles driven per year

Alcohol questionnaire

Caffeine questionnaire

Smoking questionnaire

Sleep pattern / sleep history

fMRIB safety questionnaire

Discuss full details of study timings

Give information letter (if not had already)

Visit 2 - Training

Epworth Sleepiness Score

Tracking training sitting (about 20 minutes)

Steering training 10 minutes

Tracking training supine (about 20 minutes)

Steering training 10 minutes

Demonstrate Osler test

Discuss fMRI setup / pictures / ?book visit

Discuss timing of other visits and protocol for sleep deprivation night

Sign consent

Visit 3 - Baseline assessment after normal sleep

Deliver actiwatch minimum 20 hours before

Bed time / rise time diary

Bed by 11pm

Normal night sleep at home

Up by 8am

Normal days' activities

fMRI centre 2pm (John Radcliffe Hospital)

fMRI scanner setup - tracking practice

Tracking in scanner

Visual stimulation in scanner

Structural scan

Back to the Churchill

30 minutes steering simulator
Osler test
Return actiwatch

Visit 4 - Sleep deprivation assessment (visits 4 and 5 in random order)

Deliver actiwatch minimum 20 hours before
Bed time / rise time diary
Up by 8am
Normal days' activities
Arrive Churchill 11pm for supervised sleep deprivation
Videos / games / work overnight
No stimulants, no high glucose food overnight
Breakfast 8am
fMRI centre 2pm (John Radcliffe Hospital)
fMRI scanner setup - tracking practice
Tracking in scanner
Visual stimulation in scanner
(Structural scan - only needed once)
Back to the Churchill
30 minutes steering simulator
Osler test
Return actiwatch
Taxi home

Visit 5 - Normal sleep assessment (visits 4 and 5 in random order)

Deliver actiwatch minimum 20 hours before
Bedtime / rise time diary
Up by 8am
Normal days' activities
fMRI centre 2pm (John Radcliffe Hospital)
fMRI scanner setup - tracking practice
Tracking in scanner
Visual stimulation in scanner
(Structural scan - only needed once)
Back to the Churchill
30 minutes steering simulator
Osler test
Return actiwatch
Taxi home

Subjective Daytime Sleepiness

All subjects completed the Epworth Sleepiness Score (ESS) [Johns 1991, Johns 1992, Johns 1993, Johns 1994], a self-completed questionnaire of general levels of sleepiness in eight potentially soporific situations. The score reflects the tendency to sleep over a period of time, and not just on one day. The ESS has been shown to be abnormal in subjects with a variety of sleep disorders, including obstructive sleep apnoea, and correlates well with the Multiple Sleep Latency Test (MSLT) [Johns 1994]. The ESS measures subjective sleepiness, so relies on the patient's own perception of their sleepiness. It is susceptible to deliberate errors, particularly relating to sleep tendency whilst driving [Engelmann 1997].

The Epworth Sleepiness Scale

Name.....

Date.....

Your age (Yrs)..... Your sex (male or female).....

How likely are you to doze off or fall asleep in the situations described below, in contrast to just feeling tired?

This refers to your usual way of life in recent times.

Even if you haven't done some of these things recently, try to work out how they would have affected you.

Use the scale to choose the most appropriate number for each situation:

0= would never doze

1= slight chance of dozing

2= moderate chance of dozing

3= high chance of dozing

Situation

Chance of dozing

Sitting & reading

Watching TV

Sitting inactive in a public place e.g. a theatre or a meeting

As a passenger in a car for an hour without a break

Lying down for a rest in the afternoon when circumstances permit

Sitting and talking to someone

Sitting quietly after lunch without alcohol

In a car, stopped for a few minutes in the traffic

Actigraphy (activity based monitoring)

All subjects had their movement monitored by an actiwatch (Cambridge Neurotechnology Ltd, UK). The actiwatch contains an accelerometer, which is motion sensitive. The device measures intensity and duration of activity [Sadeh 2002]. The number of counts produced by the actiwatch is proportional to the intensity of the subject's movement. The peak amplitude or intensity of acceleration of the accelerometer is recorded. The actiwatch is worn on the non-dominant wrist. The subject keeps an activity diary, enabling a correlation of the actiwatch recording with the subject's diary. Epochs are defined prior to use by the investigator, to enable logging of the captured activity data. Activity scores are represented on an actogram, epoch by epoch.

Handedness

Handedness was assessed by the Edinburgh Handedness Inventory (EHI), a self-completed questionnaire, asking subjects about which hand they would use in preference for ten every day tasks [Oldfield 1971]. Each question is scored 3 for the right hand, 2 for either hand, and 1 for left. A score of 10 - 14 indicates strongly left handed, a score of 15 - 19 indicates weakly left handed, and a score of 20 indicates neither left or right handed. A score of 21 - 25 indicates weakly right handed and a score of 26 - 30 indicates strongly right handed.

Results

Subjects were on average, strongly right handed (mean EHI 28.5, SD 2.8, range 21-30).

Edinburgh Handedness Inventory

For each of the ten activities listed below, please indicate:

1. Which hand do you prefer to use for that activity? Left, right or no preference
2. Do you ever use the other hand for the activity? Yes or No

	Which hand do you prefer to use?	Do you ever use the other hand?
Writing	Right Left No preference	Yes No
Drawing	Right Left No preference	Yes No
Throwing	Right Left No preference	Yes No
Using Scissors	Right Left No preference	Yes No
Using a toothbrush	Right Left No preference	Yes No
Using a knife (without a fork)	Right Left No preference	Yes No
Using a spoon	Right Left No preference	Yes No
Using a broom (upper hand)	Right Left No preference	Yes No
Striking a match	Right Left No preference	Yes No
Opening the lid of a box	Right Left No preference	Yes No



Confidential
Research MRI Screening Form

Name: _____

Date of Birth: _____ **Approx. Weight:** _____

COREC Approval No: _____

Please indicate if you have, or have had, any of the following:	Yes	No
Heart pacemaker	()	()
Artificial heart valve	()	()
Aneurysm clip(s)	()	()
Injury involving metal fragments (i.e. metal shavings/shrapnel)	()	()
Worked with, or machined, metal	()	()
Injury to eye involving metal (i.e. slivers, shavings, foreign body)	()	()
Metal rods/plates/screws/clips/staples, etc.	()	()
Ear implant	()	()
Nerve stimulator	()	()
Implanted pump	()	()
Orbital/eye prosthesis	()	()
Hearing aid	()	()
Dentures/fixed bridge(s)	()	()
Artificial limb/prosthesis	()	()
Tattoos/tattooed eyeliner	()	()
Surgical procedure or operation of any kind?	()	()
If yes, please list, e.g. hernia repair, detached retina repair, etc. _____		

Women Only

Sterilisation clips	()	()
Intrauterine Device (IUD)	()	()
Diaphragm	()	()
Are you pregnant, or do you suspect that you may be?	()	()

I have had the magnetic resonance scanning procedure and its risks explained to me and agree to have a magnetic resonance examination. I understand that it is not a diagnostic scan, but that if any unusual findings are noted incidentally, I will be contacted to discuss any appropriate follow-up.

Signature: _____ **Date:** _____

Witnessed by: _____ **Date:** _____

OXFORD RESPIRATORY SLEEP UNIT

Consultant/Director: Prof. John Stradling
Secretary: Denise Roberts

Consultant: Dr Robert Davies
Secretary: Amanda Webb

Sleep Clinic Nurses: Debby Nicoll & Debbie Smith

Research Nurses: Beverley Langford & Nicky Crosthwaite

Clinical Assistant:

Research Registrar: Dr Grace Robinson
Secretary: Emma Jones

The Oxford Centre for Respiratory Medicine
Osler Chest Unit
Churchill Hospital
Headington Oxford
OX3 7LJ

COREC Study Number: C01.004

Date 1.01.02

Dear

A study of brain activity during movement of the hand and eyes, before and after a night of sleep deprivation.

Thank you for your interest in the above study. The study is being done to examine the brain blood flow changes which are associated a well-documented deterioration in hand / eye coordination following sleep deprivation. This poor performance in coordinated hand / eye movements or 'tracking' leads to driving impairment and an increased motor accident rate following sleep deprivation. We are interested in the brain blood flow changes associated with this.

The study involves three scanning sessions and a practice session, and you can withdraw from the study at any time. The first session is held at the Oxford Centre for Respiratory Medicine at the Churchill Hospital. This training session takes about one hour and involves learning two simple computer games. One takes the form of a steering simulator test, which involves driving a cartoon car down a winding road. The other is a joystick-controlled game, which involves following a moving target around a screen, and tracking the target with the joystick.

Following the training session, we would ask you to come to the Oxford Centre for Magnetic Resonance Imaging, at the John Radcliffe Hospital for the first of the three scanning sessions. Each scanning session includes about 20 minutes of 'set-up' time and about one hour of actual scanning. The first two would be after a night of normal sleep, with no excess alcohol the night before, and no morning tea or coffee before the scan. Two types of scan would be performed. The first type of scan would provide a picture of your brain. Then a series of scans would measure the change in brain activity as you alternated between performing the 'tracking test' and resting, and looking at a flashing chequerboard. The test is projected onto a screen, and you would wear prism

glasses to view the screen. Both these scans use magnetism and not any X-rays. Following the scan we would ask you to come to the Churchill Hospital to measure how good you are at staying awake by asking you to lie in a darkened room while tapping a button in response to a flashing light for 40 minutes. We would also ask you to perform a 30 minute steering test.

The MRI scanner is like a tunnel, and you would lie on your back on a bed so that your head is at the center of the tunnel. Although the tunnel is quite narrow, wearing the prism glasses gives you a view of outside at all times. Some people who are prone to claustrophobia can find the closed space worrying. To allow you to decide whether this is a problem for you, we will give you an opportunity to lie in the magnet before the scan tests. Throughout a scan you would be able to contact the operators at all times, and they would immediately bring you out of the scanner if you felt uncomfortable. However, if you are claustrophobic it might be better if you did not volunteer for this study. The scanner is also rather noisy. We would give you earplugs and noise-resistant headphones to counteract this.

Because the MR scanner uses a strong magnetic field, it is very important that you do not volunteer if you have any metal implants or a cardiac pacemaker. This is important for your safety and if you are uncertain about this, please ask us. The scanning procedures we use are not a diagnostic test, but if we did detect any abnormality, we would talk to you about it and organise any advice or treatment that might be needed.

The third scanning session would be performed the morning following the night of sleep deprivation. This would be done overnight at the Oxford Centre for Respiratory Medicine. We would ask you to wear a special type of watch, which records your body movements for 24 hours before, and for the night of sleep deprivation. You can bring any work or games to occupy yourself overnight, and we will provide food and videos for entertainment. You will not be allowed to consume any caffeine containing foods or drinks for the 24 hours before, and during the night of sleep deprivation. Again following the scan, we would ask you to perform the test of staying awake and the steering test.

You will probably feel very tired after the night of sleep deprivation, and will probably not feel like doing any work that day. Even if you do not feel tired, you will also be unsafe to drive or operate machinery. If you need a taxi home, we will organise this for you.

If you have any questions or problems, please contact us. The contact telephone number is

Yours sincerely,

Dr Grace Robinson MRCP
Research Fellow in Respiratory Medicine.

Dr Robert Davies DM FRCP
Consultant Physician

OXFORD RESPIRATORY SLEEP UNIT

Consultant/Director: Prof. John Stradling
Secretary: Denise Roberts

Consultant: Dr Robert Davies
Secretary: Amanda Webb

Sleep Clinic Nurses: Debby Nicoll & Debbie Smith
Research Nurses: Beverley Langford & Nicky Crosthwaite
Research Registrar: Dr Grace Robinson
Secretary: Emma Jones

The Oxford Centre for Respiratory Medicine
Osler Chest Unit
Churchill Hospital
Headington Oxford
OX3 7LJ

COREC Study Number: C01.004

CONSENT FORM

Title of Project: A study of brain activity during movement of the hand and eyes, before and after a night of sleep deprivation.

Name of Researchers: Dr G Robinson, Dr RJO Davies, Prof RC Miall, Prof JR Stradling

- | | | |
|--|-----|-----|
| 1. I confirm that I have read and understand the information sheet | Yes | No |
| 2. I confirm that I have had the opportunity to ask questions and discuss the study | Yes | No |
| 3. I have received satisfactory answers to my questions | Yes | No |
| 4. I understand that my participation is voluntary and that I am free to withdraw
No
at any time, without giving any reason, without my medical care or legal
rights being affected | | Yes |
| 5. I would like my GP (Dr.....) to be notified about my taking
part in this study | Yes | No |
| 6. I understand that I will be unsafe to drive or operate machinery the day following
the night of sleep deprivation | | |
| 7. I agree to take part in the above study | Yes | No |

Name of Patient

Date

Signature

Name of Person taking consent
(if different from researcher)

Date

Signature

Researcher

Date

Signature

fMRI Scan Analysis

A number of pre-processing steps are required before the fMRI scan data can be analysed. Following the pre-processing steps, the data can be analysed using FEAT (FMRIB's Easy Analysis Tool). FEAT uses complex in-house computer software, including a number of automated steps. All the data pre-processing steps are within FSL, the FMRIB's Software Library (www.fmrib.ox.ac.uk/fsl). The processing steps are described below.

BET - Brain Extraction Tool

This part of FSL removes all non-brain parts of the image, using a surface model approach. There is a much greater degree of inter-subject variation in non-brain, than in brain structures [Smith 2002].

FAST - FMRIB Automated Segmentation Tool

This process segments the 3D brain image into different tissue types (grey and white matter, and CSF). It corrects for spatial intensity variations (i.e. field inhomogeneities).

FLIRT - FMRIB Linear Image Registration Tool

All brain images must be perfectly aligned before further analysis can take place. FLIRT is a linear image registration tool, which aligns the brain in each image with that in another. This involves finding which spatial transformation is necessary to move the selected image, so that it is in line with the reference image, see pages 243 and 244.

MCFLIRT - Motion Correction using FLIRT

Scan motion correction is necessary as all subjects move in the scanner to a degree. This process performs serial registration to remove motion, by registering all of the scans in the analysis group to the same reference scan. Motion artefact can result in a ring of inaccurately high statistical results at the edge of the brain, and can also reduce the significance of true areas of activation. Both translational and rotational motion is corrected for. The motion parameter output file produced in FEAT shows rotation decomposed as Euler angles ($R = R_x R_y R_z$), with translations about the centre of mass. Relative and absolute motion is also described; large jumps of movement are more detrimental than slow drifts of movement over time, see pages 241 and 242.

FEAT - FMRI Easy Analysis Tool

fMRI analysis determines which brain areas change in intensity with the input activation. The brain is analysed voxel by voxel (a voxel is a 3D pixel). Each brain voxel has a 1-dimensional time point associated with it, derived from the temporal scan sequence. Each voxel in the time series is analysed separately, and compared with the predicted response to the experimental activity. A good match implies brain activation related to the stimulus. FEAT has a number of pre-processing steps, including initial corrections to the data (slice dropout correction), slice timing correction, spatial filtering, global intensity normalisation and temporal filtering. The steps in the analysis are as described over:

Slice Timing Correction

This correction is needed as each MRI slice is taken at a slightly different time. Slice timing correction shifts each voxel's time series, so that all voxels in a given volume appear to have been captured at exactly the same time.

Spatial Filtering

Spatial filtering increases the signal to noise ratio. A Gaussian profile (bell shape) is passed over each 3D image. This profile averages each voxel locally, reducing noise and blurring the image. The width of the Gaussian profile determines the amount of image smoothing. The Gaussian profile is measured in full-width-half-maximum (FWHM), in mm. Filtering with a FWHM profile greater than the spatial resolution of the imaging system results in image noise reduction. Filtering at a size greater than the size of the activation areas reduces the signal of interest.

Global Intensity Normalisation

This process normalises all subjects' data across the group, removing the effects of image-wide signal intensity change, unrelated to the task under investigation. The process finds the mean group intensity, and multiplies all intensities by the same factor, to set the mean to a constant value. It results in all images in the sequence having the same overall brightness, which is important for the generation of the subsequent statistical map.

Lowpass Temporal Filtering

This removes unwanted high frequency noise from the data. This artefact occurs if the temporal smoothing rate is greater than the rate of change of the signal of interest.

Highpass Temporal Filtering

This process removes low frequency signals, such as cardiac and respiratory effects, and other low frequency artefacts, improving the data quality.

The General Linear Model

This is a multiple linear regression analysis model. It is set up like a simple correlational analysis, correlating each voxel's time course with the model time course. The model is set up to show what is expected from the data, and the data is fitted to the model. If the model is derived from the stimulation applied to the subject in the MRI scanner, then a good fit between the data and the model means that the data was caused by the stimulation. More than one model can be fitted simultaneously to the data.

A number of explanatory variables (EVs), or conditions are assessed against the dataset. Each EV results in a parameter estimate (PE) image, which describes how well the waveform fits the data at each voxel; the higher it is, the better the data fit. The parameter estimate image is obtained using a least squares model. The PE reflects how much of the model is explained by a particular EV. A contrast of parameter estimates (COPE) image is a linear estimation of the PEs. The null hypothesis is tested using the COPE image.

The T test image results from dividing the PE by its standard error. This image is directly related to the variance (noise level) in the model. So the T test image modifies the PE image according to the noise level - the greater the signal noise, the more the T value is reduced; reducing the significance level. The probability image (p) is produced by a mathematical transformation of the T image. The p image gives the significance of activation at each voxel - the value is low if the activation is very likely to be real. The p image is later corrected for multiple comparisons. The Z score image

is the result of converting the p image into standard deviations. So a Z of 2 means 2 standard deviations from no activation; Z is a useful way of representing the significance of activations. Each Z statistic image is generated by setting up contrast vectors. The design matrix is a graphical representation of the model and parameter contrasts. The shape of the waveform that describes each EV is selected. For the visual stimulus, the chequerboard flashes on and off, every 30 seconds, so the waveform selected is a simple on / off, 'boxcar' design, where the stimulus is on, then off for the appropriate period. For the tracking task, the variables are more complex, with 4 EVs for each tracking speed, and one for error and sleep episodes respectively. An additional 3 EVs are added for the subjects' head motion.

High pass temporal filtering determines the longest waveform processed by the model. A convolution function blurs and delays the original waveform, in an attempt to match the waveform (the input function) with the output function (the measured haemodynamic response).

The null hypothesis is determined for each brain voxel, but this causes a problem of multiple comparisons, as around 20,000 brain voxels are assessed. A modified Bonferroni correction therefore divides the 'uncorrected' p threshold by the number of brain voxels, and a cluster analysis is used, because not all voxels are independent. This involves setting the Z statistic image at an arbitrary level, and using Random Fields Theory (RFT) [Worsley 1992]. RFT helps with the theoretical problems of smoothing statistical maps of functional imaging data, by using results that give the expected Euler Characteristic (EC) for a thresholded, smoothed statistical map. The EC is essentially the number of active areas in the image after it has been thresholded. The null hypothesis is then used to determine the probability of obtaining a cluster, given its spatial extent and Z threshold.

Higher Level Analyses

Following the first-level analysis described above, a higher-level analysis is then used to assess differences between subjects, or between groups of subjects. This involves a more complex GLM, grouping subjects depending on condition (normal sleep or sleep deprivation, and pre and post CPAP), and a comparison between the different conditions.

FLAME (fMRIB's Local Analysis of Mixed Effects)

This process uses sophisticated methods for modelling and estimating the random effects components of inter-session or inter-subject analyses, and the mixed effects variance. For example, a simple (first level analysis) of a single group average will define the group mean effect. An unpaired two group difference (unpaired t-test) will estimate the two groups' variance separately. For study 1, I examined one group of subjects, under two conditions - normal sleep and sleep deprivation. For study 3, one group of subjects was also examined, again under two conditions - before and after CPAP treatment. This analysis estimates a two-group paired difference, essentially a two-sample paired t-test.

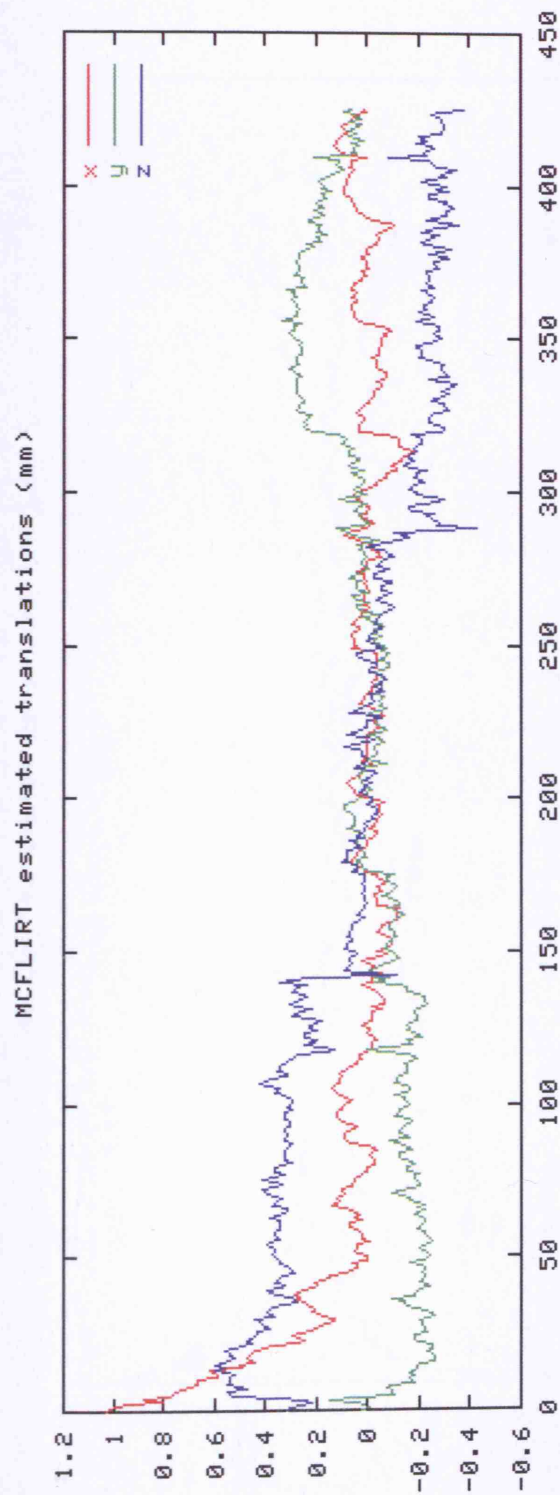
Cluster Detection

This process finds clusters and reports cluster probabilities, taking into account the problem of multiple comparisons. Clusters are formed using the Z Score Threshold, usually set at a default of 2.3. Clusters are defined as sets of voxels which touch each other in 3D, with no gaps. The Z threshold determines the size and shape of the clusters; the probability threshold (set later on) determines the computed significance of the cluster, against each cluster's size and height. Different threshold levels can be set.

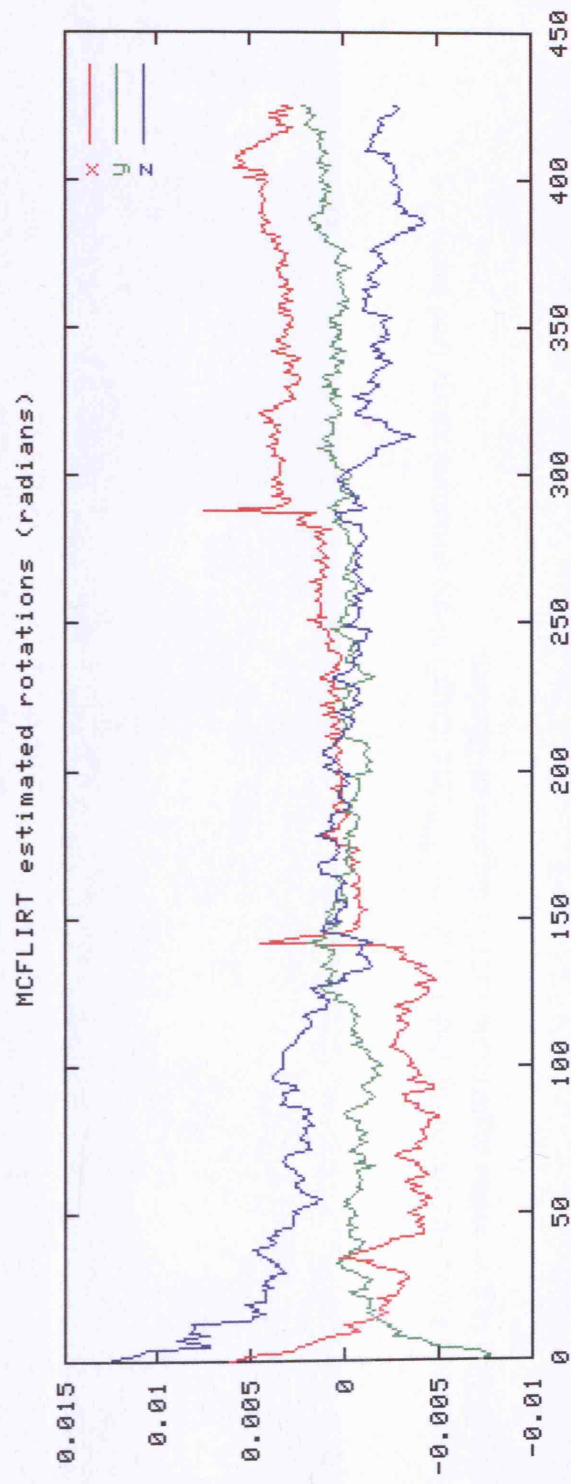
Cluster thresholding uses the Z statistic threshold to define contiguous clusters. This thresholding method is sensitive to activations. Each cluster's estimated significance is then compared with a cluster probability threshold. Significant clusters are then used to mask the original Z statistic image for the later production of coloured areas. A less sensitive thresholding alternative is voxel based correction. This uses Gaussian Random Field (GRF) theory, based on maximum height thresholding. This is less conservative than a Bonferroni type correction. Thresholding using uncorrected Z statistics, or no threshold at all can also be done. Colour rendering of the output images is calculated by default, so that the minimum Z statistic is rendered red and the highest yellow.

Local Minima / Maxima

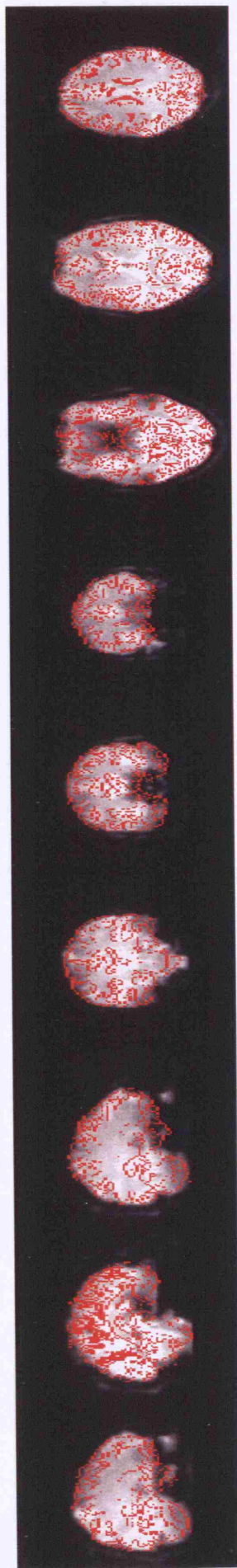
The local cluster minima and maxima from the statistical image are calculated, with the original (X, Y, Z) and Talairach coordinates reported. Brain images in 'Talairach Space' are transformed so that specific brain landmarks are registered with those of the Talairach Atlas. This means that the brain image has been centred, scaled and rotated, with the coordinate system centred on the anterior commissure. The coordinates can then be anatomically localised using the Talairach Daemon (Version 2.0, Research Imaging Centre, University of Texas Health Science Center, <http://ric.uthscsa.edu/projects/talairachdaemon.html>), a computerised, automated version of the Talairach Atlas.



Motion Correction. The MCFLIRT estimated translations in X, Y and Z dimensions for an individual subject. The X axis shows movement in mm, and the Y axis shows scanning time.



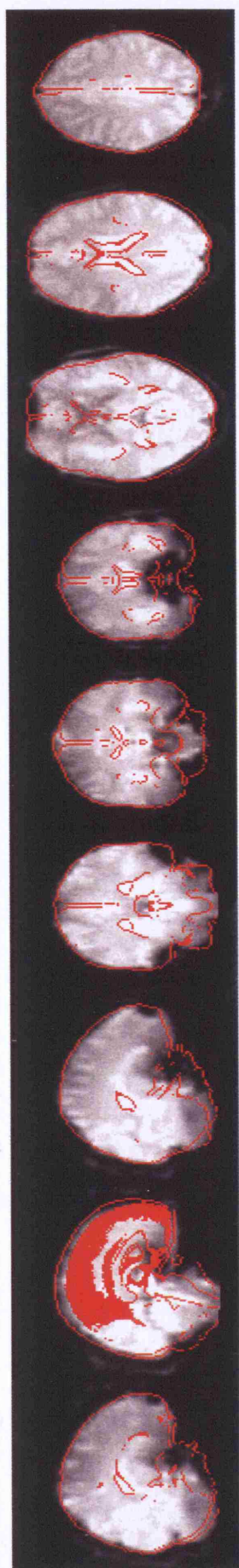
Motion Correction. The MCFLIRT estimated rotations in X, Y and Z dimensions for an individual subject. The X axis shows movement in radians, and the Y axis shows scanning time.



Registration 1 Registration of the fMRI image (underlying image) to the structural image (red lines) using FLIRT to give affine registration with 12 degrees-of-freedom.



Registration 2 Registration of the structural image (underlying image) to the standard image (red lines) using FLIRT to give affine registration with 12 degrees-of-freedom.



Registration 3 Registration of the fMRI (underlying image) to the standard image (red lines) by combining the two registrations above.

Mean location and standard deviation of visual area V5 (from Hasnain et al)

Area	Mean location (mm) (Talairach Coordinates)			Standard Deviation (mm)			Frequency of Detection
	X	Y	Z	X	Y	Z	
Left Hemisphere V5	-39.0	-71.9	-0.8	2.6	4.2	4.1	73%
Right Hemisphere V5	41.3	-64.8	-1.6	4.7	7.0	6.2	82%

GRdualt – the program used for initial tracking raw data analysis (written by Professor Miall)

```
% for analysis of generic dualt eye-hand experiments
% will read in all types of data, with luck
% and generate appropriate graph & .MAT files
% Chris Miall (revisited Sept 2001 to make version 6 compatible)
```

```
clear
close all
format short g;
col='mbckrgymbckr';
symb='do*v^xs+<>ph';
disp('USE THIS FOR DUALT DATA')
name=";
```

```
if(~exist('SortCondition')),
    SortCondition=questdlg('Sort data by', ...
        'Eye-Hand Dualt', ...
        'Speed','Time_offset','Rotation','Time_offset');
    if strcmp(SortCondition,'Time_offset'),
        SortCondition=questdlg('Time offset data with', ...
            'Eye-Hand Dualt', ...
            'Eye_Hand','Combined','Offset_only','Offset_only');
    end
end
```

```
again='Yes';
while strcmp(again,'Yes'),
```

```
    % name=find_dir('*.0*');
```

```
    [file,minj,maxj,path]=find_files('*.0*');
```

```
    name=[path file];
```

```
    ncond = getnumber('Enter no of conditions (exclude rest)',7);
```

```
    cond = zeros(1,ncond)-999999;
    x=0:100;
    x10=0:0.10:100;
    x100=x10*10-500;
    cor=zeros(100,4); %store correlation coeff & lag
    tcond=zeros(100,7); %store trial condition cues
    mcx=zeros(length(x10),ncond);
    ncx=zeros(1,ncond);
    rmserr=zeros(100,1);
    rmsvel=zeros(100,1);
    expl=zeros(1,7);
    j=1;
```

```

figure(1);
for i=minj:maxj
    %loop around looking for all good files
    eval(['xx=exist('' file '.' num2str(i,'%03d') '');' ]);
    if (xx~=0)
        eval(['load ' file '.' num2str(i,'%03d')']);
        if isletter(file(1)), eval(['dd=' file ';'']);
        else
            eval(['dd=X' file ';'']); %cope with number-names
        end
        expl=dd(1,3:end); %get trial conditions
        if size(dd,1)>2,
            dd=boxfilt(detrend(dd(2:length(dd),:),0),3); %filter,DC-remove etc
            if expl(1)>0, %active trials only from now on
                %           if expl(4)>0, %active trials only from now on

xc1=xcorr(sqrt(dd(:,2).^2+dd(:,3).^2),sqrt(dd(:,6).^2+dd(:,7).^2),50,'coeff');
            %spline interpolate here to 1 tenth of sample rate
            xc11=spline(x,xc1,x10);
            [h1,i1]=max(xc11);
            [h2,i2]=min(xc11);
            disp(['file '.' num2str(i,'%03d')'])
            switch SortCondition,
            case 'Speed',
                tmpcond=expl(4);
                %           tmpcond=expl(6); 18/12/01
            case 'Offset_only',
                tmpcond=expl(5);
            case 'Combined',
                tmpcond=expl(5) + 900*(expl(3)-1); %force indep to be most negative
            case 'Eye_Hand',
                tmpcond=expl(4);
            case 'Rotation',
                tmpcond=expl(5);
            end % switch
            if (find(cond==tmpcond))
                exx=find(cond==tmpcond);
            else
                exx=first(cond==-999999);
                cond(exx)=tmpcond;
            end
            figure;
            plot(dd(:,[2 6 3 7]));
            figure(1);
            plot(xc11,col(exx));
            hold on;
            mcx(:,exx)=mcx(:,exx)+xc11; ncx(exx)=ncx(exx)+1;

            %store all data
            tcond(j,1)=i;

```



```

        tcond(j,2:6)=expl;
        %          tcond(j,2:6)=expl(2:6); 18/12/01
        tcond(j,7)=tmpcond; % this is the one to use for plotting, sorting etc
        cor(j,1)=h1;
        cor(j,2)=(length(xc11)/2-i1)*3.8;
        cor(j,3)=h2;
        cor(j,4)=(length(xc11)/2-i2)*3.8;
        rmserr(j)=sum(sqrt((dd(:,2)-dd(:,6)).^2+(dd(:,3)-dd(:,7)).^2));
        rmsvel(j)=sum(sqrt(diff(dd(:,2)).^2+diff(dd(:,3)).^2));
        j=j+1;
    end
end
end
axis([0 1000 0.0 1.0]);
fclose('all'); % may help to avoid crashes?
cor=cor(1:j-1,:); %trim storage arrays to the final number of rows
tcond=tcond(1:j-1,:);
rmserr=rmserr(1:j-1);
rmsvel=rmsvel(1:j-1);

% sort the data by trial type & get means
cond=sort(cond);
mcc=zeros(ncond,1);
mcl=zeros(ncond,1);
merr=zeros(ncond,1);
mnerr=zeros(ncond,1);
for i=1:ncond,
    ind=find(tcond(:,7)==cond(i));
    mcc(i)=mean(cor(ind,1));
    mcl(i)=mean(cor(ind,2));
    merr(i)=mean(rmserr(ind));
    mnerr(i)=mean(rmserr(ind)./rmsvel(ind));
end

for i=1:ncond %calculate mean correlation position for the curve
    mcx(:,i)=mcx(:,i)/ncx(i);
end
[mxn,in]=max(mcx);
clear dd i1 i2 j j1 j2 v1 v2 xc1 xx h1 h2 expl exx xc11 x10;
clear maxj;

%start to plot a few figures
figure;
subplot(2,3,1);
hold on;
minpt=1.0;
for i=1:ncond
    plot(-x100*3.8,mcx(:,i),col(i));
    plot(-x100(in(i))*3.8,mxn(i),[col(i) symb(i)]);

```

```

    minpt=min([minpt mxn(i)]);
end

axis([-150 450 (1.0-(1.0-minpt)*1.5) 1.0]);
title(file);

tt=min(tcond(:,7)):range(tcond(:,7))/99:max(tcond(:,7));
subplot(2,3,2);
plot(tcond(:,7),rmserr,'o');
axis([min(tcond(:,7)) max(tcond(:,7)) 0 max(rmserr)*1.5]);
coeffs=polyfit(tcond(:,7),rmserr,2);
hold on;
plot(tt,polyval(coeffs,tt),'k');
[my,mx]=min(polyval(coeffs,tt));
title(sprintf('RMS Error; min. at: %6.2f,tt(mx)));
plot([tt(mx) tt(mx)],[0 max(rmserr)*1.5],'k')

subplot(2,3,3);
plot(tcond(:,7),rmserr./rmsvel,'o');
axis([min(tcond(:,7)) max(tcond(:,7)) 0 max(rmserr./rmsvel)*1.5]);
coeffs=polyfit(tcond(:,7),rmserr./rmsvel,2);
hold on;
plot(tt,polyval(coeffs,tt),'k');
[my,mx]=min(polyval(coeffs,tt));
title(sprintf('Norm. vel; min. err at: %6.2f,tt(mx)));
plot([tt(mx) tt(mx)],[0 max(rmserr./rmsvel)*1.5],'k')

subplot(2,2,3);
plot(tcond(:,7),cor(:,1),'o');
axis([min(tcond(:,7)) max(tcond(:,7)) (1.0-(1.0-min(cor(:,1)))*1.5) 1.0]);
coeffs=polyfit(tcond(:,7),cor(:,1),2);
hold on;
plot(tt,polyval(coeffs,tt),'k');
[my,mx]=max(polyval(coeffs,tt));
title(sprintf('Corr. Coeff; max. err at: %6.2f,tt(mx)));
plot([tt(mx) tt(mx)],[0 1.0],'k')

subplot(2,2,4);
plot(tcond(:,7),cor(:,2),'o')
axis([min(tcond(:,7)) max(tcond(:,7)) 0 max(cor(:,2))*1.5]);
coeffs=polyfit(tcond(:,7),cor(:,2),2);
hold on;
plot(tt,polyval(coeffs,tt),'k');
[my,mx]=min(polyval(coeffs,tt));
title(sprintf('Corr. Lag; min. err at: %6.2f,tt(mx)));
plot([tt(mx) tt(mx)],[0 max(cor(:,2))*1.5],'k')

orient portrait;
orient tall;

```

```

clear coeffs i minj minpt mx my mxn ncx tt x;
[name, path] = uiputfile([file '.mat'], 'Save Workspace as');
save(name,'tcond','cor','rmserr','rmsvel','mcc','mcl','merr','mnerr'); %save important
stuff to MAT file

%again=input('Enter Y to run again, or RETURN to stop: ','s');
again=questdlg('Run the program again?','Dualt','No');
end

```

GRdualt_err_TR - the program used for subsequent tracking raw data analysis, providing data excluding potential large error episodes during tracking (written by Professor Miall, modified for use in the current study)

```
% this calculates the error every TR time (assuming 6 per track)
% session and saves error, target velocity and movement velocity
% 21-7-99 - revisited 22/11/2002 and 4/7/03

clear
disp('USE THIS FOR THE TR ERRORS/CONDITIONS ONLY')

name="";

%name=find_dir('*.0*');

[file,minj,maxj,path]= find_files('*.0*');

name=[name file];

format short g;
haemlag=0;
rmserr=zeros(500,3);
j=haemlag+1;

for i=minj:maxj
    %loop around looking for all good files
    eval(['xx=exist("'" file '.' num2str(i,'%03d') '"');' ]);
    if (xx~=0),
        fprintf('\nFile %d: ',i);

        eval(['load ' file '.' num2str(i,'%03d')']);
        if isletter(file(1)), eval(['dd=' file ';' ]);
        else
            eval(['dd=X' file ';' ]); %cope with number-names
        end
        expl=dd(1,:); %get trial conditions
        if length(dd)>20, %must skip the duff ending file
            dd=boxfilt(detrend(dd(2:length(dd),:),0),3); %filter,DC-remove etc
            ls=1;
            ll=length(dd)/6;
            exx=0;
            for k=1:6,
                le=min(floor(ls+ll),length(dd));
                rmserr(j,1)=sum(sqrt((dd(ls:le,2)-dd(ls:le,6)).^2+(dd(ls:le,3)-
dd(ls:le,7)).^2));
                rmserr(j,2)=sum(sqrt(diff(dd(ls:le,2)).^2+diff(dd(ls:le,3)).^2));
                rmserr(j,3)=sum(sqrt(diff(dd(ls:le,6)).^2+diff(dd(ls:le,7)).^2));
                j=j+1;
                ls=floor(ls+ll);
            end
        end
    end
end
```

```

        end
    end
end
end

fclose('all'); % may help to avoid crashes?

%skip=input('Enter no, of TRs to skip over (dummy TRs): ');

skip=6;
disp('Skipping 6 dummy TRs');

rmserr=rmserr(skip+1:j-1,:);
err=rmserr(:,1)/(mean(rmserr(:,1))*2.0);
tvel=rmserr(:,2)/(mean(rmserr(:,2))*2.0); %normalised to 0-1 approx
mvel=rmserr(:,3)/(mean(rmserr(:,3))*2.0); %ditto
subplot(3,1,1); plot(mvel,'.-'); title('MVEL');
subplot(3,1,2); plot(tvel,'.-'); title('TVEL');
subplot(3,1,3); plot(err,'.-'); title('ERR');

[name, path] = uiputfile([file '.mvel'], 'Save data as new ASCII file');
save([path name], 'mvel','-ASCII'); %save important stuff to new MAT file

```

GRdualt_exSLP - the program used for subsequent tracking raw data analysis, providing data excluding potential sleep episodes during tracking (written by Professor Miall, modified for use in the current study)

```
% for analysis of generic dualt eye-hand experiments
% will read in all types of data, with luck
% and generate appropriate graph & .MAT files
%
% Chris Miall (revisited Sept 2001 to make version 6 compatible)

clear
close all
format short g;
col='mbckrgymbckr';
symb='do*v^xs+◇ph';
disp('USE THIS FOR DUALT DATA')
name="";

if(~exist('SortCondition')),
    SortCondition=questdlg('Sort data by', ...
        'Eye-Hand Dualt', ...
        'Speed','Time_offset','Rotation','Time_offset');
    if strcmp(SortCondition,'Time_offset'),
        SortCondition=questdlg('Time offset data with', ...
            'Eye-Hand Dualt', ...
            'Eye_Hand','Combined','Offset_only','Offset_only');
    end
end

again='Yes';
while strcmp(again,'Yes'),

    % name=find_dir('*.0*');

    [file,minj,maxj,path]=find_files('*.0*');

    name=[path file];

    ncond = getnumber('Enter no of conditions (exclude rest)',7);

    cond = zeros(1,ncond)-999999;
    x=0:100;
    x10=0:0.10:100;
    x100=x10*10-500;
    cor=zeros(100,4); %store correlation coeff & lag
    tcond=zeros(100,7); %store trial condition cues
    mcx=zeros(length(x10),ncond);
    ncx=zeros(1,ncond);
    rmserr=zeros(100,1);
```

```

rmsvel=zeros(100,1);
expl=zeros(1,7);

jj=1;
j=1;
figure(1);
for i=minj:maxj
    %loop around looking for all good files
    eval(['xx=exist('' file '.' num2str(i,'%03d') '' );']);
    if (xx~=0)
        eval(['load ' file '.' num2str(i,'%03d')']);
        if isletter(file(1)), eval(['dd=' file ';']);
        else
            eval(['dd=X' file ';']); %cope with number-names
        end
        expl=dd(1,3:end); %get trial conditions
        if size(dd,1)>2,
            dd=boxfilt(detrend(dd(2:length(dd),:),0),3); %filter,DC-remove etc
            if expl(1)>0, %active trials only from now on
                %            if expl(4)>0, %active trials only from now on

                dd2=lopass(detrend(dd(2:length(dd),:),0),1,25);
                tv=sqrt(diff(dd2(:,2)).^2+diff(dd2(:,3)).^2);
                mv=sqrt(diff(dd2(:,6)).^2+diff(dd2(:,7)).^2);
                slp=zeros(length(dd)+1,1);
                if expl(1)>0,
                    slp=[0 (mv./tv<.333 & mv<0.5+sqrt(expl(4))/2)']; %sleep is mvel less
than 1/3 tvel and mvel less than half target speed
                    %            slp=[0 (mv./tv<.333 & mv<0.5)']; %sleep is mvel less than
1/3 tvel and mvel less than half target speed
                end
                off=find(diff(slp)<-.0.5);
                on=find(diff(slp)>.0.5);
                if isempty(off),
                    if isempty(on),
                        dur=-1;
                    else
                        off=length(mv);
                    end
                end
            else
                if isempty(on),
                    on=1;
                else
                    if off(1)<on(1),
                        on=[1 on'];
                    end
                    if on(end)>off(end),
                        off=[off length(slp)'];
                    end
                end
            end
        end
    end
end

```

```

        end
    end
    dur=off-on;
    if find(dur>50),
        sleep=[];
        tmp=dur(find(dur>50));
        tmp2=on(find(dur>50));
        for ii=1:length(tmp)
            sleep= [sleep cumsum([tmp2(ii) ones(1,tmp(ii))])];
        end
        %dd(sleep,:)=[];    %chop out the sleep episodes - this leaves a step-
change in position!!
        tmp=diff(dd);    %differentiate
        tmp(sleep,:)=[];    %chop out the sleep episodes
        tmp=cumsum(vercat(dd(1,:),tmp)); %re-integrate without step-change
in position
        dd=tmp;    % replace with ex-SLP data
    end

    if length(dd)>50,    %if less than two seconds remain, bail out - not
enough data to be safe to calculate

    xc1=xcorr(sqrt(dd(:,2).^2+dd(:,3).^2),sqrt(dd(:,6).^2+dd(:,7).^2),50,'coeff');
    %spline interpolate here to 1 tenth of sample rate
    xc1l=spline(x,xc1,x10);
    [h1,i1]=max(xc1l);
    [h2,i2]=min(xc1l);
    disp ([file '.' num2str(i,'%03d')])
    switch SortCondition,
    case 'Speed',
        tmpcond=expl(4);
        % tmpcond=expl(6); 18/12/01
    case 'Offset_only',
        tmpcond=expl(5);
    case 'Combined',
        tmpcond=expl(5) + 900*(expl(3)-1); %force indep to be most
negative
    case 'Eye_Hand',
        tmpcond=expl(4);
    case 'Rotation',
        tmpcond=expl(5);
    end % switch
    if (find(cond==tmpcond))
        exx=find(cond==tmpcond);
    else
        exx=first(cond==-999999);
        cond(exx)=tmpcond;
    end
    figure;

```



```

        plot(dd(:,[2 6 3 7]));
        hold on;
        plot((slp*50)+100,'k')
        figure(1);
        plot(xc11,col(exx));
        hold on;
        mcx(:,exx)=mcx(:,exx)+xc11; ncx(exx)=ncx(exx)+1;

        %store all data
        tcond(j,1)=i;
        tcond(j,2:6)=expl;
        %           tcond(j,2:6)=expl(2:6); 18/12/01
        tcond(j,7)=tmpcond; % this is the one to use for plotting, sorting etc
        cor(j,1)=h1;
        cor(j,2)=(length(xc11)/2-i1)*3.8;
        cor(j,3)=h2;
        cor(j,4)=(length(xc11)/2-i2)*3.8;
        rmserr(j)=sum(sqrt((dd(:,2)-dd(:,6)).^2+(dd(:,3)-dd(:,7)).^2));
        rmsvel(j)=sum(sqrt(diff(dd(:,2)).^2+diff(dd(:,3)).^2));
        j=j+1;
    end
end
end
end
end
axis([0 1000 0.0 1.0]);
fclose('all'); % may help to avoid crashes?
cor=cor(1:j-1,:); %trim storage arrays to the final number of rows
tcond=tcond(1:j-1,:);
rmserr=rmserr(1:j-1);
rmsvel=rmsvel(1:j-1);

% sort the data by trial type & get means
cond=sort(cond);
mcc=zeros(ncond,1);
mcl=zeros(ncond,1);
merr=zeros(ncond,1);
mnerr=zeros(ncond,1);
for i=1:ncond,
    ind=find(tcond(:,7)==cond(i));
    mcc(i)=mean(cor(ind,1));
    mcl(i)=mean(cor(ind,2));
    merr(i)=mean(rmserr(ind));
    mnerr(i)=mean(rmserr(ind)./rmsvel(ind));
end

for i=1:ncond %calculate mean correlation position for the curve
    mcx(:,i)=mcx(:,i)/ncx(i);
end
[mxn,in]=max(mcx);

```

```

clear dd i1 i2 j1 j2 v1 v2 xc1 xx h1 h2 expl exx xc11 x10;
clear maxj;

%start to plot a few figures
figure;
subplot(2,3,1);
hold on;
minpt=1.0;
for i=1:ncond
    plot(-x100*3.8,mcx(:,i),col(i));
    plot(-x100(in(i))*3.8,mxn(i),[col(i) symb(i)]);
    minpt=min([minpt mxn(i)]);
end

axis([-150 450 (1.0-(1.0-minpt)*1.5) 1.0]);
title(file);

tt=min(tcond(:,7)):range(tcond(:,7))/99:max(tcond(:,7));
subplot(2,3,2);
plot(tcond(:,7),rmserr,'o');
axis([min(tcond(:,7)) max(tcond(:,7)) 0 max(rmserr)*1.5]);
coeffs=polyfit(tcond(:,7),rmserr,2);
hold on;
plot(tt,polyval(coeffs,tt),'k');
[my,mx]=min(polyval(coeffs,tt));
title(sprintf('RMS Error; min. at: %6.2f,tt(mx)));
plot([tt(mx) tt(mx)],[0 max(rmserr)*1.5],'k')

subplot(2,3,3);
plot(tcond(:,7),rmserr./rmsvel,'o');
axis([min(tcond(:,7)) max(tcond(:,7)) 0 max(rmserr./rmsvel)*1.5]);
coeffs=polyfit(tcond(:,7),rmserr./rmsvel,2);
hold on;
plot(tt,polyval(coeffs,tt),'k');
[my,mx]=min(polyval(coeffs,tt));
title(sprintf('Norm. vel; min. err at: %6.2f,tt(mx)));
plot([tt(mx) tt(mx)],[0 max(rmserr./rmsvel)*1.5],'k')

subplot(2,2,3);
plot(tcond(:,7),cor(:,1),'o');
axis([min(tcond(:,7)) max(tcond(:,7)) (1.0-(1.0-min(cor(:,1)))*1.5) 1.0]);
coeffs=polyfit(tcond(:,7),cor(:,1),2);
hold on;
plot(tt,polyval(coeffs,tt),'k');
[my,mx]=max(polyval(coeffs,tt));
title(sprintf('Corr. Coeff; max. err at: %6.2f,tt(mx)));
plot([tt(mx) tt(mx)],[0 1.0],'k')

subplot(2,2,4);
plot(tcond(:,7),cor(:,2),'o')

```

```

axis([min(tcond(:,7)) max(tcond(:,7)) 0 max(cor(:,2))*1.5]);
coeffs=polyfit(tcond(:,7),cor(:,2),2);
hold on;
plot(tt,polyval(coeffs,tt),'k');
[my,mx]=min(polyval(coeffs,tt));
title(sprintf('Corr. Lag; min. err at: %6.2f',tt(mx)));
plot([tt(mx) tt(mx)],[0 max(cor(:,2))*1.5],'k')

orient portrait;
orient tall;

clear coeffs i minj minpt mx my mxn ncx tt x;
[name, path] = uiputfile([file 'ex.mat'], 'Save Workspace as');
save(name,'tcond','cor','rmserr','rmsvel','mcc','mcl','merr','mnerr'); %save important
stuff to MAT file

%again=input('Enter Y to run again, or RETURN to stop: ','s');
again=questdlg('Run the program again?','Dualt','No');
end

```

Study 2 - Protocol

The effect of total sleep deprivation on visual motion and form detection in normal subjects

Visit 1 - Data collection / study eligibility

Name and contact details

Age

Height (metres)

Weight (Kg)

BMI (Kg / m²)

Epworth Sleepiness Score (must be ≤ 9)

Osler test (must reach 40 minutes)

Medication Yes / No

Past medical history

UK driving licence Yes / No

Miles driven per year

Alcohol questionnaire

Caffeine questionnaire

Smoking questionnaire

Sleep pattern / sleep history

Discuss full details of study timings

Give information letter (if not had already)

Visit 2 - Training

Tracking training sitting (about 40 minutes)

Steering training 10 minutes

Motion detection training (about 20 minutes)

Steering training 10 minutes

Form detection training (about 20 minutes)

Demonstrate Osler test

Discuss timing of other visits and protocol for sleep deprivation night

Sign consent

Visit 3 - Baseline assessment after normal sleep

Deliver actiwatch minimum 20 hours before

Bed time / rise time diary

Bed by 11pm

Normal night sleep at home

Up by 8am

Normal days' activities

Churchill Hospital 2pm

Attach EEG

Motion detection

Form detection

Tracking (20 minutes)

30 minutes steering simulator

Osler test

Return actiwatch

Visit 4 - Sleep deprivation assessment (visits 3 and 4 in random order)

Deliver actiwatch minimum 20 hours before

Bed time / rise time diary

Up by 8am

Normal days' activities

Arrive Churchill 11pm for supervised sleep deprivation

Videos / games / work overnight

No stimulants, no high glucose food overnight

Breakfast 8am

Churchill Hospital 2pm

Attach EEG

Motion detection

Form detection

Tracking (20 minutes)

30 minutes steering simulator

Osler test

Return actiwatch

Taxi home

EEG Data

Continuous electroencephalogram (EEG) recording (Embletta, Medcare, Iceland) was carried out during the motion and form detection paradigms. Three standard recording channels were used, including O1-O2. EEG analysis was by routine reporting, using standard software, by an experienced operator (not myself). Sleep stage analysis of the data showed that 23 of the 24 subjects remained awake for the whole of both recordings. One subject (a male aged 21) had 3 periods of stage 1 sleep during the post sleep deprivation recording, for a total of 3.5 minutes. These three periods were roughly 1.2 minutes each, and spaced evenly throughout the recording period. The raw EEG data is not presented in this thesis. Continuous eye movement video recording confirmed attention and eye fixation during performance of both paradigms in 23 of the 24 subjects.

Study 3 - Protocol

A pilot study: The effects of OSA on fMRI brain activation during visual stimulation before and after CPAP treatment

1. Baseline / eligibility assessment (Visit 1)

Name and contact details

Age

Height (Metres)

Weight (Kg)

BMI (Kg / m²)

Neck / waist / hip / chest measurements

Epworth Sleepiness Score (must be ≥ 10)

Sleep study dip rate (≥ 10 , $> 4\%$ dips / hr)

Medication Yes / No

Past medical history (no neurological disease)

UK driving licence Yes / No

Miles driven per year

Alcohol questionnaire

Caffeine questionnaire

Smoking questionnaire

fMRIB safety questionnaire

Discuss full details of study timings (CPAP set-up date)

Give information letter (if not had already)

2. Tracking and driving training (Visit 2)

Steering training 10 minutes

Tracking training (about 20 minutes)

Steering training 10 minutes

Demonstrate Osler test

Discuss fMRI setup / pictures / ?book visit

Discuss timing of other visits and protocol for CPAP set-up

Sign consent

3. Assessment pre CPAP treatment (Visit 3)

Normal days activities

fMRI centre 2pm (John Radcliffe Hospital)

fMRI scanner setup

Visual stimulation in scanner

Structural scan

Back to the Churchill

Tracking test

30 minutes steering simulator

Osler test

4. CPAP set-up (Visit 4)

Standard CPAP set-up

5. Assessment after CPAP treatment (Visit 5)

Bring CPAP machine

Normal days activities

fMRI centre 2pm (John Radcliffe Hospital)

fMRI scanner setup

Visual stimulation in scanner

Structural scan (only needed once)

Back to the Churchill

Tracking test

30 minutes steering simulator

Osler test

Download data from autoset

Review compliance, pressure and mask leak data

Change to fixed pressure machine

Travel expenses

Book clinic follow-up (3 months CPAP clinic)

OXFORD RESPIRATORY SLEEP UNIT

Consultant/Director: Prof. John Stradling
Secretary: Denise Roberts

Consultant: Dr Robert Davies
Secretary: Amanda Webb

Sleep Clinic Nurses: Debby Nicoll & Debbie Smith
Research Nurses: Beverley Langford & Nicky Crosthwaite
Clinical Assistant:
Research Registrar: Dr Grace Robinson
Secretary: Emma Jones

The Oxford Centre for Respiratory Medicine
Osler Chest Unit
Churchill Hospital
Headington Oxford
OX3 7LJ

COREC Study Number: C01.004

Date

Dear

A study of brain activity during visual stimulation in patients with sleep apnoea.

We are writing to ask for your help with a study which involves magnetic resonance imaging (MRI) of the brain to measure brain activity. We are doing this study to try to understand why patients with sleep apnoea such as yourself sometimes have trouble in co-ordinating hand and eye movements. This is important since it is probably one of the things which makes patients with sleep apnoea more likely to have motor accidents. Before they are treated, patients with sleep apnoea are about 5 times more likely to have car accidents than people who are not affected by this problem. This falls to normal with treatment.

If you agree to help us, we would ask you to come to the Churchill Hospital for a training session (which takes about two and a half hours), during which we would ask you to perform a simple computer game, which takes the form of a driving simulator test. This involves steering a cartoon car along a winding road. We would also give you a chance to practice a 'tracking test'. This is another type of computer game, which involves following a moving target with your eyes and using a small joystick to track the moving target.

We would then ask you to come to the Oxford Centre for Functional Magnetic Resonance Imaging on the John Radcliffe Hospital site for two scanning sessions. Each scanning session includes about 30 minutes for a 'set up' period and about one hour of actually scanning. We would perform two types of brain scan as you performed some simple tasks. The first type of scan would provide a picture of your brain. Then a series of scans would measure the change in brain activity as you looked at a flashing chequerboard. The test is projected onto a screen, and you would wear prism glasses to view the screen. These scans use magnetism and not any X-rays. Following the scan we would ask you to come to the Churchill Hospital to measure how good you are at staying

awake by asking you to lie in a darkened room while tapping a button in response to a flashing light for 40 minutes. We would also ask you to repeat the steering test, and a tracking test.

The MRI scanner is like a tunnel, and you would lie on your back on a bed so that your head is at the center of the tunnel. Although the tunnel is quite narrow, wearing the prism glasses gives you a view of outside at all times. Some people who are prone to claustrophobia can find the closed space worrying. To allow you to decide whether this is a problem for you, we will give you an opportunity to lie in the magnet before the scan tests. Throughout a scan you would be able to contact the operators at all times, and they would immediately bring you out of the scanner if you felt uncomfortable. However, if you are claustrophobic it might be better if you did not volunteer for this study. The scanner is also rather noisy. We would give you earplugs and noise-resistant headphones to counteract this.

Because the MR scanner uses a strong magnetic field, it is very important that you do not volunteer if you have any metal implants or a cardiac pacemaker. This is important for your safety and if you are uncertain about this, please ask us.

After you have had the first scan and tests we would start you on the nasal continuous positive airway pressure treatment (often shortened to just CPAP) which has already been explained to you by your doctor. After about one month we would ask you to repeat the MRI brain scans, the 'tracking test', the test of ability to stay awake, the steering simulator computer game. Comparison of these results with those you performed before starting CPAP treatment will allow us to see if the way the brain controls hand and eye coordination has changed with your treatment. At the end of the study your CPAP machine will be changed to a different model. All these tests will be completed in less time than is the waiting time to start CPAP usually.

You are free to decide not take part in this study and you can withdraw at any time. If you choose not to take part, it will not affect your treatment in any way. We would reimburse your travel expenses.

We suggest that you keep this letter in case you need to show it to anyone concerned with your medical care. If you agree to take part in the study, we would write to your GP informing him of your participation. The scanning procedures we use are not a diagnostic test, but if we did detect any abnormality, we would talk to you about it and organise any advice or treatment that might be needed.

If you have any questions or problems, please contact us. The contact telephone number is

Yours sincerely,

Dr Grace Robinson MRCP
Research Fellow in Respiratory Medicine.

Dr Robert Davies DM FRCP
Consultant Physician

OXFORD RESPIRATORY SLEEP UNIT

Consultant/Director: Prof. John Stradling
Secretary: Denise Roberts

Consultant: Dr Robert Davies
Secretary: Amanda Webb

Sleep Clinic Nurses: Debby Nicoll & Debbie Smith
Research Nurses: Beverley Langford & Nicky Crosthwaite
Research Registrar: Dr Grace Robinson
Secretary: Emma Jones

The Oxford Centre for Respiratory Medicine
Osler Chest Unit
Churchill Hospital
Headington Oxford
OX3 7LJ

COREC Study Number: C01.004

CONSENT FORM

Title of Project: An fMRI study of brain activity in patients with obstructive sleep apnoea performing co-ordinated eye and hand tracking tasks before and after treatment with nasal continuous positive airway pressure.

Name of Researchers: Dr G Robinson, Dr RJO Davies, Prof RC Miall, Prof JR Stradling

- | | | |
|--|-----|----|
| 1. I confirm that I have read and understand the information sheet | Yes | No |
| 2. I confirm that I have had the opportunity to ask questions and discuss the study | Yes | No |
| 3. I have received satisfactory answers to my questions | Yes | No |
| 4. I understand that my participation is voluntary and that I am free to withdraw at any time, without giving any reason, without my medical care or legal rights being affected | Yes | No |
| 5. I would like my GP (Dr.....) to be notified about my taking part in this study | Yes | No |
| 6. I agree to take part in the above study | Yes | No |

Name of Patient

Date

Signature

Name of Person taking consent
(if different from researcher)

Date

Signature

Researcher

Date

Signature

1 for patient; 1 for researcher; 1 to be kept with hospital notes

OSA Tracking Training

As for the normal subjects, patients with OSA were carefully trained to stable performance on the tracking task.

Practice

Posa1.bat was used.

This runs Posa1a.def (hand tracking only, 5 x speed 100) = 7.5 minutes

Posa1b.def (hand and eye tracking, 5 x speed 50) = 7.5 minutes

Posa1c.def (faster hand and eye tracking, 5 x speed 50, 100, 150, 200) = 7.5 minutes

Posa1.bat

```
@echo off
cd c:\fmri\prog
input name
cls
if "%1"=="?" GOTO USAGE
if "%1"==" " GOTO USAGE
if "%1"=="JUNK" GOTO START
if "%1"=="junk" GOTO START
if exist c:\fmri\data\%1\NUL GOTO NEWNAME
if exist c:\fmri\data\%1\PRAC1\NUL GOTO NEWNAME
if exist c:\fmri\data\%1\PRAC2\NUL GOTO NEWNAME
if exist c:\fmri\data\%1\PRAC3\NUL GOTO NEWNAME
if not exist c:\data\%1 mkdir c:\data\%1
:START
echo.
echo This is a short practice session.
echo.
echo 1. You will see a blue screen, on which there
echo   are two yellow lines making a cross-hair. There
echo   are also a red square and a red circle.
echo.
echo 2. After a few seconds, the red symbols turn white and
echo   the square will start to move. Use the joystick with
echo   your preferred hand to control the movement of the
echo   square.
echo.
echo 3. You must try to keep the square as close to the cross
echo   hairs as possible.
echo.
echo 4. You must also keep your eyes on the circle as much as
echo   possible.
echo.
echo 5. When the symbols turn red, you can rest for a few seconds
echo   until they move again.
echo.
pause
cls
```

```

atr_adc 18 c:\fmri\def\Posa1a.def 6 1.00 350 c:\fmri\prog\joystick.cal 24 1000 0 0
%1\PRAC1
echo.
echo This is the next short practise session. This display is the same.
echo.
echo 1. After a few seconds, the red symbols turn white and
echo both will start to move. Use the joystick to control the
echo movement of the square.
echo.
echo 2. You must try to keep the square as close to the cross
echo hairs as possible.
echo.
echo 3. You must also keep your eyes on the moving circle as much as
echo possible.
echo.
echo 4. The direction of the white circle tells you which direction to
echo move the joystick. So if your eye move left, moving the joystick
echo towards the left should help you keep the square on the crosshairs.
echo.
echo 5. When the symbols turn red, you can rest for a few seconds
echo until they move again.
echo.
pause
cls
atr_adc 18 c:\fmri\def\Posa1b.def 6 1.00 350 c:\fmri\prog\joystick.cal 24 1000 0 0
%1\PRAC2
cls
echo.
echo This stage is very similar to the last one. The targets
echo will move faster and faster.
echo.
echo Remember you must keep your eyes on the moving circle
echo and you must try to keep the square on the cross-hairs.
echo.
pause
cls
atr_adc 18 c:\fmri\def\Posa1c.def 24 1.00 350 c:\fmri\prog\joystick.cal 24 1000 0 0
%1\PRAC3
cls
echo.
echo The session is complete. Thank you.
echo.
echo.
cls
goto END
:NEWNAME
echo.
echo. !!!!!!!!!!!!!!!!!!!!!!!!!!!!!!!
echo The name chosen has already been used.
echo Please chose a new one

```

```

echo. !!!!!!!!!!!!!!!!!!!!!!!!!!!!!!!
dir c:\data\*.
echo. !!!!!!!!!!!!!!!!!!!!!!!!!!!!!!!
pause
goto END
:USAGE
echo.
echo Usage: %0 SUBJECT_NAME
echo      e.g:%0 smith
echo.
echo      use maximum of 8 letters, no punctuation characters
echo.
pause
atr_adc ?
:END

```

Posa1a.def

1	EXPL REST	0	0	0
7	IMPL COORD	2	0	100
7	IMPL COORD	2	0	100
7	IMPL COORD	2	0	100
7	IMPL COORD	2	0	100
7	IMPL COORD	2	0	100

Posa1b.def

1	EXPL REST	0	0	0
6	IMPL COORD	3	0	50
6	IMPL COORD	3	0	50
6	IMPL COORD	3	0	50
6	IMPL COORD	3	0	50
6	IMPL COORD	3	0	50

Posa1c.def

1	EXPL REST	0	0	0
6	IMPL COORD	3	0	50
6	IMPL COORD	3	0	50
6	IMPL COORD	3	0	50
6	IMPL COORD	3	0	50
6	IMPL COORD	3	0	50
1	EXPL REST	0	0	0
6	IMPL COORD	3	0	100
6	IMPL COORD	3	0	100
6	IMPL COORD	3	0	100
6	IMPL COORD	3	0	100

6	IMPL COORD	3	0	100
1	EXPL REST	0	0	0
6	IMPL COORD	3	0	150
6	IMPL COORD	3	0	150
6	IMPL COORD	3	0	150
6	IMPL COORD	3	0	150
6	IMPL COORD	3	0	150
1	EXPL REST	0	0	0
6	IMPL COORD	3	0	200
6	IMPL COORD	3	0	200
6	IMPL COORD	3	0	200
6	IMPL COORD	3	0	200
6	IMPL COORD	3	0	200
1	EXPL REST	0	0	0

Real tracking task

This program runs Rosa1.def. Total length of task = 43 x 18 second blocks = 774 seconds = 12.9 minutes. A shorter task was used for the subjects with OSA, as in general they found the task much more difficult than the normal subjects, and their concentration time was generally shorter.

osatest.bat

```
@echo off
cd c:\fmri\prog
input name
cls
if "%1"=="/" GOTO USAGE
if "%1"==" " GOTO USAGE
if "%1"=="JUNK" GOTO START
if "%1"=="junk" GOTO START
if exist c:\fmri\data\%1\NUL GOTO NEWNAME
if exist c:\fmri\data\%1\PRAC1\NUL GOTO NEWNAME
if exist c:\fmri\data\%1\PRAC2\NUL GOTO NEWNAME
if exist c:\fmri\data\%1\PRAC3\NUL GOTO NEWNAME
if not exist c:\data\%1 mkdir c:\data\%1
:START
pause
cls
atr_adc 18 c:\fmri\def\Rosa1.def 25 1.00 350 c:\fmri\prog\joystick.cal 25 1000 0 0
%1\REAL1
cls
echo.
echo The session is complete. Thank you.
echo.
echo.
cls
goto END
:NEWNAME
```



```

echo.
echo. !!!!!!!!!!!!!!!!!!!!!!!!!!!!!!!
echo The name chosen has already been used.
echo Please chose a new one
echo. !!!!!!!!!!!!!!!!!!!!!!!!!!!!!!!
dir c:\data\*.
echo. !!!!!!!!!!!!!!!!!!!!!!!!!!!!!!!
pause
goto END
:USAGE
echo.
echo Usage: %0 SUBJECT_NAME
echo      e.g:%0 smith
echo.
echo      use maximum of 8 letters, no punctuation characters
echo.
pause
atr_adc ?
:END

```

Rosa1.def

1	EXPL REST	0	0	0
6	IMPL COORD	3	0	50
6	IMPL COORD	3	0	100
6	IMPL COORD	3	0	200
6	IMPL COORD	3	0	150
6	IMPL COORD	3	0	100
1	EXPL REST	0	0	0
6	IMPL COORD	3	0	200
6	IMPL COORD	3	0	50
6	IMPL COORD	3	0	150
6	IMPL COORD	3	0	200
6	IMPL COORD	3	0	100
1	EXPL REST	0	0	0
6	IMPL COORD	3	0	50
6	IMPL COORD	3	0	100
6	IMPL COORD	3	0	50
6	IMPL COORD	3	0	150
6	IMPL COORD	3	0	200
1	EXPL REST	0	0	0
6	IMPL COORD	3	0	150
6	IMPL COORD	3	0	50
6	IMPL COORD	3	0	200
6	IMPL COORD	3	0	150
6	IMPL COORD	3	0	100
1	EXPL REST	0	0	0
6	IMPL COORD	3	0	200

6	IMPL COORD	3	0	50
6	IMPL COORD	3	0	100
6	IMPL COORD	3	0	200
6	IMPL COORD	3	0	150
1	EXPL REST	0	0	0
6	IMPL COORD	3	0	100
6	IMPL COORD	3	0	150
6	IMPL COORD	3	0	50
6	IMPL COORD	3	0	200
6	IMPL COORD	3	0	100
1	EXPL REST	0	0	0
6	IMPL COORD	3	0	50
6	IMPL COORD	3	0	200
6	IMPL COORD	3	0	100
6	IMPL COORD	3	0	150
6	IMPL COORD	3	0	50
1	EXPL REST	0	0	0